SURFACE STUDIES IN ULTRA HIGH VACUUM

by

ALAN KEITH GREEN

A dissertion submitted for the
Degree of Doctor of Philosophy
in the
Department of Chemistry
of the
University of Aston
in Birmingham

October 1975.

SUMMARY

An ultra high vacuum system capable of attaining pressures of 10^{-12} mm Hg was used for thermal desorption experiments. The metal chosen for these experiments was tantalum because of its suitability for thermal desorption experiments and because relatively little work has been done using this metal. The gases investigated were carbon monoxide, hydrogen and ethylene. The kinetic and thermodynamic parameters relating to the desorption reaction were calculated and the values obtained related to the reaction on the surface.

The thermal desorption reaction was not capable of supplying all the information necessary to form a complete picture of the desorption reaction. Further information was obtained by using a quadrupole mass spectrometer to analyse the desorbed species. The identification of the desorbed species combined with the value of the desorption parameters meant that possible adatom structures could be postulated.

A combination of these two techniques proved to be a very powerful tool when investigating gas-metal surface reactions and gave realistic values for the measured parameters such as the surface coverage, order of reaction, the activation energy and pre-exponential function for desorption.

Electron microscopy and X-ray diffraction were also used to investigate the effect of the gases on the metal surface.

PREFACE

This dissertation, which is being submitted for the degree of Doctor of Philosophy in the University of Aston in Birmingham, is an account of the work done under the supervision of Dr S. J. Moss in the Department of Chemistry of the University from October 1971 to October 1974. Except where references are given in the text, the work described herein is original and has not been nor is being submitted for a degree at any other University.

Alan Green

A. K. Green
October 1975

ACKNOWLEDGEMENTS

I wish to express my gratitude to the following:-

My Mother and Father for all their encouragements and financial support during my earlier education.

Mr J. Walford, now deceased, who above anyone else was responsible for my earlier education.

Dr S. J. Moss for many hours of patient discussion and guidance during the past three years.

All other members of the University who have helped with the work, especially Professor M Page, Dr M. Painter, Mr M. Houghton, Mr V. Laight and Mr Herricks, the Glassblower.

My wife Sandra for her patience, encouragement and support during the work and also for her suffering and excellent typing in the production of this thesis.

Many thanks

Alan Green.

Alan Green.

CONTENTS

LIST OF FIGURES

TABLES

1 INTRODUCTION AND LITERATURE SURVEY

1.1 INTRODUCTION

1.1.1 The Clean Metal Surface

A "clean" surface may suggest various meanings to different authors and readers. Throughout this thesis the word "clean" refers to a surface that is completely free of contamination, i.e. there are no foreign molecules on the surface.

Now at normal temperatures and pressures gas molecules collide with the surface many times a second. For methane a gas with a molecular weight of 16 the rate of collision will be 3×10^{23} collisions in a second and for carbon dioxide there will be 2×10^{22} collisions in a second. Values of the same order of magnitude are found for all common gases. This shows the surface is saturated with atoms and molecules in a fraction of a second. It is not possible because of this to make meaningful studies of gas metal surface reactions at normal temperatures and pressures.

If the temperature of the metal is increased the molecules which have been adsorbed on the surface will be desorbed. The temperature at which they desorb will depend on the adsorbed species. If the temperature is raised to fractionally below the melting point of the metal, all the molecules that are capable of being desorbed, will have been desorbed, producing a clean surface. In order to maintain a clean surface the pressure of the gas in contact with the surface must be maintained at a suitably low level. Increasing the temperature of a metal in the presence of oxygen

at atmospheric pressure will lead to oxidation and this is so in the case of tantalum where a white flaky tantalum oxide forms.

The rate of collision, μ , per cm^2 per second of a gas of molecular weight m at a pressure p torr and a temperature T K is given by the kinetic theory of gases as (1)

$$\mu = p/(2 \pi m k T)^{\frac{1}{2}} \quad \ldots\ (1\text{-}1)$$

where k is Boltzmann's constant and the pressure is given in torr where

$$1 \text{ torr} = 1 \text{ mm Hg} = 133.32 \text{ N } m^{-2} \quad \ldots\ (1\text{-}2)$$

At room temperature where T = 300 K

$$\mu = 2 \times 10^{21} \, p/m^{\frac{1}{2}} \text{ collisions } cm^{-2} \text{ sec}^{-1} \quad \ldots\ (1\text{-}3)$$

for a gas of molecular weight 28 such as nitrogen, carbon monoxide or ethylene, then at atmospheric pressure the number of collisions per cm^2 per sec is 3×10^{23}. When the pressure is reduced to the high vacuum region 1×10^{-6} mm Hg the number of collisions per cm^2 per sec is 4×10^{14}. The number of atoms exposed on the surface of a metal such as tungsten is approximately 1×10^{15} (2). Assuming the sticking probability is about unity a monolayer would form in a few seconds at this pressure. When the pressure is reduced further into the ultra high vacuum region, $p = 1 \times 10^{-10}$ mm Hg, the calculated number of collisions per cm^2 per second for a gas with molecular weight 28 is 4×10^{10} and a monolayer will be formed in 8 hours.

To prepare a surface layer, the sample gas is usually allowed into the system so that the pressure rises two to three orders of magnitude above the background, then the background gases will be less than 1% of the gas in the system. To be able to do this and

still allow the gas to adsorb in the 10^{-8} to 10^{-9} mm Hg range we must be able to reduce the pressure in the system down to the 10^{-11} to 10^{-12} mm Hg range. This is very close to the minimum pressure that can be obtained in a working vacuum system which is of the order of 10^{-14} to 10^{-15} mm Hg range but at these pressures it is very difficult to obtain a pressure gauge that will give reliable results.

From these calculations on the ultra high vacuum region it can be seen that once the filament has been cleaned it will remain in a clean state for a short period. It is during this time that the sample gas will be adsorbed. The temperature of the filament will be rapidly increased and the pressure increase in the system due to the gas leaving the filament surface will be recorded. When the gas is allowed to adsorb in the 10^{-8} mm Hg range a monolayer will form on an area 1 cm square in 5 minutes assuming the sticking probability is unity. A monolayer of gas being desorbed will give a large pressure rise in the system used for the experiments, for instance a monolayer of ethylene increased the pressure by 4 orders of magnitude. A monolayer may be considered to be a large unit in the flash desorption studies in this thesis.

1.1.2 The Ultra High Vacuum Region

The ultra high vacuum region is considered to be the region below 1 x 10^{-9} mm Hg pressure range (3). Pressures down to the 10^{-8} mm Hg range are obtained by very careful working with conventional pumps and gauges. Provided all leaks as far as possible are eliminated and the pumps are capable of obtaining this pressure range it is only a matter of technique to reach the required pressure. To obtain

pressures below this certain other considerations have to be taken into account, such as the requirement of special joints, preliminary purging with non-contaminating gases and most importantly, the ability to bake out the whole system at above 473 K for at least twenty-four hours. The apparatus has to be heated to above 473 K and because of this special materials must be used to stop leaks occurring during expansion and contraction.

Recently however the ultra high vacuum region has become relatively easily attainable. A major problem before 1950 was measurement of the low pressures reached. The X-ray limit was the problem with the conventional ion gauge and this was not overcome until the work of Bayard and Alpert (4).

The development of the Bayard and Alpert gauge was a major breakthrough and meant that the ultra high vacuum pressures could now be measured reliably and that experiments could be carried out in this region. Surface studies were now undertaken by many workers using a variety of new techniques. Many of these could be used with the flash filament work which will be the main subject of this thesis and all this work gave a better understanding of surface behaviour.

Surface studies are undertaken in order that scientists may obtain a clearer picture of what is taking place when a gas is allowed onto a surface. The surfaces usually investigated are metal surfaces especially tungsten. Various kinetic parameters are calculated and these give an indication of the strength of the bonds holding the gas to the surface, the behaviour of the gas on the surface under various condition, and mechanisms of adsorption and

desorption. Analysis of the products after desorption of the gas will also help to elucidate mechanisms of adsorption and desorption. No one particular surface technique can do all these investigations but a combination of results from two or more of the techniques is usually valuable.

A survey of some of these techniques is the subject of the next section. The technique of Flash Desorption will receive a more detailed discussion in a later section.

1.2 TECHNIQUES OF SURFACE STUDIES

1.2.1 General

There are broadly two approaches to surface studies in ultra high vacuum conditions. One series of techniques analyses the surface and changes in the surface occurring during the experiment. These techniques include field ion and field emission microscopy. The second series of techniques is concerned with conditions in the gas phase close to the surface; i.e. flash desorption experiments.

Those techniques that look directly at the surface should be such that they do not interfere and change the surface interactions. It is the effect of the gas on the surface that we are investigating and not the changes in the gas-metal surface interaction due to the technique. Those techniques that look at the gas phase and not directly at the surface must be able to relate the results obtained in the gas phase to the interactions on the surface.

1.2.2 Adsorption on Evaporated Metal Films (5)

In this technique the gas phase is monitored while adsorption is taking place on a clean thin metal surface. The advantage of

using an evaporated metal film is that it gives a much larger surface area than a filament or wire. The evaporated metal film may also be produced initially in a very clean state and under ultra high vacuum conditions it will remain in this state for some time. The metal film is evaporated onto the surface of the vessel and because of this the surface of the film is up to 1000 sq cms whereas the surface area of a filament will be up to 10 sq cms and the surface area of a wire less than this. The number of molecules needed to form a monolayer on a film will be of the order 10^{18} which is many more than the 10^{15} molecules needed on a filament.

To produce the film the metal needs to be outgassed at a temperature, just below the temperature where it will evaporate, and this could take several days. The surface onto which the metal is going to be evaporated also needs to be outgassed by baking the system. This eliminates the evolution of gas from the glass which could contaminate the surface. The metal is evaporated in vacuum and the film forms on a substrate which is usually glass but could be mica or the face of a crystal. The glass is usually at a temperature of 273 K.

The vessel may be a specially designed commercial calorimeter. The experimental gas is allowed into the presence of the film in small doses and the heat of adsorption of each gas sample is observed. By varying the amount of gas adsorbed each time the variation of the heat of adsorption with surface coverage can be observed.

Metals are ideal for this technique and most metals have been used but also work has been done on alloys and non metals which can be evaporated. The variety of surfaces that can be investigated is

one of the advantages of the technique.

The disadvantage of the technique is that the area of the film is not accurately known. The roughness factor of the surface needs to be known but the exact area of the film is very hard to estimate. The errors involved in this would only be very small and results obtained in a variety of systems in different laboratories are reproducible.

1.2.3 Field Emission Microscopy

The field emission microscope is used to study surface properties when adsorption occurs. The properties of the surface monitored are the work function and the surface structure. A field emission microscope is shown diagrammatically in Fig. 1 (6).

A sharp tip is produced in a metal filament and this tip is mounted on a support loop. The tip usually has a radius of less than 1000 Å. The tip is situated in the centre of a glass vessel whose inner surface has been covered with an electrically conducting fluorescent screen. A large potential is applied to the screen and this produces a very high electric field at the tip, typically 6×10^7 V cm^{-1}. Electrons are then able to tunnel through the high energy barrier under the influence of this potential and they travel to the screen. The electrons after being accelerated have sufficient energy to excite the phosphor and this produces a much magnified image of the surface in U H V conditions. The magnification will be about 10^6. The variation of the work function over the whole surface will give light and dark areas on the fluorescent screen. The support loop can be heated or cooled and the temperature of the tip varied. The field emission microscope has a high magnification, high

FIG. 1 The Field Emission Microscope.

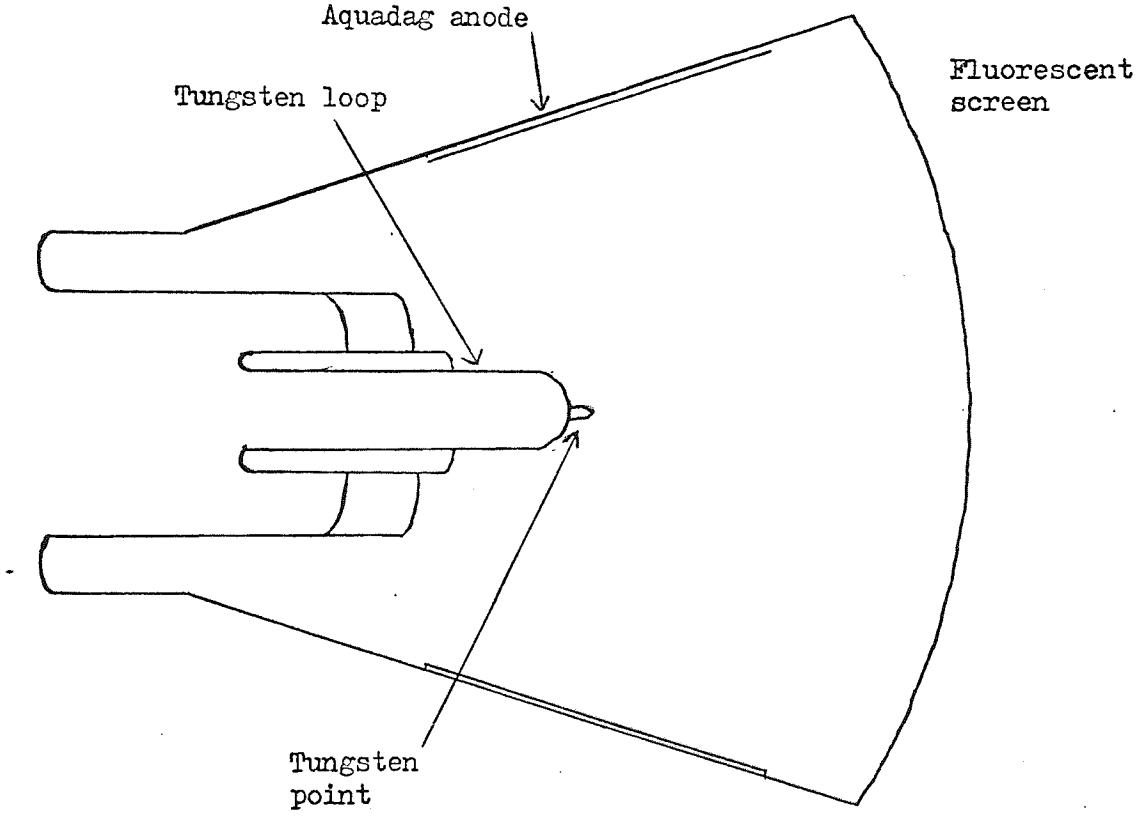

Tungsten point

resolving power of 20 Å and can be used over a range of operating temperatures and it is this that makes it such a useful tool for surface studies.

The field emission microscope was used by Gomer, Wortman and Lundy (7) to investigate the interaction of hydrogen and oxygen with tungsten. The tip was cooled to a temperature where diffusion would not occur and one side only was then covered in gas. This was done by putting a source of the gas into the vessel and heating it electrically. Only one side of the tip faced the gas supply and any molecules missing the tip were condensed on the cold sides of the vessel. The temperature of the tip was allowed to rise until diffusion began to be seen and the boundary between the covered and clean sides of the tip began to move across the tip as the molecules diffused. The movement of the gas from physisorbed sites to chemisorbed sites on the clean surface was clearly observed. For oxygen migration started at 27 K whereas for hydrogen it was less than 20 K.

This shows what a very useful technique field emission is but care must be taken that the very high electric field near the surface does not have any influence on the adsorbed gas on the surface.

1.2.4 Field Ion Microscope

Information about the field ion and field emission microscope was first published by Muller (8). The field ion microscope is similar to the field emission microscope with the polarity of the applied potential reversed. The advantage of the field ion microscope over the field emission microscope is that it has a higher

resolving power and individual atoms can be seen. The disadvantage is that the very high fields at the tip can make all but the most strongly held atoms desorb and this means only a limited range of metals and adsorbants can be investigated.

In the field ion microscope a gas such as hydrogen or helium which has a low molecular weight is let into the system at a pressure of 10^{-3} torr. In the very high field region near the tip the gas is ionized by quantum mechanical tunnelling and the positive ions produced are accelerated to the fluorescent screen where they produce a greatly magnified image of the surface. The high resolution means that for surfaces where the atoms are far apart then the bright spots seen are pictures of individual atoms.

Anderson (9) has used the field ion microscope to investigate oxygen adsorption on a tungsten system. He saw that the oxygen which had been adsorbed was rapidly desorbed on heating, leaving a tungsten surface which was heavily eroded with many atoms having been moved.

1.2.5 Low Energy Electron Diffraction (LEED)

Davidson and Germer (10) in their classic experiment showed that low energy electrons were diffracted by the surface. These electrons have low energy and so only the surface layers are effected. The positions of the reflected electrons are measured and the wavelength of these electrons is given by

$$\lambda = (150.4/V)^{\frac{1}{2}} \qquad \ldots\ (1\text{-}4)$$

where λ is the wavelength in angstroms and V is the accelerating potential. In this case the atomic spacing is given by Bragg's Law:

$$n\lambda = 2d \sin\theta \qquad \ldots\ (1\text{-}5)$$

here θ is the diffraction angle. The low energy electrons are diffracted onto a fluorescent screen. By bombarding a clean single crystal surface the spots obtained should be clear and well defined. Although LEED is a powerful tool it has several drawbacks. Detailed interpretation of LEED results is difficult at present although much effort is currently being expended on clarifying the theoretical background (11). Improved results have been obtained using more complicated theories. The second drawback is that the electrons may cause a change in the surface structure.

The gas used should be of a low molecular weight compared to the metal and in this case the gas atoms should have no effect on the pattern and any change in the LEED pattern obtained therefore must be due to the adsorption of the gas on the metal.

LEED studies of the adsorption of xenon on graphite have been performed by Morrison and Lander (12). The xenon is adsorbed at 90 K and at low surface coverages a liquid-like phase is formed. At higher temperatures the diffraction features become blurred but an interesting point is that each xenon atom occupies a surface area of 15-17A^2 which leads to the suggestion that the atom is laterally compressed by the forces of the surface.

1.2.6 Auger Electron Spectroscopy

The same system can be used for Auger studies as for LEED studies. Auger is concerned with the emission of secondary electrons from inner shells. The primary beam used in the LEED experiment is used with an energy of 3-3.5 times the potential needed to ionize the electrons in the inner shell. The incident beam will remove

the secondary electrons from the inner shell as shown in Fig. 2. The gap in the electron levels in the inner shell will be filled by an electron from a higher level dropping into the gap and releasing an amount of energy. The energy will be emitted as a photon or captured by another electron and be used by this electron to escape from the surface. This is known as the Auger effect and it is this electron that we are concerned with. Although the effect has been known since 1925 it is only recently that it has been possible to trace these Auger electrons from the background of secondary electrons. The problem was overcome by Harris in 1967 (13).

By measuring the energies of the emitted electrons an Auger spectrum can be obtained. Auger electron spectra have been obtained for most elements up to gold with the exception of hydrogen, helium and singly ionized helium which lack the necessary electrons.

Auger electron spectroscopy can be used to observe the surface of metals and is particularly useful in identifying contaminants on the surface of the metal. It can also be used in conjunction with LEED since Auger is applicable to not only single crystal but polycrystalline and amorphous materials.

Haas, Grant and Dooley (14) have used the Auger electron spectrometer to investigate the adsorption of oxygen and carbon monoxide on various transition elements such as tungsten, molybdenum, niobium and tantalum. The spectra obtained show a shift in the energy of the Auger electrons when the oxygen is adsorbed on the surface and the spectra obtained from the adsorption of carbon monoxide on tantalum and niobium show that the carbon monoxide is

FIG. 2 Auger Energy Level Diagram.

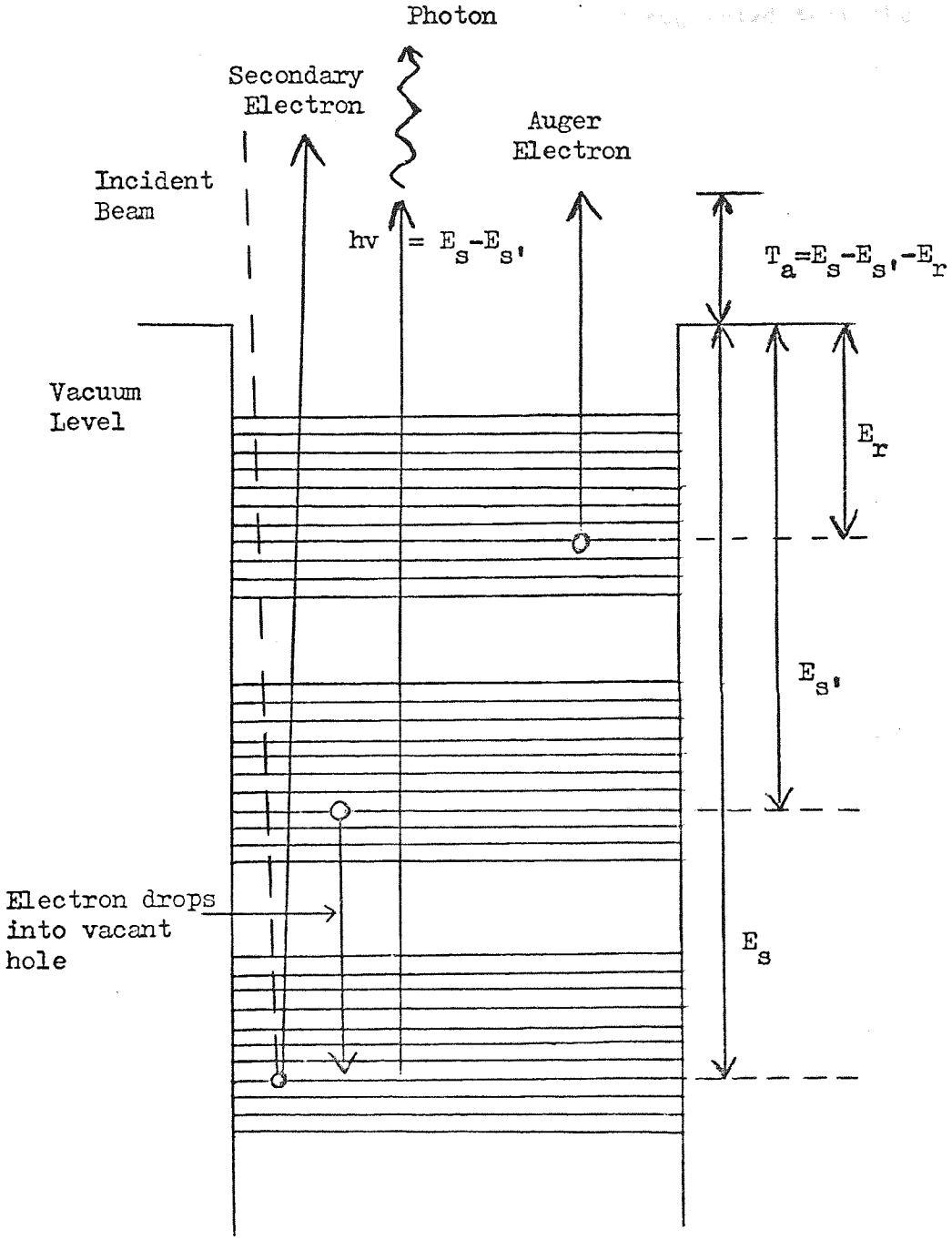

decomposed to carbon and oxygen on the surface even at room temperature. This was unexpected and it was suggested that the shift is due to a shift in the electron density from the surface atoms to the carbon monoxide.

1.2.7 Photoelectron Spectroscopy

When light of short wavelength, usually ultra violet with an energy of 21 eV from helium, falls on a molecule it can eject an electron from the outer molecular orbitals. The energy of the electrons emitted from a molecule is recorded and the resulting spectrum is analysed and this gives a measure of the energy levels in the molecule. The energy of the light is used in overcoming the binding energy of the electron to the molecule and any extra energy goes into giving kinetic energy to the electron. The energy which goes into ejecting the electron from the molecule is the ionization energy of the molecule and so the photoelectron spectra can be used to give a measure of the ionization potentials. The photoelectron spectrum is a record of the number of electrons detected at each value of the kinetic energy. The light is monochromatic and so each photon of light energy supplies the same amount of energy.

Using two approximations

(1) Each band in the spectrum corresponds to ionization from a single molecular orbital,

(2) Each occupied molecular orbital of binding less than hf gives rise to a single band in the spectrum,

the relationship between the photoelectron spectrum and the molecular electronic structure is simple. The photoelectron spectrum is a

FIG. 3 Idealized Photoionization Process and Photoelectron Spectrum of an atom.

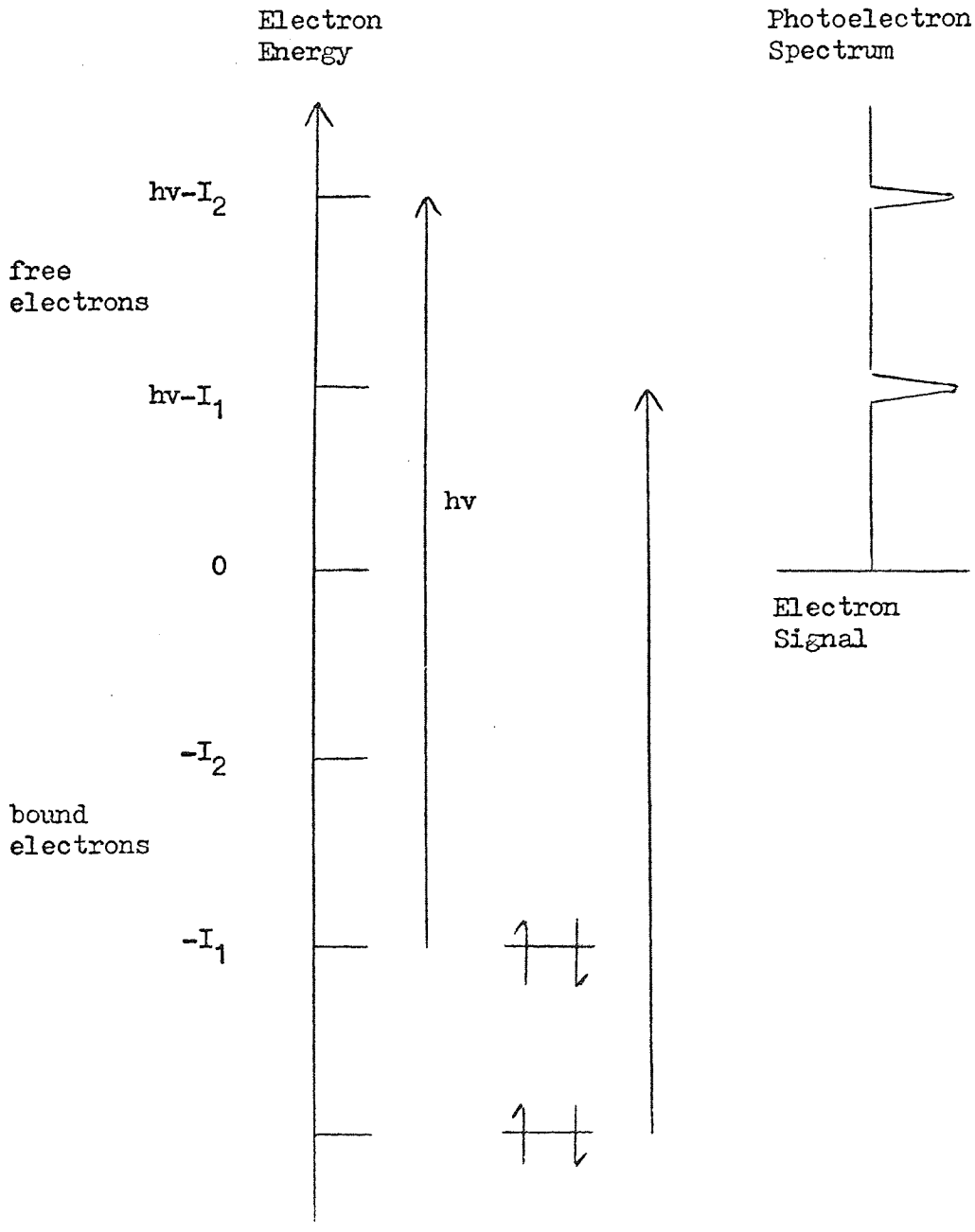

reflection of the molecular orbital diagram similar to that shown in Fig. 3. However these rules are simplified and deviations do occur. A typical photoelectron spectrum is shown in Fig. 4 for mercury.

Photoelectron spectroscopy can be used on all systems but it is especially valuable in the case of adsorption on various surfaces. Here the change in the molecular orbitals of both the surface and the adsorbing gas can be seen when adsorption takes place.

This technique is a relatively new technique and offers great potential for furthering our knowledge of the processes that occur when a gas is adsorbed on a metal surface. Being a new technique comparatively little work has been done in this field although a start has been made studying adsorbed layers by ultraviolet photoelectron spectroscopy by Bordass and Linnett (15). The technique was first investigated in the early 1960's by Turner (16) who was working in London.

This technique has been used to investigate the perfluoro effect by Brundle (17,18). This is a substitution effect where hydrogen is replaced by fluorine and when this happens it is found that the σ electron ionization potentials are shifted to much higher energies than the π electron ionization.

1.2.8 Electron Stimulated Desorption

This method of investigating the surface of a metal involves bombarding the surface with a beam of low energy electrons of energy from 10 eV to 600 eV. In this case the adsorbed molecules desorb as positive ions because of the interaction with the low energy electrons. The ions which have been desorbed are analysed by a

FIG. 4 Photoelectron Spectrum of Mercury Excited By He 1(584 Å) Radiation

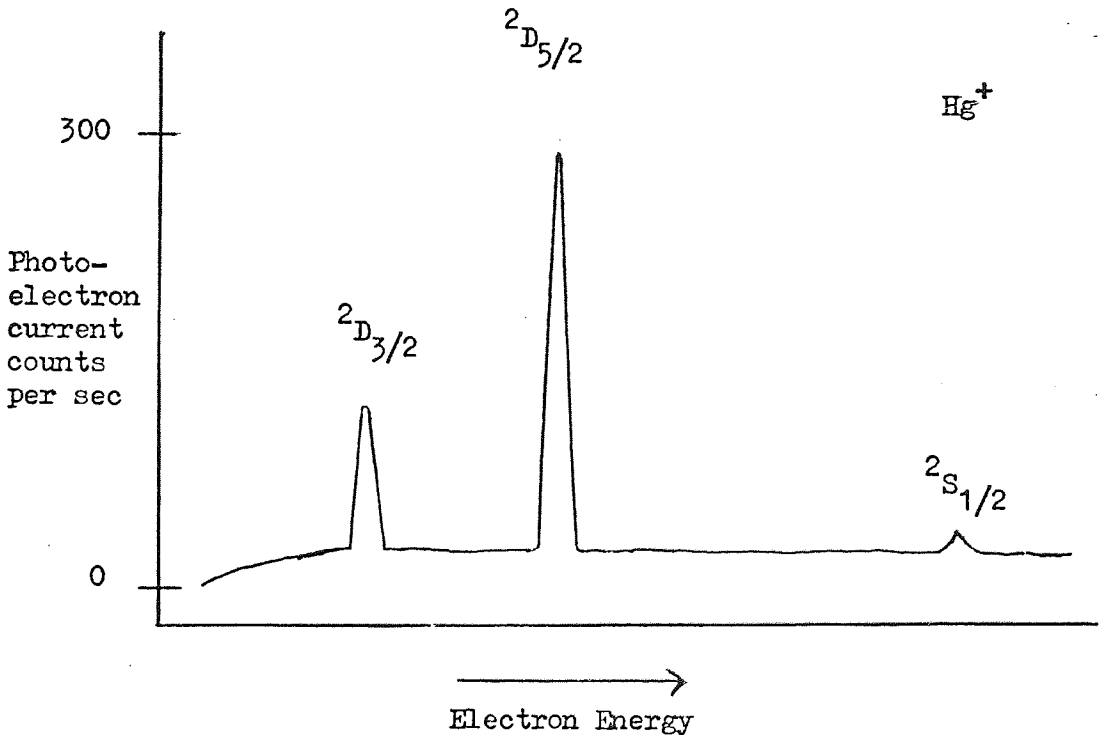

mass spectrometer and identified. The use of an electron multiplier and careful design of the mass spectrometer means that electron beam currents as low as 2×10^{-7} amps can be obtained and this reduces any effect that the electron beam has on the surface and the adsorbed species.

Much of the initial work in this field on the desorption of neutrals and ions by electron impact was done by Redhead (19) and Menzel and Comer (20). A more sophisticated system was designed by Nishijima and Propst (21) and this system was used to investigate the action of O_2, CO, CO_2, N_2 and H_2 on a polycrystalline tungsten surface (22).

A combination of the electron stimulated desorption technique and flash desorption experiment was used by Goymour and King (23) to investigate the action of CO on tungsten and shows the value of combining these surface techniques. Further work by King, Madey and Yates (24) combined electron stimulated desorption studies and the flash desorption technique. A number of oxide and oxygen atom states were found by the thermal desorption technique for the adsorption and desorption of oxygen on polycrystalline tungsten. Two states of adsorbed oxygen were found by electron stimulated desorption and attempts were made to correlate this information with the thermal desorption information and obtain a clearer picture of the mechanism of adsorption.

1.2.9 Mass Spectrometry

The mass spectrometer will measure the change in the gas phase due to adsorption and desorption from the filament. If the mass spectrometer used is also a partial pressure analyser then the

kinetics of the adsorption and desorption can also be worked out. Sensitive mass spectrometers are capable of measuring the very low pressures involved in the desorption experiments but this will be at the extremes of the sensitivity of many instruments.

The identification of the desorbed species is a very important part of the analysis. The desorbed species can throw light on the nature of the adsorbed species although other information and other experiments have to be carried out before the adsorbed species can be positively identified. If ethane peak 30 was found in the mass spectrum after adsorption of methane it would suggest that the adsorbed species could be CH_3, however other details would have to be known before the species could be conclusively identified. The mass spectrometer information means that a complete picture of the system can be made. If a mechanism for adsorption is postulated the mass spectrometer evidence can be used to confirm its validity.

Ageev (25) has used a time of flight mass spectrometer as a partial pressure measuring device for a flash filament experiment. The desorbed species are identified and the kinetics of the reaction are calculated from the pressure peaks. Gasser (1) has shown how mass spectrometers are useful in identifying the catalytic action of metal surfaces on gas reactions. The decomposition of organic gases has been followed by Robertson and Morgan (26). In ultra high vacuum the decomposition of ethyne and ethene on niobium surfaces was investigated.

1.3 FLASH DESORPTION

1.3.1 Prologue

The kinetic parameters for surface processes can be related to

each other using various equations. These equations must be related to the parameters obtained from the vacuum system so that the unknown kinetic parameters can be found. Since vacuum systems are not mathematically minded it is found that the equations do not always hold in all cases and certain assumptions have to be made and justified. When a vacuum system is designed it is necessary to think carefully about what is going to be measured and how these parameters are to be related to the unknown ones.

The study of gas-metal surfaces has been of interest to the chemist and physicist for many years. In 1912 Langmuir (27) did work on gas reactions with metals and Urbach (28) in 1930 used a continuous heating technique to study rate measurements. However it was not until recently that it was possible to obtain a clean metal surface in ultra high vacuum conditions. Since this time a lot of work has been done on gas metal surface reactions, many experiments using the flash filament method.

It is this technique, the flash filament technique, that is to be the subject of this thesis. This technique needs to be used with one of the other ultra high vacuum techniques if the maximum amount of information is to be obtained. A mass spectrometer is used to give further information. The theoretical background behind the analysis of the results will be given later but this theoretical work has been developed over many years by a succession of workers.

1.3.2 The First Work on Flash Desorption

The credit for the development of the flash filament technique should go to Becker and Hartman (29,30). In 1953 they published a

paper in which they used the flash filament technique combined with a field emission microscope to study the adsorption of nitrogen on a tungsten surface (31). This was one of the first vacuum systems to use the Bayard-Alpert design of ionization gauge and the system was capable of achieving pressures of 10^{-9} to 10^{-10} torr.

Using the kinetic theory they obtained the expression

$$\Delta M = KV \Delta p = AM_1 \theta \qquad \ldots\ (1\text{-}6)$$

where A is the area of the filament, M is the number of molecules per cm^2, K is the number of molecules per litre for p = 1 torr, V is the volume of the system and Δp is the pressure rise. $\theta = \frac{M}{M_1}$, so that when $\theta = 1$ one monolayer has been adsorbed and in this case $M_1 = 1.25 \times 10^{14}$ molecules per cm^2. Since A, K, V and M_1 are known and Δp is measured then θ the surface coverage in monolayers can be calculated. By varying the adsorption time t and calculating θ, a graph of the change in surface coverage with time could be obtained.

By using a mass balance equation for the system we get

$$M_1 \, d\theta/dt = V p S - E \qquad \ldots\ (1\text{-}7)$$

where $M_1 d\theta/dt$ is the rate of increase of the desorbed molecules, E is the rate at which molecules are lost by evaporation and V is the rate at which the molecules strike the surface when p = 1 torr. Since S is the sticking probability, V p represents the rate of collision at pressure p. It is shown for $\theta < 1.8$, E is negligible compared to V p s and so

$$S = \frac{M_1}{Vp} \frac{d\theta}{dt} \cdot \qquad \ldots\ (1\text{-}8)$$

It is found that at 300 K, the sticking probability remains constant at 0.5 for $\theta = 0$ to 1 but after this the sticking probability drops rapidly to 10^{-4} at $\theta = 2$. The results in the form of the pressure and sticking probability against time graphs are shown in Fig. 5 for nitrogen adsorbed on a tungsten surface. The results show that the analysis gives results of the expected order of magnitude.

A pumped system with a constant leak rate is used and the pumping speed is calculated and found to be constant but no term is used in the equation (1-7) to account for any molecules lost by pumping. This method of analysis did not show if there was more than one adsorbed state since only a small pressure rise was seen over the whole flash. It is assumed that the total rise in pressure is due to nitrogen atoms being desorbed. The surface was flashed at 2300 K to clean it and the nitrogen was allowed to adsorb. After this the filament was flashed at 2300 K and the increase in pressure monitored.

After a decade of work in this field Ehrlich (32) produced a lengthy and valuable review in which he gave a detailed account of the theory. A more detailed version of Ehrlich's paper is also available (33). He used a closed system with no pumping during the experiment but used a term NS_E in his equations to take account of the molecules lost by adsorption on the walls, pumping by the gauge and any escaping to the traps.

Applying the conservation of mass to the system we get

$$V\, dN/dt = F_F - NS_F + F_A - NS_E \qquad \ldots\ (1\text{-}9)$$

FIG. 5 Sticking Probability and Pressure Against Time Graphs Obtained By Becker and Hartman for Nitrogen on Tungsten.

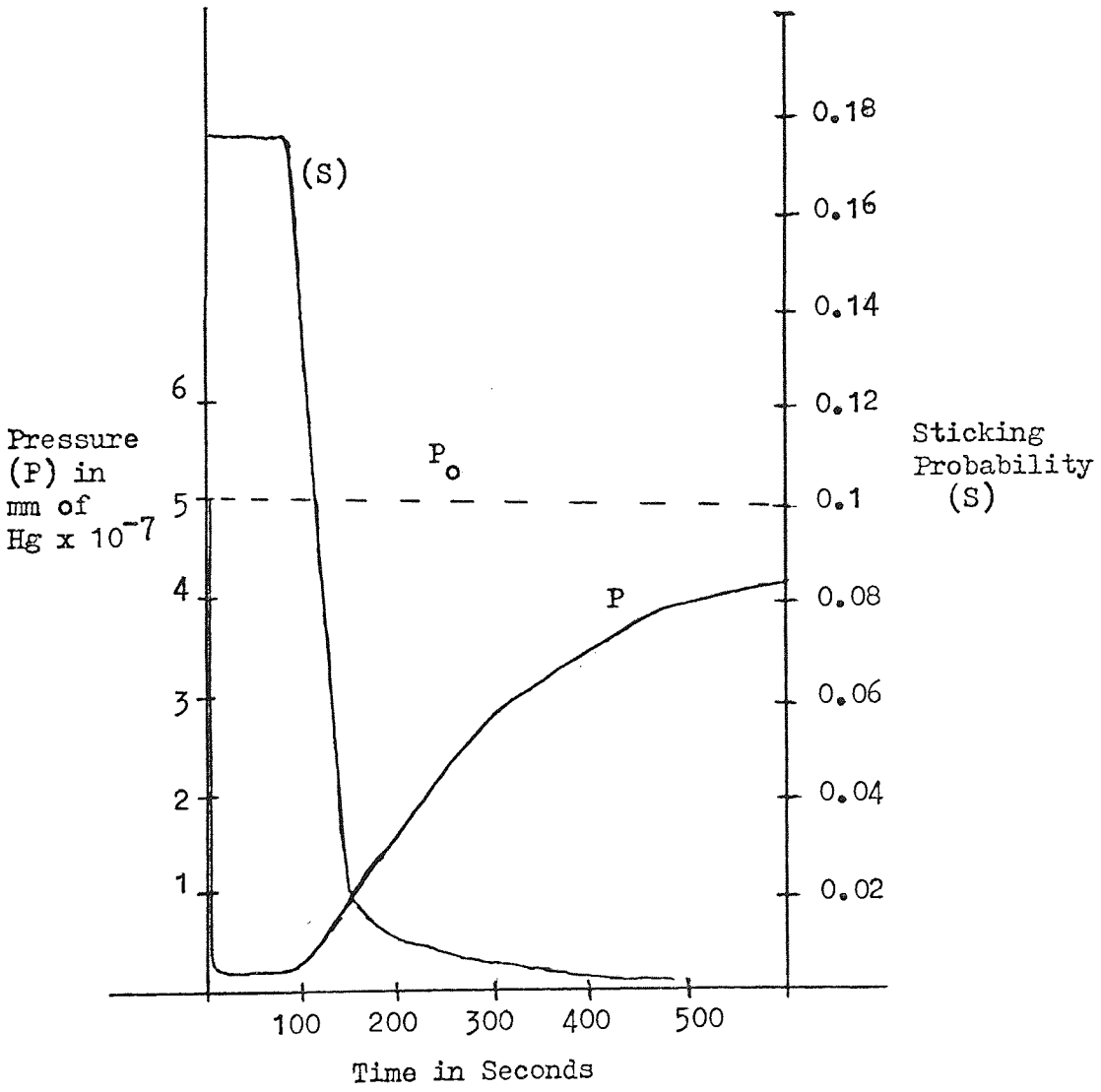

where N is the gas density at any instant, V is the volume of the system, F_F is the rate of desorption from the filament, F_A is the rate of supply of gas from any leaks and NS_F is the rate of depletion through re-adsorption on the sample. F_A and S_E are maintained constant and independent of time. Now if the rate of re-adsorption and the leak rate from a reservoir are negligible during the flash then equation (1-9) becomes

$$V\, dN/dt = F_F - NS_E \qquad \ldots\ (1\text{-}10)$$

and ΔN can be shown to be equal to

$$\exp\left[-S_E t/V\right] \int_o^t (F_F/V) \exp\left[-S_E t/V\right] dt \qquad \ldots\ (1\text{-}11)$$

Prior to the experiment the temperature rise with time was investigated and found to be linear of the form

$$1/T = a_o + b_o\, t \qquad \ldots\ (1\text{-}12)$$

where a_o and b_o are constants calculated by substituting for T at various times. It was assumed that this equation for the temperature rise was obeyed at all times during the flash.

Using the Arrhenius equation of the form

$$F_F/A = -dn/dt = n^x\, v_x \exp\left[-\Delta H/RT\right] \qquad \ldots\ (1\text{-}13)$$

where v_x is the pre exponential function, n the surface coverage, ΔH the activation energy and x the order of reaction 1 or 2. Combining (1-12) and (1-13) followed by integration, when x = 1, leads to

$$\Delta N/\Delta N_x = 1 - \exp\left[x\right] \qquad \ldots\ (1\text{-}14)$$

FIG. 6 Ehrlich's Graphs Used to Calculate the Order of Reaction.

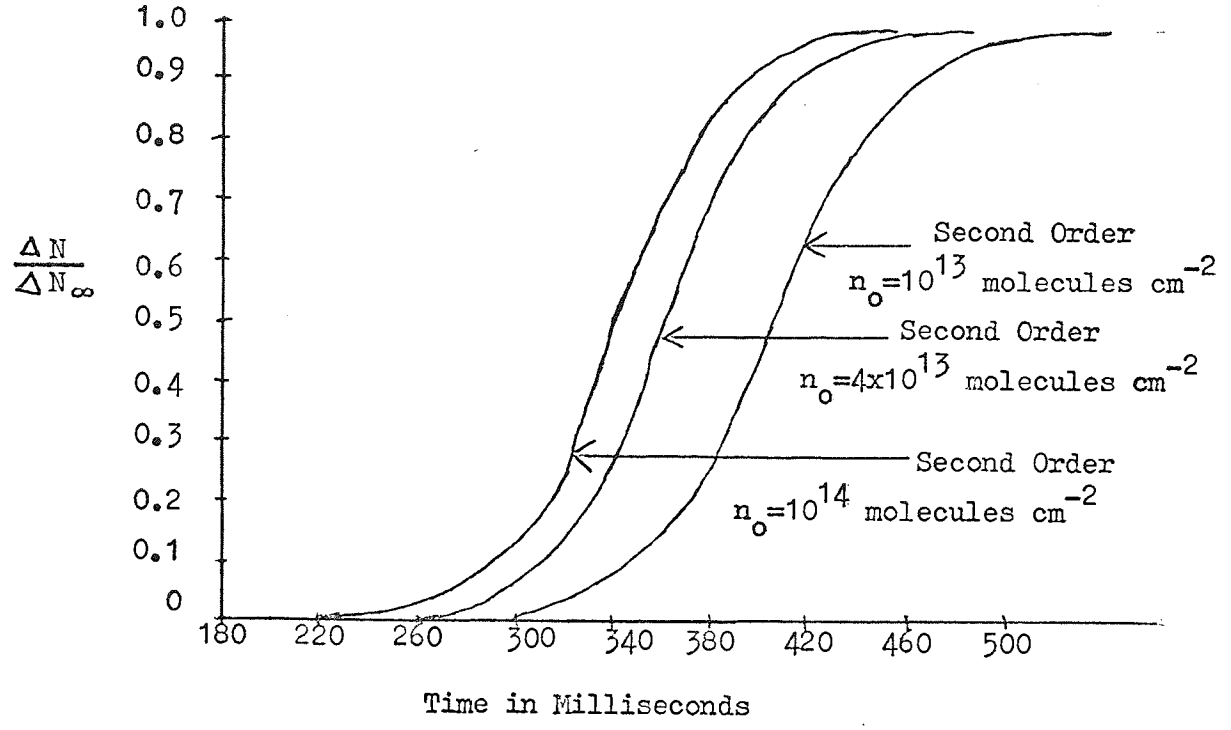

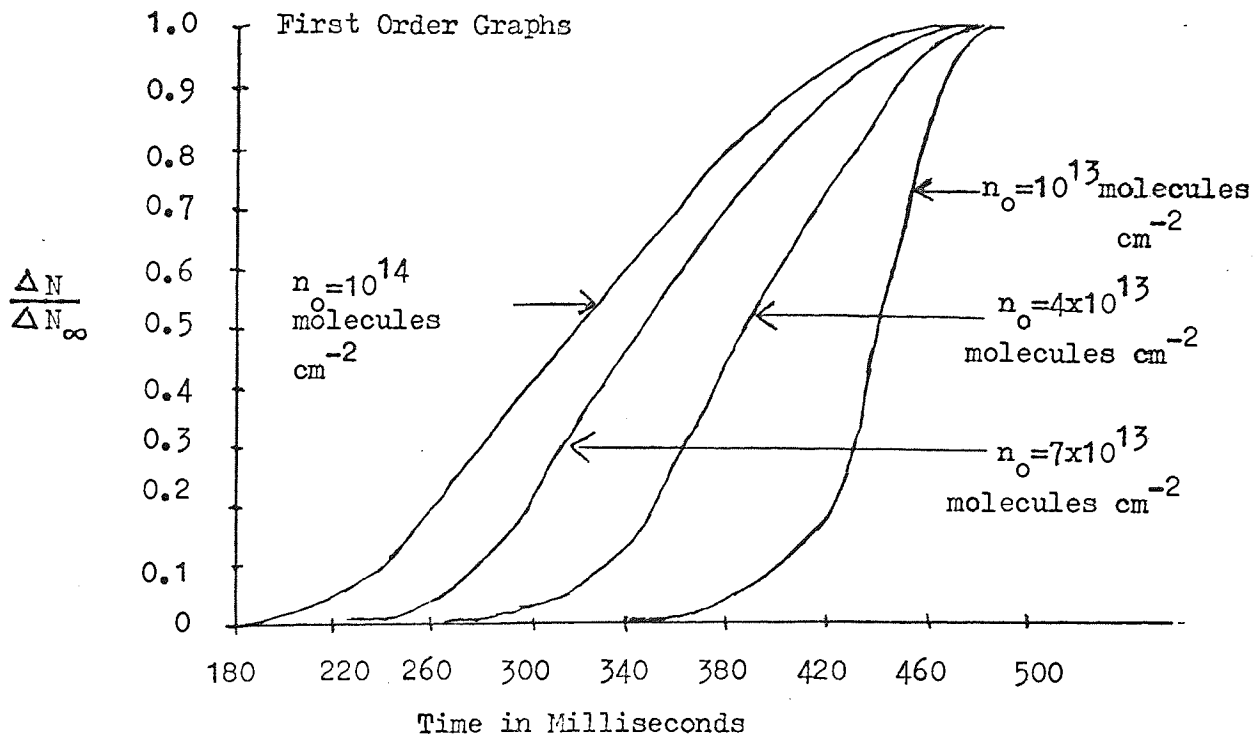

and when x = 2

$$\Delta N / \Delta N_x = n_o X / [1 + n_o X] \quad \ldots\ldots (1\text{-}15)$$

where

$$X = \left[Rv_x / -b_o \Delta H \right] \exp \left[- \Delta Ha_o / R \right] \exp \left(\left[- \Delta Hb_o t / R \right] - 1 \right) \quad \ldots\ldots (1\text{-}16)$$

x is determined by comparing the evolution curves shown in Fig. 6. The shape of the curves indicate whether x is 1 or 2.

A similar approach was used by Smith and Aranoff (34) who proposed a theory of desorption for gases using a linearly rising temperature and used this for both first and second order kinetics when there was a leak into the system and also for a closed system. The activation energy and order of reaction could be calculated but the method involved making some approximations and also some trial and error curve fitting. This paper developed the theory and was not applied to a gas-metal system and it is not possible to criticise the results obtained.

Redhead (35) investigated methods of analysing flash desorption data. He used two linear variations of temperature with time, one similar to Ehrlich's and the second one is a reciprocal variation of the form

$$1/T = (1/T_o) - \alpha t \quad \ldots\ldots (1\text{-}17)$$

He applied the conservation of mass to the SYSTEM

$$AN(t) + L = KS_p + KV \, dp/dt \quad \ldots\ldots (1\text{-}18)$$

where A is the area of the sample, N is the desorption rate, V is the volume of the system, L is the leak rate and S is the pumping speed.

FIG. 7 Effect of Increasing the Pumping Speed as Shown By Ehrlich.

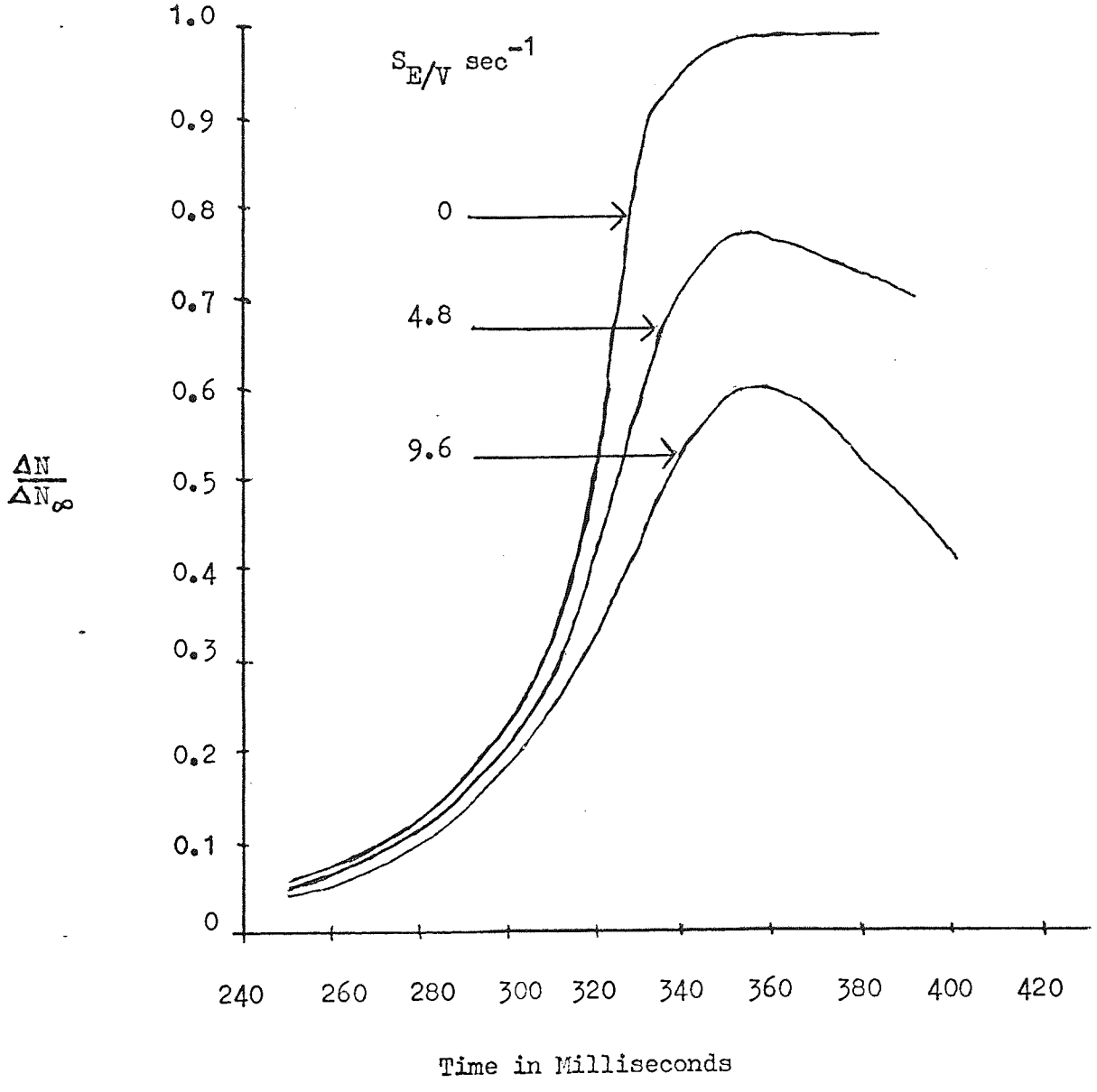

$K = 3.27 \times 10^{19}$ molecules per litre at p = 1 torr and T = 295 K.

Redhead assumed that there is no re-adsorption on the sample during the flash and that adsorption on the walls of the system is negligible.

Then at equilibrium

$$L = K S P_e \qquad \ldots\ (1\text{-}19)$$

Combining (1-18) and (1-19) and putting $p^* = p - p_e$

$$dp^*/dt + p^*/\gamma = a N(t) \qquad \ldots\ (1\text{-}20)$$

where $a = A/KV$ and $\gamma = V/S$

Now the rate of desorption from unit surface area is

$$N(t) = -d\sigma/dt = v_n \sigma^n \exp(-E/RT) \qquad \ldots\ (1\text{-}21)$$

where n is the order of the desorption reaction, σ is the surface coverage, v_n is the rate constant and E is the activation energy of desorption. We assume a linear variation of temperature $T = T_o + \beta t$ and assume that E is independent of the surface coverage. Now (1-20) is solved to find the temperature at which the desorption rate is a maximum. For n = 1

$$E/RT_p^2 = (v_1/\beta) \exp(-E/RT_p) \qquad \ldots\ (1\text{-}22)$$

for n = 2

$$E/RTp^2 = (\sigma_o v_2/\beta) \exp(-E/RTp) \qquad \ldots\ (1\text{-}23)$$

where σ_o is the initial surface coverage and σ_p is the surface coverage at $T = T_p$. It can be seen that T_p is independent of coverage for the first order reaction but varies with the surface coverage for a second order reaction. For the first order reaction

if the value of v_1 is assumed to be 10^{13} sec^{-1} then the activation energy can be calculated. The activation energy can be found without assuming v_1 by varying β and plotting log T_p against log β since

$$E/RT_p + 2 = d(\log \beta)/d(\log T_p) \quad \ldots\ (1\text{-}24).$$

For the second order case the surface coverage σ_o has to be found by calculating the area under the curve of the desorption rate as a function of time and by plotting $\log(\sigma_o T_p^2)$ against $1/T_p$ a straight line of slope E/R is obtained and then v_2 is found by substituting in (1-23).

By varying the temperature in a reciprocal fashion the relation between E and T_p is

$$n = 1,\ E/R = (v_1/\alpha) \exp(-E/RT_p) \quad \ldots\ (1\text{-}25)$$

$$n = 2.\ E/R = (v_2\sigma_o/\alpha) \exp(-E/RT_p) \quad \ldots\ (1\text{-}26).$$

By substituting into the above equations the known parameters obtained from the experimental system the other parameters can be calculated. Redhead discusses how the order of reaction is determined from the curves of $\Delta N/\Delta N_\alpha$ against time. From the shape of the curves for the desorption rate against sample temperature the constancy of the activation energy may be investigated. This method can only be used however for the case where the peaks are clearly resolved from each other. The equation of the desorption rate curve is found to be

$$\ln(N_p/N) = (E/R)(1/T - 1/T_p) + (T/T_p)^2 \exp(-E/R[1/T - 1/T_p]) - 1$$

$$\ldots\ (1\text{-}27)$$

which shows the curve to be asymmetric about the maximum at temperature T_p. Redhead goes on to take into account the effect of a finite

FIG. 8 Redhead's Results for the Desorption of Hydrogen From Tungsten After 14 Minutes Adsorption Time.

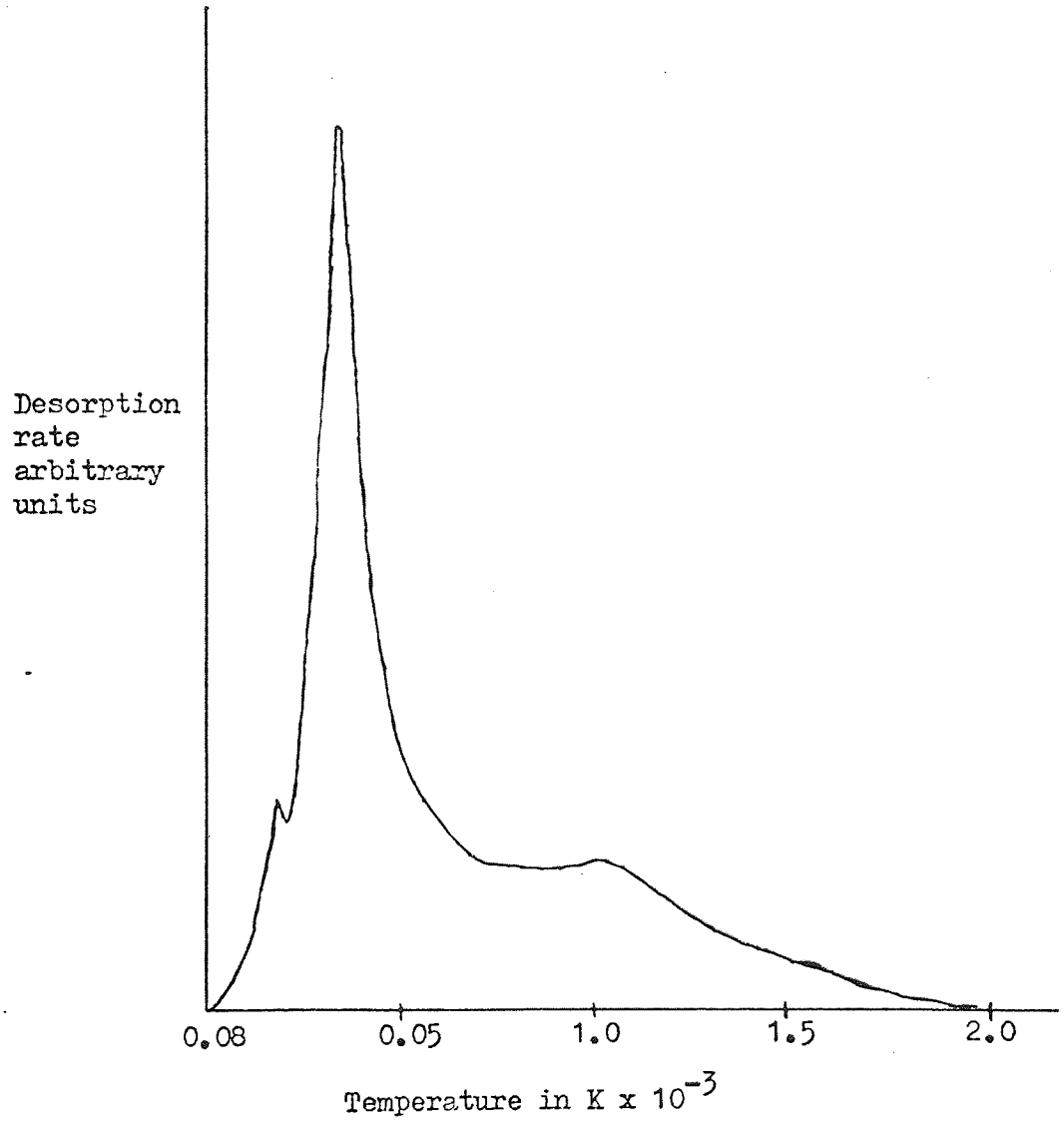

pumping speed from which we obtain equations which are more complicated but which can be used to calculate the experimental parameters. Fig. 8 shows the results obtained by Redhead, the experimental curves and Fig. 9 the graphs from which the order of reaction was found.

Work similar to Redhead's was performed by Carter (36) and in his paper he considered three types of surface. One which has binding states of constant energy, one which has discrete energy heterogeneous sites and a third which has a continuum of heterogeneous sites. In the papers considered so far all the adsorption has been on sites which have a single activation energy but Carter goes on to investigate the problem of discrete energy heterogeneous sites where the equations become quite complex and for the case of a continuum of sites, he states that the best and probably only method of deducing site concentrations is a numerical summing technique.

1.3.3 Theoretical Papers During the Last Decade

Many papers have been published by Ageev and Ionov in the last ten years. The first of the papers gave a short account of the theoretical approach they used in their analysis. The gas balance equation they used is (37)

$$-dN/dt = (1/AkT_o) \left[VdP/dt + S \Delta p \right] \qquad \ldots\ (1\text{-}28)$$

where dN/dt is the adsorption rate, T_o is the temperature at the beginning of the flash, V is the volume, A is the surface area and k is Boltzmann's constant.

An Arrhenius equation of the form

$$-dN/dt = N^v C e^{-E/kT} - S \mu p \qquad \ldots\ (1\text{-}29)$$

where E is the activation energy for desorption, v is the order of

FIG. 9 Redhead's Theoretical Desorption Rate Curves for First and Second Order Reactions.

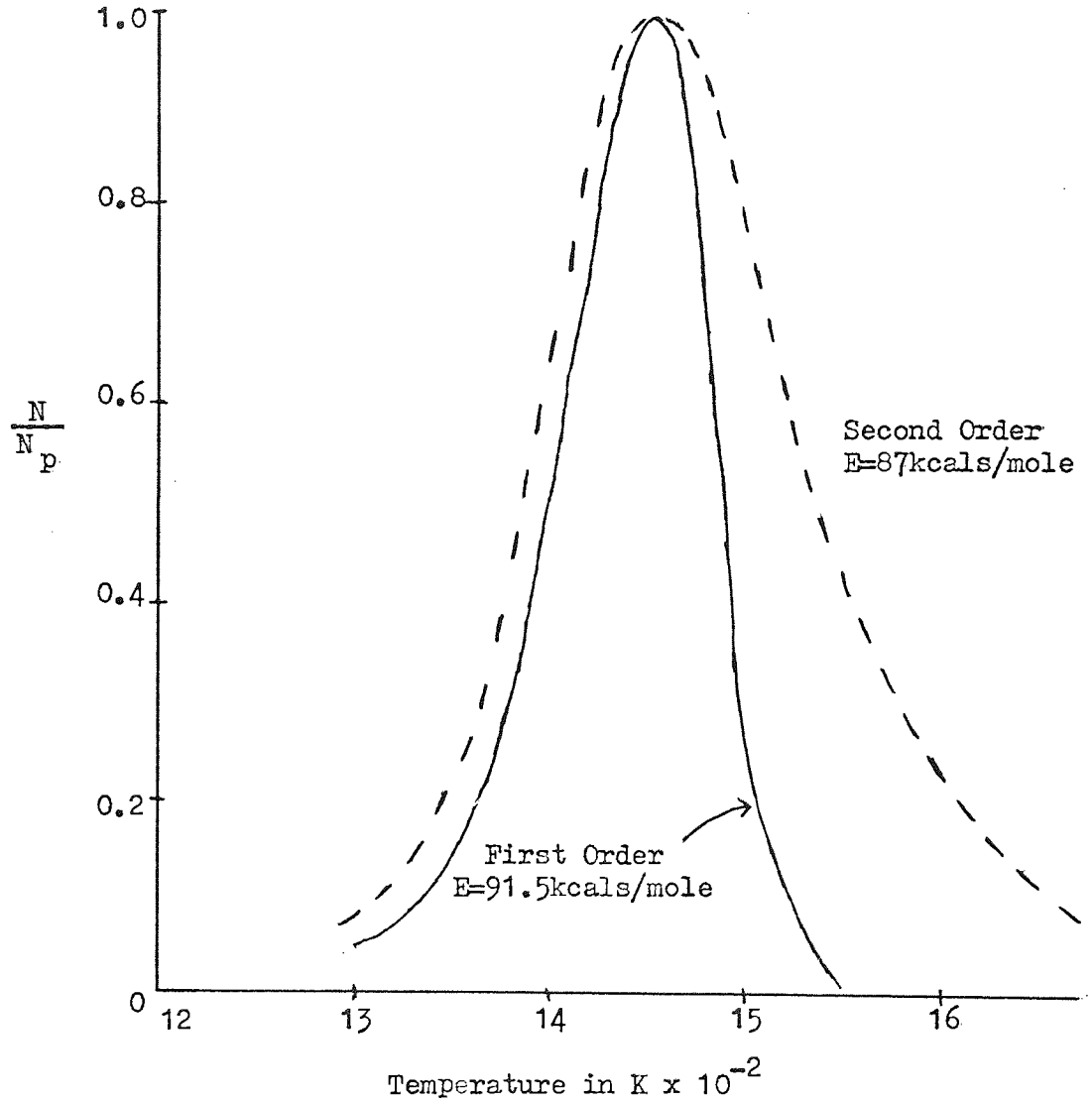

reaction, C is the rate constant and $\hat{s}$ is the adhesion coefficient. μ_p is the number of molecules colliding with unit surface area in unit time. When the desorption rate is high (1-29) becomes

$$-dN/dt = N^v \, C \, e^{-E/RT} \qquad \ldots\ (1\text{-}30)$$

The number of molecules Ng desorbed from 1 cm^2 at time t is given by

$$Ng(t) = N_1 - N_{(t)} = (1/AkT_o) \left[V \, \Delta p + S \int_o^t \Delta p dt \right] \qquad \ldots\ (1\text{-}31)$$

and here the integral is solved graphically. The value of S is determined from equation (1-28) when dN/dt = 0, knowing the desorption curve and equation (1-31) then the degree of coverage θ at the beginning of the flash can be found. The number of molecules dN_a adsorbed in time dt_a on the adsorbent surface is given by

$$dN_a = \hat{s} \mu p_o \, dt_a \qquad \ldots\ (1\text{-}32)$$

and hence the value of the adhesion coefficient or sticking probability can be found.

Fig. 10 shows the desorption curves obtained by Ageev and Ionov for the desorption of CO off a tungsten surface. From their results three desorption states are seen, α, β_2 and β_3. The β_3 peak was found to be 1st order and the β_2 peak second order. The values of the activation energy determined were 2.4 for the β_3 peak and 1.6 eV for the β_2 peak. Fig. 11 shows the relation between the number of adsorbed molecules Ng and the adsorption time t. Ageev and Ionov obtained results which were of the expected order of magnitude and the analysis shows the technique to be a very valuable technique.

Hansen (38) at the Iowa State University has published many papers on flash desorption and he has taken into account the possible

FIG. 10 Desorption Curve for Carbon Monoxide from Tungsten Obtained by Ageev.

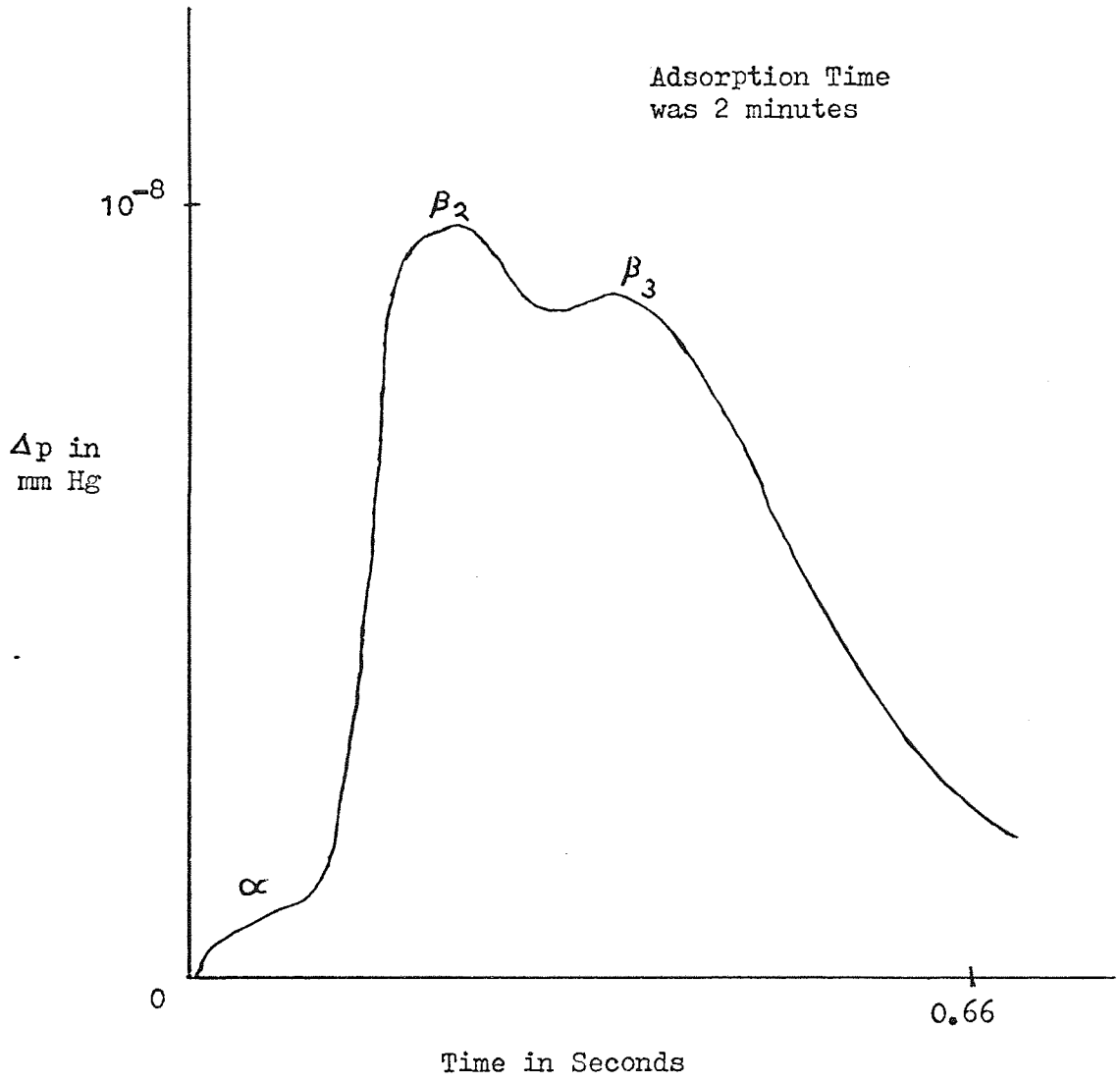

FIG. 11 Relation Between Adsorption Time and 1) Number of Adsorbed Molecules (N) and 2) The Adhesion Coefficient (S) for the Adsorption of CO on Tungsten.

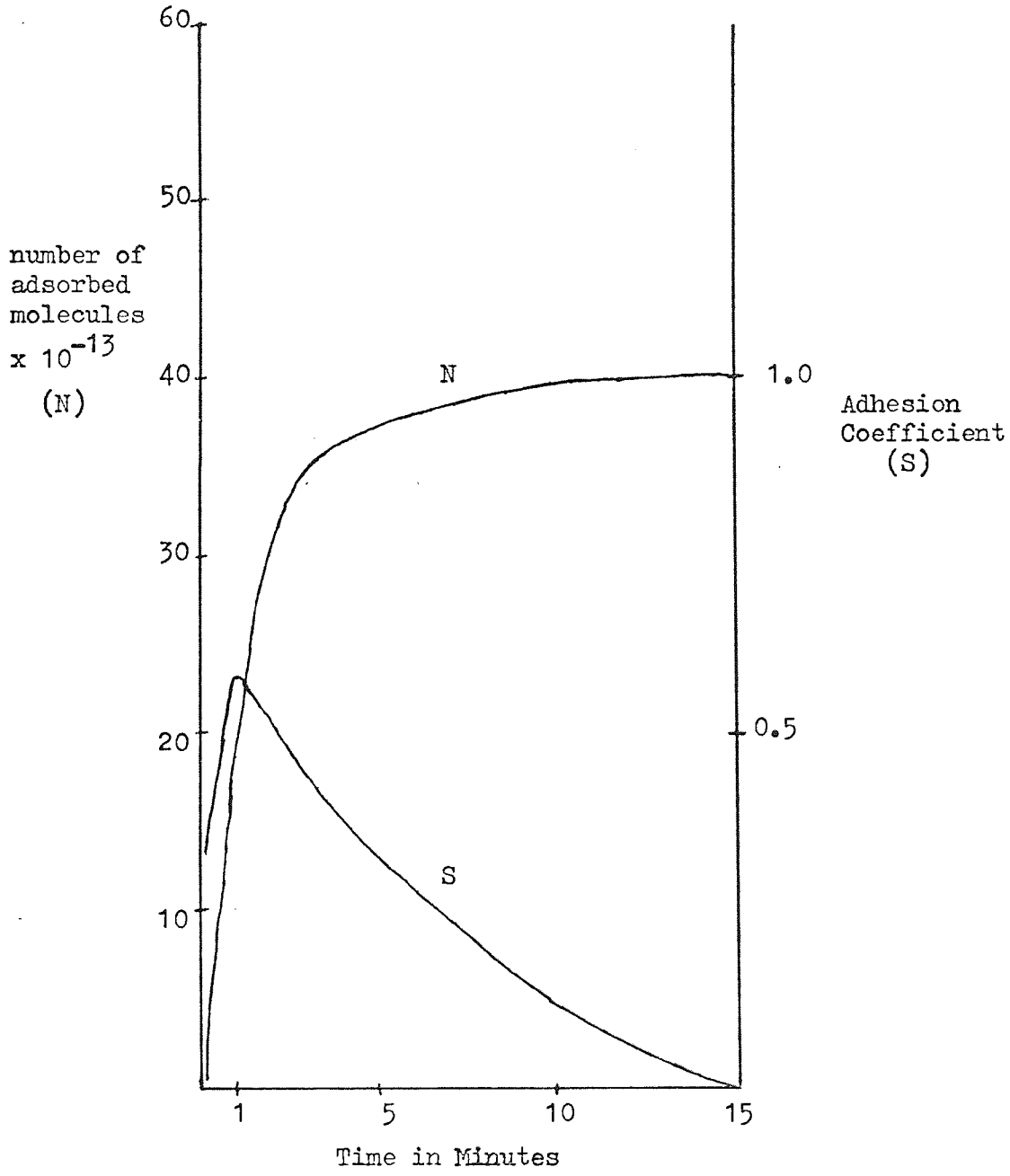

variation of the activation energy with surface coverage. The conservation of mass was applied to the vacuum system

$$dN/dt = -A\ dn/dt - SN/V + L \qquad \ldots\ (1\text{-}33)$$

Assuming the number of molecules is proportional to the pressure this becomes

$$-dn/dt = \left[V/AkT_o\right]\left[d\Delta P/dt + S\Delta P/V\right] \qquad \ldots\ (1\text{-}34)$$

Now assuming the activation energy is independent of surface coverage and using the Arrhenius equation

$$-dn/dt = v_k n^k \exp\left[-\Delta H/RT\right] \qquad \ldots\ (1\text{-}35)$$

Using the linear variation of temperature $1/T = a + bt$ we obtain for first order reactions when $k = 1$

$$\ln(\ln n_o/n) = -\Delta H/RT + \ln\left[Rv_1/\Delta H(-d(1/T)/dt)\right] \qquad \ldots\ (1\text{-}36)$$

for second order reactions when $k = 2$

$$\ln(n_o - n/nn_o) = -\Delta H/RT + \ln\left[Rv_2/\Delta H\ (-d(1/T)/dt)\right] \qquad \ldots\ (1\text{-}37)$$

If either equation gives a straight line this tells you the order of reaction and the gradient of this line is $-\Delta H/R$.

If the activation energy varies with surface coverage neither will give a straight line and an equation of the type:-

$$-dn/dt = v\ n^2 \exp\left[(-\Delta H_o - \propto n)/RT\right] \qquad \ldots\ (1\text{-}38)$$

is used for a second order reaction. This equation is solved by using a computer to fit the best results when the other parameters have been calculated. The order of reaction is found in a similar method to that suggested by Ehrlich. Graphs of $(n_o - n)/n$ against time are plotted and the general trends are observed.

The results obtained are shown in Fig. 12 for hydrogen on tungsten.

FIG. 12 Hansen's Results for the Desorption of Hydrogen from Tungsten.

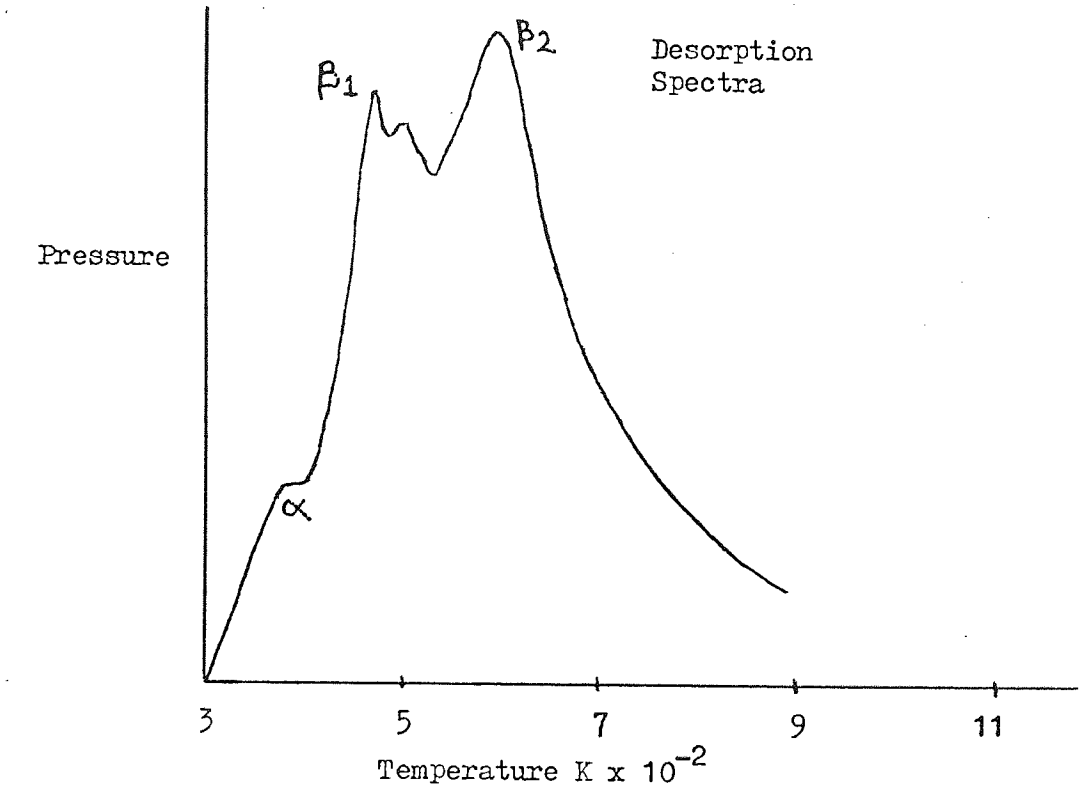

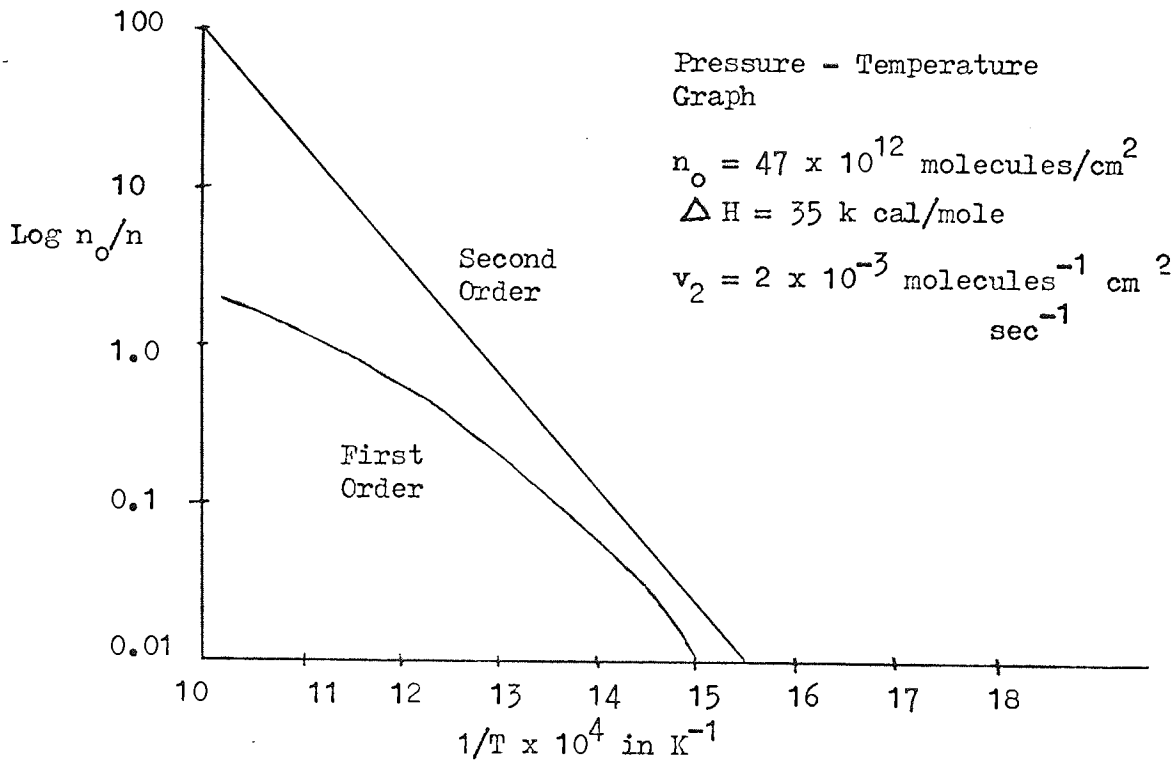

The value for the surface coverage is of the order 10^{13} to 10^{14} molecules per cm^2. The activation energy of desorption was found to be 35 kcals $mole^{-1}$ obtained from the gradient of the second order graph. This is for one of the two peaks obtained and these were desorbed at temperatures of 405 K and 470 K. It was found that a small variation in activation energy with surface coverage occurred and α was equal to 14 with a surface coverage of 3.8×10^{13} molecules per cm^2.

The Arrhenius equation has been combined with the transition state theory (39,40,41) so that thermodynamic parameters such as the entropy of activation can be calculated as well as the kinetic parameters. Petermann calculated the activation energy and pre-exponential function from the rate of reaction and this is used to calculate the entropy. The limitations of using the transition state theory are presented especially in the case of a very slow unimolecular reaction. Investigations of carbon dioxide on many transition-metal surfaces have been performed by Degras who used the Arrhenius equation together with the thermodynamic relationship

$$\gamma = h/kT \exp \left[\Delta F/RT \right] \quad \ldots\ldots (1\text{-}39)$$

where ΔF is the free energy change per mole. Lapujoulade used a similar approach. He considers the vacuum system and how this effects the equations describing the system. He assumes the pumping speed remains constant during the flash and no re-adsorption occurs on the filament and onto the cell walls. He makes the point that the pumping speed depends on the history of the system and would be expected to vary.

Petermann (42) further considers the application of the transition state theory to thermal desorption experiments. The rate constant and the temperature are calculated and using each set of points a graph is plotted of ln Kh/kT against 1/T. From the absolute rate theory if the value of the activation energy and entropy are constant the plot will give a straight line of gradient $\Delta H/R$ and of intercept $[\ln r + \Delta S/R]$ where r is the transmission coefficient. The results in Fig. 13 give a straight line over a small experimental range and this he extrapolates to other regions. This method is not very convincing since the assumption that the straight line holds over the other regions is not proven.

Amenomiya (43) has considered how to calculate the rates of adsorption and desorption from the adsorption curves. Amenomiya and Cvetanovic (44) have proposed an interpretation of thermal desorption data. The method is used by Amenomiya to analyse problems in chemical catalysis but could also be applied to flash filament work. A linear heating schedule, the Arrhenius equation and a material balance equation of the type (1-40) is used

$$-v_m \, d\theta/dt = v_m k_d \, \theta - k_a C(1-\theta) \qquad \ldots\ (1\text{-}40)$$

where v_m represents the amount of sample desorbed per unit volume of the solid phase when the surface coverage θ is unity. k_a and k_d are the rate constants for adsorption and desorption. At the desorption peak maximum where $T = T_m$ and $dC/dT = 0$ then

$$(k_d)_m = A \exp(-Ed/RT_m) = \beta E_d/RT_m^2 \qquad \ldots\ (1\text{-}41)$$

For any known rate of heating β ($T = T_o + \beta t$), the activation

FIG. 13 Petermann's Graph Used to Deduce ΔH and ΔS.

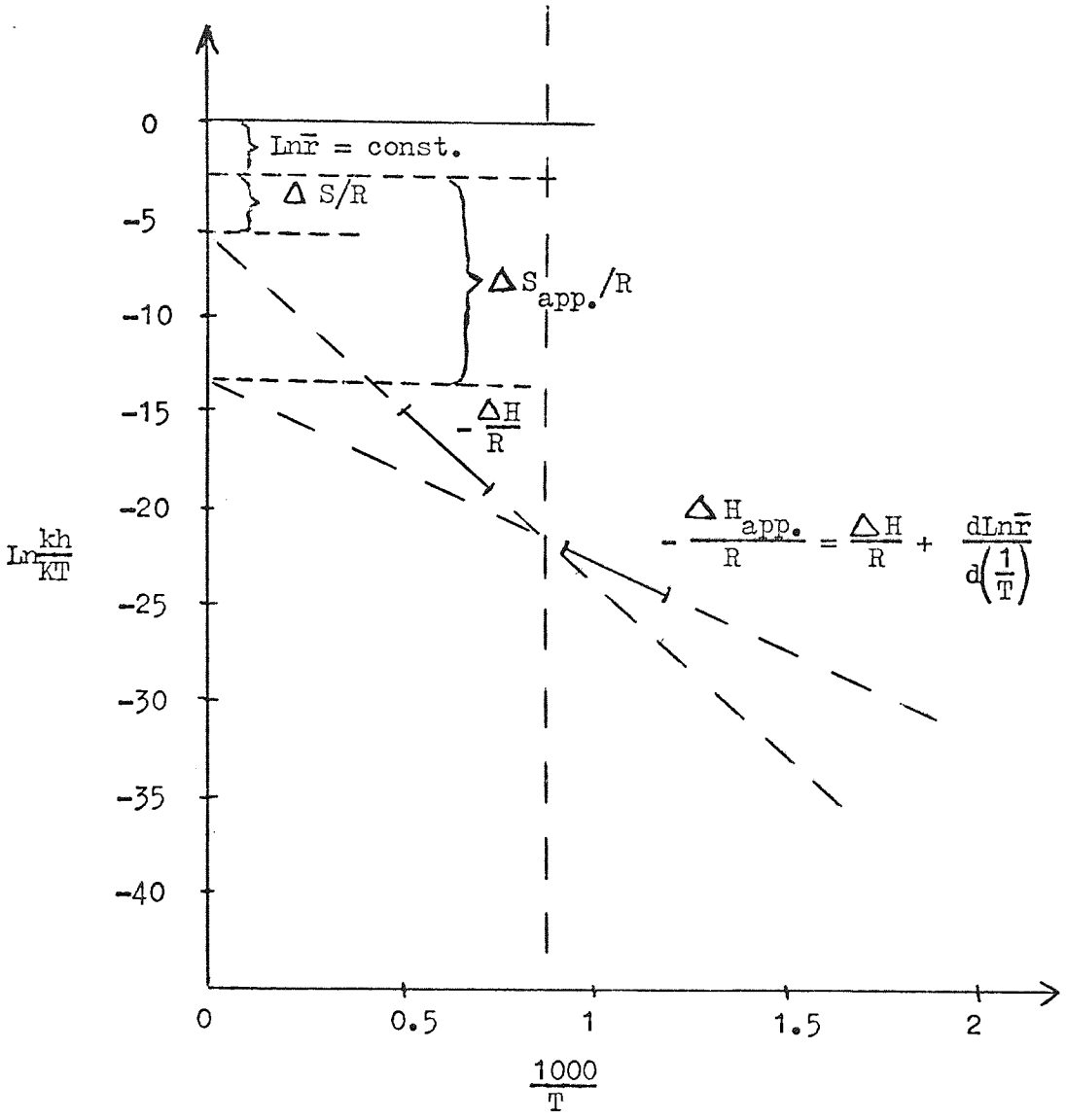

Table 1. Summary of Theoretical Treatment by Other Workers.

Author	Ref	T variation	Theoretical Equations	Extraction of		System	Thermodynamic Parameters
				E	x		
Becker and Hartman	29	Linear	Conservation of mass equation	Intercept of a graph	-	N_2 on W	-
Ehrlich	32	$1/T = a_o + bt$	Arrhenius Equn and conservation of mass	Substitution in equation	Shape of curves at various σ_o	CO on W	-
Redhead	35	$\frac{1}{T} = \frac{1}{T_o} + at$ $T = T_o + bt$	Arrhenius Equn and conservation of mass	Substitution taking $\nu = 10^{13}$ sec^{-1}	Trend of curves at various σ_o	H_2 on W	-
Carter	36		SIMILAR TO REDHEAD				-
Ageev and Ionov	37	$\frac{dT}{dt}$ = constant	Arrhenius Equn and conservation of mass	Substitution into equation or slope of graph	Best straight line for x = 1 or x = 2	O_2, H_2, CO_2 on W	-
Hansen	38	$\frac{1}{T} = a + bt$	Arrhenius Equn and conservation of mass	Gradient of graphs	Graphs of $\left(\frac{n_o - n}{n_o}\right) - t$	H_2, N_2, C_2, H_2 C_2H_4 on Ir	-
Petermann	39	-	Arrhenius Equn and absolute rate theory	Graph of $\ln \frac{Kh}{kT} - \frac{1}{T}$	Assumed to be first order	H_2 on Ni	ΔS, F/F_n from Transition state theory
Degras	41	-	Arrhenius Equn and absolute rate theory	Graphically	-	Co on Ni, Mo, W, Nb, Co	-

Cont:

Table 1 Continued.

Author	Ref	$T_{variation}$	Theoretical Equations	Extraction of		System	Thermodynamic Parameters
				E	x		
Amenomiya and Cvetanovic	43	$T = T_o + bt$	Arrhenius Equn and conservation of mass	Graphically 1/T	-	Ethylene on alumina catalyst	-
Page and Jennings	45	linear	Arrhenius Equn and conservation of mass	Graph against 1/T	Best straight line	O_2 on T_a	ΔS, from transition state theory

energy is defined by equation (1-41). Provided the pre-exponential factor is known or can be assumed E_d can be found. By varying β, E_d may be found with assuming a value of A. Thus the experimental parameters may be found. This method of analysis could be applied to flow systems to calculate the various parameters.

Page and Jennings (45) have taken into account many other factors which influence vacuum systems, such as desorption on the walls, pumping by the gauges, external leak rate and re-adsorption on the filament. Many of these are shown to be negligible and the final equation obtained is similar to that obtained by Ageev et al.

1.3.4 Summary

Many methods for analysing flash desorption data have been thoroughly covered in the literature over the previous years. The method used depends on the parameters measured but for a standard desorption spectrum a mass balance equation for the system is incorporated with an Arrhenius type equation as the definition of the experimental activation energy. From a combination of these two equations the various kinetic parameters are found. The absolute reaction rate may be used if thermodynamic parameters such as the entropy and partition functions are to be found. The method used for analysis depends on the particular vacuum systems properties and the parameters which are measured. These have to be related to the parameters to be investigated.

1.4 RESULTS OF SOME EXPERIMENTAL INVESTIGATIONS

1.4.1 Gas Metal Interfaces

It is beyond the scope of this thesis to review all the gas-metal systems investigated. The number is ever increasing and it would be

Table 2. a) Adsorption and Desorption of the Common Gases from Various Metals

Metal / Gas	W	Ta	Mo	Ir	Ni	Fe
H_2	Redhead(35)	Trasatti(91)	Pasternak(89)	Hansen(38)	Petermann(42)	Porter(87)
O_2	Ageev(53)	Ageev(55) Jennings(63)			King(93)	
N_2	Becker and Hartmann (31)			Hansen		
CO	Redhead(61) Ehrlich(32)	Gasser(56)	Degras(40)		King(93) Degras(40)	Porter
CO_2	Ageev(25)				Page	
C_2H_4				Hansen	Moss(90)	Greenhalgh(88)

b) Chemisorption on Metal Films

Gas	Very Fast Chemisorption	Slow Chemisorption	No Chemisorption Up To 0^oC
H_2	Ti,Zr,Nb,Ta,Cr,Mo,W,Fe,Co,Ni,Rh,Rd,Pt,Ba	Mn, Ge	K,Cu,Ag,Au,Zn,Cd,Al,In,Pb,Sn
O_2	All metals except Au	-	Au
N_2	Ti,Zr,Nb,Ta,Mo,W	Fe,Ba	As for H_2 plus Ni,Rh,Pd,Pt
CO	As for H_2 plus La,Mn	Al	K,Zn,Cd,In,Pb,Sn
CO_2	As for H_2 less Rh,Pd,Pt	Al	Rh,Pd,Pt,Cu,Zn,Cd
CH_4	Ti,Ta,Cr,Mo,W,Rh	Fe,Co,Ni	-
C_2H_6	As for CH_4 plus Ni	Fe,Co	-
C_2H_4	As for H_2 plus Cu,Au	Al	As for CO
C_2H_2	As for H_2 plus Cu,Au,K	Al	As for CO less K
NH_3	(W,Ni,Fe)?	-	-
H_2S	W,Ni	-	-

a major task for any one person to undertake. Transition metals have been used extensively in a variety of techniques mainly because of their experimental suitability, being stable at the high temperatures involved in the flash desorption technique. Other surfaces have also been used and in a great variety of forms, single crystals, powders and evaporated metal films as well as filaments. The adsorbents used vary from the chemically inert gases to more reactive gases such as oxygen and organic gases and from there to the adsorption of the elements of group one in the periodic table, such as sodium, potassium and caesium. A review will be made of the more common gases used in flash desorption experiments but hydrogen, carbon monoxide and ethylene will be omitted until the results of the present study are discussed. Table 2 makes an attempt to show the large variety of surfaces and adsorbents investigated throughout the years.

1.4.2 Nitrogen as Adsorbent

The adsorption of nitrogen on tungsten was one of the first gas-metal surfaces to be investigated by the flash filament method (31). The flash filament method was used in conjunction with a field emission microscope. The rate at which nitrogen is adsorbed on tungsten, the sticking probability and the activation energy were found. The activation energy was found to be dependent on surface coverage being equal to 5000 cals/g mole when the surface coverage is 2 monolayers and this decreases to 100 cals/g mole when the surface coverage is up to one monolayer. The system was not pumped and no attempt was made to resolve the various states of adsorbed nitrogen and no interpretation of the results were made in this paper.

Hickmott and Ehrlich (46,47,48,49) used the flash desorption technique to investigate the adsorption of nitrogen on tungsten and

FIG. 14 Desorption Spectra of Nitrogen from Tungsten Obtained by Hickmott and Ehrlich.

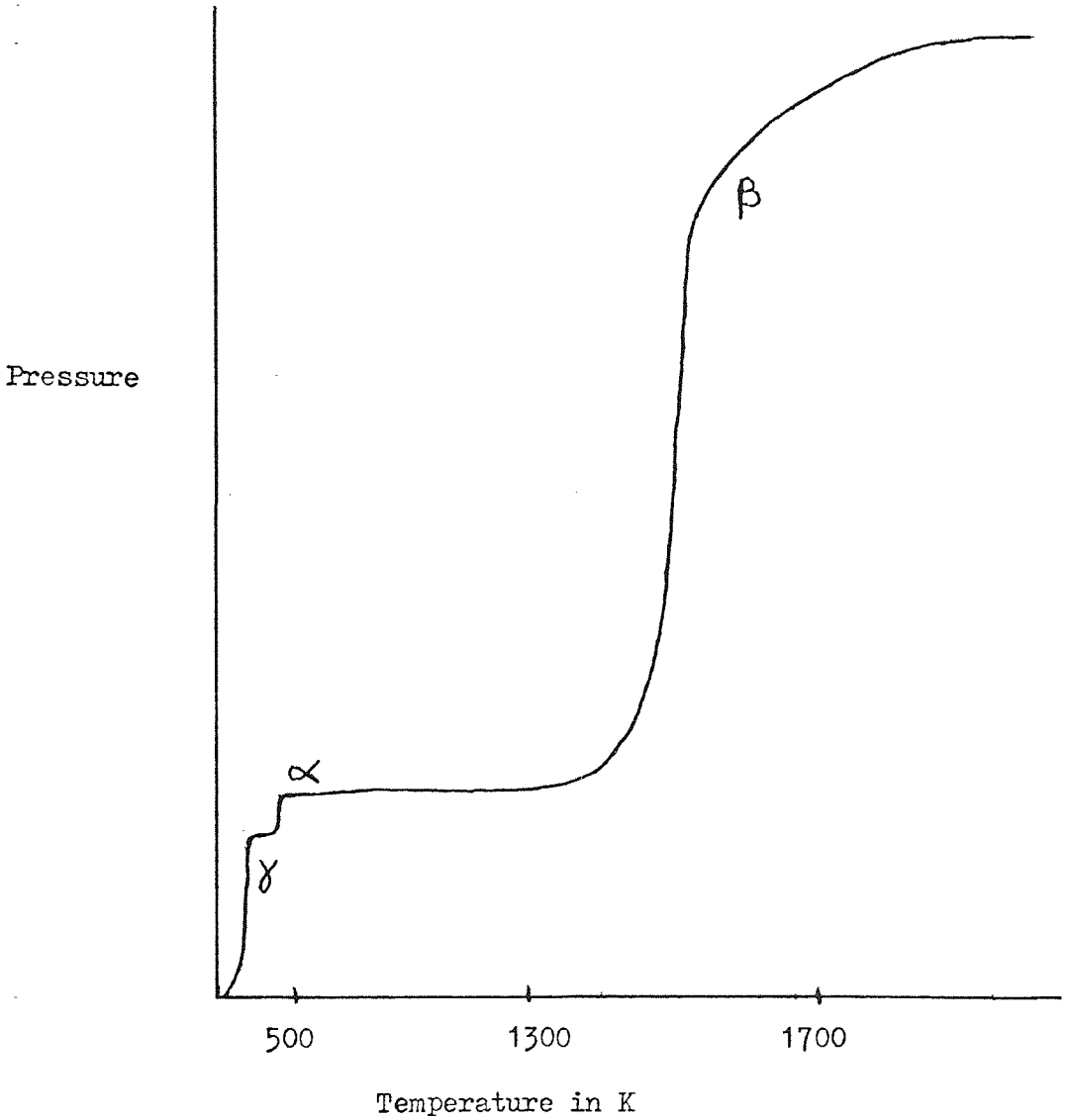

found three peaks which were designated γ, α and β in order of their increasing temperature. The γ peak occurred at temperatures below 200 K, the α peak in the range 350 K to 450 K and the β peak at the higher temperatures of 1350 K to 1800 K. The kinetics of each peak were investigated separately and the β peak was found to be second order showing that the nitrogen dissociated on adsorption and the activation energy of the β peak was found to be 81 kcals mole^{-1} up to a surface coverage for the β peak of 1.5×10^{14} molecules cm^{-2}.

It was found that the γ peak was independent of the other peaks and this adsorption state was connected to the surface by some kind of electron exchange. The α and β peaks effect each other so that the peak heights and temperature of desorption change and the conclusion from this is that at higher surface coverages the α state molecules exchange with gas phase molecules at a significant rate. The order of reaction is found to be second order and this leads to the suggestion that the nitrogen is adsorbed as atoms and two of these "adatoms" have to come together before the nitrogen is desorbed. It is also suggested that the surface structure effects the activation energy of desorption and heat of adsorption.

Further work has been performed by Hansen (36) who analysed both the α and β peaks. The α peak was found to obey first order kinetics and the β peak second order. The maximum surface coverage for the α peak was found to be 6.6×10^{12} molecules cm^{-2} and the α peak was found to have an activation energy of desorption of 19.2 kcals mole^{-1}. This was found from the slope of the $(n_o - n)/n_o$ against 1/T curve where n_o is the maximum surface coverage and T is the temperature. The β peak, which occurred in the temperature

range 1350 K to 1900 K, was found to have an activation energy of 73 kcals mole^{-1} which was obtained by a similar method to that used with the α peak. The maximum surface coverage for this peak was found to be 2.1 x 10^{14} molecules cm^{-2}. This paper was concerned with the use of the flash filament techniques being used to obtain the various kinetic parameters and comparing the results with those obtained by other techniques. No attempt was made to relate the findings to the surface but many systems were considered. It was suggested that since a great deal of work has been done on the nitrogen and tungsten system that this system was ideal for use in the calibrating of vacuum systems.

Rigby (50) has identified a further peak the β_1 in the desorption spectrum of nitrogen from tungsten. The β peak has been resolved into two, of which the β_1 obeys first order kinetics and the β_2 second order kinetics. The activation energies for desorption are found to be 73 and 75 kcals mole^{-1} for the β_1 and β_2 peaks respectively. The resolution obtained in separating the peaks was not good and it is difficult to make an accurate kinetic analysis of the two overlapping peaks.

A comparison of the binding states of nitrogen on (100) tungsten and (100) molybdenum has been made by Hans and Schmidt (51). Both tungsten and molybdenum are isoelectronic and it is found that when nitrogen is adsorbed on these two metals the adsorbed states are very similar. Two states are found when nitrogen is adsorbed on the (100) plane of tungsten. These two states are the γ and β states and two similar states are found for the (100) plane of molybdenum. The technique used was flash desorption mass spectrometry and this

was combined with results obtained from low energy electron diffraction studies.

When the nitrogen is adsorbed on molybdenum the γ state has an activation energy of 9.7 ± 1 kcals mole^{-1} and the β peak which is second order has an activation energy of 87 ± 3 kcals mole^{-1}. For nitrogen the γ peak is similarly first order with an activation energy of 9.2 kcals mole^{-1} and the β is second order with an activation energy of 80 kcals mole^{-1}. It is noted that at high surface coverages there is a broadening of the second order peaks and the suggested reason is that the activation energy may depend on the surface coverage. Also observed was the fact that the saturation amounts in the two systems between those obeying first order kinetics and those obeying second order kinetics was in the ratio 2:1. The interactions of the molecular orbitals of the nitrogen with the metal surface are considered. The 4d and 5d orbitals of the metal interact with one of the 2p orbitals of nitrogen and the other two 2p orbitals of the nitrogen are parallel to the surface. The tungsten 5d orbital has a greater extension than the 4d orbital of the molybdenum and because of the possible greater overlap with the tungsten this could account for the slightly different kinetics especially the small difference in the activation energy.

When nitrogen is adsorbed on a filament with many crystal surfaces three desorption states are seen the α, β and γ. The β may be resolved into further peaks but when the (100) crystal surfaces is considered only two states the γ and β are found. This suggests that the various adsorption states are due to adsorption on different crystals planes. The activation energies and kinetic parameters from

the various states have been calculated and in some cases the activation energy was found to depend on the surface coverage. More work is being performed investigating the adsorption of nitrogen on particular crystal surfaces.

1.4.3 Oxygen

Oxidation and reduction are two very important chemical processes. This is especially so with catalysts using metal surfaces and it is understandable why a large amount of the literature is devoted to the study of oxygen on metal surfaces.

Eisinger (52) studied the adsorption of oxygen on tungsten. The tungsten surface was a single crystal ribbon whose surface was normal to the [113] direction. With a surface coverage of 2×10^{14} atoms cm^{-2} the sticking probability was found to be 0.2 but with a surface coverage of 1.2×10^{15} atoms cm^{-2} the sticking probability is 0.001. The maximum surface coverage obtained was 1.23×10^{15} atoms cm^{-2}. The [113] plane has three different surface atoms, each being connected to a different number of nearest neighbours. (I) is connected to 4 nearest neighbours, (II) five nearest neighbours and (III) seven nearest neighbours. Eisinger suggests three separate adsorption states depending on the combination of the above surface atoms to which they are connected. These adsorption sites in order of their decreasing stability are in terms of the above labelled (I, I, II), (I, II, II) and (II, II, III). This model is largely conjectural but field emission microscopy by Becker has supported this interpretation. Most of the adsorbed oxygen is desorbed as oxygen for the surface coverage up to a monolayer.

Ageev (53,54) using a time of flight mass spectrometer and the flash method has investigated the behaviour of oxygen on many metal surfaces including tantalum, tungsten and niobium. The desorption of oxygen from a tungsten ribbon was studied and it was found that oxygen was desorbed from the tungsten in two atomic states, the β_1 and β_2. The activation energies for desorption were found to be for the β_1 peak 4.1 $\pm$ 0.1 eV (395.6 kJ mole^{-1}) and for the β_2 peak 7.8 $\pm$ 0.6 eV (752.6 kJ mole^{-1}). The desorption curves are shown in Fig. 15. Further work by Ageev (49) investigated the formation of tungsten oxides due to the interaction of oxygen with a tungsten ribbon. When the surface coverage of oxygen is more than a monolayer the desorbed species are found to be tungsten oxides WO_2, WO_3 with a trace of $(WO_3)_2$, $(WO_3)_3$ and O_2. The mass spectrometer was set to follow the desorption of one species through the flash. The desorption of O_2 and a small amount of O^+ occurred at low temperatures. The desorption of the WO_2^+ and the WO_3^+ both occurred at higher temperatures and two desorption phases occurred for each of these species. The activation energy and the order of reaction was calculated for each of these states, these were

β_1 phase WO_2: E = 2.2 $\pm$ 0.1 eV and v = 2 (212 kJ mole^{-1})

β_1 phase WO_3: E = 2.1 $\pm$ 0.1 eV and v = 2 (202 kJ mole^{-1})

β_2 phase WO_3: E = 3.6 $\pm$ 0.3 eV and v = 2. (347 kJ mole^{-1})

From the results it was concluded that with surface coverages of less than one monolayer the oxygen exists as atoms but with larger surface coverages of more than a monolayer the oxygen exists as O_2 molecules. The desorption of the oxides occurred in the low temperature range of 1100 to 1600 K.

FIG. 15 Ageev's Results for Desorption of Atomic Oxygen from Tungsten.

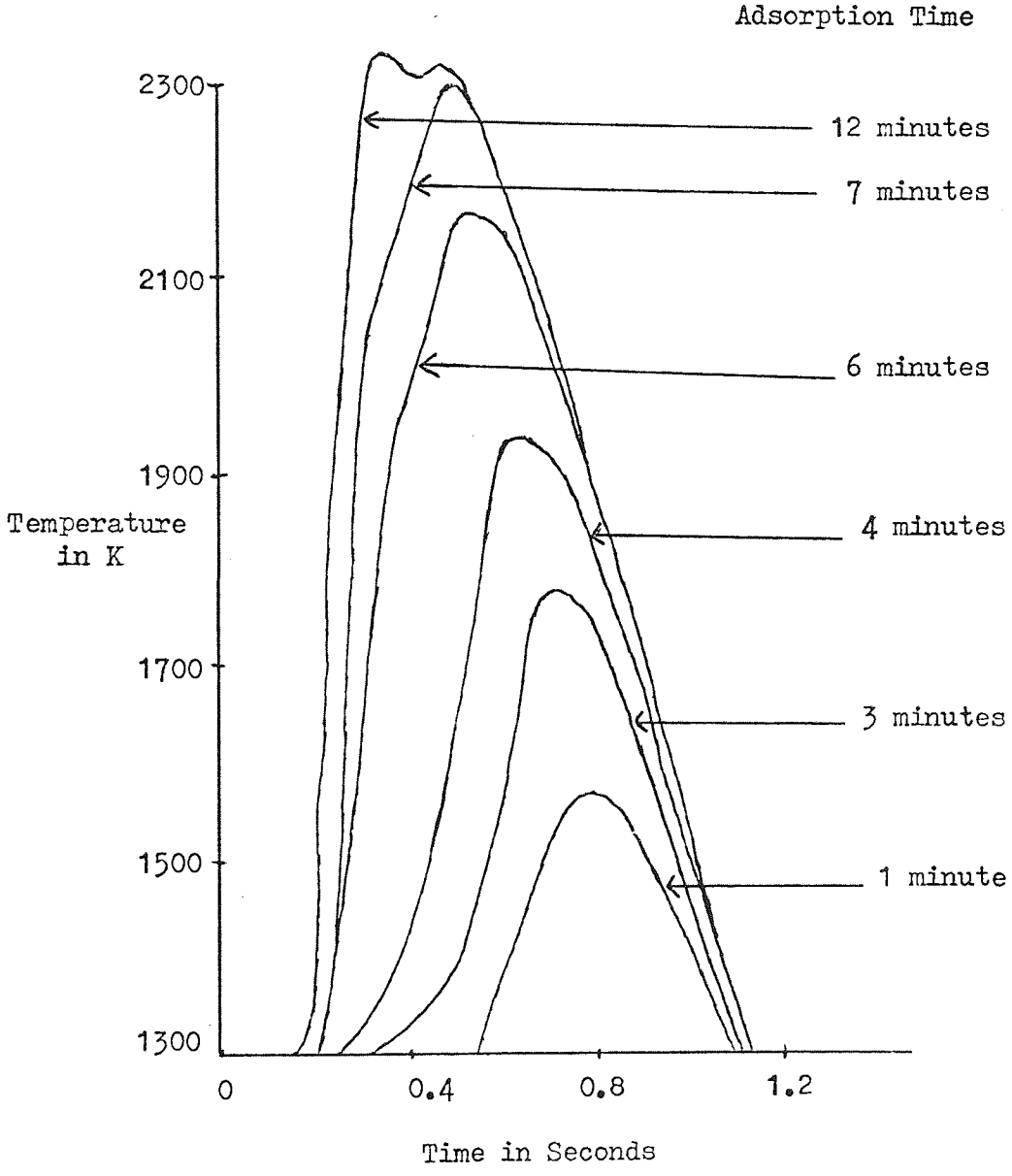

Other metal-oxygen reactions have been studied by this method. When oxygen was allowed to adsorb on niobium and flashed the desorbed species was found to be NbO. The activation energy for the desorbed species was 6 $\pm$ 0.3 eV (578 $\pm$ 28 kJ mole^{-1}). Only one desorption peak was found and this at temperatures greater than 1700 K.

The adsorption of oxygen on tantalum has been studied by both Ageev (55) and Gasser (56). Ageev used the time of flight mass spectrometer and found only one desorption maximum and this was analysed and discovered to be due to TaO. No oxygen was desorbed and these results were similar to those obtained by Ageev for niobium but in contrast to those for tungsten and rhenium. The activation energy for the desorption of the TaO peak was 5.7 $\pm$ 0.2 eV (550 kJ mole^{-1}). A flow chart to show the interaction of the oxygen being adsorbed on the tantalum surface is shown in Fig. 16.

Gasser used an omegatron radio frequency mass spectrometer to investigate the reaction of oxygen with tantalum and tungsten. It was found that the activation energy of the oxygen on tantalum was more than that for tungsten and so the bond which held the oxygen to the tantalum was stronger.

Electron stimulated desorption (57) and many other ultra high vacuum techniques have been used to study the adsorption and desorption from the surface of many metals. The electron stimulated desorption results revealed that at low surface coverages only atomic oxygen was desorbed but at higher coverages the metal oxides of tungsten were desorbed.

FIG. 16 Scheme of Interaction Between Oxygen Molecules and a Tantalum Surface.

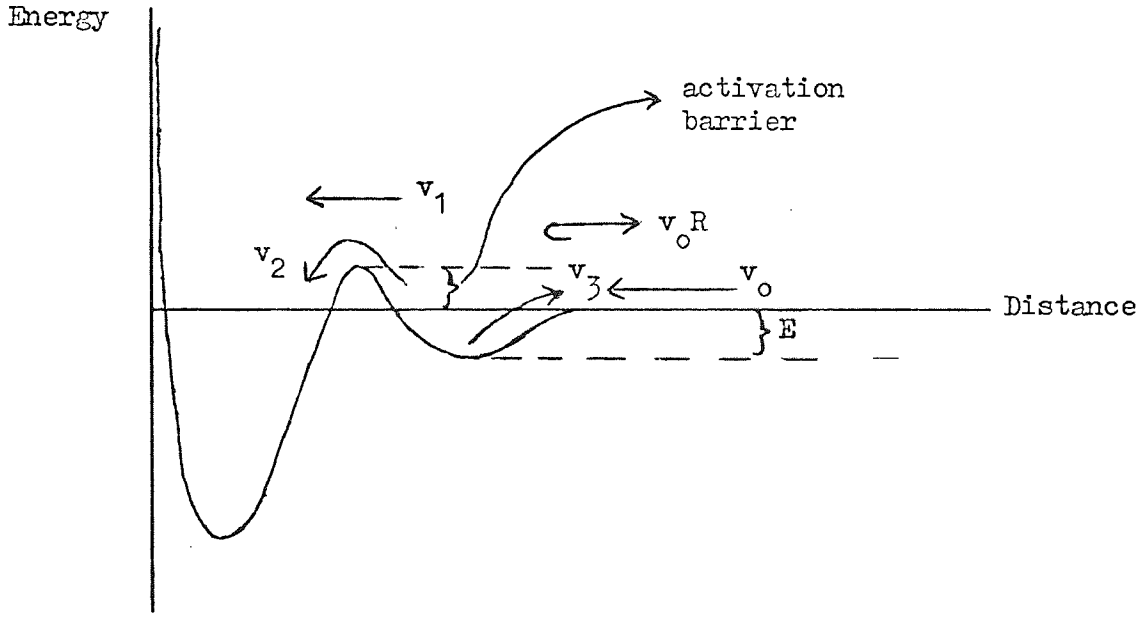

The arrows indicate the directions of the flows of oxygen molecules interacting with the tantalum

1.4.4 Organic Gases

Comparatively little work has been done on organic gases compared to the mass of literature on relatively simple gases such as carbon monoxide and nitrogen. The organic gases are regarded as contaminants in a vacuum system especially long chain hydrocarbons which can be adsorbed on the filament. The reactions of organic gases are much more complicated than the simple gases. The effect of the gases on the system also have to be considered, e.g. whether they are pumped at the same rate and whether the pressure gauge is reliable for these gases. Chemical changes in the filament may also severely complicate the results, particularly carbide formation on the surface.

Only the simpler organic gases have been investigated so far, these include methane, ethane, ethylene and acetylene. The work has been concerned with the decomposition of the molecules on the surface of the metal and the mechanisms of the reactions. Much of the work has been performed by Hansen (58) who used the flash method to investigate the adsorption of organic gases on iridium. The gases he used were both ethylene and acetylene. The acetylene gave two desorption peaks at approximately 480 K and 660 K and also a very low temperature peak at 110 K. By following the mass 26 and mass 2 through the flash using a mass spectrometer it is seen that the low temperature peak (110 K) is due to the acetylene which was physisorbed. The two higher temperature peaks were due to the desorption of hydrogen and none of the higher peaks were due to the desorption of hydrocarbons. Field emission studies suggested

the following reaction mechanism

$$CH \equiv CH \longrightarrow C_2 \text{ (adsorbed)} + 2H$$

where the acetylene is completely dissociated on adsorption.

Organic gases have been studied using other ultra high vacuum techniques, for instance the field emission microscope (59) to investigate the reaction of ethane and ethylene on nickel.

The reactions involved when an organic gas is adsorbed in a vacuum system are very complex, the effect of the wall, pumps and gauges may all influence the reaction. Many of the radicals produced are very reactive and their behaviour in a vacuum system is still somewhat of a mystery. This field still allows scope for careful study before the behaviour of organic gases on surfaces in a vacuum system is thoroughly understood.

2 EXPERIMENTAL APPARATUS

2.1 THE VACUUM SYSTEM

2.1.1 General Introduction

In order to obtain results which are both accurate and meaningful care is needed to be put into the design of the apparatus. The basic necessity in the apparatus is a filament which is connected by electrical leadthroughs to an energy source which is used for heating the filament. This filament has to be in a system which is capable of being pumped down to the ultra high vacuum pressure region. To allow the system to be pumped down below the 10^{-8} torr region the system has to be heated to a temperature of at least 473 K and this means that the ultra high vacuum part of the system must be placed in an oven.

2.1.2 Factors Limiting Ultra High Vacuum

In order to reach the ultra high vacuum pressure region in the system several factors which seriously affect the lowest pressure available need to be taken into account. The system needs to be sealed off from the atmosphere by special leak valves and the joints connecting the various pieces of the apparatus should also be of a leak tight nature. At these pressures the smallest leak from the atmosphere outside will seriously limit the lowest pressure obtainable. The system needs to be capable of being "baked out", that is heated to a temperature of above 473 K for several hours. The gas initially in the system prior to pumping should be one which will be pumped easily and one which is easy to remove from the system. The pumps and gauges used in the system need also to have special features so that they in no way limit the performance of the system.

Fig. 17 Front View of the Apparatus.

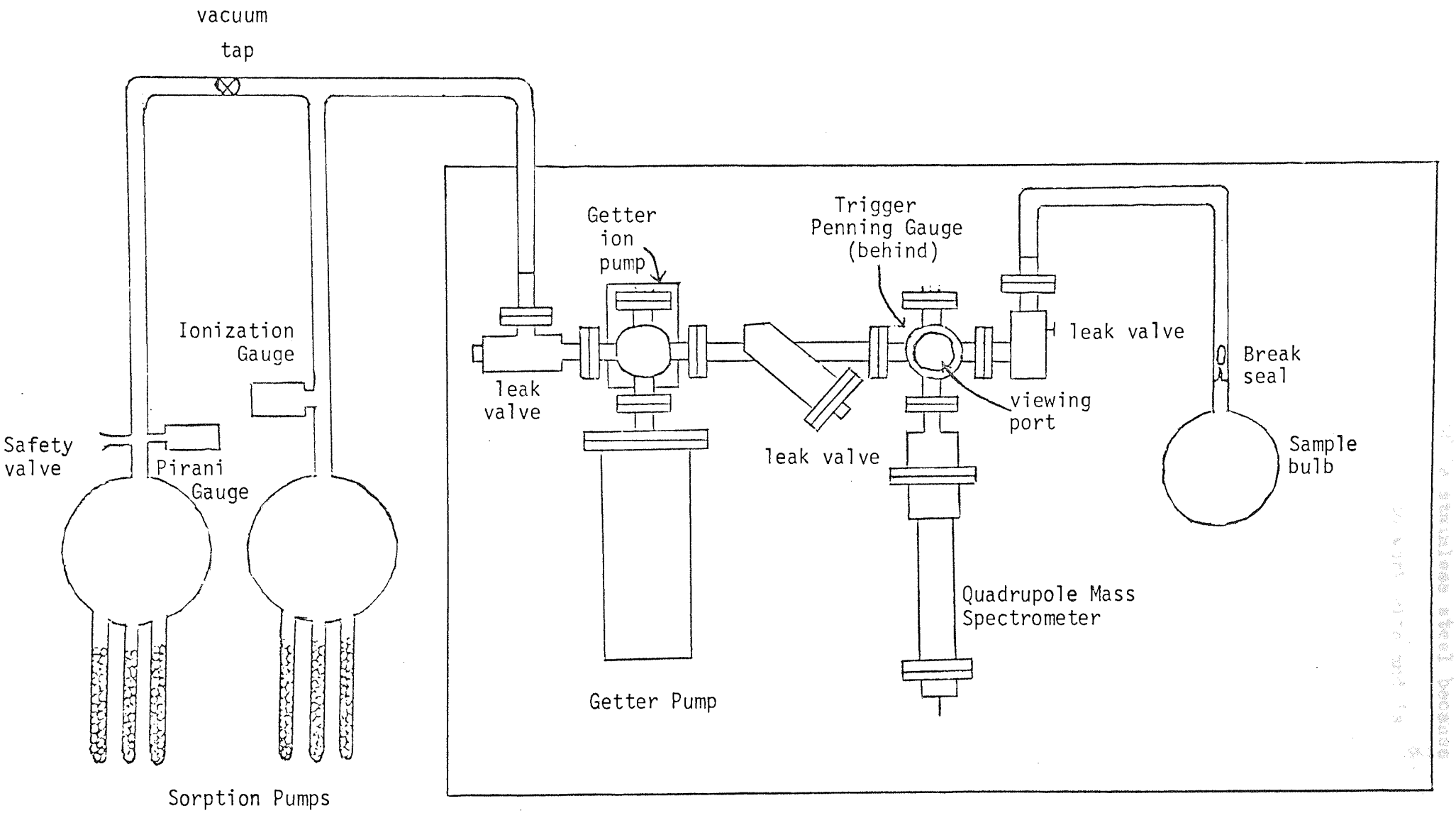

The material the system is made of is stainless steel because this material is easy for the manufacturers to work with and is strong and able to stand the low pressures which are obtained in this work. Stainless steel is impermeable to most gases but hydrogen is known to diffuse through it slowly and as the temperature rises the rate of diffusion increases (60). The stainless steel components, two symmetrical six-way adaptors, two reducer couplings, the titanium sublimation pump housing, three high vacuum leak valves and the getter ion pump were all supplied by Vacuum Generators Ltd (61). The viewing port was made of "Kodial" glass and was suitable for baking up to 673 K and was oxidation resistant. The glass was connected to the metal by a glass to metal seal so that during the baking both the glass and metal expand together and no leaks occur.

The whole system which was to be pumped down to the ultra high vacuum region had to be set in an oven so that it could be heated to a temperature above 473 K (62) for a long period of time. The purpose of this is to remove the gas that has been adsorbed on the system walls, into the system so that it can be pumped away by the pumps. Without this "bake-out" the lowest pressure obtainable would be 10^{-8} torr but much lower pressures are obtained with the heating of the system.

The air contains a small percentage of inert gases and about 20% oxygen. Inert gases along with long chain hydrocarbon and vacuum grease are undesirables when the internal constituents of a vacuum system are considered. These are very hard to remove and are pumped away very slowly or not at all. Air contains 1% of inert gases but when the air has been pumped for several minutes

the action of the pumping is to concentrate the inert gases. The sensitivity of the vacuum gauges varies for different gases. Most gauges are calibrated using one gas which is normally nitrogen. Oxygen in the case of the trigger gauge has a sensitivity of only 0.9 (63) compared to nitrogen. It is essential therefore that the gas in the system is one of which the sensitivity is known. Nitrogen obtained by "boiling off" from liquid nitrogen is found to be pumped down easily by most pumps. For these reasons the gas in the system at the beginning of the pump down is usually arranged to be nitrogen. This is done by passing nitrogen into the system several times before the experiment begins. After taking this trouble to eliminate any unwanted material from the system it is common sense to ensure that the pumps and gauges do not constitute a source of contamination.

2.1.3 Vacuum Joints (64)

The simple vacuum joint consists of a ground glass cone and socket which are held tight together by a spring. A thin smear of vacuum grease is usually applied so that the joint is absolutely leak free. This design works well for vacuums down to 10^{-6} torr but for vacuums below this a more sophisticated type of joint is needed. There are two types of ultra high vacuum joints, those that need to be opened and closed and those which remain tightly shut.

The first type are sealed with soft metal "O" rings. The metal is usually twenty four carat gold or soft lead which is cheaper but it is not regarded as being as good since the lead cannot be baked to such high temperatures. These "O" rings are placed between two geometrically planar surfaces which are as flat as possible. If a horizontal joint is needed the "O" rings may be kept in place using a spigot ring. The gold "O" rings are made from approximately a

ten thousandth of an inch gold wire and are supplied by A.E.I. Ltd. The size of the vacuum tubing will determine the number of nuts and bolts used to tighten the joint. With the "O" ring in position the nuts and bolts are tightened either alternately around the circle or in order around the circle until the distance between the two surfaces is just less than a six thousandth of an inch. The threads of the bolt are treated with a lubricant to ensure easy opening and closing after baking.

The joints which need to be opened and closed have to be sealed using a copper "O" ring. For this joint the two sides of the joint have a small knife edge projecting from the flat surface. The knife edge "bites" into the copper surface and forms an air tight joint. This joint is tightened similar to the gold joint except that it only has to be tightened down evenly on all sides once the knife edge has bitten into the copper. The leak valves in the vacuum system also use this principle for sealing off the system. The copper sealing pad is situated on the end of a screw thread. When the screw is turned the sealing pad is moved to open or close the tube. On the outside of the apparatus is a mark which may be adjusted to a mark on the knob at the end of the screw thread and this allows the screw to be tightened to the same position each time. The copper is always set tight against the knife edge and if the screw is tightened too far then the valve must always be tightened to the same position.

The expansion of the gold and copper is similar to that of stainless steel and during the bake-out no leaks should occur but the apparatus joints should be checked in case a leak has occurred.

2.1.4 The Bake-out

The ultra high vacuum part of the apparatus has to be heated

to a temperature of at least 473 K for a long period of time and this is termed the "bake-out". The apparatus has to be set in an oven, and this oven is made out of asbestos sheet which is set on a steel frame and has two asbestos doors on the front of the apparatus. This asbestos oven is surrounded by an insulating shield which consists of an asbestos wool attached to a hardboard sheet which is supported by a steel frame. The electrical connections to the heaters, pumps and filament all pass through the insulators by special connections. Without this bake-out the maximum lowest pressure obtainable would be 1×10^{-8} torr because of the adsorbed gas on the sides of the vacuum system.

The heating elements for the oven is nichrome wire which is wound round an asbestos sheet attached inside the oven. There are four heaters made of Nichrome 3 wire supplied by British Driver Harris. The wire is connected directly to the mains and take a current of 13 amps.

The temperature of the oven is measured by a copper-constantin thermocouple which was previously calibrated in boiling oil as the variable hot junction and ice as the cold junction. The voltage difference was measured on a digital voltmeter. The temperature of the oven must not be raised by more than 100 K per hour (63) because the expansion of the apparatus and the "O" rings might result in leaks. This means that the heater has to be switched on and off spasmodically and these heaters should be switched on alternately so that each part of the oven is equally heated.

The gas which is desorbed from the walls and other surfaces are pumped by the ion pump which is able to stand these temperatures while working. The oven needs to be left on for forty-eight hours

so that all the surfaces in the vacuum system are heated to the temperature of the oven. Because of the low pressures in the system the only ways that heat can be transferred to the filament and the getter pump filaments and mass spectrometer rods is by conduction. The effects of radiation and convection would be negligible. This means that the oven has to be hot for the time it takes for the heat to be conducted by the connections to the various internal elements of the vacuum system so that these may be degassed as well as the walls of the system. This is why the oven is left on for at least forty-eight hours.

When the oven is switched off once again the oven must cool down at a rate of not more than 100 K per hour once again so that no leaks occur due to contraction of the joints.

2.1.5 Design of the Apparatus

The vacuum system has to be set up so that the measurements taken from the gauges are an accurate representation of what is happening in the vacuum system. We must be able to relate these measurements to what is happening on the surface of the filament. The measured pressure rise is due partly to the gas desorbed from the filament and partly by degassing of other parts of the system (65). The pressure measured by the gauge should be a measure of the gas coming off the surface but since the gauge is not situated on the surface of the filament, other effects of the system mean that the measured pressure has to be corrected. The further away from the surface the larger the correction factor that needs to be used and the harder it is to estimate. It is essential to have the pressure measuring gauge near to the filament so that the pressure reading is taken in the vicinity of the surface. A spectrum is recorded on an oscilloscope of the pressure against the time after the start. The further away from the filament the pressure gauge is, the greater the time delay in

recording the pressure rise and this would lead to inaccurate results. The gauge must not be so close to the surface that the natural workings of the gauge effect the surface reactions. The vacuum tube between the gauge and the filament must not form a constriction and effect the flow of gas and the same applies between the filament and the mass spectrometer. The mass spectrometer needs to be close to the filament so that any ions negative, positive and neutrals do not have time to react with the walls of the system and other atoms before they reach the mass spectrometer. The peaks of the mass spectrometer are then an accurate representation of the atoms and molecules leaving the surface. The ions and molecules should not be allowed to be adsorbed on the sides of the system before they are analysed. The tubing of the system should not be too large to provide a large surface area of adsorption and should not be so small that the flow of gas is restricted and right angled bends should be avoided (63). The pumps should be placed sufficiently far away from the filament so as not to effect the surface reactions and the spectrum obtained. The pumps need to be separated from the reaction vessel by a leak valve so that the pumping rate may be adjusted. The mass spectrometer and the gauge should be situated between the pumps and the filament so that all the gas that is desorbed from the filament is pulled towards the pump through the gauge and the mass spectrometer. The effect of the pumps has to be estimated in the analysis.

2.2 VACUUM PUMPS

2.2.1 General Review

There are many different types of vacuum pump which (66) perform in many different ways and affect the system in different ways. Not all pumps can be started at atmospheric pressure and

some need a second pump to act as a backing pump. The pumps for an ultra high vacuum system should not be the cause of any contamination which will stop the system from being pumped down and also effect the surface of the metal which is being investigated.

2.2.2 The Rotary Pump

This pump has a vane which rotates in a chamber at a high speed. This vane pushes the air out of the system and gives the pump a pumping speed of 1 litre per second. It is used for pumping vacuum systems down from atmospheric to 1 x 10^{-3} torr range. When used with a liquid nitrogen trap it is a very useful pump and is used in pumping a system from atmospheric pressure. The disadvantage of this pump is that it cannot obtain very low pressures and since no trap is 100% efficient some oil vapour from the pump will find its way into the system.

2.2.3 Diffusion Pumps

The principle (67) on which the mercury or oil diffusion pump works is still a matter of discussion amongst scientists. A volume of mercury or oil is heated and the vapour rises up a central tube which is brought to a jet at the top. The vapour molecules, which are heavy, pass through the jet and are directed downwards. These molecules collide with molecules of gas from the vacuum system and give these molecules which are generally light a preferential velocity towards the entrance to the backing pump. These light molecules are removed by the backing pump from the system and the heavy molecules condense on the cold sides of the condenser and return to the mercury.

Mercury has a high vapour pressure and because of this tends to spread out of the pump into the vacuum system. Traps are

needed to prevent the mercury contaminating the system. The mercury condensing in the traps needs to be able to be transferred back to the pump. When the vapour leaves the jet a certain amount of spread occurs and this allows some molecules of the gas to travel back in the opposite direction to the direction of pumping. This phenomena is known as "backstreaming" and is one of the disadvantages of the pump.

The backing pump is used to reduce the pressure in the system when the heating of the diffusion pump is started. The lowest pressure obtainable using a diffusion pump depends on the size of the diffusion pump which is measured by the size of the pump near the nozzle. The pumps are usually made of glass or stainless steel because mercury does not attack either of these but it does attack many other metals.

Large diffusion pumps which are made of stainless steel and are attached to an apparatus which can be baked are capable of lowering the pressure to 10^{-10} torr (64). This is the value quoted for a 9" diffusion pump. Smaller diffusion pumps can be used for reducing the pressure down to only 10^{-4} torr.

2.2.4 Adsorption Pumps

The general principle of this pump is that gases are adsorbed on a refrigerated surface. This was first noted by Dewar in 1875 (68). The adsorption capacity depends upon the surface area available. The adsorbing agents used in the pumps are molecular sieves called zeolites. These are basically alumino silicates of the form $Na_2OAl_2O_3$ n SiO_2 x H_2O (69). These zeolites consist of small cavities interconnected by pores which increase the surface area greatly. When these pellets are lowered to liquid nitrogen

FIG. 18 The Sorption Pumps.

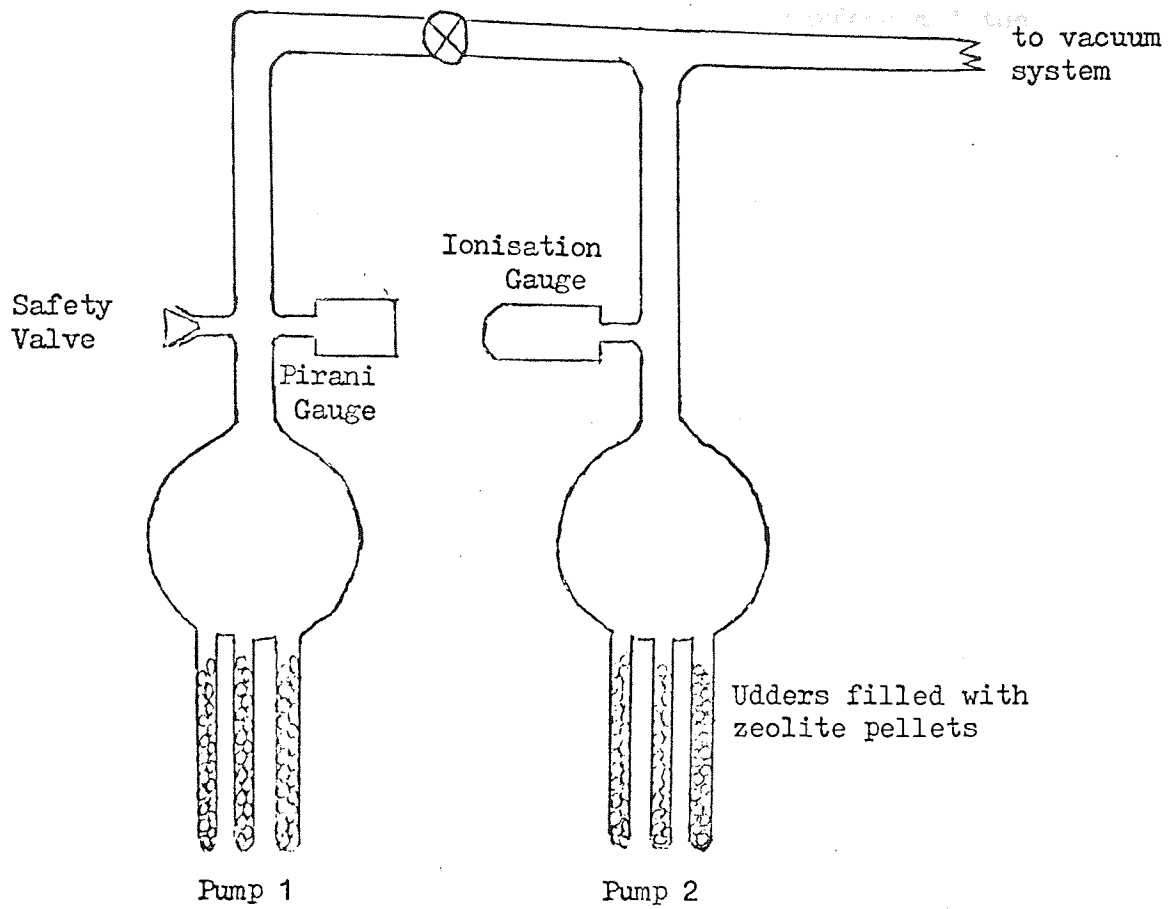

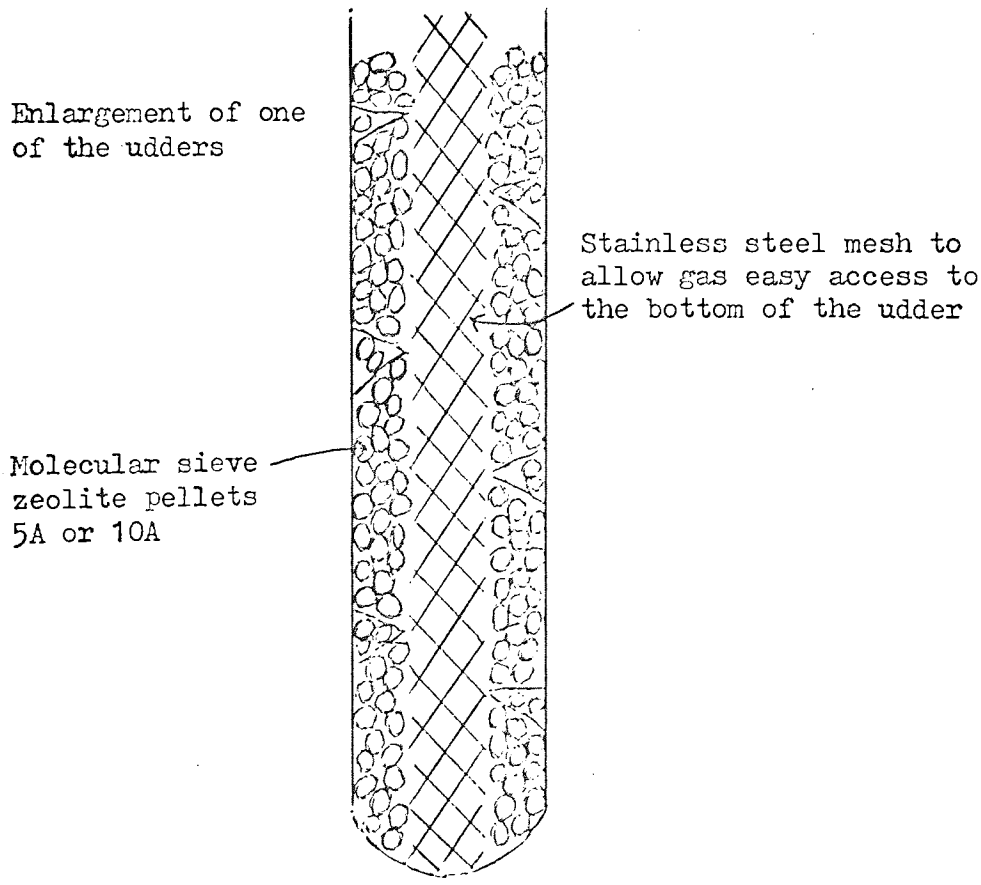

temperatures the gas is adsorbed onto the cold surface and the pressure falls. The size of the pores decides the pumping efficiency of the pumps. A five Angstrom molecular sieve will adsorb gases with a molecular diameter of less than five A. If the sizes of the pores is increased the size of the molecules adsorbed will be increased but the surface area available will be slightly decreased and so the pumping capacity of the pump will be slightly reduced. The best use of these pumps is obtained by "purging out" the system before hand so that the pumps have only to pump small diatomic gas such as nitrogen and not long chain hydrocarbons and vacuum grease.

The zeolite is usually held in a series of long tubes protruding from the bottom of the pump. These tubes are usually about twelve inches long by about an inch wide and contain 100 grams of zeolite. A steel gauze runs down the centre of each tube so that gas has easy access to the zeolite at the bottom of the tube. The number of tubes and amount of zeolite depends on the volume to be pumped.

The molecular sieve is usually heated to 523 K to remove gas which is adsorbed on the pump at room temperature and this may be quite a considerable amount. After this heating, on subsequent cooling one pump, containing 0.5 kg of zeolite and pumping a volume of two litres of "boiled off" liquid nitrogen, may obtain pressure of less than 1×10^{-3} torr. If the pump has to pump a larger volume such as eight litres, the lowest pressure obtained is 3×10^{-3} torr. However by using a combination of two pumps, pumping a volume of eight litres, pressures down lower than 1×10^{-7} torr have been obtained. It has been shown by Cope (70) that zeolites produce optimum low pressures when pumping down "boiled off" liquid nitrogen

FIG. 19 The Pump Down of Various Gases By The Sorption Pumps.

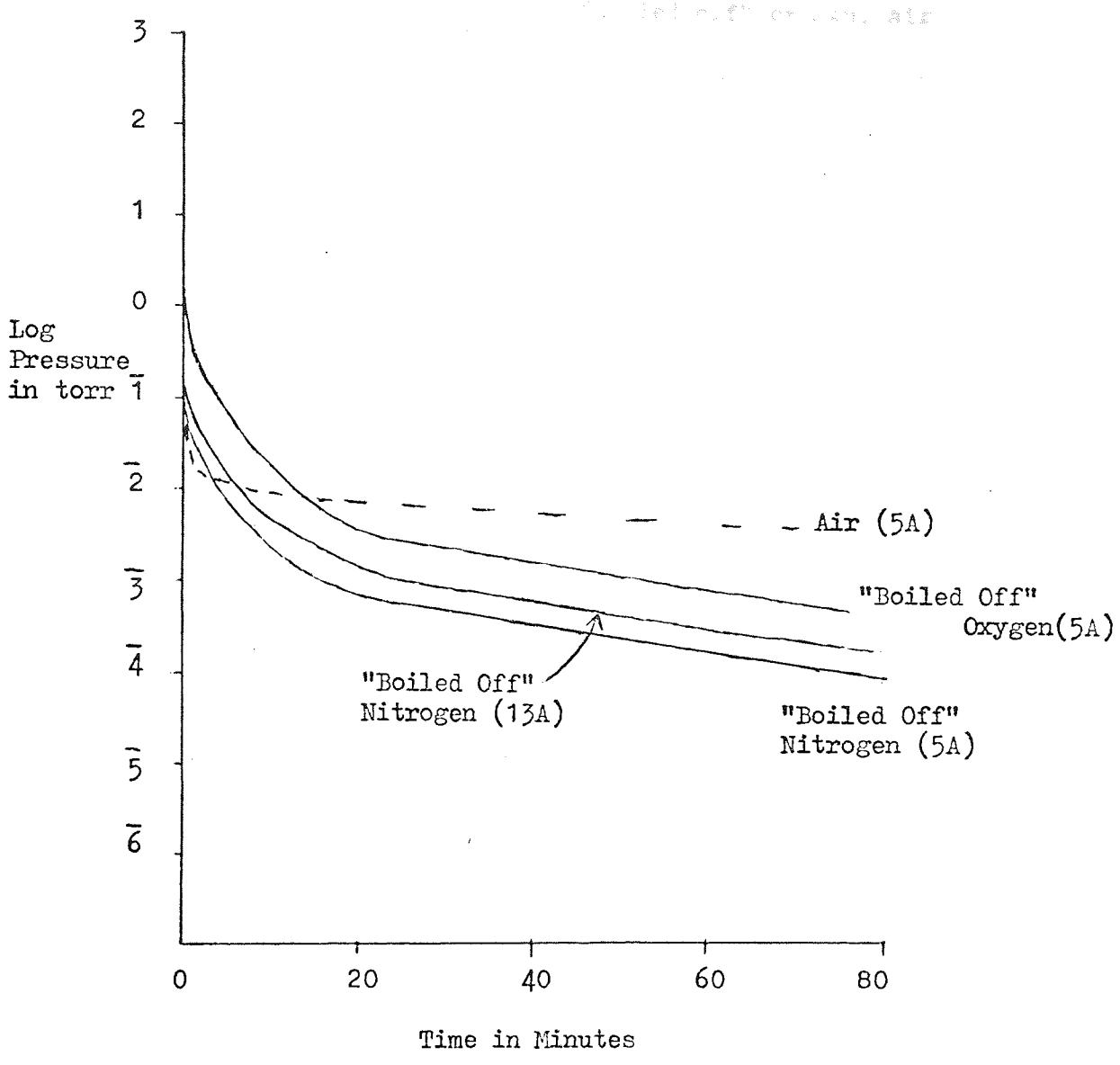

and results are not quite as good for "boiled off" oxygen, air and cylinder nitrogen. This is shown in Fig. 19. The pump does not pump inert gases, hydrogen and water vapour very efficiently but one of the advantages of an adsorption pump is that it does not contaminate a vacuum system in any way.

2.2.5 Getter Pumps

This pump again uses the principle of adsorption of gases on a cooled surface (64). In the case of this pump the adsorbing surface is the getter material. This can be zirconium, molybdenum, niobium but is usually 85% titanium and 15% molybdenum. Filaments of these materials are heated by resistance heating with a current of 40 amps which is obtained from a set of accumulators connected in series with the filament. The getter material evaporates from the filament surface and forms a thin layer on the outer casing of the pump. It is on this surface that the gas is absorbed when the evaporated layer is cooled in liquid nitrogen. Depending on the pressure of the system which determines the useful pumping lifetime of the layer, the time between successive evaporations is determined. This second layer which is evaporated onto the first layer buries the gas which has been adsorbed on the previous layer as well as providing a new layer for adsorption. In a getter pump are several filaments which are flashed in turn. This pump does not constitute a source of hydrocarbon contamination or other kind of contamination. Gases such as oxygen, nitrogen, hydrogen and water vapour are pumped out of the system, however inert gases are not pumped out because they will not adsorb on the titanium film. The inert gases need to be removed from the system beforehand. For a system in which inert gases are being investigated this type of pump is used so that the

FIG 20 The Titanium Sublimation Pump.

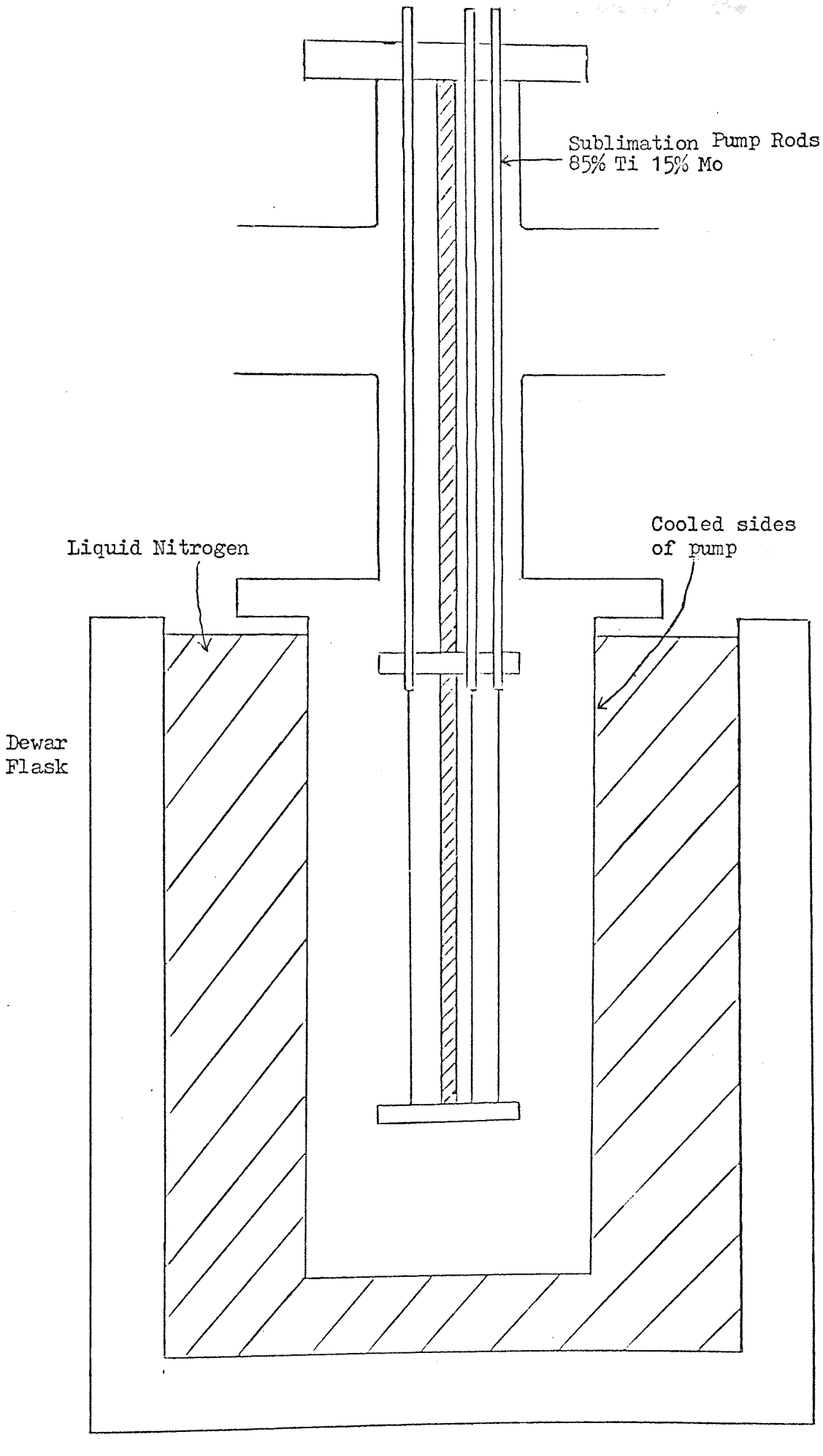

background gases are pumped but the inert gases are not. The pumping speed of this pump is very high when the metal surface has just been deposited and for obvious reasons the pumping speed is dependent on the sticking probability for a particular gas. The pump is usually used in the pressure range 10^{-3} to 10^{-12} torr. Use of the pump at pressures above 10^{-3} torr will result in shortening the life of the filament. The filaments need de-gassing for several hours before use at 30 amps. The pump can be baked but cannot be used during bake-out.

A second type of getter pump is one in which the getter is sublimed by electron bombardment from a molten ball and requires a means for mechanically feeding in the titanium wire. However this does provide a constant stream of evaporated getter for adsorption.

2.2.6 Getter Ion Pumps

There are two types of ion pump namely the sputter ion pump and the getter ion pump (64). In the sputter ion pump positive ions formed in a cold cathode discharge are accelerated to the cathode which is made of titanium. The collision expel s atoms of titanium which are then collected on the cold anode wall and these form a clean surface which chemisort s the gas as in the getter pump. In the getter ion pump the titanium is evaporated as in the getter pump. The gas is pumped by chemisorption at the hot surface. Inert gases are pumped very slowly by this pump and are removed by being buried in the layer of titanium when they collide with it at great velocity. However the titanium layer sometimes wears away and the buried inert gases are allowed back into the system and this is known as the memory effect. The

Table 3
Comparison of properties of UHV pumps

Type of Pump	Traps Required	Starting Pressure (torr)	Pumping efficiency		Pump Cooling	Hydrocarbon Contamination	Advantages	Disadvantages
			active gases	rare gases				
Turbo-pump	None	10^{-2}	12-18	12-18	Water	Oil	No traps, no working fluids.	Low compression ratio, difficult to outgas, some noise and vibration.
Diffusion pump								
a) Mercury	L N_2	up to 100	5-10	5-10	Water	Oil from backing pump	Fluid thermally stable.	Toxic fluid, reacts with metals. Requires trap.
b) Oil	L N_2	0.5	10-20	10-20	Water	Oil	Fluid non toxic, trapped at RT.	Must be efficiently trapped.
Cryopumps	None	Atmospheric	50-90	50-90	Cryogenic fluid	Oil from backing pump	100% system wall area can pump.	H_2 and H_e hard to pump requires constant supply of fluid.
Getter pumps	None	10^{-2}	45	0	None	None	Simple.	No rare gas speeds, limited pump life.

Cont:

Table 3

Comparison of properties of UHV pumps (Continued)

Type of Pump	Traps Required	Starting Pressure (torr)	Pumping efficiency		Pump Cooling	Hydrocarbon Contamination	Advantages	Disadvantages
			active gases	rare gases				
Ion pumps								
a) Getter-ion		5×10^{-3}	45	0.6	Water	None	No trap.	Low rare gas speeds, limited pump life.
b) Sputter-ion	None	2×10^{-2}	15	0.15-5	None	None	No trap.	Pumping speed decreases at low pressures, Memory effect.
c) Orbitron		5×10^{-2}	45	2	Water	None	No magnet, no trap, no Memory effect.	Limited getter life, low rare gas speeds.

getter ion pump is superior to the sputter ion pump in that it does cover the titanium with a fresh layer and so makes it harder for the memory or historical effect to take place. The pump works at a voltage of 8000 volts between the anode and cathode and a magnetic field sustains a Penning discharge in the pump. The pump is capable of being baked and working while at a temperature of greater than 523 K. The pump works between pressures of less than 1×10^{-4} torr down to the 10^{-12} torr range. Since the pump works on the Penning gauge principle it can also act as a gauge and measure pressure accurately by measuring the current between 10^{-4} torr and 10^{-9} torr. The pump once again does not constitute a source of contamination and the pumping speed depends on the sticking probability of the various gases.

2.2.7 Summary of the Pumps Used

To limit contamination to a minimum the pumps used in the ultra high vacuum system used in this work were a getter pump and titanium getter pump. These pumps both had no serious lower limit to the pressures they could attain in the achievable ranges and both have pumping speeds which are sufficiently high to reduce the pressure quickly. A combination of both these pumps will pump most gases but especially nitrogen which was the original occupant of the system. Inert gases are only pumped very slowly though and should be avoided. The use of both these pumps means that the pressure has to be reduced to below 10^{-4} torr before the other pumps may be switched on. The pressure is reduced by using a combination of sorption pumps which are capable of reducing the pressure from atmospheric to 10^{-7} torr. When preparing the sample gases a mercury diffusion pump was found to be acceptable when used with a series of traps and backed

by a rotary pump which also reduced the pressure from atmospheric.

2.3 VACUUM GAUGES

2.3.1 Review

There are a great many vacuum gauges capable of measuring pressure anywhere between atmospheric and 10^{-12} torr (71). Table 4 shows that no one gauge is capable of measuring the full range. Atmospheric pressure and small changes in this are measured accurately by a barometer whilst pressures in the range 1 to 760 torr are measured using a manometer or Bourdon gauge. Pressures lower than this require the use of a Pirani or McLeod gauge. Several gauges are capable of measuring pressures in the ultra high vacuum region such as the Bayard Alpert gauge, the inverted magnetron gauge and the Penning trigger gauge. Several factors need to be taken into account when choosing vacuum gauges. The first is the pressure range to be measured, the accuracy of the pressure measurements, contamination of the vacuum system and whether the gauges can be baked.

2.3.2 The Pirani Gauge

The gauge works on the principle that the thermal conductivity of a filament is related to the pressure of the gas surrounding it (72). If a filament has a steady voltage applied across it, the temperature of the filament will be dependent on the heat transfer away from the filament. The resistance is dependent on the temperature and therefore also on the thermal conductivity and the pressure. By measuring the resistance the pressure can be calculated.

A Wheatstone bridge circuit is used to calculate the resistance of the filament. A constant voltage is applied across the two ends

Table 4 Useful Range of Pressure Measurement for Vacuum Gauges.

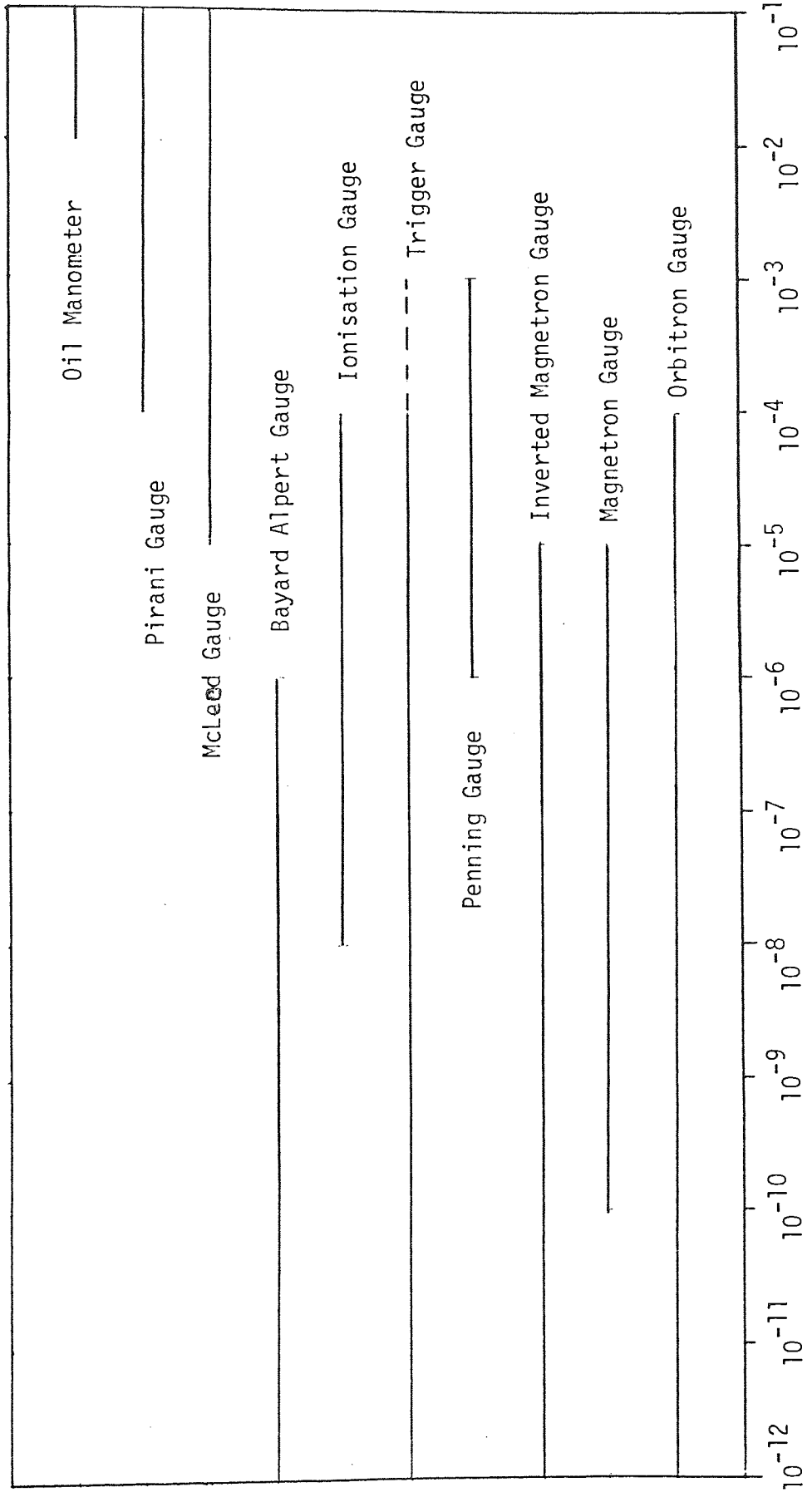

of the bridge. The bridge galvanometer has to be set to zero and this is done by using a pressure which is effectively zero to the bridge. This pressure is less than 10^{-6} torr and when this pressure is obtained the galvanometer is adjusted to zero by altering the resistance R_1 in Fig. 21. The two resistances R_2 and R_3 are equal resistances and the resistance R_4 is approximately equal to that of R_1 and that of the Pirani gauge at the effectively zero pressure. When the gas pressure increases the galvanometer becomes out of balance and this can be used as a measure of the pressure in the vacuum system.

The Pirani gauge has an upper limit of 10^{-1} torr because the filament temperature is not as sensitive until this range. The lower limit is usually set by fluctuations in the voltage supply and gas temperature. The usual lower limit is 10^{-4} torr but for accurate measurement is 1×10^{-3} torr. The most sensitive range is the 10^{-3} torr range.

2.3.3 McLeod Gauge

This gauge was designed in 1874 to measure pressures (73) accurately below 10^{-2} torr. A volume of gas at a low pressure is compressed into a smaller volume which causes the pressure to rise. This higher pressure is measured with the mercury manometer principle. The gauge is calibrated to the lower pressure either by calculation or by actual experimental setting. There are several disadvantages to this gauge. The mercury in the gauge poses a contamination problem and so the gauge must be sealed off from the vacuum system with a liquid nitrogen trap. The gauge is bulky and requires constant attention because it cannot give continuous pressure readings. The gauge is set a slight distance

FIG. 21 a) Pirani Gauge - Wheatstone Bridge Circuit

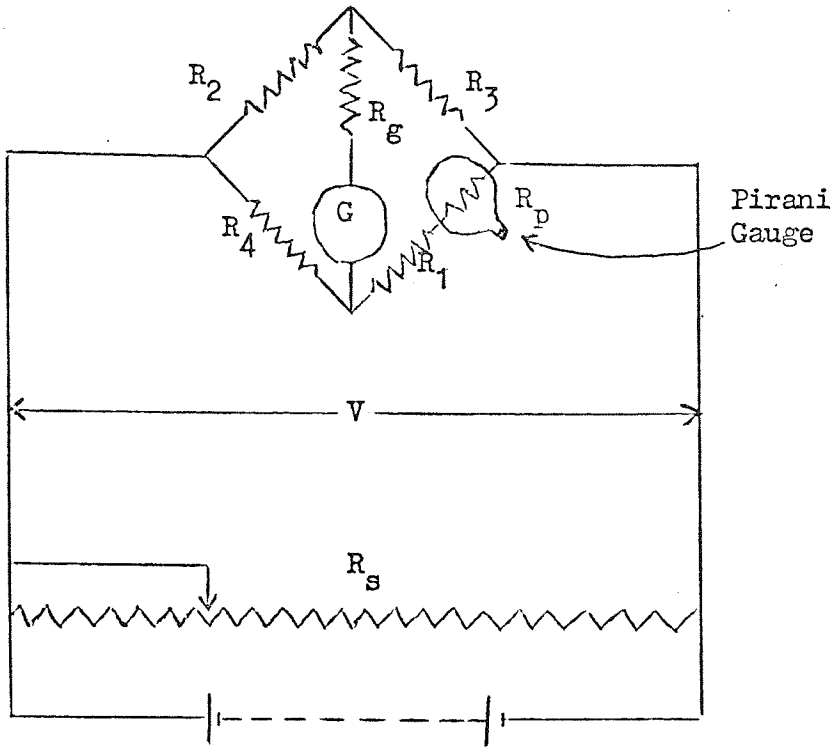

b) The Swivel McLeod Gauge.

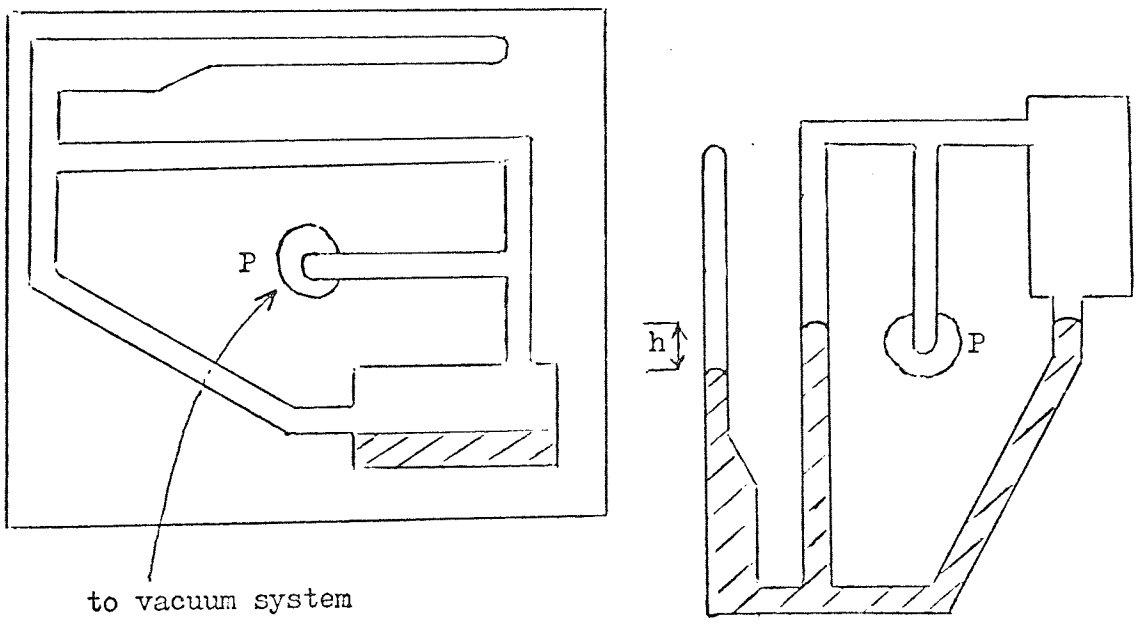

away from the vacuum system and needs connecting tubing and joints. Pressure from 1 torr down to 10^{-3} torr can be measured but the most sensitive range is the 10^{-1} torr to 10^{-2} torr range. A swivel McLeod gauge is more conveniently used nowadays and this is shown in Fig. 21. This gauge pivots about a point P and when the gauge is not measuring pressure the gauge rests so that all the mercury is in the bulb. To measure the pressure the gauge is pivoted so that a quantity of gas is trapped by the mercury in the sealed off limb. The rise of the mercury up this limb is a measure of the pressure in the system.

2.3.4 Ionization gauge (Hot Cathode Gauges)

A simple triode valve structure of cathode, grid and collector is used (71). The cathode is a hot filament which is heated by the emission current which in this case is 0.75 mV. Electrons are emitted from the cathode and these are accelerated towards the grid which is at a positive potential with respect to the cathode. These electrons ionize any gas molecules they meet on their travels and these positive ions are attracted to the collector which is at a negative potential with respect to the cathode. This positive ion current is a measure of the gas pressure in the system and also of the emission current but as this is always kept constant this does not effect the measurement of the pressure. The gauge is usually calibrated against another already calibrated gauge for a gas such as nitrogen for which the gauge then has a sensitivity of one. The sensitivity of the gauge for other gases varies depending on the gas. The degassing of the filament and other parts of the gauge is usually taken into account in the control box. The gauge is connected to the system by a short wide tube because the gauge

can act as a pump and this enables the pumping action due to adsorption on the glass and other surfaces to be uniform throughout the gauge. The pumping action of the gauge may be quite considerable. The gauge is used for measuring pressures between 10^{-4} torr and 10^{-8} torr. The structure of the gauge is shown in Fig. 22. The cathode is a filament of either pure tungsten, thoriated tungsten or platinum alloy placed centrally in the gauge and supported by two steel wires which also act as electrical connections. The filament is encircled by a grid which is shaped as a cylindrical wire helix. This wire is usually molybdenum held in place by two nickel supports which act as electrical connections. The ion collector is an open ended nickel cylinder. The gauge is usually made of glass with metal leadthroughs and connected directly to the system.

The limits of the gauge are between 10^{-4} torr and 10^{-8} torr. The discharge cannot begin until the pressure in the system is 1×10^{-3} torr otherwise the filament will burn out. At 10^{-8} torr X-rays falling on the collector surface release photoelectrons which strike the grid and cause incorrect readings.

To lower the limit of a hot cathode gauge further the size of the cathode has to be reduced as was first shown by Bayard and Alpert (4). The size of the collector was reduced by a factor of 10^{-3} and the whole arrangement was inverted so that the collector was on the inside and the filament was on the outside. This enabled pressures down to 10^{-11} torr to be measured. Reducing the size of the collector even further brings in added problems of supporting a very thin filament. The commercial Bayard Alpert gauge is designed for easy assembly, robustness and will measure pressure

FIG. 22 The Ionisation Gauge

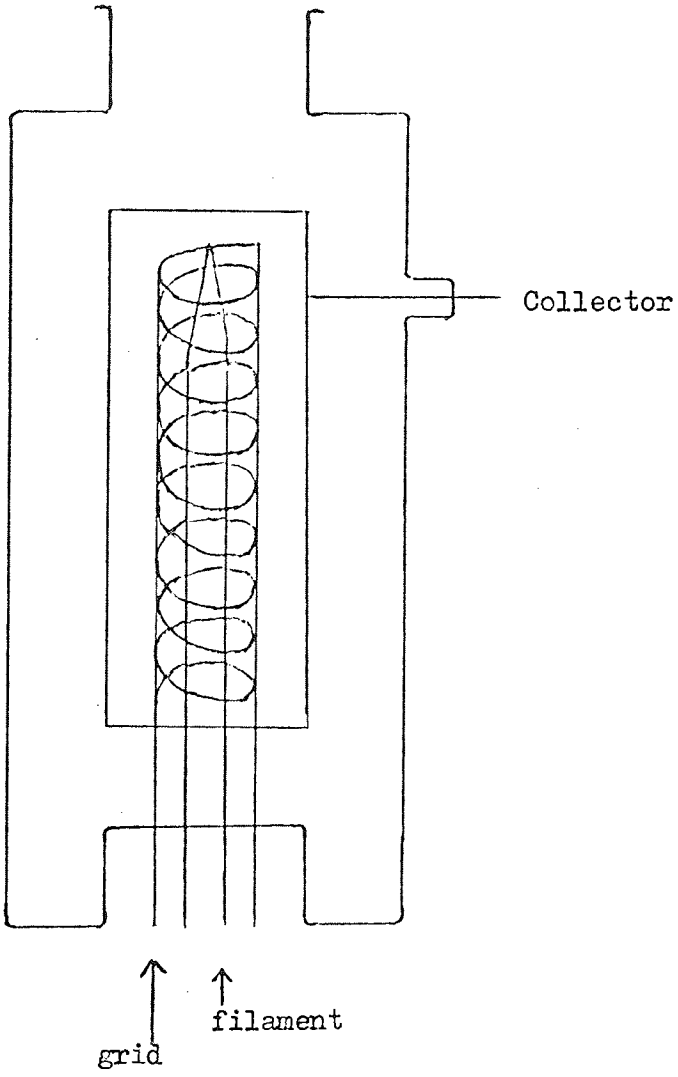

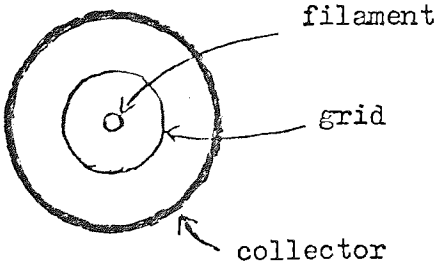

down to 10^{-11} torr. Gauges may be adapted for use at lower pressures but generally these are not as useful for general use. The gauges have to be capable of being baked.

2.3.5 Cold Cathode Gauges (Penning Gauges)

The Penning gauge is a form of cold cathode ionization gauge (74). An anode in the shape of a ring is set with a flat cathode plate on either side on it. The two cathode plates are connected together electrically so that a large voltage difference can be applied across them. The electrodes are set in a glass envelope which is connected to the vacuum system. A permanent magnet is then placed around the envelope, the magnetic field running perpendicular with the plane of the ring. The magnetic field is usually 400-600 gauss. With a DC voltage of 2 kV operating between the anode and the cathode the discharge waits for the appearance of an electron, this electron may be produced by photoelectric emission or cosmic rays or else it may occur naturally in the system when the pressure is high enough. The electron travels from the cathode towards the anode. The electron passes through the anode ring and continues travelling towards the cathode. The cathode repells the electron back towards the anode ring, passes through the ring again and is again repelled by the cathode, the whole cycle repeating itself until the electron is finally captured by the anode. This process greatly increases the path length of the electron. When the electron collides with a neutral atom this atom is changed to a positive ion and this ion is attracted to the cathode. The greater path length produced by this method means that there is an increase in the number of positive ions

produced. The ion current can be measured on a 0-100 μ A moving coil galvanometer because of this increase in the ion current. At pressures higher than 10^{-5} torr the discharge sometimes refuses to start and so a small tungsten filament is placed near the electrode in order to start the discharge. The basic geometry of the Penning gauge was described by Penning and Nienhuis (75). The gauge has a high pumping speed and the output varies non linearly with pressure and this means that the gauge has to be calibrated against another gauge such as a Bayard Alpert gauge. The gauge is very easy to use and there is no X-ray limit. The Penning gauge works in the pressure range 10^{-3} torr to 10^{-6} torr.

A variation of the Penning gauge will measure pressures down to 10^{-13} torr and this is the trigger Penning gauge. The anode instead of being a ring is a cylinder and this increases the sensitivity of the gauge. The trigger gauge combines the robust properties of the Penning gauge with a far better low pressure performance than that of the hot cathode ion gauge because of the higher sensitivity and the absence of an X-ray limitation. The trigger gauge has a filament behind a small hole in one of the cathodes so that when an electron is needed this filament can be heated and supply an electron. The discharge once started is self sustaining. However for more accurate pressure measurements the hot cathode gauges are used.

2.3.6 Summary

The gauges used in the ultra high vacuum system must be capable of being baked to 473 K. The gauge for measuring the pressure change during the flash must be able to record a change of pressure of 2-3 magnitudes in a very short time. The gauge used to measure this pressure change and the ultra high vacuum pressure in general is the

FIG. 23 The Penning Trigger Gauge.

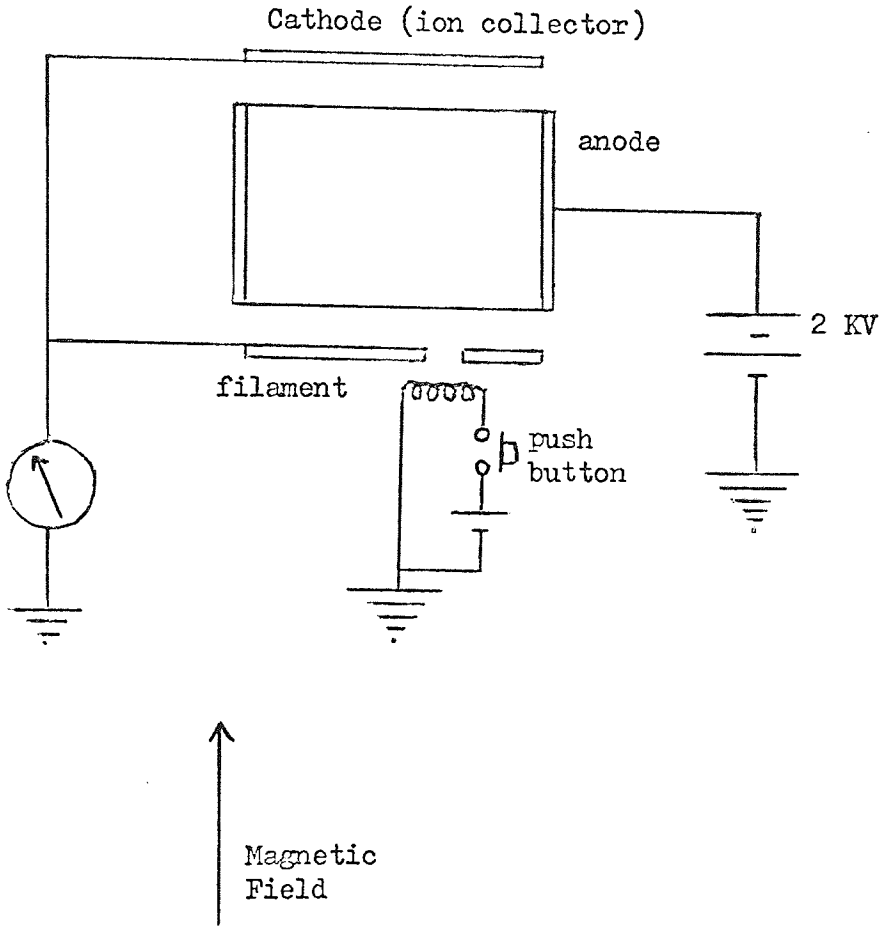

trigger Penning gauge. An ionization gauge is used on the sorption pumps as well as a Pirani gauge so that the pump down of the sorption pumps can be monitored between atmospheric and 10^{-7} torr. These gauges do not contaminate the system and are easy to use because they do not need constant attention. For use on standard vacuum lines a manometer is used for pressure measurements down to 1 mm of mercury and below this a McLeod gauge and Pirani gauge were used.

2.4 REACTION SYSTEM AND MEASURING DEVICES

2.4.1 The Filament

The size of the filament is limited by the apparatus. We would like the filament to be as long as possible to reduce the errors in the calculations. However because of the size of the system, the limitation of the power in the batteries and the size of the pressure rise, the size of the filament is limited. The size of the system is not a serious limitation to the size of the filament. If the filament is too long or too thin the voltage drop across the filament will be very large and the highest temperature obtainable will decrease. If the surface area of the filament is too large and the power available unlimited the pressure rise caused by the flash could be too great for the gauge after adsorption at a relatively high pressure say 10^{-7} torr.

The filament is spot welded onto stainless steel supports which are attached directly to two leadthroughs to the outside of the vacuum apparatus. Good electrical contact is essential and the filament must also be a sufficient distance away from the sides of the apparatus, to stop the filament being earthed but more important not to let the other parts of the system interfere with the filament. On heating, the filament will expand and this should be allowed for

in the design.

The position of the filament in the apparatus is a very important parameter. It is set so that it can be observed in a viewing port so that visual observation can be made. The position of the filament in regard to the pumps, gauges, samples and mass spectrometer needs also to be taken into account.

2.4.2 Mass Spectrometer

The number of mass spectrometers available for vacuum work is very large. The type of mass spectrometer used on the apparatus was a quadrupole mass filter (76). The principle of operation was first described by Paul and Steinwedel (77) and an operating mass spectrometer using this principle was described in 1955 (78). The principle of the quadrupole mass filter is to make the path, the ions describe in the spectrometer, dependent only on the mass M for a given voltage ratio applied to the sets of rods. Only ions in the mass range $(M + \triangle M)$ will perform stable oscillations down the full length of the spectrometer to be received at the collector, the remainder will move in unstable paths and move outside the main axis of the mass spectrometer.

The quadrupole mass filter consists of two sets of rod electrodes suspended in a stainless steel cylinder as shown in Fig. 24. To each of these rods a DC voltage is applied with a high frequency AC voltage superimposed on top of it. The equations of motion of the ions produced by this field are,

$$m \frac{d^2x}{dt^2} + \frac{e}{r_o^2} (U - V \cos wt)x = 0 \qquad \ldots\ (2\text{-}1)$$

FIG. 24 Quadrupole Mass Spectrometer.

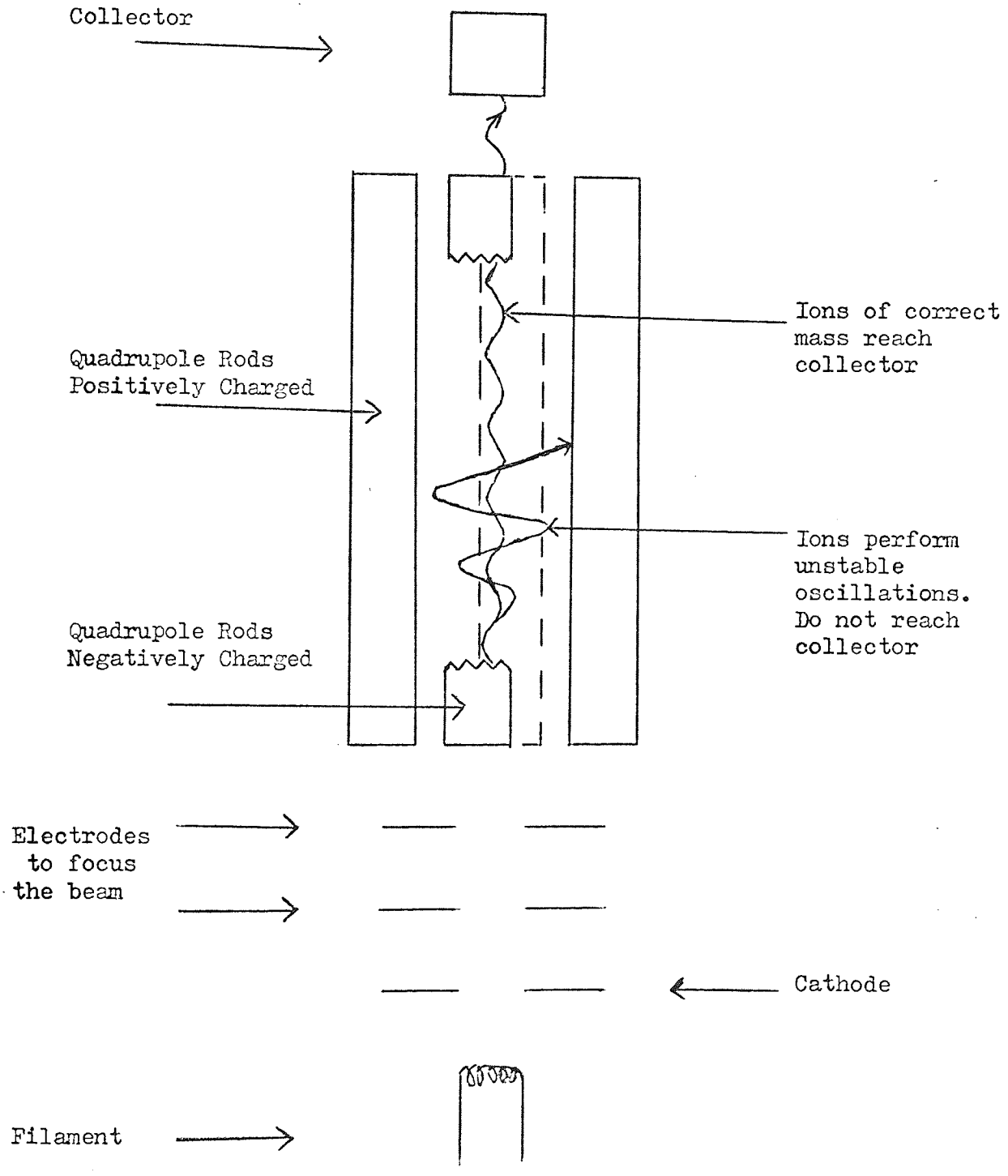

$$m \frac{d^2y}{dt^2} - \frac{e}{r_o^2}(U - V \cos wt)y = 0 \qquad \ldots\ldots (2\text{-}2)$$

$$\frac{d^2z}{dt^2} = 0 \qquad \ldots\ldots (2\text{-}3)$$

here m is the mass of the ion, r_o the radius of the rod, U is the value of the DC voltage and V represents the high frequency alternating voltage. Equation (2-3) shows that there is no acceleration in the z direction which runs parallel to the length of the rods. Equations (2-1) and (2-2) can be transformed into the Mathieu differential equation

$$\frac{d^2x}{d\xi^2} + (a - 2q \cos 2\xi)u = 0 \qquad \ldots\ldots (2\text{-}4)$$

The solution of this equation shows that the ions perform complex oscillations perpendicular to the direction of motion which is along the z axis down the mass spectrometer. For given values of U, V, the frequency w and rod radius r_o the path described by the ions is only dependent on the mass of the ion M or a small mass range $(M + \Delta M)$. Ions which have other masses all perform unstable oscillations and are filtered out when they hit the quadrupole rods and exterior of the mass spectrometer. A mass spectrum is produced by varying the ratio 2 U/V or by varying the DC voltage and high frequency alternating voltage. This produces a mass scan line which passes over the stable region of the ions produced. The value of the ratio which determines the mass scan line also determines the resolution of the device. The variation of the voltages is done

automatically during the scan.

An ion source is required to ionize the neutral atoms so that they can be analysed by the mass spectrometer. A Wehnelt ion source is used to ionize the ions and pass them in a well focussed beam into the spectrometer. The ion source is shown in Fig. 25. A voltage is applied across the filament and electrons emitted from the filament are attracted towards the anode. They pass the anode and travel towards the extraction tube which has a small negative potential and so the electrons turn back towards the anode where they are collected on the opposite side to the filament. On their travels they ionize any neutral atoms that they meet in the central cavity and these ions are attracted towards the extraction tube because of the negative potential on it. The neutral atoms enter the ion source through the hole in the nipple. The extraction tube is only very small and so a high electron density is needed near the tube and the electrons are focussed by a negative voltage on the Wehnelt electrode. A small voltage focusses the electrons but a too high voltage effects the heating current by suppressing the emission from the filament.

The ions after passing through the spectrometer are collected by a Faraday cup at the opposite end of the spectrometer to the ion source. This Faraday cup is connected to a pre-amplifier which leads to an amplifier and recorder. The response time of the amplifier and recorder have to be taken into account when choosing these instruments. The mass spectrometer can sweep its full spectrum in a fraction of a second to several minutes and the devices have to be capable of responding to such sweeps.

FIG. 25 Quadrupole Mass Spectrometer Circuit.

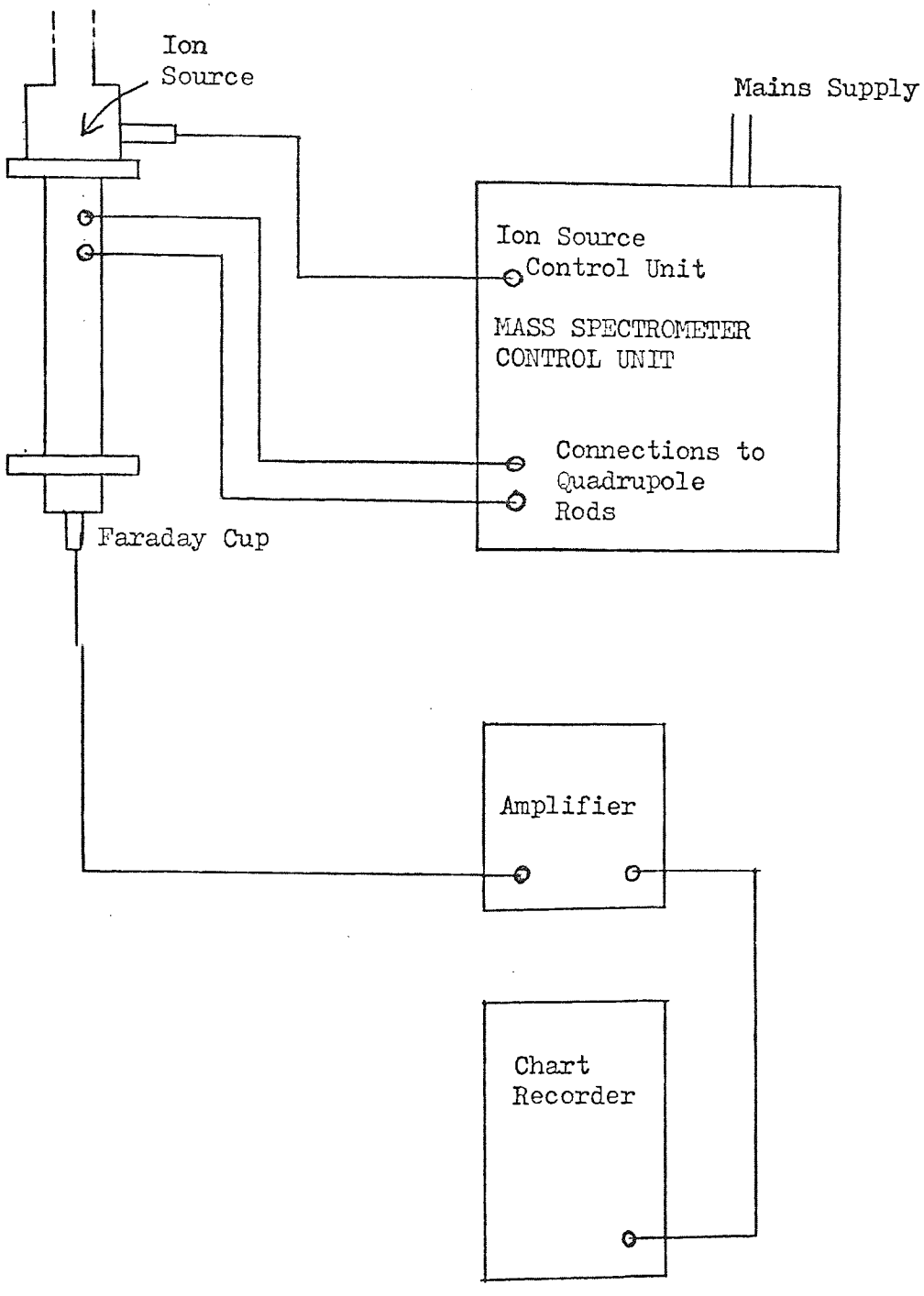

One advantage of the quadrupole is that it is relatively small, easy to handle and does not require a magnet. The scanning time is short and may be varied and the resolution of the peaks is good. The mass spectrometer is capable of detecting peaks when the pressure in the system is very low, when it is used with a sensitive amplifier. The quadrupole system is capable of being used whilst it is being baked. The disadvantage of the quadrupole is that it is capable of detecting peaks only up to a mass range of 200 a.m.u. After this the total number of mass units above this are all combined in one peak at the end of the scan. The apparatus because of its size is not as sensitive as the larger instruments and cannot be used at pressures higher than 10^{-4} torr.

2.4.3 Electrical Circuit to the Filament

The power needed to flash the filament depends on its thickness width and length. The power to our filament was supplied by two 12 volt heavy duty batteries. These were connected in parallel but if larger currents were needed could be connected in series. These accumulators were connected in series with a variable carbon resistor which was used to adjust the current and were needed because of the high currents which would be required. A 0-50 amp ammeter was connected in series so that the current could be measured approximately and then also connected in series was a switch. In the "on" position of the switch the filament was connected but in the "off" position a battery charger was connected to the batteries to keep them on constant charge when not in use. A flasher unit which consisted of a multivibrator circuit and relay was set in series with the power source and filament. This unit could be adjusted so that the relay's terminals were shut for a given time

and as soon as they shut an impulse would be sent to trigger an oscilloscope connected to the unit. The flasher unit was set to be on for 1.2 seconds every 15 seconds approximately but this could be adjusted. In order to measure the current passing through the circuit a shunt was placed in series with the filament so that by measuring the voltage across this known resistance, the current could be calculated by using Ohm's law. The voltage drop across the filament has to be measured and this is done by connecting the two sides of the filament to an oscilloscope. It must be ensured that the circuit is only earthed at one point otherwise erroneous results will occur. The circuit diagram for the filament is shown in Fig. 26. Connections to the filament are made into the ultra high vacuum apparatus by means of leadthroughs in a special connection to the apparatus.

2.4.4 Collection of Results

The results of the flash filament experiment are obtained on an oscilloscope. Because of the speed of the flash a photograph is taken of the behaviour of the trace. The negative is developed and then the negative may be used on an enlarger so that the enlarged picture can be traced onto log graph paper. This enables the value of the pressure to be calculated more easily.

The results from the mass spectrometer are collected on an x-y recorder or on the oscilloscope. The mass spectrometer can be set so that it takes some time to scan the whole spectrum, up to six minutes. This far exceeds the slowest speed of the trace on the oscilloscope and so the x-y recorder is used so that on a slow speed the whole trace can be recorded. The output of the amplifier

FIG. 26 Circuit for Flash Desorption Experiment.

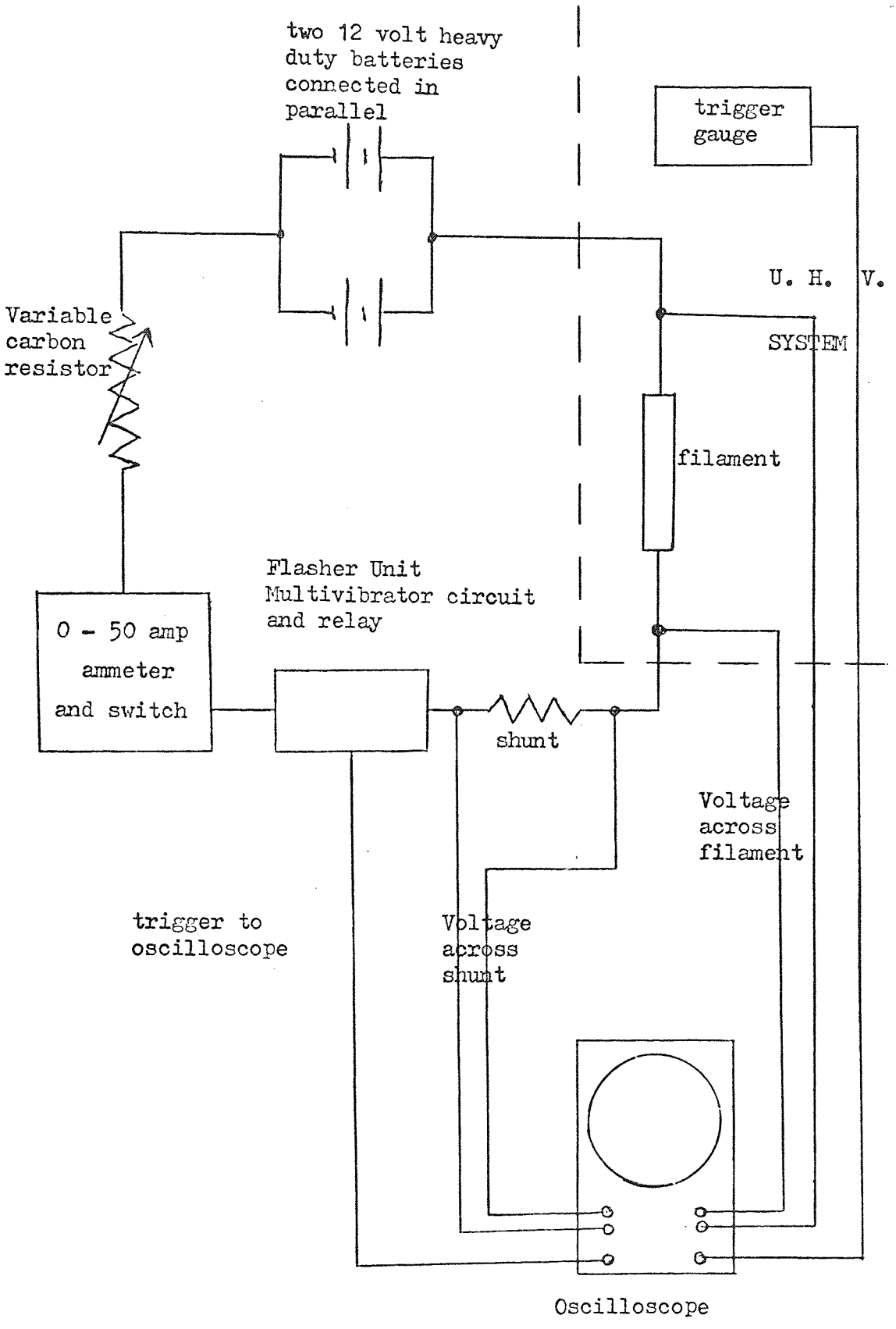

can be adjusted to suit both the x-y recorder and the oscilloscope. The x-y recorder is set so that on the lowest sensitivity a full scale deflection is 8 mV. The response of the recorder is much slower than that of the oscilloscope and so the mass spectrometer is set on a slower scan time.

When a fast response is needed the response must be followed on the oscilloscope. The sensitivity is adjusted to correspond to the output of the amplifier but the oscilloscope trace can be used to follow the mass spectrometer scan when only the lower end of the spectrum is considered. The mass spectrometer can be used to follow the variation of one particular peak during the flash. The variation of this peak can be followed on either the oscilloscope or the x-y recorder but for the quicker response during the flash the oscilloscope is preferred.

3 EXPERIMENTAL TECHNIQUE

3.1 VACUUM APPARATUS

3.1.1 Introduction

The flash desorption technique only became available for research purposes after 1950, this was because an ultra high vacuum system was needed and only after 1950 could the ultra high vacuum region be easily obtained. The filament is placed at the centre of the reaction vessel and the desorption effects are monitored by the pressure gauge. The increase in pressure is usually very fast and so this is usually observed on an oscilloscope. These desorption traces are analysed and the unknown kinetic parameters found by the relationships shown in Chapter 4.

3.1.2 The Apparatus

The filament is cut from a tantalum sheet supplied by Goodfellow Metals Ltd. With a sheet of tantalum, the size of the filament could be cut to the required dimensions. The sheet was 0.0025 cms in thickness and it was found that the most suitable dimensions were 6 cms by 0.25 cms. If a longer filament was used then the voltage drop across the filament was too great for the energy supply to raise the temperature to the required limit. The filament was spot welded to a stainless steel support which was connected one end to each of two leadthroughs in a flange. This flange was connected to one arm of one of two symmetrical six way adaptors supplied by Vacuum Generators Limited, as was the remainder of the stainless steel vacuum apparatus. One of the other arms was connected to a leak valve which was used to allow the sample gases into the system. The sample gases were stored in glass sample bottles connected to a glass metal joint which in turn was connected to a flange, which joined the other

end of the leak valve. A break seal type of separation was used to separate the sample from the system while the system was pumped down. On the other vertical arm of the six way adaptor, opposite the filament leadthroughs, was a reducer coupling to allow the mass filter amp three quadrupole mass spectrometer to be connected to the apparatus. This reducer coupling had a compartment section directly above the quadrupole mass spectrometer so that the ion source could be fitted. A flange to hold a Faraday cup was attached to the bottom of the mass spectrometer so that the ions could be collected and the ion current measured. This part of the vacuum was sealed off as shown in Fig. 27. The ion source, quadrupole mass spectrometer and Faraday cup were supplied by Varian Associates Limited. A viewing port was attached to another of the six way adaptor's limbs so that the filament could be observed during the reaction. This allowed the temperature of the filament to be measured by an optical pyrometer during de-gassing and cleaning. On the limb of the six way adaptor opposite the viewing port was a trigger Penning gauge supplied by Vacuum Generators. This was used to measure the pressure in the system and the pressure variation during the flash. Connected to the remaining limb of the six way adaptor opposite the leak valve for the samples was another leak valve which separated the filament from the vacuum pumps and could be used to alter the pumping speed. This leak valve was connected to another six way adaptor to which the pumps were connected. The vertical top limb of the six way adaptor was used for leadthroughs to a getter pump which was attached to the other vertical limb. The body of the pump was connected to a reducer coupling connected to the six way adaptor and the getter rods for the pump were connected

FIG. 27 Position of the Mass Spectrometer and Filament.

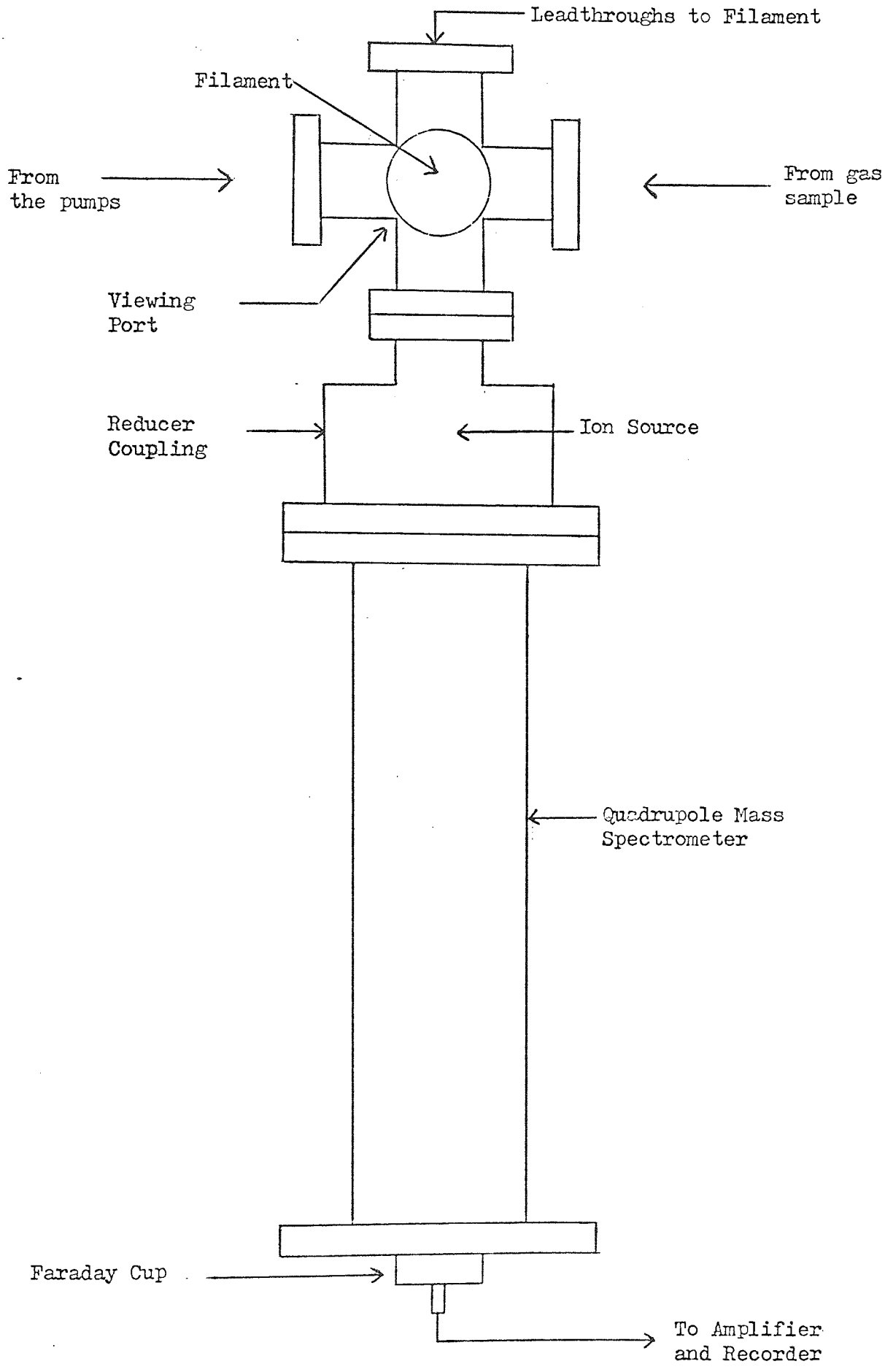

to the leadthroughs from the top flange. A getter ion pump also supplied by Vacuum Generators was connected to one of the horizontal limbs. The getter ion pump could be left on without close attention since it was protected by a cut out mechanism and so this pump was in continuous use during the pump down rather than the getter pump which required continuous attention. On the horizontal limb of the six-way adaptor opposite the leak valve was another leak valve which marked the extremity of the ultra high vacuum part of the system and served to keep out the atmosphere and isolate the ultra high vacuum system. To this leak valve was connected a flange on which was a glass to metal seal and the glass tube attached to this passed outside of the oven used for the bake out to the second of two sorption pumps which were used to pump the system down to a pressure where the pumps in the vacuum system could be started with no harmful effects. The two sorption pumps were separated by a glass vacuum tap so that they could be used independently of each other. To the second of the two pumps was connected an ionization gauge supplied by Mullard and to the first pump was connected a Pirani gauge. Also on the first pump was a safety valve since it was this pump that was used to absorb large quantities of gas and release it to the outside. The pumps were made by the University Glass Blower, Mr B Sabin. An asbestos oven was put round the whole ultra high vacuum section of the apparatus leaving leadthroughs for the various connections and several nichrome wire heating elements were set, attached to the oven around the high vacuum apparatus.

3.2 THE PUMP DOWN

3.2.1 Purging Out

In order to obtain the best results the whole system needs to be "purged out" with liquid nitrogen before the pump down procedure begins. This means that the apparatus is flushed out several times with liquid nitrogen "boiled off" from a container. This process removes air and other gases from the system and leaves it full of nitrogen gas. This has certain advantages over leaving the system full of air. Air contains inert gases and these are not pumped at all or pumped very slowly by the titanium getter pump and the ion-pump respectively. So by removing the inert gases this increases the efficiency of the pumps. The pumping speed is greatest when the system contains "boiled off" nitrogen only and the ultimate lowest pressure obtainable by using the sorption pumps only is lowest when the system is full of "boiled off" nitrogen. Gauges and pumps are usually calibrated for nitrogen.

The vacuum tap between the two sorption pumps is closed and the molecular sieve in sorption pump no 2, that is the one attached directly to the vacuum system is put in an oven and heated to 500 K. The other vacuum taps in the system are left open. The molecular sieve in pump no 1 is also heated to 500 K. Pump no 1 is left open to the atmosphere by leaving the safety valve open and the pressure in pump no 2 is relieved periodically by opening the vacuum valve. After several hours at this temperature when all the adsorbed gas in the molecular sieve pellets has been desorbed the safety valve is shut. By opening the safety valve "boiled off" nitrogen is then blown into the system by means of a tube and air is expelled from

the pump through the safety valve which when the nitrogen is exhausted is shut. The liquid nitrogen vessels were small and because of this, this procedure was repeated three times. When the pump was "purged" the safety valve was replaced and the oven removed. The "udders" were then immersed in liquid nitrogen and the pressure was recorded on a Pirani gauge. The vacuum valve was opened and the whole system was pumped down the 10^{-2} torr region. The vacuum valve was shut and the liquid nitrogen removed so that the pump desorbed all the adsorbed gas and again the safety valve was taken out periodically to release the pressure. The pump was again purged out with liquid nitrogen as before, only after the last time the vacuum valve was opened so that the liquid nitrogen could enter the remainder of the vacuum system. The vacuum valve was then closed. The sorption pump was once again pumped down with liquid nitrogen and the whole procedure repeated. This was done in excess of ten times to ensure all the inert gases had been removed from the system. Each time the percentage of nitrogen in the system increased until finally it is hoped that the percentage of inert gas is negligible.

3.2.2 Pumping Down with the Sorption Pumps

Cope (70) has shown that lower pressures are obtainable when the gas in the sorption pumps is "boiled off" nitrogen rather than oxygen, nitrogen from other samples or air. After the system has been purged out with "boiled off" nitrogen the sorption pumps should be sufficiently full of it to be pumped down. With the vacuum tap between the two pumps shut the heater should be removed from sorption pump no 2 and put around the "udders" of pump no 1. The temperature is increased to 500 K and the safety valve released periodically

FIG. 28 Diagram Showing the Sorption Pumps in Relation to the Ultra High Vacuum System.

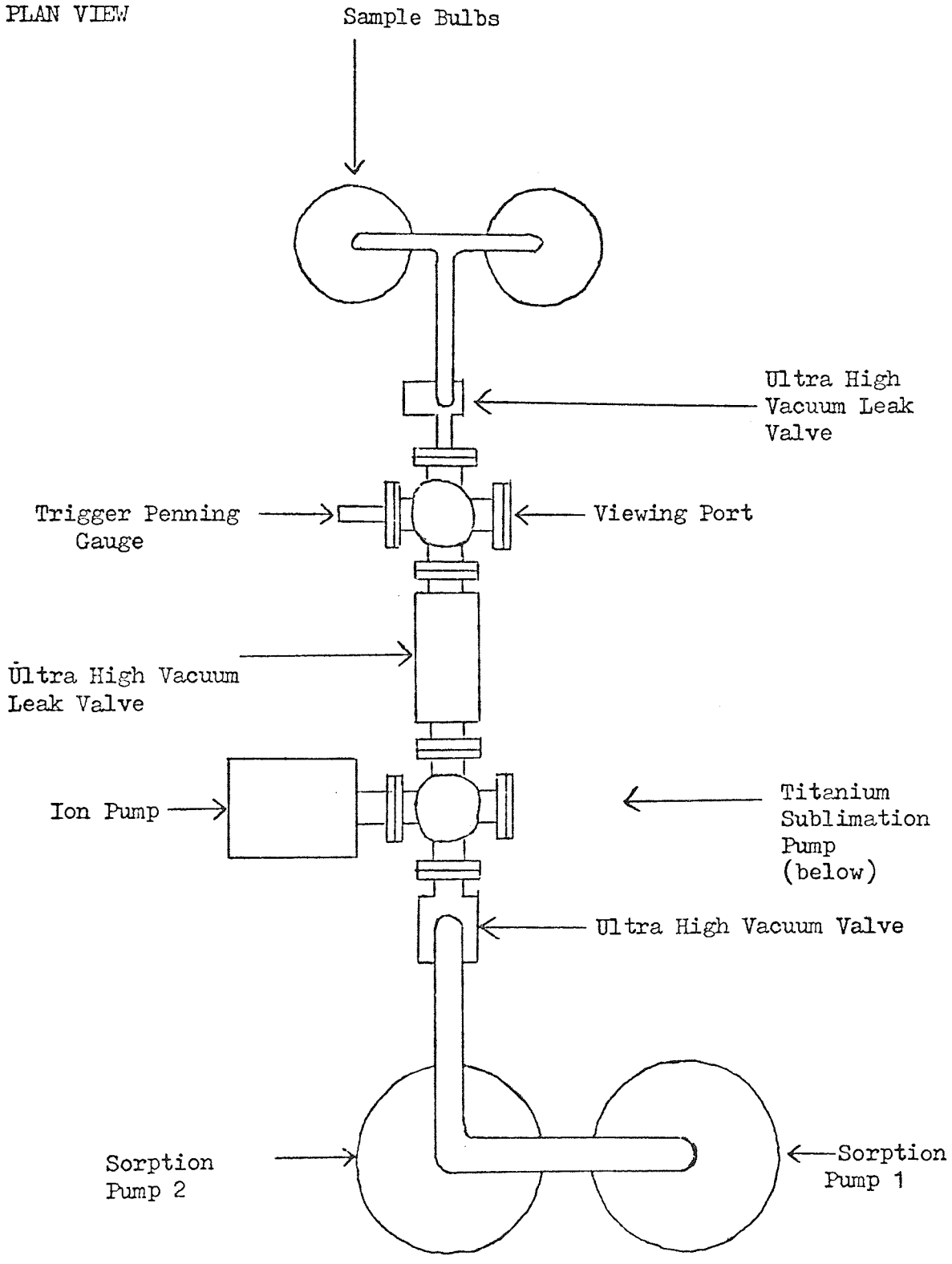

to relieve the pressure. When the desorption of gas from the molecular sieve had stopped the sorption pump was again "purged out" with "boiled off" nitrogen to ensure that any contaminant gas from the molecular sieve was flushed from the pump.

The heater was then removed from pump no 1 and put on the second sorption pump and the temperature again increased to 500 K. The heater was an asbestos box around the sides of which was wound nichrome wire. The two ends of the wire were connected to a variable transformer connected to the mains. The voltage across the heater could be adjusted between 0-240 volts. A voltage of about 30-35 volts gave the required temperature.

After heater no 1 had cooled down for a time the udders were immersed in liquid nitrogen and the pressure drop as a function of time was measured. The lowest pressure obtainable was in the 10^{-4} torr range pumping down a volume of about 3 litres. The vacuum tap between the two pumps was then opened slowly and gas was allowed to flow from the rest of the system into pump no 1. The pump was allowed to pump down the whole system for several hours until an ultimate low pressure was reached. The vacuum tap between the two pumps was closed and the liquid nitrogen removed from under pump no 1. The desorbed gas was let into the atmosphere by releasing the safety valve at various intervals. When all the desorbed gas had been released the liquid nitrogen was again placed around the "udders" of sorption pump no 1. The cycle was repeated and this time an ultimate low pressure was achieved, lower than the previous ultimate low pressure.

FIG. 29 Graph Showing Rate of Pumping of Various Gases.

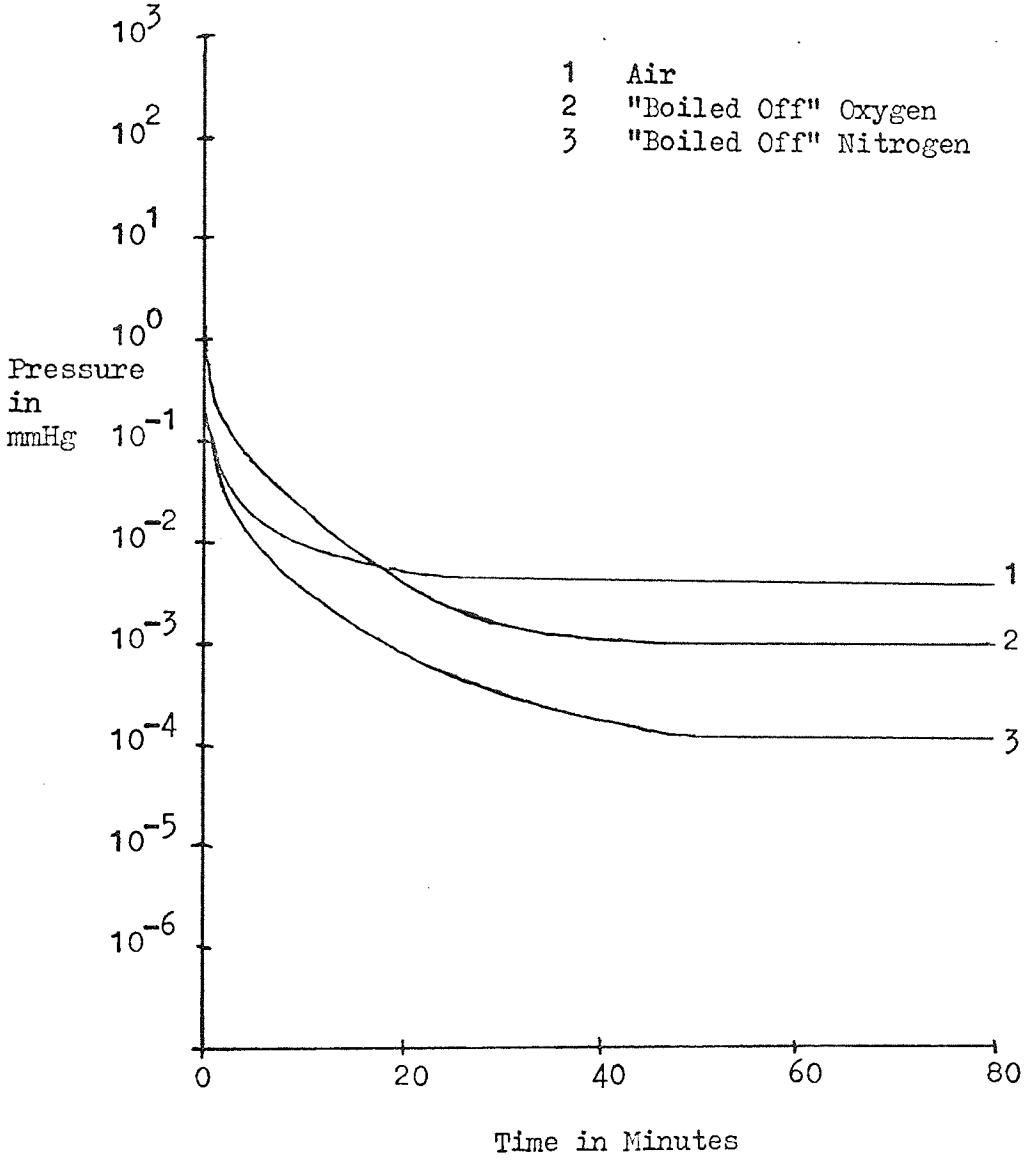

The purpose of the sorption pumps is to achieve a pressure of less than 10^{-4} torr so that the ion pump and titanium sublimation pumps can be started up. Once a pressure in the 10^{-3} range can be achieved by using pump no 1 only then the vacuum tap between the two pumps can be closed and pump no 2 can be put into action.

The heater is removed from pump no 2 and the liquid nitrogen substituted in its place. The pressure measuring device for the range atmospheric to 10^{-3} torr was a Pirani gauge attached to pump no 1 but for readings in the 10^{-4} to 10^{-7} torr range an ionization gauge was used. Before the ionization gauge could be switched on the pressure needed to be in the lower range of the Pirani gauge 10^{-4} torr. If the ionization gauge was switched on before this it would result in the filament burning out. The ionization gauge, when it was switched on, also acted as a pump and supplemented the action of the sorption pump. The trigger Penning gauge attached to the ultra high vacuum part of the apparatus could also be switched on in the 10^{-4} torr range if necessary.

By using the second sorption pump the pressure was reduced into the 10^{-7} torr range measured on the ionization gauge. This pressure is easily low enough to enable the other gauges and pumps to be activated. The ultra high vacuum tap separating the sorption pump from the ultra high vacuum system could be closed. The sorption pumps then having been used successfully could be allowed to reach a state where they did not require constant attention and the various gauges associated with them switched off.

3.2.3 Pump Down with the Getter Ion Pump and Titanium Sublimation Pump

When the pressure has been reduced below the 10^{-4} torr range the Getter-ion pump and trigger Penning gauge can be switched on. The getter pump could also be used if needed. The getter-ion pump initially pumped down slowly from the 10^{-5} torr range but when left overnight had pumped down into the 10^{-8} torr range. The system would not pump down any lower than this without a bake-out. After the bake out was completed the pressure had dropped to the 10^{-10} torr range since the getter-ion pump had been working during the bake out. The getter pump was started. This was done by immersing the pump in liquid nitrogen and cooling down the outer surface of the pump. One of the rods had a current of between 40-43 amps passed through it for 1½ minutes. The pressure in the system rose initially but when the current was turned off fell to a lower value than before. The pumping speed and the pumping efficiency depended on the pressure and for the lower pressure ranges the longer was the period between activating the pump. Table 5 shows the time periods for different pressure ranges. The use of this pump enabled the apparatus to pump down to the 10^{-10} torr range.

The pressure in the ultra high vacuum system was measured by a trigger Penning gauge. This gauge was switched on in the 10^{-4} torr range and measures the pressure on a logarithmic or linear scale depending on the setting of the dials. The gauge worked at a potential of 2000 kV and this as well as the zero had to be checked at daily intervals.

When the pressure had reached the 10^{-10} torr range it was possible

Table 5. Time Between Flashing the Titanium Sublimation Pump Filaments.

Pressure range in mm Hg	'on' Time in Minutes	Time Between flashes in Minutes
10^{-6}	1½	15
10^{-7}	1½	30
10^{-8}	1½	120
10^{-9}	1½	480
10^{-10}	1½	1440

to start taking readings from the apparatus. The trigger gauge needed to be kept on the log scale to measure increases of pressure over two or three orders of magnitude. It was not possible to activate the titanium sublimation pump during the period of adsorption and the flash since this would upset the results which were to be obtained and so the pump was activated before the adsorption time began and it would pump down for many hours.

3.2.4 The "Bake-out"

Once the pressure has reached the 10^{-8} torr range it cannot be decreased without the process of baking out. The ultra high vacuum part of the apparatus is contained in an asbestos oven. Around the inside of the oven is wound nichrome heating wire to allow the oven to be heated to 523 K. During the bake out the trigger Penning gauge is disconnected but the getter ion pump continues with its operation. After removing all but the necessary connections, which are heat proof, the doors at the front of the oven are screwed into position. The connections to the filaments are made through the asbestos walls. The whole oven is now covered by heat shields. These are hardboard pieces supported by stainless steel frames to which has been fixed a layer of heat resisting material such as oven foil covering asbestos wool. Any gaps in the heat shields have to be plugged but some gaps have to be left to allow connections to the filament and thermocouple.

The temperature of the oven is measured by a copper constantin thermocouple. The cold junction of the thermocouple is an ice bath and the hot junction the oven. The thermocouple has previously been calibrated in boiling oil as the hot junction and a plot of change in voltage in millivolts against temperature made. The voltage

FIG. 30 Calibration Chart for the Thermocouple.

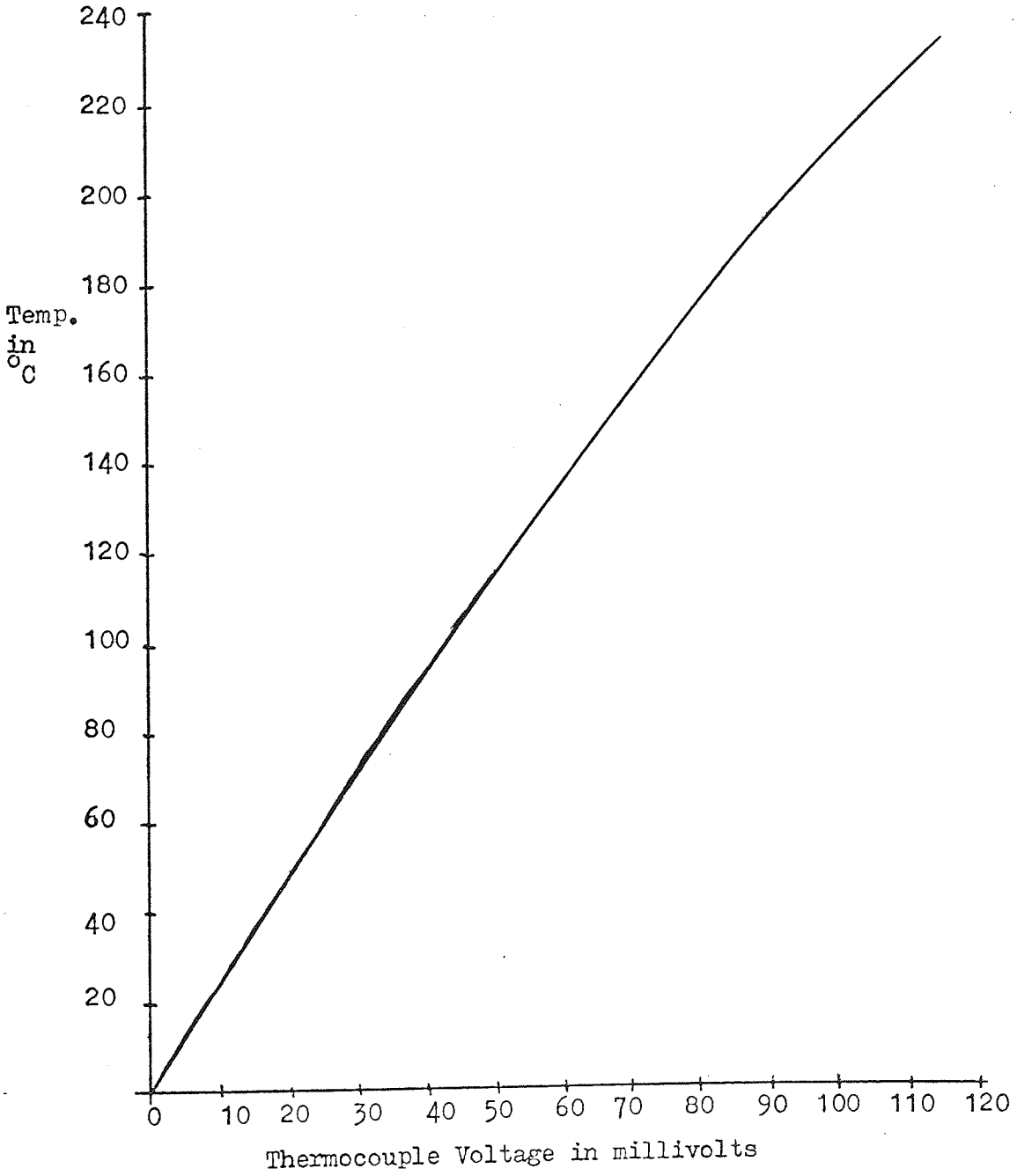

across the thermocouple is measured by a digital voltmeter.

The temperature of the oven must not rise at a rate greater than one hundred degrees centigrade per hour or else the expansion of the ultra high vacuum apparatus could cause leaks. It is important therefore to plot a graph of temperature against time as the experiment is performed so that the heating rate does not exceed the said amount.

The heating wire is connected directly to the mains. In the oven there are three heaters and these are switched on and off alternately so that each side of the oven is heated equally. When the oven is first switched on the temperature rises very quickly and a long "off" time is needed, but gradually the temperature can be increased so that one heater is needed on all the time and eventually both heaters can be left on to reach a final ultimate temperature.

The oven should be kept on for a maximum of forty-eight hours and if possible for as long as two weeks. The only way the connections to the filament can be heated is by conduction along them and this takes time. The getter ion pump must have time to pump the system down as low as possible.

When the heater is switched on the pressure rises from the 10^{-8} torr range up to the 10^{-5} torr range. This is eventually pumped down back to the 10^{-8} torr range and when the oven is eventually back at room temperature the pressure falls into the 10^{-11} torr range. The pressure during the bake-out is measured on the ion pump pressure gauge.

When the heater is switched off the temperature should not be

allowed to fall at a rate greater than 100 K per hour, although this is not a great problem and one will find that with efficient heat shields when both heaters are switched off the temperature does not fall at a rate greater than this.

While the oven is on at the maximum temperature the filament is flashed to desorb gas from the filament and the getter pump filaments are left on, each at 30 amps for an hour.

3.3 FLASH DESORPTION EXPERIMENTS

3.3.1 Electrical Connections

In order to flash the filament the leadthroughs need to be connected to a power supply. This is done using the circuit shown in Fig. 26. The 12 volt accumulators are kept on a continuous trickle charge when not in use so that they are capable of providing a large current when needed. The flashing device is set by using a combination of capacitors in a multivibrator circuit to allow the current to flow for about 1.2 seconds and the accuracy of this can be checked on an oscilloscope. The oscilloscope is connected to the trigger and when the relay switches on the oscilloscope is triggered. The magnitude of the current is controlled by two carbon resistors which may be varied by a screw control. The current is measured on an ammeter which gives approximate values and serves as a guide. The actual current is measured by calculating the voltage drop across a shunt, the resistance of which is accurately known. The voltage across the shunt is measured by the oscilloscope since two wires, one from each side of the shunt, are connected one to the oscilloscope and one wire is earthed. The voltage drop across the filament is measured similarly. However the voltage drop measured here is that

from a large number of components and this must be taken into account when calculating the resistance of the filament. By taking the temperature with an optical pyrometer and at the same time calculating the resistance of the circuit the value of the resistance of the other part of the circuit, apart from the filament, can be calculated. Great care must be taken when setting up a circuit with so many earths not to get an earth loop and it is an advantage to earth all the various earths to the same place. The trigger Penning gauge control box is also connected to the oscilloscope. The output from the gauge along this lead is 0.2 volts per decade and so by setting the oscilloscope trace to 0.2 volts per cm, each centimeter on the oscilloscope grid corresponds to 1 order of magnitude rise in pressure. By taking the equilibrium pressure before the flash a reference point on the grid can be found and by this method the increase in pressure is calibrated. The gauge was set on a logarithmic scale so that large rises in pressure could be followed.

The mass spectrometer is connected up as shown in Fig. 25. The output of the Faraday cup is connected to an amplifier which in turn is connected to a recording device, a chart recorder. As the mass spectrometer scans the range or the peak the output of the Faraday cup is plotted directly onto the chart.

3.3.2 Adsorption and Desorption

Before the experiment takes place the filament needs to be cleaned. This was done by flashing it to 2300 K for several minutes before the experiment. We are presuming that at this temperature all adsorbed gases are desorbed from the filament. When the filament was clean it could be set at 2300 K and the sample gas let into

the system at a pressure of a hundred times that of the background gas. The adsorption time was started when the filament was switched off. This was done so that the sample gas can adsorb on a clean filament and not one contaminated with background gas. The pressure at which the gas was allowed to adsorb was noted. After the adsorption had been completed the sample was shut off again and the excess gas in the system was pumped away. When an equilibrium pressure was reached its value was noted. The sample was now ready to be flashed and the gas adsorbed on the filament could be desorbed. The oscilloscope was set for a single sweep and the current needed to raise the temperature to an acceptable value had been set beforehand. The flashing device was switched on and this automatically triggers the apparatus and the camera on the oscilloscope photographs the single sweep.

The experiment was repeated with varying adsorption times and temperature-time relationship. A background run was performed to assess the increase in pressure due to the background. The negative in the camera was developed and the numerical value of the experimental parameters was calculated.

By trial and error methods the temperature at which a good, clear, well resolved peak was obtained could be found. In the case where more than one peak was found the situation can be more complicated and the peaks may overlap. In this case to obtain a clear picture of the first peak the filament would be flashed at a low temperature so that only the first peak was seen on the oscilloscope. To see a clear picture of the second peak it was necessary to allow the gas to absorb at a temperature which was greater than that at which the first peak was desorbed and lower than that temperature which will effect the adsorption and desorption

of the second peak.

The pressure rise during the desorption process must not rise above 1×10^{-4} torr otherwise the protect mechanism on the pressure gauge will operate and the gauge will "cut out". Once again trial and error tests will show what the maximum expected pressure will be and the pressure of adsorption of the gas may be used to increase or lower the maximum pressure.

The mass spectrometer will be used to identify the species desorbed during the flash. This was done by analysing the mass spectrometer trace which was obtained during the flash. The system was prepared as for the flash desorption experiment. The gas is allowed to adsorb on the sample and the background gas was pumped away. A mass spectrum of the background was taken so that one was able to see what the background gases were. The system was sealed off from the pumps so that the gases that are desorbed are not pumped away before the mass spectrum can be taken. The current was switched on and the temperature of the filament raised slightly. Because of the response time and the time of scan of the mass spectrometer it was not possible to take a mass spectrum very quickly. It takes about six minutes for a complete scan of the full spectrum. The filament was left at this low temperature during the scan. The temperature was once again raised and another full scan was completed. This was repeated for many temperature rises so that a complete change in mass spectrum during the flash can be observed. The approximate temperatures at which the desorption peaks come off the filament can be estimated from the flash desorption experiments. If the mass scale was set on a

specific peak then we can follow this peak during the flash. The main purpose of the mass spectrometer was that we were able to identify the desorbed species and this information could be used with kinetic information to give a clearer indication of surface phenomena. If more than one species was desorbed during a particular temperature this could be seen from the mass spectrometer work.

The mass spectrometer will give a spectrum with the pressure in the 10^{-9} torr range but here the resolution was very poor and the peaks obtained were just distinguishable from the background noise. In order to receive peaks which were well resolved and of a suitable height then a pressure of greater than 1×10^{-7} torr was needed. This was usually obtained when the gases are desorbed from the filament but if this pressure is not reached the experiment will have to be repeated at higher adsorption times. The mass spectrometer can also be used to give an idea of the kinetics of the surface using it as a partial pressure device. Leaks, impurities and the background gases could be investigated using the mass spectrometer and action could be taken using this information.

3.3.3 Oscilloscope Display

A four-trace oscilloscope was used. The two traces which were obtained on a conventional oscilloscope were each split. The time of sweep of the oscilloscope could be varied from a number of milliseconds per cm to a maximum of five seconds per cm. The voltage could be varied from 10mV per cm to 5 volts per cm. For the flash, the time of sweep was set at 2 seconds and at the start of the flash a 9 volt pulse triggered the oscilloscope. Since the

flash lasts for just over a second the pump down at the end of the flash was also seen on the trace. The pressure trace was set on 0.2 volts per cm since this fitted the output of the gauge control unit. The voltage per cm for the voltage change across the shunt and the filament depended on the maximum temperature that had to be obtained. It was found that the voltage drop across the shunt was a matter of a number of millivolts but the voltage drop across the filament circuit was several volts.

The time of the flash was checked by having the trace on continuously and by flashing the filament. The time of flash could be observed from the time between where the voltage suddenly increased and when the voltage dropped suddenly. This was repeated several times.

The number of volts per cm for each of the traces was checked by putting a known voltage across at each of the settings. It was found that the oscilloscope settings were accurate.

When the voltage settings were set to the lowest limit it was found that distortion occurred due to the mains 50 cycles per second ripple. It was therefore preferable if these low settings could be avoided because of the difficulty in measuring the exact increase in the voltage.

3.4 MASS SPECTROMETRY

3.4.1 Assembly of the Mass Spectrometer

The mass spectrometer was attached to the vacuum apparatus by means of a reducer coupling. The ion source fitted into the reducer coupling and this was allowed for in the design of the reducer coupling which had to be specially made. Onto this reducer

coupling was fitted the mass spectrometer and onto the end of the mass spectrometer the collector flange with a Faraday cup.

The ion source had to be assembled and fitted onto the mass spectrometer prior to fixing onto the apparatus. The ion source was assembled with a 1/1000 inch tantalum filament which was used to ionize the neutral species. The ion source clipped firmly onto the top of the mass spectrometer. The connections to the filament and for the various voltages to be applied were made between the ion source and the mass spectrometer. The leadthroughs to the ion source were situated on the mass spectrometer itself.

The mass spectrometer flanges had lead 'O' rings between them. These were tightened down until the soft lead was squashed between the two flanges and formed a leak tight seal. The Faraday cup collector was situated at the bottom end of the mass spectrometer held in a flange also connected to the mass spectrometer by a lead 'O' ring.

The apparatus was pumped down with the various vacuum pumps. The pressure obtained without a bake out was the upper reaches of the 10^{-8} torr range. It was found that when the mass spectrometer was baked a large amount of de-gassing occurred. Care had to be taken not to let the pressure rise too high so that the pump cut out. However even after seventy-two hours baking a large amount of de-gassing still occurred. Also care had to be taken with the lead 'O' rings since with the expansion and contraction leaks were found to occur.

3.4.2 Operation

The connections to the mass spectrometer were made from the

control unit. The Faraday cup connection was connected to the amplifier and the amplifier output was connected to the recorder. The ion source was also connected to the mass spectrometer control box.

The mass spectrometer scan was set to the required degree and when switched on was observed to be working. The filament current was checked, this was 6 amps. The recorder was zeroed and set and the amplifier set on a low sensitivity. The focussing voltages on the ion source were adjusted so that the most sensitive condition of the mass spectrometer was found. The time of the scan was set and the scanning time and the amplifier and recorder were set so that the output of the amplifier could be mapped out on the recorder.

3.4.3 Result Collection

The zero on the recorder was set. The setting on the amplifier was selected and the zero was readjusted with the backing-off switch. The mass scan switch was then adjusted to the set range, usually position 1 for a slow scan and the movement of the pen of the x-y recorder was traced out on a sheet of graph paper. One of the scales was a time scale and the other was a voltage scale depicting a voltage which was proportional to the number of ions collected at the Faraday cup.

To calibrate the scale so that we could recognise the unknown peaks, gas that produced known peaks had to be leaked into the system. This was done with acetone, methyl alcohol and carbon tetrachloride. The sample gas was analysed on the MS9 mass

spectrometer by Mr M Houghton and the peaks obtained and identified on the large mass spectrum were compared with the peaks found on the quadrupole mass spectrometer. The analysis showed that the sweep was very nearly linear, only varying slightly from linearity at high mass values. The distance between two peaks at low masses was found to be 0.7 of a unit on the graph paper or 0.07 inch.

These sample gaswere pumped out of the system thoroughly and the apparatus set up for the actual gas to be investigated. The apparatus was purged out with nitrogen and a large background peak at 28 was found.

The filament was flashed and the sample gas allowed to desorb on the filament at a given pressure and an analysis of this gas was done whilst it was adsorbing. The sample gas was shut off and the apparatus allowed to pump down. The filament was shut off from the pumps and a background spectrum was again taken. The filament was flashed and again a spectrum was observed. The experiment was repeated with the filament left on during the mass spectrometer run. An analysis of the increase in pressure due to the background gas had been done beforehand. When the filament was flashed after adsorption, the desorbed gases may have been re-adsorbed before they could be analysed by the mass spectrometer, and if the filament was left on desorption from the walls could become a problem.

The experiment could also be repeated and left open to the pumps but in this case some species may be preferentially pumped and their peak considerably reduced compared to the others.

The various peaks which were seen to increase during the flash may now be independently investigated. The voltages on the mass spectrometer rods were set on a particular peak. This was done using the heliopods on the control box and setting each one on a particular peak was done quite simply. Each of the peaks was now observed through the flash. This was more easily seen on the oscilloscope because of its faster response. The two disadvantages with the oscilloscope were its fast scan time and that the voltages we were dealing with were near the oscilloscopes limit of detection.

However how each peak behaves and its proportional increase could now be observed. Each desorbed species may be analysed and identified.

By varying the pressure and observing the peak height of the particular peaks a graph of pressure against the corresponding peak height voltage could be plotted. This was a straight line showing that the peak voltage was proportional to the pressure. The peak height indicated the partial pressure of the peak in the system.

3.5 PREPARATION OF THE GAS SAMPLES

3.5.1 The Need for Pure Samples

The gas samples are obtained as pure as practically possible. Some gases may be obtained as being 99% pure but others, especially organic gases are contaminated with minor contaminants which are produced by the splitting of the main molecule and also by addition of hydrogen to the main structure. In the case of ethylene for

example species found along with the ethylene are CH_2^+, CH_3^+, CH_4^+, $C_2H_3^+$, $C_2H_5^+$ and C_2H_6 along with any background gases that are present.

When we consider an adsorbed state on a metal it is necessary to know what the structure of the adsorbed molecule is as well as where the adsorbed molecule came from so that the mechanism of adsorption can be estimated. It is a great asset therefore if the gas surrounding the metal has only one structure and formula or that one species greatly outnumbers the other species present.

Also if more than one species is present the quantitative results may be affected. If more than one species is adsorbed at a particular site or binding energy then it is very difficult to differentiate between the two. Also one species may be preferentially adsorbed and unless the experiment had been done with a pure sample previously this information could not be found.

It can be seen from mass spectrometric evidence that purification of the gas samples by the method used helps to achieve a purer sample as well as providing an easy method for obtaining the samples in the sample bulbs.

3.5.2 Apparatus

I would like to thank the University Glass Blowers, Mr Herricks, Mr Sabin and Mr Cutforth for all their hard work and advice in the construction of this apparatus.

The apparatus consists of a mercury diffusion pump which has a rotary pump which acts as a backing pump to it as well as being able to pump the system down on its own. To the diffusion pump is

Fig. 31 Apparatus Used to Prepare the Gas Sample in the Sample Bulb.

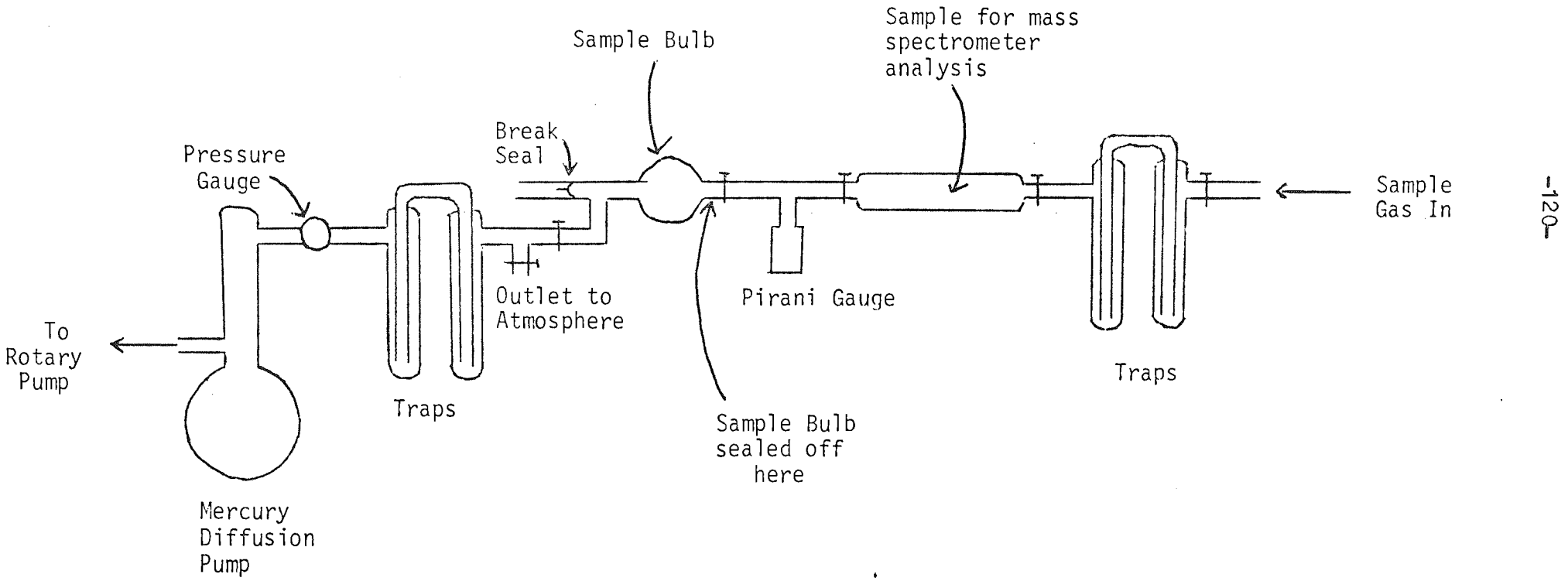

connected a series of traps which prevent mercury vapour from the diffusion pump and oil vapour from the rotary pump getting into the system. Although no pump is 100% efficient this series of traps prevented so much mercury from getting into the system that none at all was detected throughout the experiment. These traps were connected to an outlet to the atmosphere which allowed the system to be flushed out without effecting the pumps. The sample bulb was next attached. This was based on a 500 ml round bottom flask with a break seal and passage allowed for the gas to pass through the sample bulbs and for connections to the rest of the apparatus made. A Pirani gauge was then attached on a side arm between the sample bulb for the apparatus and the sample bulb for the mass spectrometric work. This second sample bulb was then attached to the apparatus and this was then connected to another trap. One of these contained molecular sieve pellets which would be used to trap the gas. The gas cylinder was then connected to the end of the traps by a rubber tube.

The pressure in the system was measured by a mercury manometer, a McLeod gauge and a Pirani gauge. The Pirani gauge was only useful for measuring the ultimate low pressure in the system. It would have been more useful to have a McLeod gauge in its place but this would have introduced mercury into the system between the traps. The McLeod gauge and the mercury manometer were placed between the diffusion pumps and the traps. The mercury manometer was used to measure pressures between 760 and 1 torr and below this the McLeod gauge was used.

The vacuum joints used were greased joints held together

strongly with clips. Care was taken with the grease so as not to contaminate the system more than was necessary. The use of greased joints was necessary since financial and experimental problems of the alternative methods could not be overcome.

3.5.3 Method

The apparatus was set up as above with great care being taken when making the joints and greasing the taps so that no leaks should occur. The rotary pump was set working and allowed to pump the system and the pressure was reduced to at least 0.1 torr which was measured on the mercury McLeod gauge. The system was checked for leaks and when all was leakproof the mercury diffusion pump was switched on. The pressure in the system was reduced to less than 0.01 torr on the McLeod gauge and the pressure on the Pirani gauge in the vacuum system was reduced to 0.02 - 0.025 torr. The sample bulbs and other apparatus which could be heated were warmed to degas the bulbs and system and remove any water vapour which was trapped in the system. An oven was put around the molecular sieve pellets and the temperature raised to 573 K which de-gassed and activated the pellets. During this period both the sample bulbs were de-gassed by heating gently. This removed quite a lot of water vapour which was present in the system and also moved other desorbed gases from the sides of the bulbs.

The pumps were then isolated from the system and the system again checked for leaks which might have occurred during the heating of the system. The gas from a gas cylinder was then allowed into the system and allowed to purge out the system by passing through it for 30 minutes whilst the system's sample bulbs were

again heated.

For ethylene and carbon monoxide the following method was then used. The system was closed from the gas cylinder and the oven removed from the molecular sieve. The molecular sieve was then placed in a liquid nitrogen containing dewar and the pressure in the system was monitored whilst the gas was adsorbed on the molecular sieve. When sufficient gas had been adsorbed the pumps were allowed to remove any excess gases from the system. The pressure in the system was reduced to less than 0.01 torr again measured on the Pirani gauge. The pumps were again isolated from the system and the molecular sieve allowed to warm up. The pressure in the system was observed and when the pressure had increased by 20 torr the molecular sieve was sealed off from the system and the liquid nitrogen was placed under it again. The pumps were allowed to pump away this first 20 torr of gas in which would be concentrated the lower molecular weight fraction of the contaminants of the sample gas. When the pressure had once again reached less than 0.01 torr the system was ready to be used for collecting the gas for use. The molecular sieve was again allowed to warm up and the pressure in the system was allowed to increase to 30 torr when once again the molecular sieve was isolated from the system, leaving on it the higher molecular weight impurities of the sample gas. The vacuum taps on the sample bulbs were closed and the one for the vacuum system was taken to the Glass Blower for sealing off and the other sample tube was taken for a mass spectrometric analysis. This mass spectrum was used to show that in fact the gas we had collected was indeed the sample gas and that it was

not contaminated with any products from a leak which may have occurred.

In the case of hydrogen the method of preparation was slightly different due to a special property of hydrogen. When the molecular sieve is at liquid nitrogen temperatures if hydrogen is passed through it the hydrogen will be allowed to pass whereas any higher molecular weight impurity will be adsorbed on the sieve. After collection of the hydrogen in the sample bulbs the pressure was reduced slightly for use in the vacuum system.

When the vacuum system is baked out the temperature rises by a factor of two and this would double any pressure in a sealed vessel. In order to reduce any chance of explosion the pressure in the sample bulbs is reduced below atmospheric to about thirty torr.

3.5.4 Mass Spectra

The mass spectra analysis in Tables 6, 7 and 8 show a comparison between the sample obtained for use and the sample obtained straight from the cylinder. It also shows what impurities are present and shows that no extremely harmful compounds are to be put into the vacuum system, such as long chain hydrocarbons. In all cases of the mass spectra obtained no peak above forty-four was observed to increase when compared with background spectra taken both before and after the sample run. A typical mass spectrum and background run is shown in Fig. 32.

An analysis of the carbon monoxide spectrum shows that predominantly the sample is 95% carbon monoxide. This percentage increases to 98.6% after treatment. No trace of an increase in

FIG. 32 Mass Spectrum of Ethylene and the Background Spectrum.

Mass Spectrum of Ethylene from the MS9

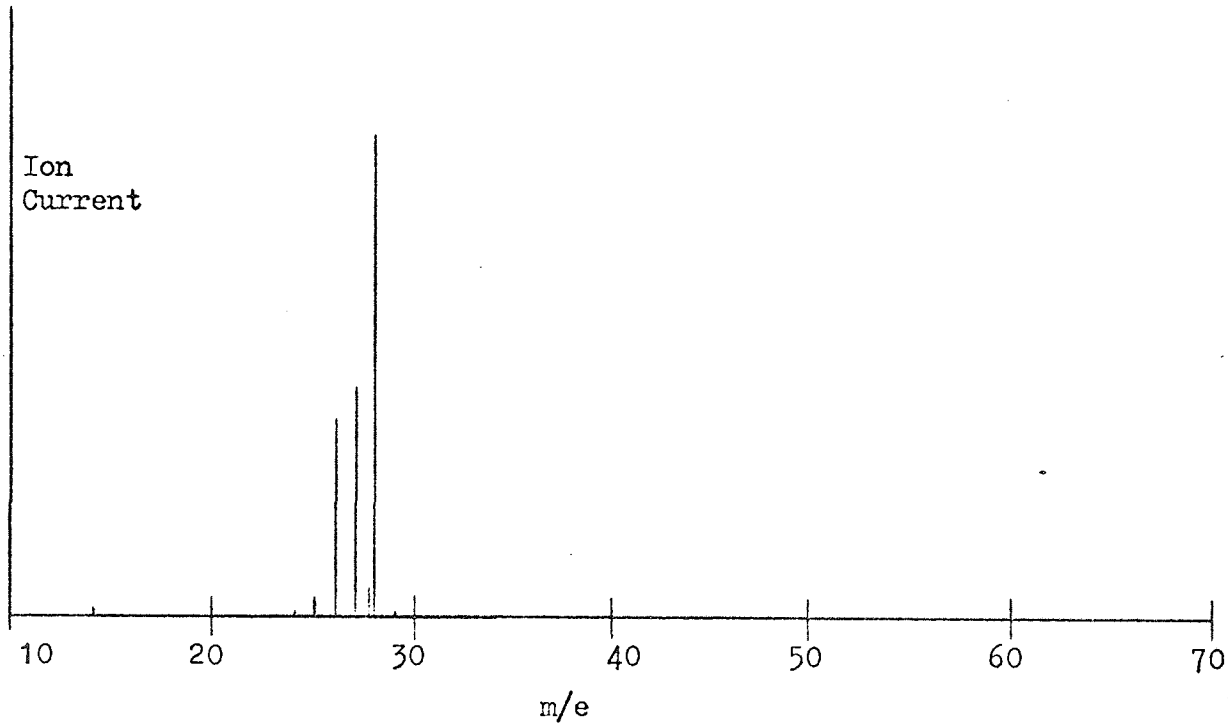

Background Spectrum (x 10)

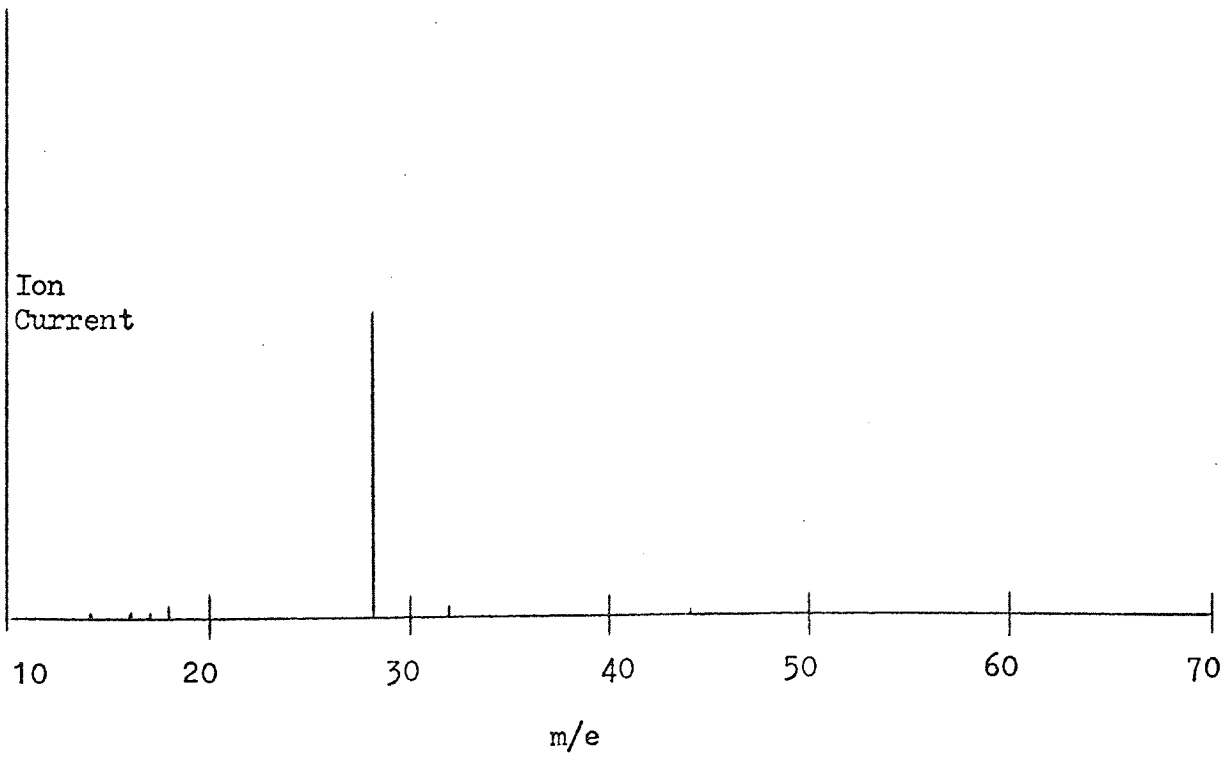

Table 6. Mass Spectrometric Analysis of Carbon Monoxide by MS9 Mass Spectrometer.

PEAK	CYLINDER SAMPLE			PREPARED SAMPLE			PERCENTAGE INCREASE OF PREPARED SAMPLE
	Sample Peak Background	Increase of Peak	%	Sample Peak Background	Increase of Peak	%	
12	15 0	15	0.3	110 0	110	0.3	
14	12 12	0	-	110 110	0	-	
16	20 14	6	0.1	25 7	18	NEG	Smaller
17	7 7	0	-	4 4	0	-	
18	70 50	20	0.4	24 24	0	-	Smaller
20	6 6	0	-	2 2	0	-	
26	11 0	11	0.2	2 0	2	NEG	Smaller
27	16 5	11	0.2	3 2	1	NEG	Smaller
28 1st Peak CO	5500 150	5350	95.7	29500 0	29500	98.6	3% Increase
28 2nd Peak N_2	3500 3500	0	-	3000 3000	0	-	

Table 6 Continued

PEAK	CYLINDER SAMPLE			PREPARED SAMPLE			PERCENTAGE INCREASE OF PREPARED SAMPLE
	Sample Peak Background	Increase of Peak	%	Sample Peak Background	Increase of Peak	%	
29	80 15	65	1.2	240 9	231	0.7	Smaller
30	24 0	24	0.4	20 0	20	NEG	Smaller
32	730 640	90	1.7	61 53	8	NEG	Smaller
44	13 13	0	-	31 10	21	NEG	Very slightly larger

Table 7. Mass Spectrometric Analysis of C_2H_4 by MS9 Mass Spectrometer.

PEAK	CYLINDER SAMPLE			PREPARED SAMPLE			PERCENTAGE INCREASE OF PREPARED SAMPLE
	Sample Peak Background	Increase of Peak	%	Sample Peak Background	Increase of Peak	%	
12	10 0	10	NEG	14 0	14	NEG	-
14 N_2	80 80	0	-	10 10	0	-	
14 CH_2^+	100 0	100	NEG	140 0	140	NEG	
15	3 0	3	NEG	9 0	9	NEG	
18	40 17	23	NEG	28 28	0	-	
25	370 0	370	0.2	150 0	150	NEG	
26	3500 1	3499	21.7	5100 3	5097	20.8	Down
27 $C_2H_3^+$	4100 4	3996	24.8	5700 14	5686	23.2	Down
27 $C_2H_3^{2+}$	9 0	9	NEG	10 0	10	NEG	

CONT:

Table 7 Continued.

PEAK	CYLINDER SAMPLE			PREPARED SAMPLE			PERCENTAGE INCREASE OF PREPARED SAMPLE
	Sample Peak Background	Increase of Peak	%	Sample Peak Background	Increase of Peak	%	
28 N_2^+	4200 4200	0	-	720 720	0	-	
28 $C_2H_4^+$	7800 0	7800	48.1	12600 0	12600	51.5	Up 3.4
29	150 12	138	0.1	180 1	179	NEG	Down
30	0 0	0	-	1 0	1	-	
32	720 710	10	NEG	15 15	0	-	

Table 8. Mass Spectrometric Analysis of Hydrogen by MS9 Mass Spectrometer.

PEAK	CYLINDER SAMPLE			PREPARED SAMPLE			PERCENTAGE INCREASE OF PREPARED SAMPLE
	Sample Peak Background	Increase of Peak	%	Sample Peak Background	Increase of Peak	%	
2	2700 5	2695	94.3	5700 14	5686	99.8	5.5
14	70 80	-	-	40 60	-	-	
16	15 14	1	0.03	8 8	-	-	
17	16 6	10	0.3	7 7	-	-	
18	110 70	40	1.3	5 6	-	-	
27	5 3	2	0.06	6 4	2	0.03	Down
28	3000 2900	100	3.4	670 670	-	-	
32	530 530	-	-	150 150	-	-	
36	16 10	6	0.18	40 30	10	0.17	Down
44	50 50	-	-	16 16	-	-	

nitrogen, oxygen or water vapour is found which indicates that no leaks occurred and the heating treatment removed all the water vapour from the system. The main contaminants of the cylinder sample are peaks at 12 which are due to carbon, 16 and 32 due to oxygen and a peak at 18 due to water vapour. Also peaks occur at 26, 27 and 29, 30 probably due to subtraction and addition to the main peak. After treatment it can be seen that the oxygen and water vapour peaks disappear. All the other peaks remain the same or are fractionally reduced except for the 40 and 44 peaks which are very slightly increased. The 44 peak is probably due to carbon dioxide which since some carbon is found suggests a small amount of dissociation to the basic elements and then the addition of the oxygen radical to a carbon monoxide molecule but this occurs in approximately 1 in 10,000 cases. The analysis shows that the percentage of carbon monoxide is increased with the treatment but the carbon monoxide is the main component of the gas by a long way.

The mass spectrum of ethylene shows that the only major percentage increase is the ethylene peak. A high resolution spectrum had to be taken to differentiate between nitrogen 28 peak and ethylene 28 peak. Fragmentation peaks of the ethylene were found in the cylinder sample CH_2^+, CH_3^+, a 26 peak, 27^+ and 27^{2+} peak and a 29 peak. The major peak was the ethylene peak but two other large peaks were the 26 and 27 peak. After treatment the only peaks of reasonable size were the 25, 26, 27 and 28 with the 25 peak being relatively small. This is to be expected since the low mass

and high mass peaks should be removed by the molecular sieve but the range of peaks around 28 should be more concentrated.

These results show that the treatment provides a way of collecting a gas sample as well as improving the purity of the sample. The improvement in the sample peak can be seen as well as the fact that no impurity not expected from the fragmentation of the major peak is seen.

The analysis for hydrogen shows that hydrogen was 99.8% of the sample. The purity of the sample increased by 5% this is shown by the analysis in Table 8.

3.6 DIRECT SURFACE OBSERVATIONS

3.6.1 Techniques Used

An electron microscope was used to examine the surface. This gave an idea of the surface structure. The crystal structure and variations in the surface is observed. The change in the structure after the filament had been heated was also observed. The surface structure could give an indication to the mechanisms of adsorption and desorption.

An X-ray analysis of the surface was also made. By analysing the energies of the X-rays after striking the filament the elements on the surface were identified. This technique is limited to elements above fluorine. For our purposes hydrogen, carbon and oxygen can not be detected but if higher atomic weight gases and adsorbates were used this would be a powerful technique. For instance if fluorine was used and this turned the surface into the metal fluoride then the components on the surface would be identified.

An X-ray power diffraction photograph of the metal after treatment and exposure was also obtained. This showed the crystal

structure of the surface and also if any involatile metal-gas compounds had been formed on the surface. It had been shown on this apparatus that when methyl iodide was adsorbed on the surface (3), metal carbide was formed on the tantalum surface in substantial amounts.

3.6.2 Scanning Electron Microscope (79)

The scanning electron microscope is used to investigate the surfaces of metals and most other surfaces. It's operation is very similar to an optical microscope. However for an optical microscope surface detail with dimensions much less than the wavelength of light ($\ll$ 5460 Å) will not be resolved.

In order to obtain a picture of the surface where the structure is resolved the wavelength of the source of radiation must be reduced. The wavelength of an electron beam is given by

$$\lambda \simeq \sqrt{150} / \sqrt{V} \quad \text{Å} \qquad \ldots\ldots (3\text{-}1)$$

and for an electron accelerated through 100 volts the wavelength of an electron beam is 1.22 Å. However the normal accelerating voltage for an electron microscope is 50-100 kV and so the wavelength of the electron beam (for 100 kV) is 0.04Å.

Comparing this to the wavelength of light 6×10^3 Å it is seen that the wavelength has been reduced by a factor of 10^5. The resolution of the microscope over an optical microscope should be improved by 10^5 but because of the spherical aberration of the magnetic lenses used in the microscope, which cannot correct for non paraxial rays efficiently , the resolving limit of the electron microscope is found to be about 4 Å which is three to four orders of magnitude better than the optical microscope.

FIG. 33 The Electron Microscope.

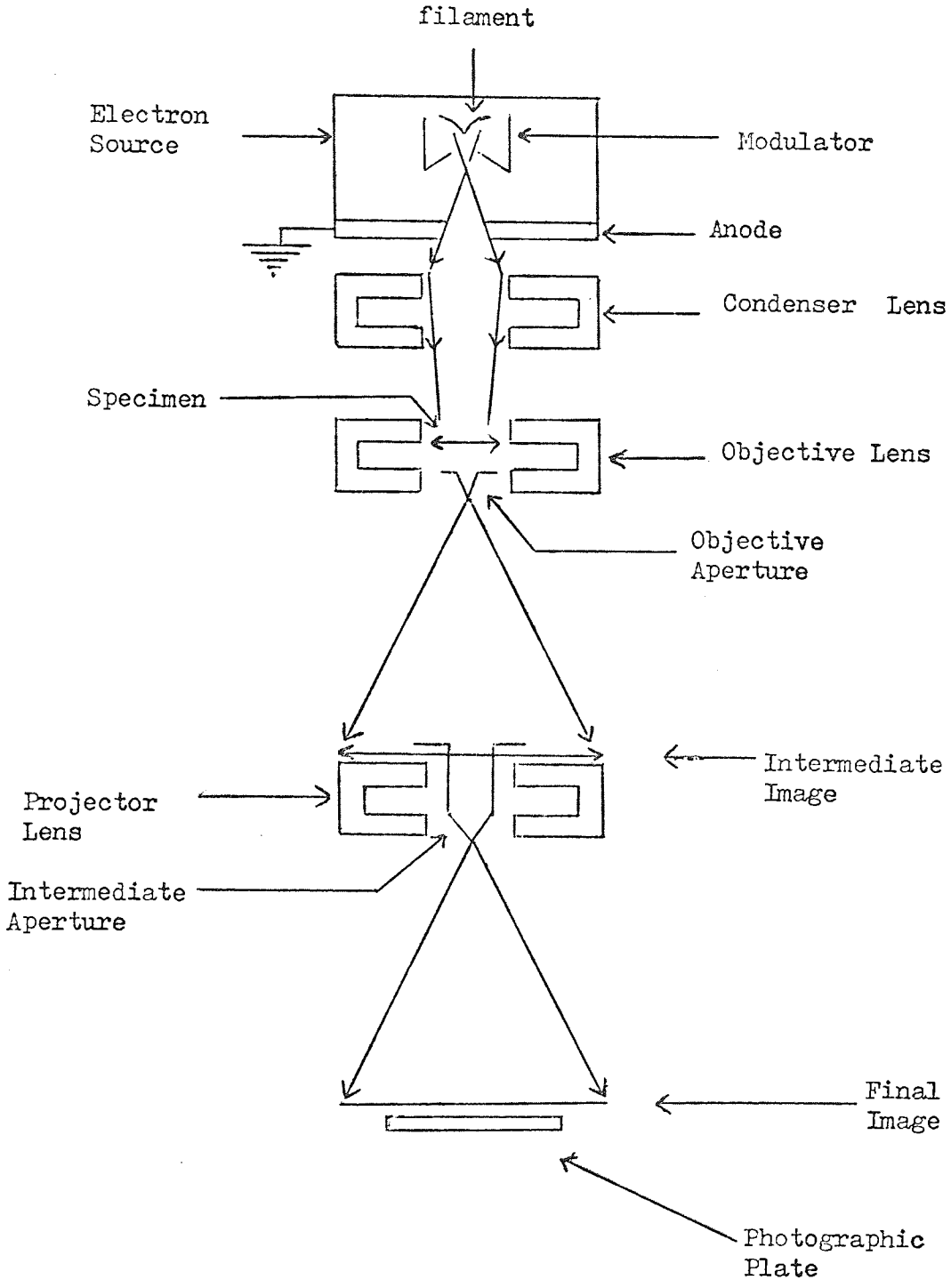

The essential features of an electron microscope are shown in Fig. 33. A filament produces an electron beam which is accelerated to the anode. This beam is then focussed on the specimen by a magnetic condenser lens. If the specimen is a thin film the transmitted electron beam is focussed by the objective lens and projector lens onto a photographic plate.

The scanning electron microscope shown in Fig. 34 is slightly different from the transmission electron microscope. High resolution and a wide range of magnification from x 20 up to x 50,000 are possible, as well as a large depth of field. It does not have such a high resolution as the transmission microscope.

A very narrow electron beam which has been focussed onto the specimen is used to scan the specimen and the secondary electrons produced are collected and used to give a picture of the surface of the specimen. The secondary electrons are collected in a charged cup and this current is amplified and used to produce a picture of the surface on a cathode ray tube. A photograph is taken of the scan.

The magnification can be altered without having to refocus the microscope. The magnification is altered by adjusting the area of scan on the specimen.

3.6.3 Electron Probe Microanalysis

This technique can be used to analyse the elements on the surface of the metal surface. However only elements with atomic numbers greater than fluorine can be identified with our analyser. Our analyser has been used to identify the elements in a speck of dust which has contaminated the surface after removal from the vacuum system.

FIG. 34 The Scanning Electron Microscope.

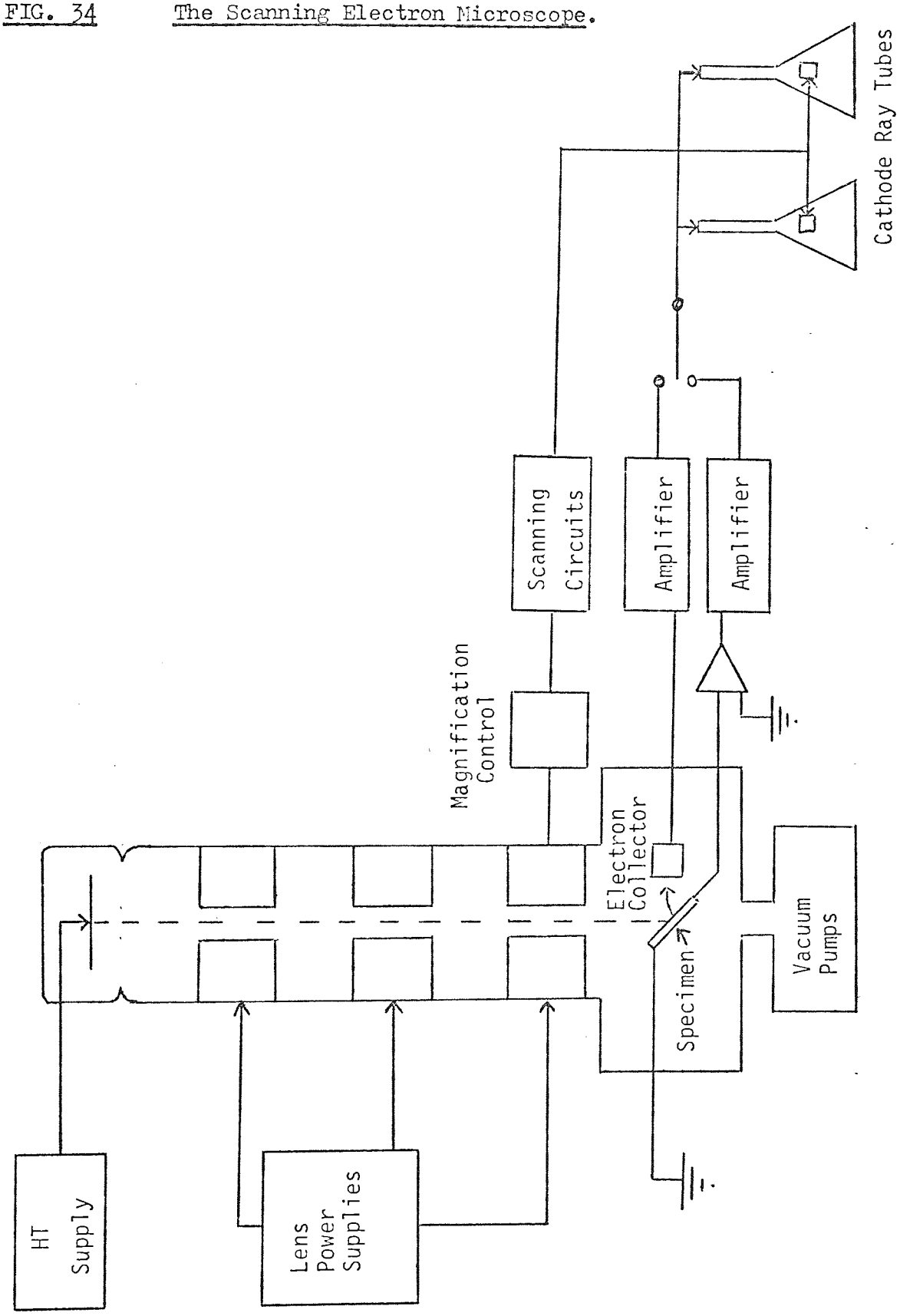

An electron beam is once again used to investigate the surface. This electron beam is bombarded onto a small area of the surface and the X-rays given off are analysed by means of an X-ray crystal spectrometer. X-rays can be analysed by means of either their wavelength or in this case their frequency or energy. The energy distribution of the X-rays given off is characteristic of the elements that the electron beam is scanning and so the surface elements are analysed.

3.6.4 X-ray Diffraction (80)

The X-ray diffraction data can be used to give crystallographic structure details. However our specimen has many crystal orientations and so the pattern we get is not a series of sharp lines. The diffraction pattern obtained can also be used to identify the surface metal. Tantalum carbide gives a different diffraction pattern from tantalum metal and so the technique gives us information about the metal-gas compounds formed on the surface.

The specimen, preferably in the form of a cylindrical wire is situated at the centre of an X-ray powder diffraction camera. In our case the specimen was a ribbon filament. The circular circumference of the camera holds a photographic film into which there are two holes 180° apart. A monochromatic X-ray beam impinges on the surface and the X-rays are reflected both forwards and backwards. X-rays that pass through the specimen are allowed to pass out of the camera through the hole opposite the X-ray source. The reflected X-rays are collected on the light sensitive film and this can be developed and analysed. By comparing the results obtained to the X-ray powder data file (A.S.T.M. Index) the element

Fig. 35 Electron Probe Microanalysis Results.

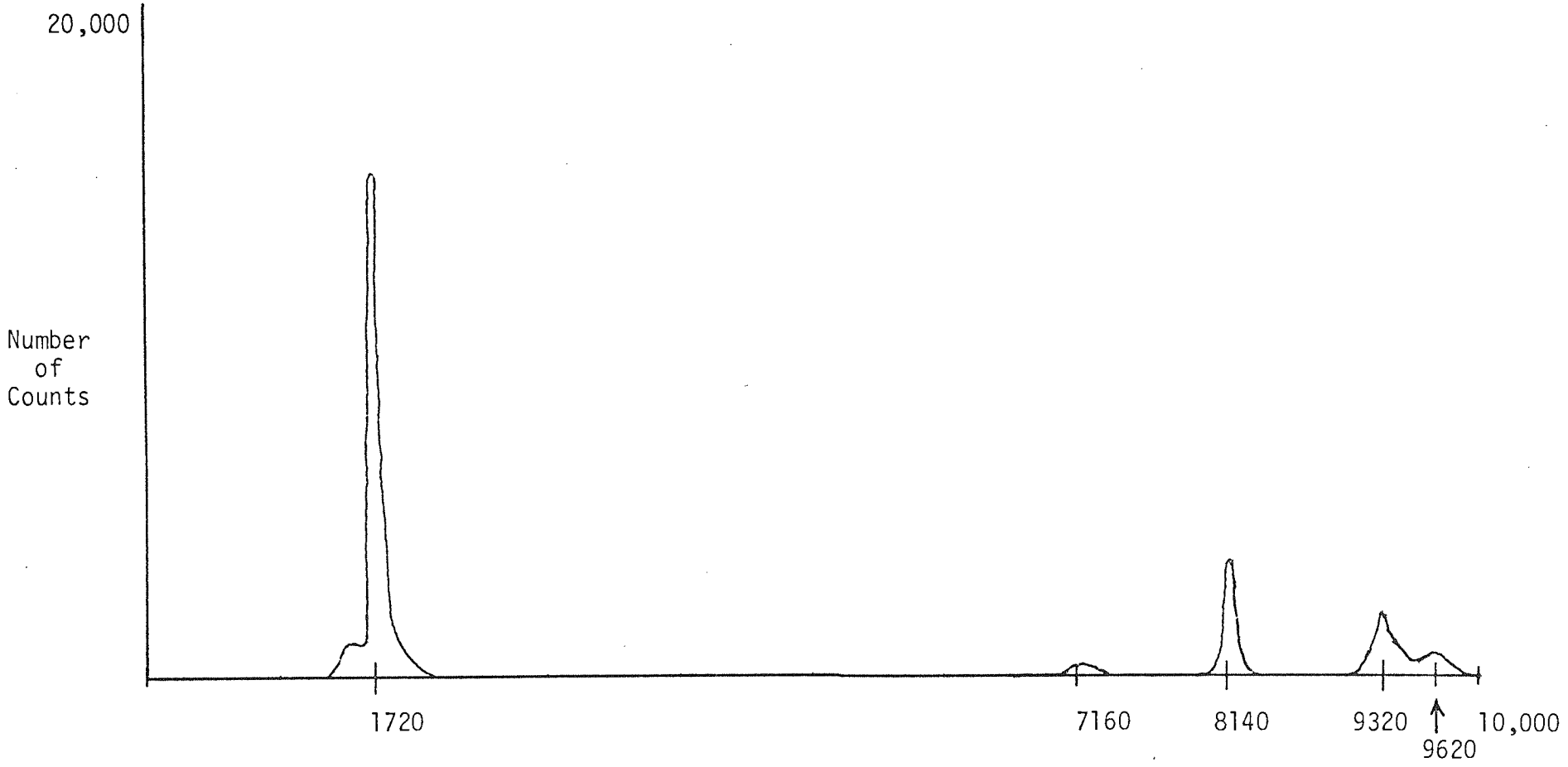

or compound and its crystallographic history can be found.

3.6.5 Results

The results obtained from the electron probe microanalysis were not very enlightening as expected. Since elements with atomic numbers less than fluorine could not be detected and all the gases used had atomic numbers less than fluorine it was not expected that anything other than tantalum would be found. The results obtained from the electron probe microanalysis are shown in Fig. 35. This is in fact the electron probe microanalysis spectra of tantalum which was obtained for all the specimens used. The technique would be a very useful technique for adsorbed elements with atomic numbers greater than fluorine. Fig. 36 shows an electron microscope picture of the surface of a tantalum filament. After removal from the apparatus the filament was contaminated with dust. When observed under the electron microscope at (1560) times magnification the spot of dust can be seen. The picture shows a 4.8×10^{-3} cm sided piece of the filament. The length of the spot of dust is 9.6×10^{-4} cm long and this was analysed by the electron microprobe technique and one of the spots of dust was found to be silicon and the second spot contained calcium, magnesium and chlorine. The analysis of such a small sample shows the value of the technique.

Electron microscope pictures have been taken of the filament before treatment in the U.H.V. apparatus. These photographs are shown in Figs. 37 and 38. Fig. 37 shows low magnification pictures at magnification of 405 x and 825 x. The surface at 405 x looks quite flat but the 825 x picture shows more surface structure. The

FIG. 36 An Electron Microscope Photograph of a Dust Particle on the Surface of the Filament.

Magnification x 1560

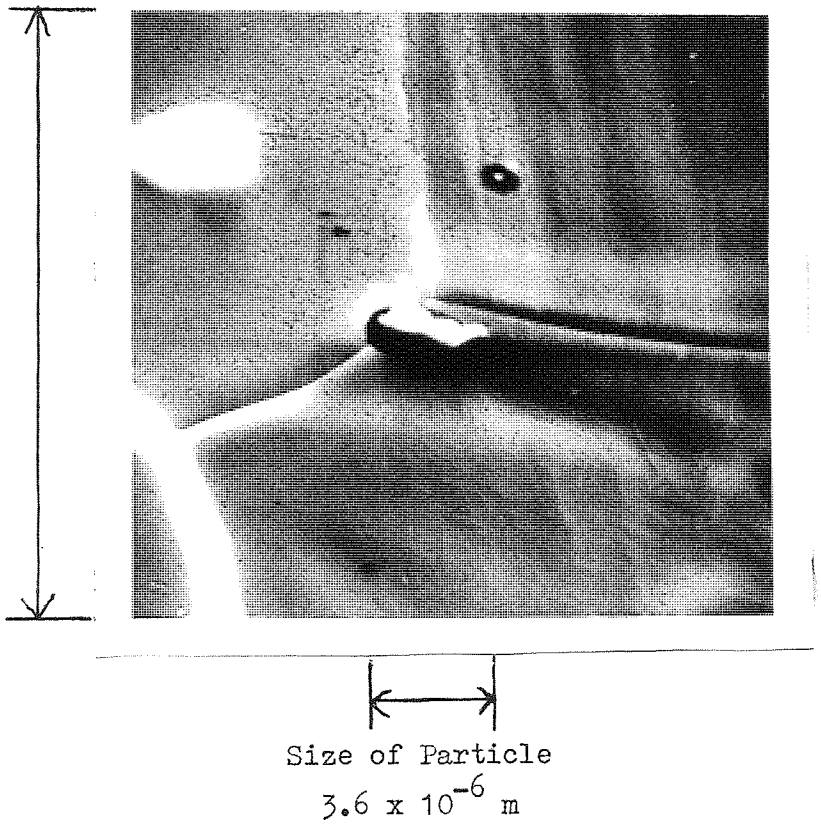

Using Electron Probe Microanalysis:-

Bright Spot is Silica
Dark Particle is Made Up of Magnesium, Calcium and Chlorine

FIG. 37 The Filament Before the Experiments I.

Magnification x 405

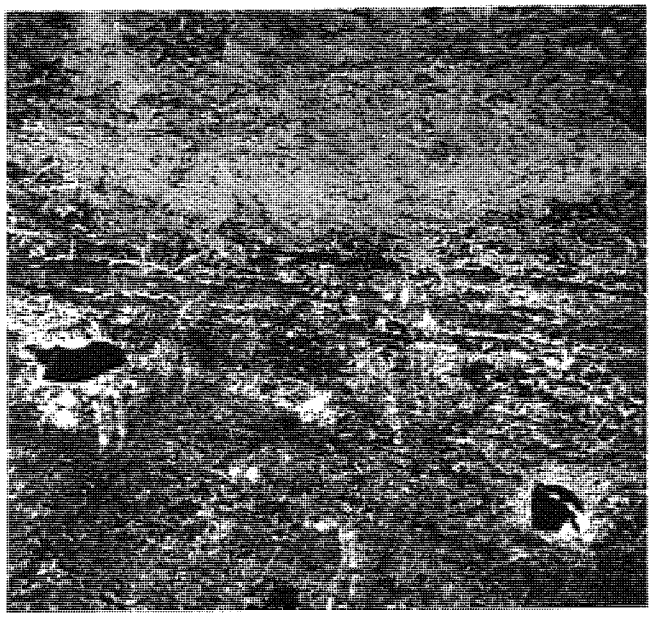

Magnification x 825

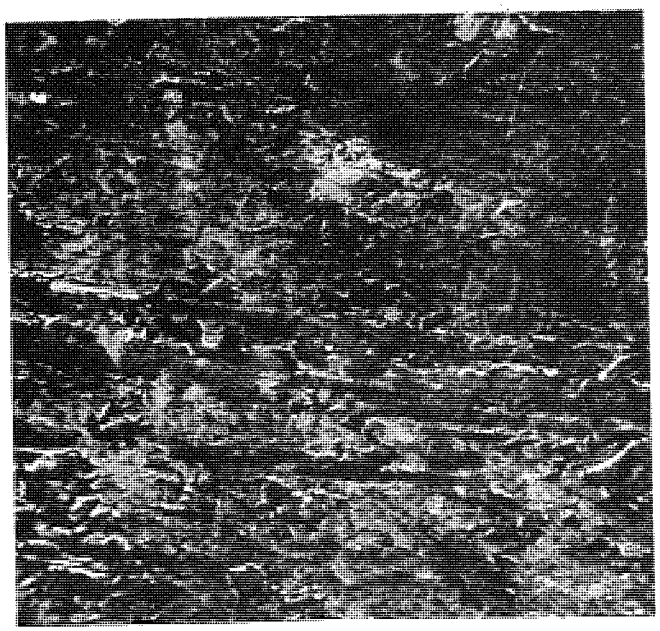

FIG. 38 The Filament Before the Experiments II.

Magnification x 1650

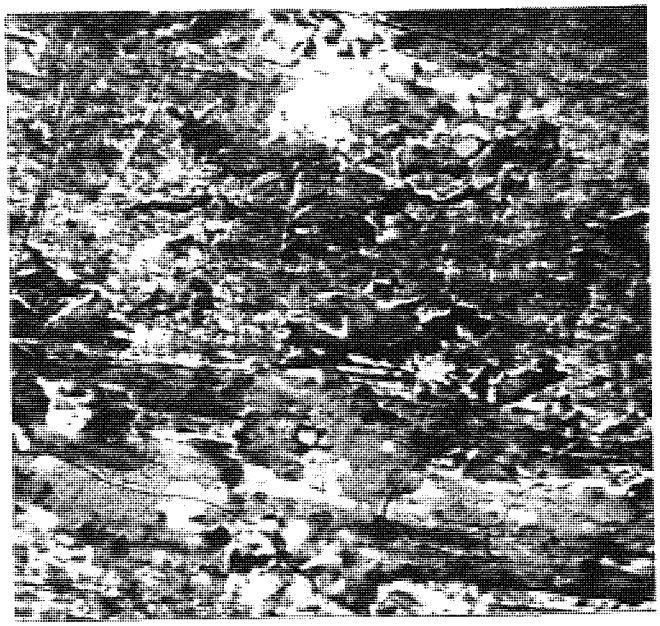

Magnification x 4050

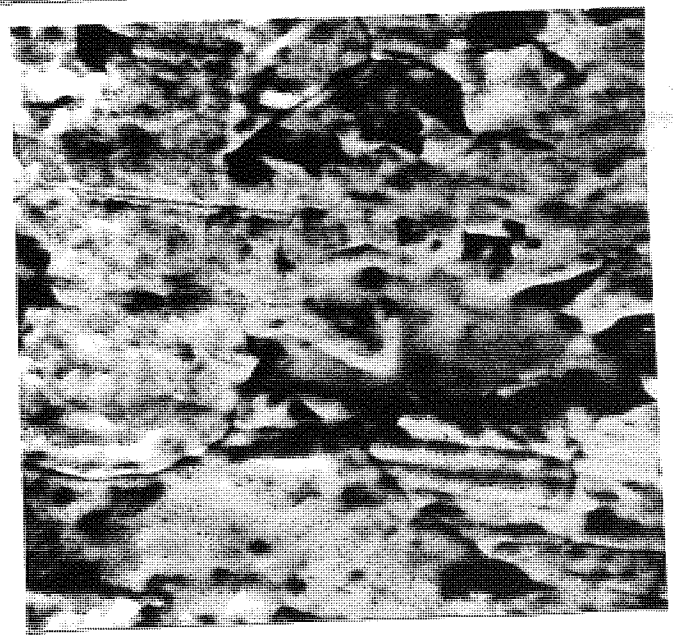

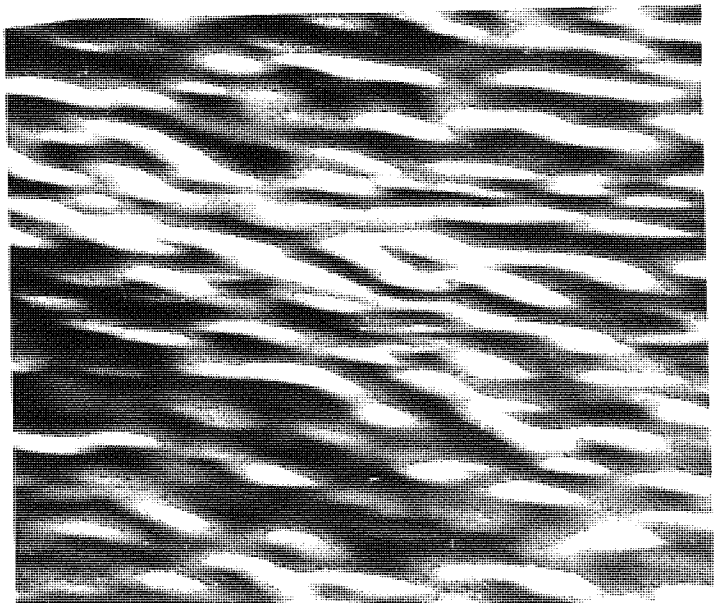

Magnification x 10 K

surface is not flat but contains various uneven features. Fig. 38 shows the surface at magnifications of 1650x and 4050x. The surface structure is shown in more detail. Here it can be seen that the surface is rough but it contains no crystal boundaries. The area shown in the high magnification picture is a square of sides 7.4×10^{-4} ins.

Fig. 38 shows a very high magnification picture. The magnification here is 10000x and the sides of the square represent 7.6×10^{-4} cms. The resolution is very poor and little information about the surface structure is forthcoming. The useful magnification for our purposes is about 6 K.

Electron microscope pictures were taken, after treatment of the filament, in the region near to the place where it was spot welded to the support. These pictures are shown in Fig. 39 for magnifications of 200x, 800x, 1600x and 2600x. The shaded area on the picture indicates the presence of the support. The 200x picture shows the crystal boundaries occur in a region near to the support and this shows the heat treatment had some effect up to the support. The other pictures show the surface in the region close to the support is similar to the surface throughout the filament. It does not appear that the support has much effect on the crystal structure caused by the heat treatment, except for a region of 1×10^{-2} cm near to the support. The size of the larger individual crystals near to the support can be measured and they are found to be 2×10^{-3} cms in length.

Fig. 40 shows the centre of the filament after heat treatment and adsorption experiments with the CO. This filament is very similar to the filament surface obtained when the filament was heated

FIG. 39 The Used Filament Showing the Region Near the Support.

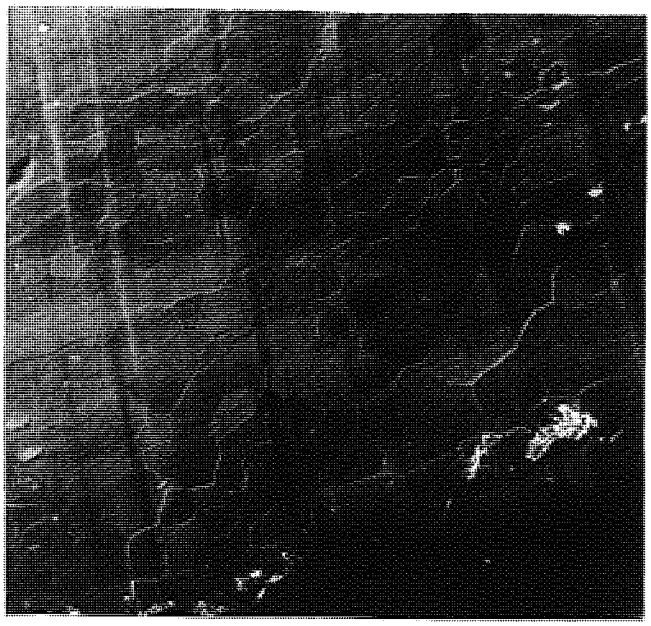

Magnification x 200

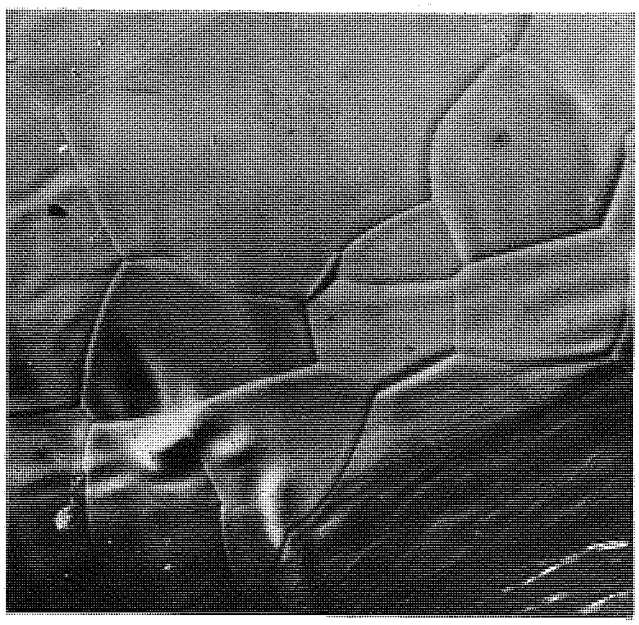

Magnification x 800

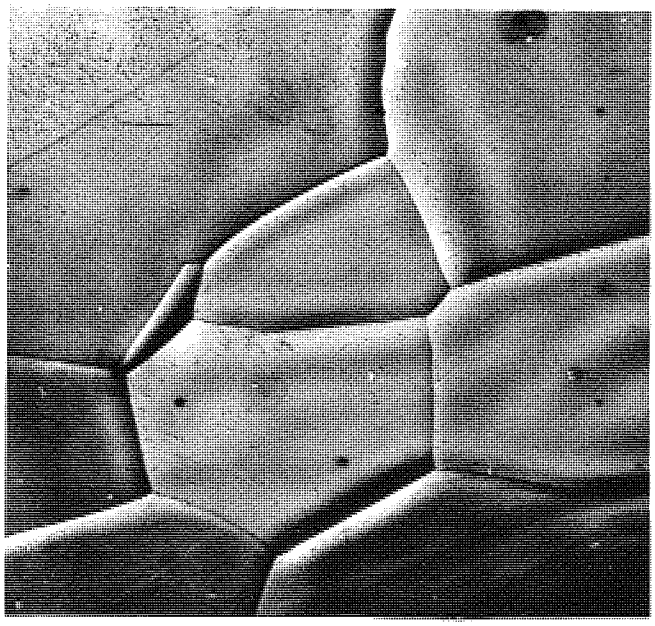

Magnification x 1600

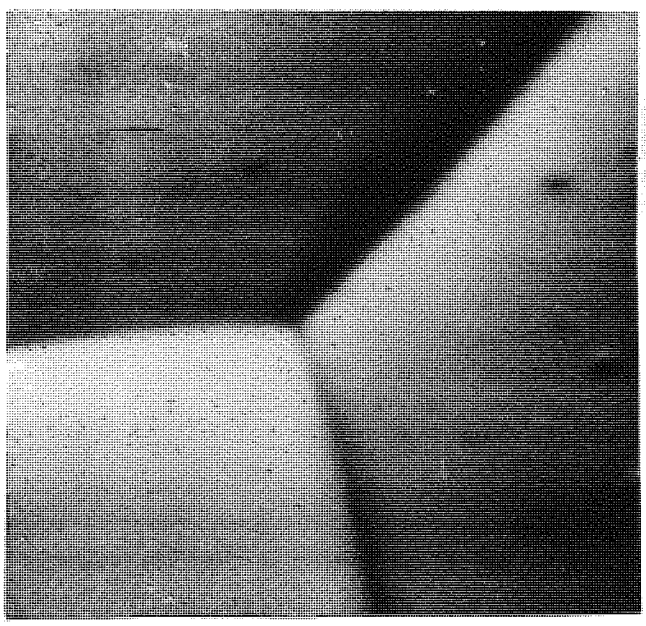

Magnification x 2600

FIG. 40 The Filament After the Carbon Monoxide Experiments.

Magnification x 150

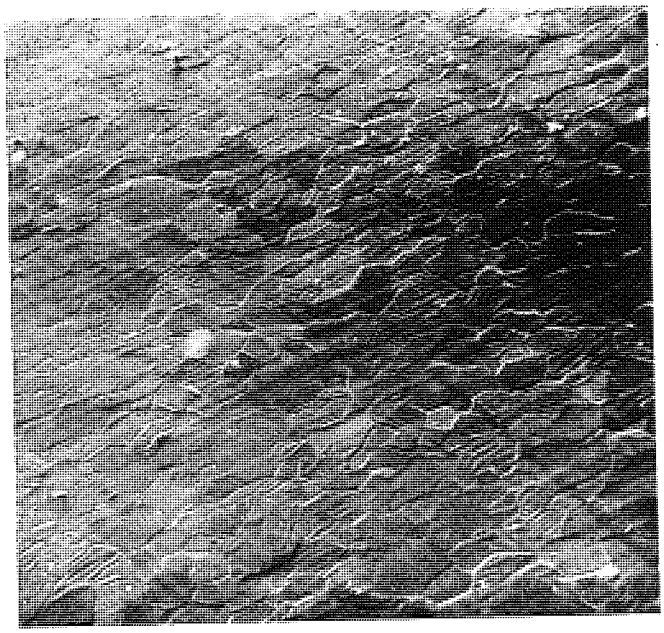

Magnification x 1500

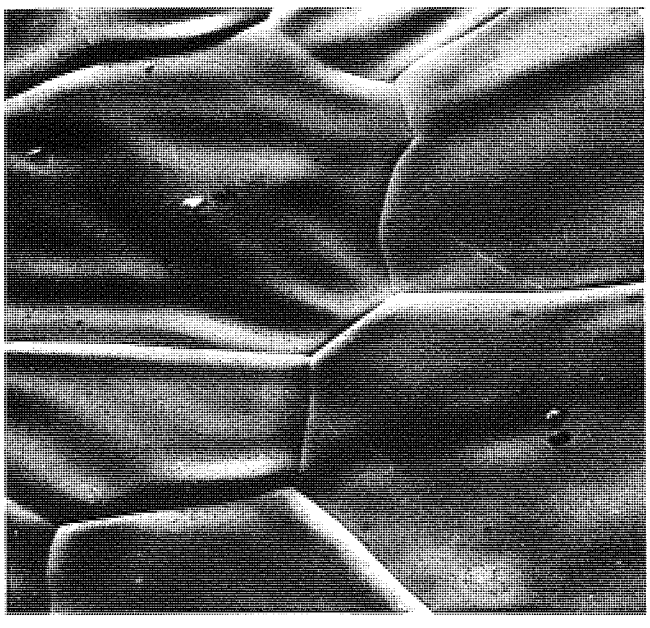

under a high vacuum condition. This tends to indicate the gas does not react and form compounds with the surface. So for carbon monoxide it seems that the gas is adsorbed and then desorbed without the formation of any metal-carbonyl or metal-oxide compounds.

Figs. 41 and 42 show the surface after it had been heated in ethylene and desorption experiments performed. The various crystal boundaries are obscured by a surface coating. The surface is no longer smooth but ingrained and on the top appeared to be strands of a fibrous compound. The pictures shown are for magnifications of 200x, 500x, 1 K and 2 K.

The results of the X-ray diffraction are shown in Figs. 43 and 44. In Fig. 43 a picture of the untreated tantalum, and also the tantalum sample after treatment with carbon monoxide and in Fig. 44 the tantalum sample after treatment with ethylene. The sample after treatment with carbon monoxide closely resembles the X-ray diffraction photograph for pure tantalum whereas with the X-ray diffraction photograph for the sample treated with ethylene the two photographs differ greatly.

By measurements taken off the photograph, use of Bragg's law and a search through the A.S.T.M. index it was found that the diffraction photograph obtained after treatment and flashing with ethylene was of tantalum carbide. The evidence supports the idea that ethylene dissociates to some extent when it is adsorbed on the tantalum.

The change in appearance of the metal after ethylene adsorption also indicates that it is not the same as at the start. The metal after treatment with carbon monoxide still was a metallic silver colour. The metal after treatment with ethylene had a darker surface.

FIG. 41 The Filament After the Ethylene Experiments I.

Magnification x 200

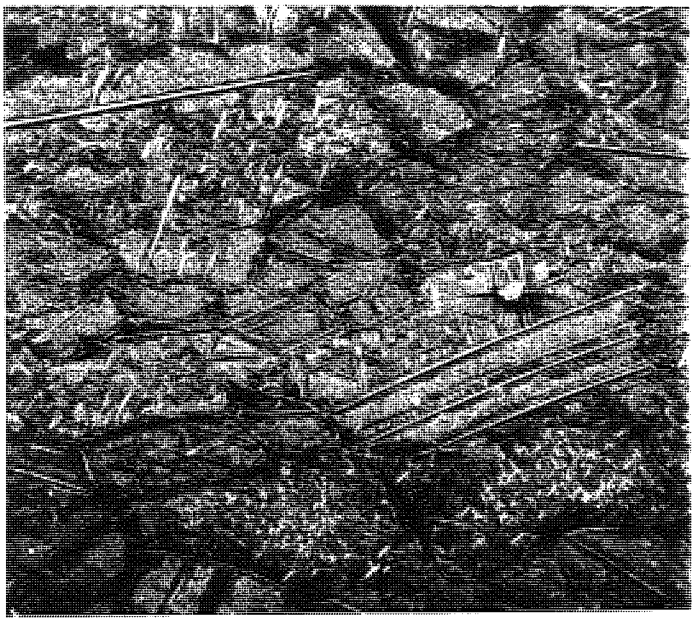

Magnification x 500

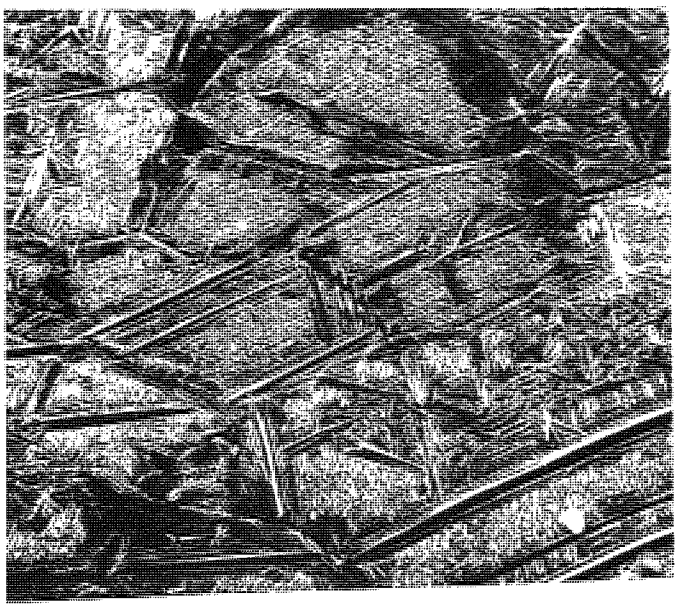

FIG. 42 The Filament After the Ethylene Experiments II.

Magnification x 1000

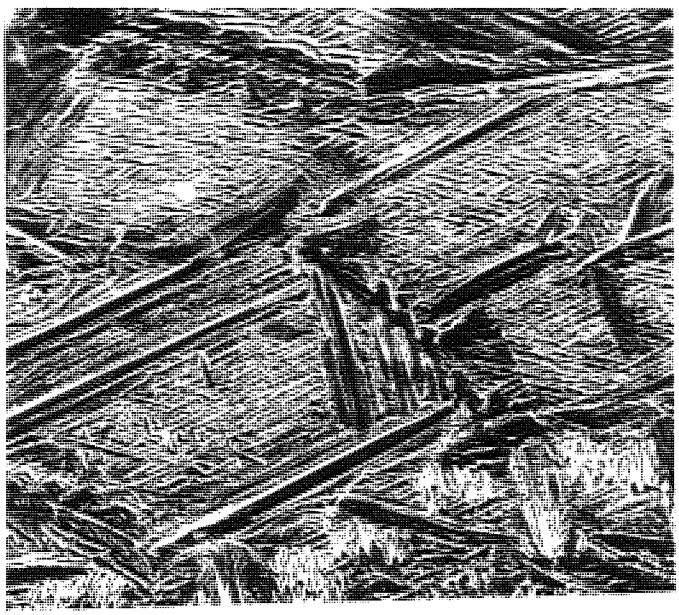

Magnification x 2000

Fig. 43 X-Ray Diffraction Results for Carbon Monoxide.

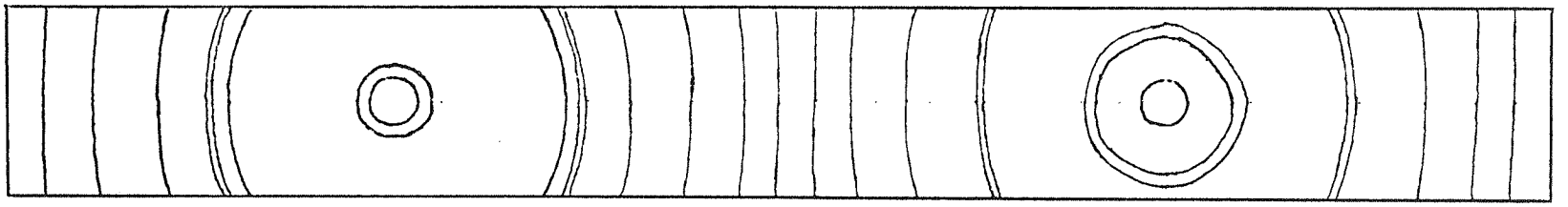

X-ray Diffraction Pattern Before Treatment with Carbon Monoxide

(X-ray Diffraction Pattern of Tantalum)

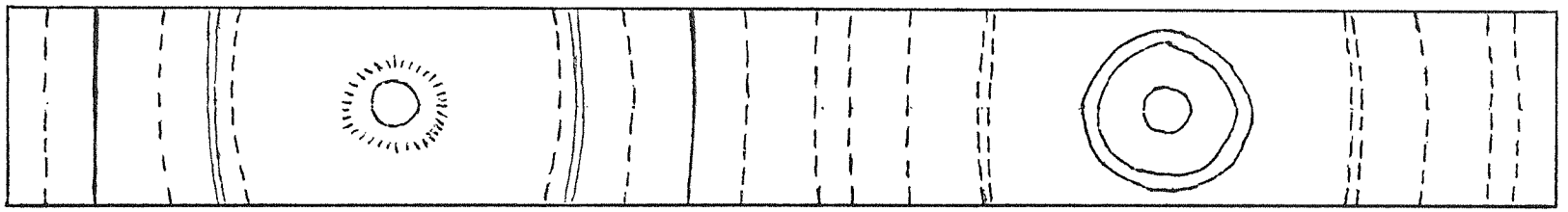

X-ray Diffraction Pattern Obtained After Treatment with Carbon Monoxide

Fig. 44 X-Ray Diffraction Results for Ethylene.

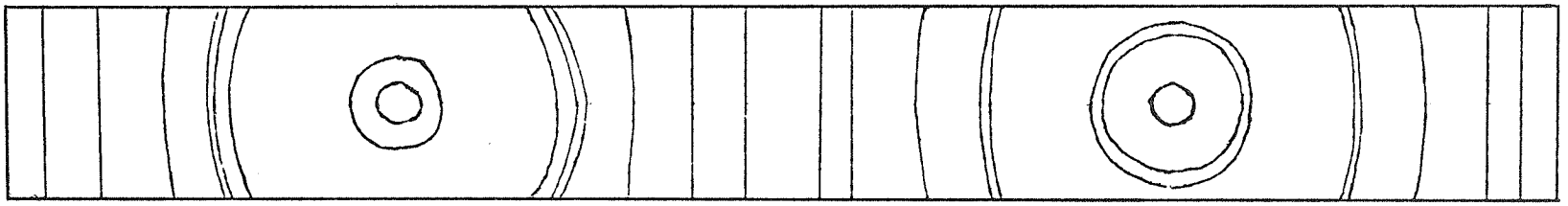

X-ray Diffraction Pattern Before Treatment with Ethylene
(X-ray Diffraction Pattern of Tantalum)

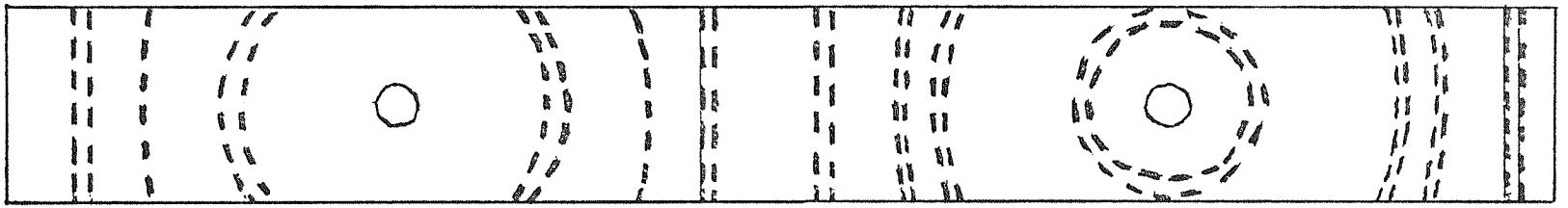

X-ray Diffraction Pattern Obtained After Treatment with Ethylene
(X-ray Diffraction Pattern of Tantalum Carbide)

These investigations of the surface before and after treatment with carbon monoxide, hydrogen and ethylene show the only effect noticeable after treatment with carbon monoxide and hydrogen is due to the rapid heating but with the ethylene a more drastic change has occurred and a compound has been formed on the surface which is probably tantalum carbide.

Investigations to find whether this layer was a surface layer or whether it went right through the material did not give any useful information due to the limitations of the stereoscan, however it is thought that the layer was only a surface layer. The X-ray diffraction also could not be used because the sample was too thin to obtain any satisfactory results.

4 GENERAL THEORETICAL APPROACH

4.1 ANALYSIS OF THE OSCILLOSCOPE TRACE

4.1.1 Introduction

In order to establish some meaning from the masses of numbers that can be obtained from the experimental data a connection must be established between the known parameters and the unknown parameters. We must find a path so that we can go from the experimentally measured parameters to those that cannot be measured directly. These experimentally measured parameters are the temperature, the pressure, the pumping speed and the time and these are related to other parameters such as the rate of the reaction, the order of the reaction, the surface coverage at the start of the flash and its change throughout the flash and finally the experimental energy of activation.

This chapter shows the ways of relating these various measurements as well as comparing this approach with the methods used by other workers. In the end however it is the accuracy of the experimental results that determines how a given method is used and the reliability of the end result.

The results are obtained from an oscilloscope, the front of which is photographed during the flash. The picture obtained is shown in Fig. 45 . The x axis of the grid is a time scale and for the flash each centimeter on the grid (which is the space between two consecutive lines) is equal to 0.2 seconds and so the full time of sweep of the oscilloscope spot is 2 seconds. The y axis of the grid is in volts per cm, the exact value being varied by a switch on the front of the oscilloscope for each of the traces.

There are three traces on the oscilloscope. One measures the

FIG. 45 A Thermal Desorption Spectra.

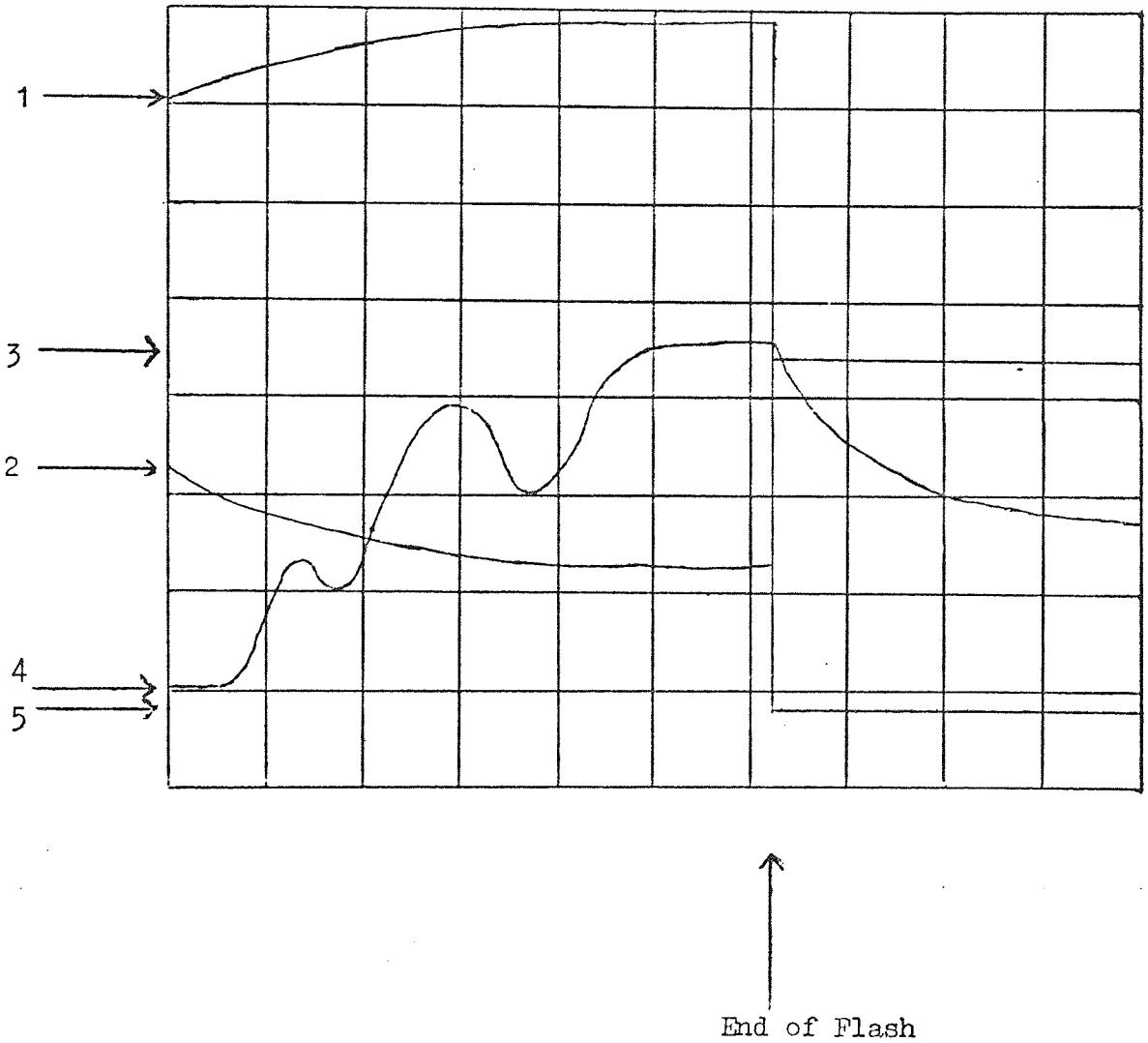

1 Voltage across filament
2 Voltage across shunt
3 Zero for voltage across shunt
4 Pressure curve
5 Zero for voltage across filament.

output of the pressure gauge and so any variation in the trace represents a pressure increase or decrease. The output of the pressure gauge on the log scale was found to be 0.2 volts per decade and by setting the dial on the oscilloscope at this value each centimeter on the grid represented an order of magnitude rise in pressure. The two other traces measured voltage changes, one across a known resistance and the other across the filament and part of the filament circuit. These two traces were used together so that the variation of temperature during the flash could be calculated.

The number of peaks in the desorption spectra shows the number of adsorbed states. Each of these states will be analysed. The higher the temperature the peak occurs at, the stronger are the bonds which hold the molecule to the surface.

If the variation of the peaks with adsorption time is observed any interaction of the peaks and the way the peaks effect each other can be observed.

The volume of the system and the surface area of the filament were both measured by physical methods. The pumping speed was calculated from the decrease in pressure with time at the end of the flash. The flash lasted for approximately 1.2 seconds and the remaining 0.8 seconds of the sweep were used for the pumping speed measurement.

The pressure measured by the gauge and read off the oscilloscope is a total pressure measurement due to all species present. From this has to be taken the equilibrium pressure and the increase in pressure due to the background. The increase due to the background was measured from a background flash prior to the actual flash.

This final pressure increase that was obtained was plotted on

a graph against the time at which the pressure occurred. This time should be related to the temperature by a linear relationship and provided this is the case then whether temperature or time is plotted the result obtained is the same. However if the temperature time relationship is not linear then the temperature should be used instead of the time.

The gradient of this curve at any point t, $(dp/dt)_t$ can be found either manually or by obtaining an equation for the curve and differentiating. This value can now be used to calculate the rate of desorption at any time or temperature.

The rate of desorption $(dn/dt)_t$ is equal to a constant multiplied by the $(dp/dt)_t$ term obtained plus a correction factor which accounts for the number of molecules lost during pumping. Since $(dp/dt)_t$, the volume, the surface area, the pumping speed and the constant are known then the rate of desorption can be calculated.

A graph of the rate of desorption at time t, $(dn/dt)_t$ against the time t can be plotted and the total area under this graph gives the value of the total surface coverage. The surface coverage at any time during the flash may also be found by subtracting from the total surface coverage the number of molecules desorbed up to a time t. This is done by subtracting an area under the graph from time t = 0 to t = t from the total area under the graph.

The experimental energy of activation can be found now along with the order of reaction. A graph of $-\ln\left[(dn/dt)/\sigma_o - \sigma_t)^x\right]$ against the reciprocal of the temperature for various values of the order of reaction x is now drawn. The value of x which gives the best straight line graph gives the order of reaction and the gradient of this line gives the experimental energy of activation.

The desorbed species is identified by mass spectrometric analysis. This will give information about the state of the adsorbed species. It shows whether the species is dissociated on desorption, desorbed as the gaseous radical or whether it forms complexes with the metal and is desorbed as the metal complex. Without this mass spectrometric identification of the desorbed species it would not be possible to suggest a mechanism for the adsorption and desorption of the gas. Each of the species which are desorbed can be identified and also the components of the background and if necessary the mass spectrometer may be used for leak testing.

All the information collected can then be used to suggest a mechanism for the adsorption and desorption of the gas. Other information may also be found such as the entropy which can also be used to give further information about the surface.

4.1.2 Calculation of the Temperature

In many experiments in both physics and chemistry one parameter is varied whilst another one is observed and its variation noted. The flash desorption experiment is very similar although many parameters are taken into account it is simply an experiment where the temperature is varied and the change in pressure noted. In these simple terms it is easy to see why it is important to be able to measure the temperature and know what temperature gives rise to a particular pressure increase.

As long as the temperature is changing we can make the assumption that the pressure change in the system over a short period of time is due to this change in temperature. The pressure in the system can change without a change in temperature being responsible. As we can see at the end of flash, many seconds after the filament has cooled down, the gas is still being pumped away and the pressure changing. If there is a linear relationship over the temperature

rise between the temperature and the time then for our purposes we can use the change in time in our equations and graphs as being equal to the change in temperature.

If the relation between the temperature and time is of the form

$$A\,t = T - T_o \qquad \ldots\ (4\text{-}1)$$

a linear relationship where t is the time in seconds, A is a constant, T is the temperature at time t and T_o is a constant being the temperature when t = 0, the temperature at the beginning of the flash.

Differentiating (4-1) we get

$$A\,dt = dT \qquad \ldots\ (4\text{-}2)$$

and shows the simple relationship between the change in temperature and the change in time and for a given time change we get a corresponding temperature change.

On the desorption spectra one trace gives the voltage drop across a known resistance, the shunt. The current through the circuit is given by Ohm's law

$$I = (X - X_o) \times S_I/E \times R_s \qquad \ldots\ (4\text{-}3)$$

where X_o is the zero of the voltage trace and so $(X - X_o)$ is the distance in cms between the two lines, S_I is the sensitivity scale of the trace in volts/cm and E is the enlargement factor calibrated by the fact that the distance between two grid lines on the scale should be 1 cm. R_s is the resistance of the shunt.

Similarly the voltage drop across the filament may be calculated using the equation

$$V_f = (Y - Y_o) \times S_v /E \qquad \ldots\ (4\text{-}4)$$

where $(Y - Y_o)$ is the voltage difference related to the voltage zero and S_v is the sensitivity factor for the trace. The resistance of the filament circuit R_c at a particular time is given by Ohm's law

$$R_c = V_f / I \qquad \ldots\ (4\text{-}5)$$

where R_c is the sum of the resistance of the filament, the contact resistances, the leadthroughs and the wire connection.

The resistance of the filament R_f is found by subtracting the resistance of the remainder of the circuit R

$$R_f = R_c - R \qquad \ldots\ (4\text{-}6)$$

R is found by physical measurements and calculations using known physical parameters. The resistivity of the filament σ is related to the resistance by the equation

$$\sigma = R_f A/L \qquad \ldots\ (4\text{-}7)$$

where A is the cross sectional area of the filament and L is the length of the filament. Wang and Lee (81) have published the results of the variation of resistivity of tantalum against temperature. Therefore from the values obtained for the resistivity the temperature can be calculated. The resistivity of tantalum varies with temperature in a way described by equation (4-8)

$$\sigma = A + BT + CT^2 + \ldots \qquad \ldots\ (4\text{-}8)$$

where A, B and C are constants.

Fig. 46 shows a typical temperature against time graph. It can be seen that the temperature rises quickly up to a maximum which occurs after approximately 0.6 seconds. Up to this point however the temperature does rise linearly with time. A series of flashes to different temperature maxima shows that the maximum

FIG. 46 Graph Showing Temperature Against Time for Various Maximum Temperature.

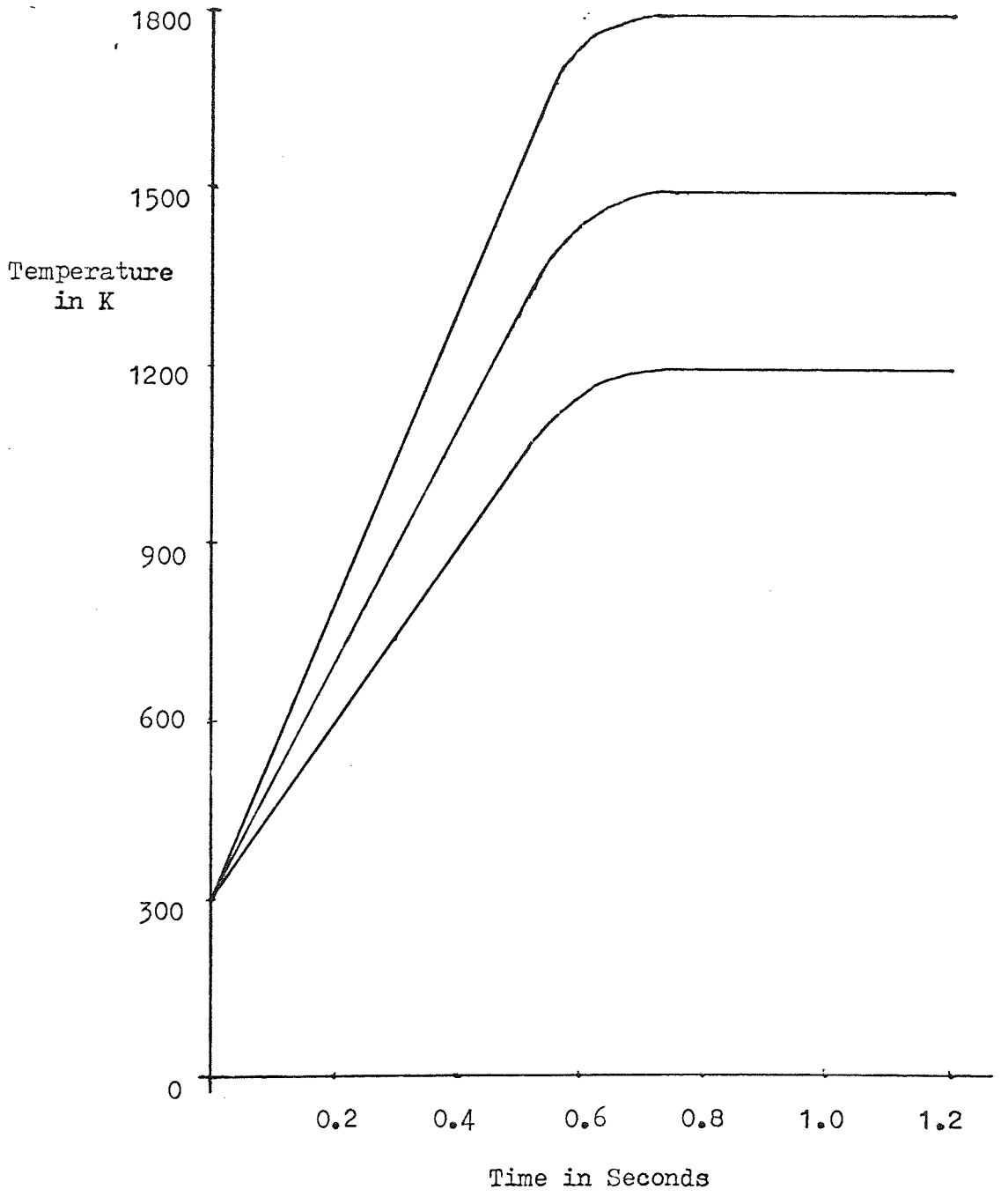

is always reached after about 0.6 secs and only the rate of heating, the gradient of temperature against time graph, measured before this changes.

4.1.3 The Pumping Speed

The measured pumping speed is that due to all effects which reduce the number of molecules in the vacuum system. That is pumping by the pumps, adsorption on the walls of the system and re-adsorption on the filament.

The pumping speed is defined by

$$dp_t/dt = -S_E(P_t - P_E)/V \qquad \ldots. (4\text{-}9)$$

where S_E is the total pumping speed for the whole system and V is the volume of the vacuum system.

If the pressure at t_1 is P_1 and at t_2 is P_2, rearranging

$$\frac{d P_t}{P_t - P_E} = -\frac{S_E}{V}\, dt \qquad \ldots. (4\text{-}10)$$

$$\int_{P_2}^{P_1} \frac{dP_t}{P_t - P_E} = -\frac{S_E}{V} \int_{t_2}^{t_1} dt \qquad \ldots. (4\text{-}11)$$

here assuming S_E is a constant independent of t.

$$\ln \frac{(P_1 - P_E)}{(P_2 - P_E)} = -\frac{S_E}{V}(t_1 - t_2) \qquad \ldots. (4\text{-}12)$$

this equation gives, when rearranged, a value for the pumping speed in terms of experimentally known parameters.

$$S_E = \frac{V}{(t_2 - t_1)} \ln \frac{(P_1 - P_E)}{(P_2 - P_E)} \qquad \ldots. (4\text{-}13)$$

FIG. 47 The End of the Oscilliscope Trace Showing the Reduction in Pressure at the End of the Flash.

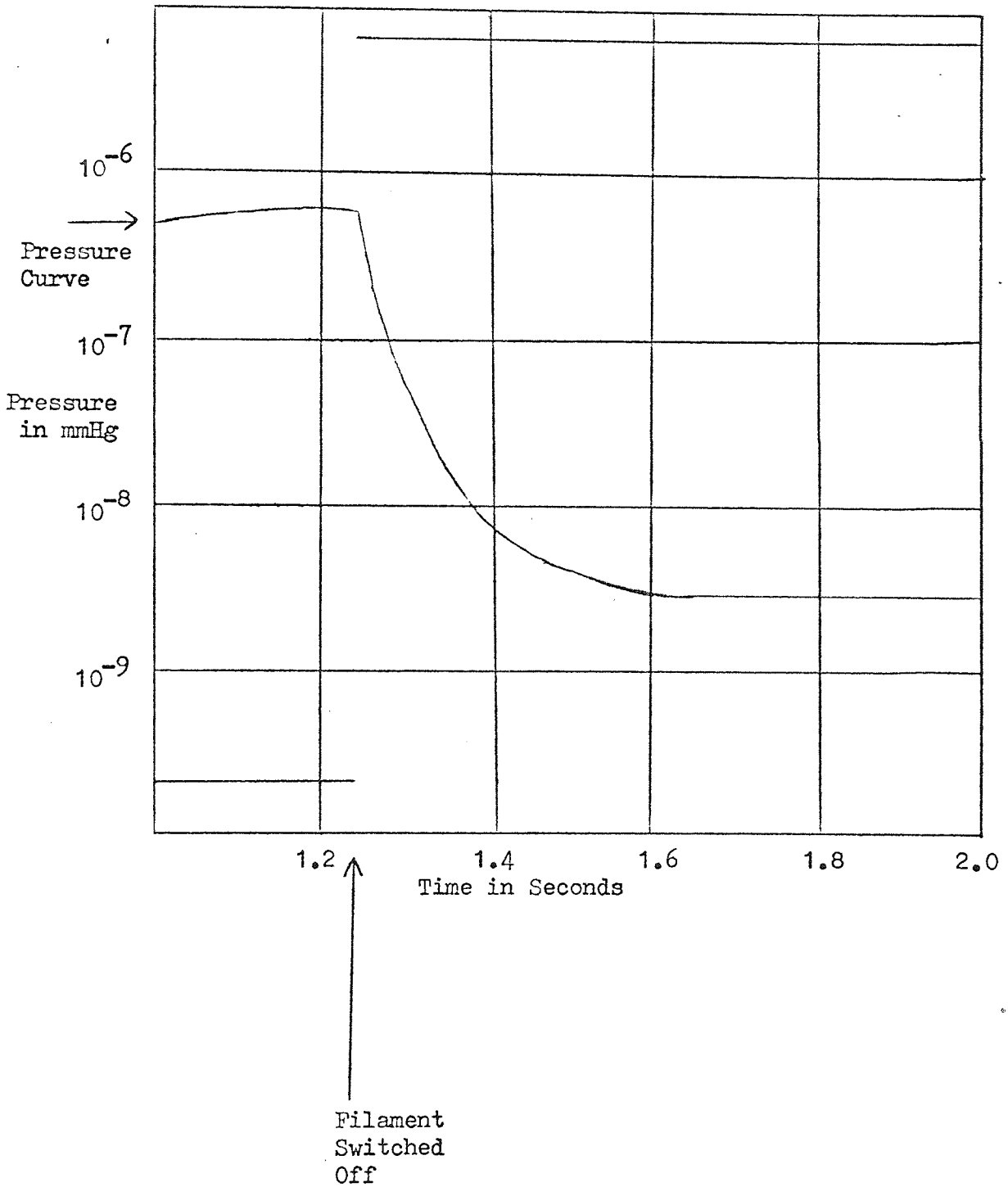

now if we assume P_1 and P_2 >> P_E as is sometimes the case we can omit P_E

$$S_E = \frac{V}{(t_2 - t_1)} \ln \frac{P_1}{P_2} \quad \text{.... (4-14)}$$

Now by substituting the values obtained from the pump away at the end of the flash into this equation the pumping speed can be calculated. Fig. 47 is a graph showing a typical reduction in pressure due to pumping at the end of the flash.

4.1.4 Calculation of the Pressure

The output of the trigger Penning gauge was transferred to an oscilloscope. One of the traces on the oscilloscope represented the pressure in the system. The output of the trigger gauge control unit was 0.2 volts per decade and when this was transferred to the oscilloscope one cm on the oscilloscope represented an order of magnitude rise in pressure. By noting the pressure at the beginning of the flash this gives a point to calibrate the trace.

A picture is taken of the oscilloscope trace and the negative obtained is enlarged so that the pressure can be more easily read off the enlargement. By enlarging onto log graph paper the pressure is read off easily.

We need to know the increase in pressure due to the sample gas coming off the filament. From the total pressure in the system we must subtract the increase in pressure due to the background gases and the pressure in the system at the beginning of the flash. The value obtained at a particular time will be the total pressure measurement from all the desorbed species coming off the filament, due to the gas sample. This value can now be used in the analysis.

4.2 USE OF THE BASIC PARAMETERS

4.2.1 The Rate of Desorption

One of the main objectives of the experiment is to calculate the rate of desorption $(dn/dt)_t$. Once this value has been found it is simply mathematics to calculate the remaining parameters. The rate of desorption is given by equation (4-32) and since all the terms in this equation are known the rate of desorption can be calculated.

The experiment begins with the adsorbed gas on the filament in the steady state with its surroundings. The number of molecules being adsorbed on the surface is equal to the number being desorbed in the same time, a dynamic equilibrium. When the filament is flashed this steady state is disturbed and atoms, molecules and ions are desorbed from the filament. Before the flash the pressure in the system will remain constant because of the dynamic equilibrium.

RATE OF GAS ENTERING THE SYSTEM PER UNIT TIME = RATE OF GAS LEAVING THE SYSTEM PER UNIT TIME

.... (4-15)

When the filament is flashed the equilibrium will be disturbed.

In any real system (45) there will be a steady leak rate (L) which may have been introduced deliberately as with a flow system or may be minimised by careful attention to vacuum techniques. The walls of the system will also be de-gassing due to adsorbed gases which will have the same effect as a leak (D). There will also be de-gassing from the filament (F). The rate of gas entering the system in unit time will be,

Rate of gas entering = L + D + F .... (4-16).

If $(dn/dt)_f$ is the rate of supply of gas from the de-gassing of the filament during the flash, n the number of molecules, then by combining L and D the total amount of gas entering the system from anywhere but the filament is $(dn/dt)_L$ in a time interval dt. Equation (4-16) becomes,

$$\text{Rate of gas entering} = (dn/dt)_L + (dn/dt)_f A \qquad \ldots\ (4\text{-}17)$$

where A is the surface area of the filament. Now the rate of loss of gas from the system will be due to the pumping system V or by adsorption on the walls of the system (W) or by re-adsorption on the filament (Z) per unit area.

$$\text{Rate of gas leaving system} = W + Z + V \qquad \ldots\ (4\text{-}18)$$

now if N is the gas density in the system and S_E the pumping speed due to all effects removing gas from the system such as the pumps, the pumping effect of the gauge and the reduction in pressure due to adsorption on the systems walls. Then equation (4-18) becomes

$$\text{Rate of gas leaving system} = + NS_E + RA \qquad \ldots\ (4\text{-}19)$$

where $RA = Z$ and $NS_E = W + V$. By using equation (4-15), which is the mass balance equation for the system,

$$\begin{array}{lcll} \text{CHANGE IN GAS DENSITY PER UNIT TIME} & = & \text{RATE OF GAS ENTERING} & - \text{RATE OF GAS LEAVING THE SYSTEM} \end{array}$$

$$\ldots\ (4\text{-}20)$$

Substituting (4-17) and (4-19)

$$V\left(\frac{dN}{dt}\right) = +\left(\frac{-dn}{dt}\right)_f A + \left(\frac{-dn}{dt}\right)_L - NS_E - RA$$

$$\ldots\ (4\text{-}21)$$

where V is the volume of the system.

We will now assume that the number of molecules readsorbed during the flash will be very small. The chances that a molecule that has acquired the energy to desorb will be adsorbed on a surface which is higher in temperature than the one from which it was desorbed are very small and so this assumption is valid. Any molecule which escapes from the immediate vicinity of the filament has a much greater chance of being adsorbed on the walls of the system which has a much larger area than the filament. The time of the flash is also relatively short and so this also reduces the chances of a molecule being readsorbed. We will also assume that $(-dn/dt)_L$, the leak rate, is relatively small compared to $(-dn/dt)_f$ and so can be neglected.

Then,

$$V(dN/dt) = (-dn/dt)_f \; A - NS_E \qquad \ldots\ (4\text{-}22)$$

We shall assume that the ideal gas laws may be applied to the system, then

$$PV = n R T \qquad \ldots\ (4\text{-}23)$$

now V is in litres, P in atmospheres, n in moles of gas and T in degrees absolute.

$$n = NV/L \qquad \ldots\ (4\text{-}24)$$

Since N = number of molecules per litre (as used in 4-21) and L is Avogadro's number.

$$P = \frac{N R T}{L} \qquad \ldots\ (4\text{-}25)$$

It can be seen that if R, T, V and L are constant,

$$P \propto N, \text{ so}$$

$$P = \frac{1}{Q} N = \frac{N}{Q} \qquad \ldots\ (4\text{-}26)$$

Here Q is the proportionality constant and is equal to

$$Q = \frac{L}{RT} \qquad \ldots\ (4\text{-}27)$$

$$= 0.2446 \times 10^{23} \text{ molecules atm}^{-1}$$

changing atmospheres to torr

$$Q = 3.219 \times 10^{19} \text{ molecules torr}^{-1} \qquad \ldots\ (4\text{-}28)$$

$$= 3.219 \times 10^{19} \text{ molecules m}^{2} \text{ N}^{-1}$$

substituting in equation (4-26)

$$N = 3.219 \times 10^{19} \text{ P molecules litre}^{-1} \qquad \ldots\ (4\text{-}29)$$

now differentiating (4-29) with respect to time gives

$$dN/dt = 3.219 \times 10^{19} \ dP/dt \qquad \ldots\ (4\text{-}30)$$

substituting in equation (4-22) for (4-29) and (4-30)

$$V \frac{dP}{dt} \ 3.219 \times 10^{19} = + \left(\frac{-dn}{dt} \right)_f A - 3.219 \times 10^{19} \ P \ S_E$$

$$\ldots\ (4\text{-}31)$$

where V is the volume of the vacuum system. This equation gives the rate of desorption in terms of experimentally measured parameters

$$\left(- \frac{dn}{dt} \right)_f = \frac{3.219 \times 10^{19}}{A} \left[V \frac{dP}{dt} + P \ S_E \right] \qquad \ldots\ (4\text{-}32)$$

The negative sign in front of the rate of desorption is because

we are taking adsorption as being a positive process. A is the surface area of the filament, which is twice the length multiplied by the width, assuming it to be so thin that desorption from the edges is negligible. This gives the rate of desorption in terms of rate per cm^2.

Of the two terms in the bracket the first term gives the number of molecules desorbed from the filament per sec per cm^2 and the second term is a correction factor for the number of molecules lost by pumping. When the pressure is increasing and gas is being desorbed from the filament the VdP/dt is the largest term but when this goes negative the PS_E term compensates for the loss of molecules. Fig. 48 shows the effect of these terms on the various graphs. The maximum in the dP/dt against time curve occurs before the maximum in the P against t curve. The $(dP/dt)_t$ curve goes negative and the effect of the PS_E term shows in the $(dn/dt)_t$ against time graph when this term keeps the graph positive. If the $(dn/dt)_t$ graph goes negative then this indicates that adsorption is occurring during the desorption process which is against one of the basic assumptions that we have made.

In equation (4-32) all the terms are known. A and V are measured using physical methods. The pressure P is calculated as indicated and the $(dP/dt)_t$ term is measured by calculating the gradient to the P against t graph at time t. The pumping speed S_E is calculated by the method suggested.

A typical rate of desorption against time curve is shown in Fig. 49. The rate of desorption rises sharply to a maximum and then drops sharply back to the base line where it tails off. The graph is roughly symmetrical about the maximum.

FIG. 48 Graphs showing 1) Pressure Against Time, 2) $(dP/dt)_t$ Against Time, 3) $(dn/dt)_t$ Against Time.

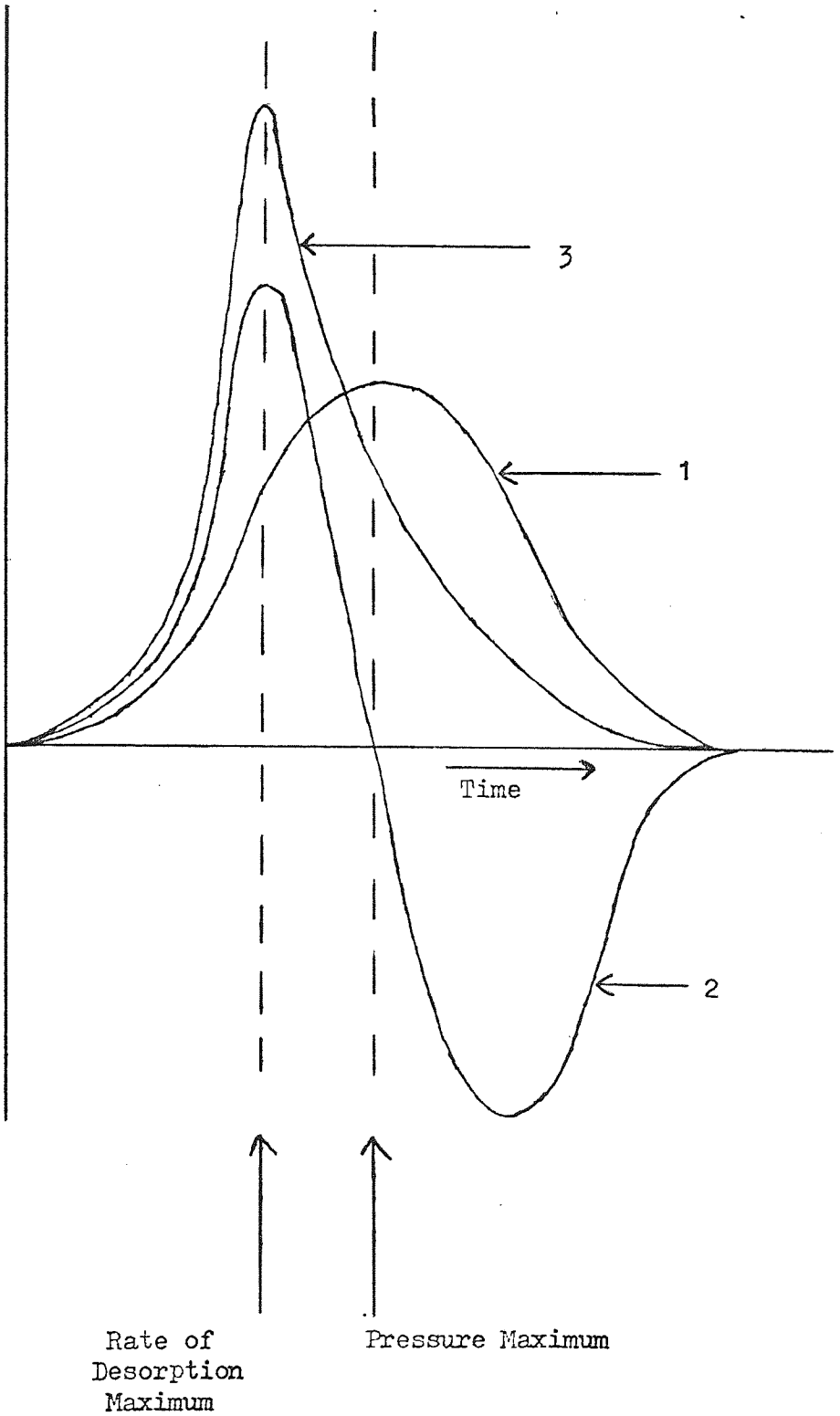

4.2.2 The Surface Coverage

The surface coverage is the number of molecules that have been adsorbed on the surface per cm^2. These molecules are desorbed when the filament is flashed. To calculate the surface coverage we must add the number of molecules desorbed in each small period of time. The calculation of the surface coverage is mathematically expressed as

$$\sigma_o = \int_{t=0}^{t=t_{end}} \left(\frac{-dn}{dt}\right)_t dt \qquad \ldots\ (4\text{-}33)$$

This gives the total surface coverage which is given by the number of molecules desorbed between time t = 0, the start of the flash and $t = t_{end}$, the end of the flash.

The surface coverage at any time during the flash is the number of molecules that remain on the surface at that time. At the beginning of the flash the surface coverage is a maximum and this decreases to zero when all the molecules have been desorbed from the filament at the end of the flash. The surface coverage at any time is given by the mathematical expression

$$\sigma_t = (\sigma_o - \theta_t) = \int_{t=0}^{t=t_{end}} \left(\frac{dn}{dt}\right)_t dt - \int_{t=0}^{t=t} \left(\frac{dn}{dt}\right)_t dt$$

$$\ldots\ (4\text{-}34)$$

where the number of molecules desorbed up to time t = t has been taken from the total surface coverage to leave the number of molecules still on the surface. Here σ_o is the total surface coverage, σ_t is the surface coverage at time t, that is the number of molecules left on the surface at time t, and θ is the number

of molecules desorbed in the time interval t = 0 to t = t.

Equation (4-34) is solved graphically by calculating the area under the $(dn/dt)_t$ against time graph. This gives the total surface coverage. The surface coverage at any time can be found as shown in Fig. 49. The area under the graph from time t = 0 to time t = t is subtracted from the total area under the curve, and this gives the surface coverage at any time t. The surface coverage is calculated in molecules per cm^2 but can be more easily used if monolayer units are used.

4.2.3 Evaluation of the Order of Reaction and Activation Energy

The order of reaction and the experimental energy of activation are two very important parameters that we must know in order to try to postulate a mechanism for the adsorption and desorption of the gas from a metal surface. ~~The order of reaction gives the number of bonds which are broken in the rate determining stage of the reaction and gives information about the transition state.~~ The experimental energy of activation gives us the strength of the bond which binds the atom or molecule to the metal surface. The actual value can give us information on the type of binding that is involved.

In 1889 Arrhenius (82) postulated a relationship between the rate constant k_d and the experimental energy of activation provided that this is independent of temperature. This law has been applied to many chemical systems since this time and has been found to be remarkably accurate. It states

$$k_d = A\ e^{-E_{exp}/RT} \qquad \ldots\ (4\text{-}35)$$

here A is known as the frequency factor or pre-exponential factor but is only a frequency in the case of first order reactions.

FIG. 49 Graph of $(dn/dt)_t$ Against Time Used to Measure the Surface Coverage.

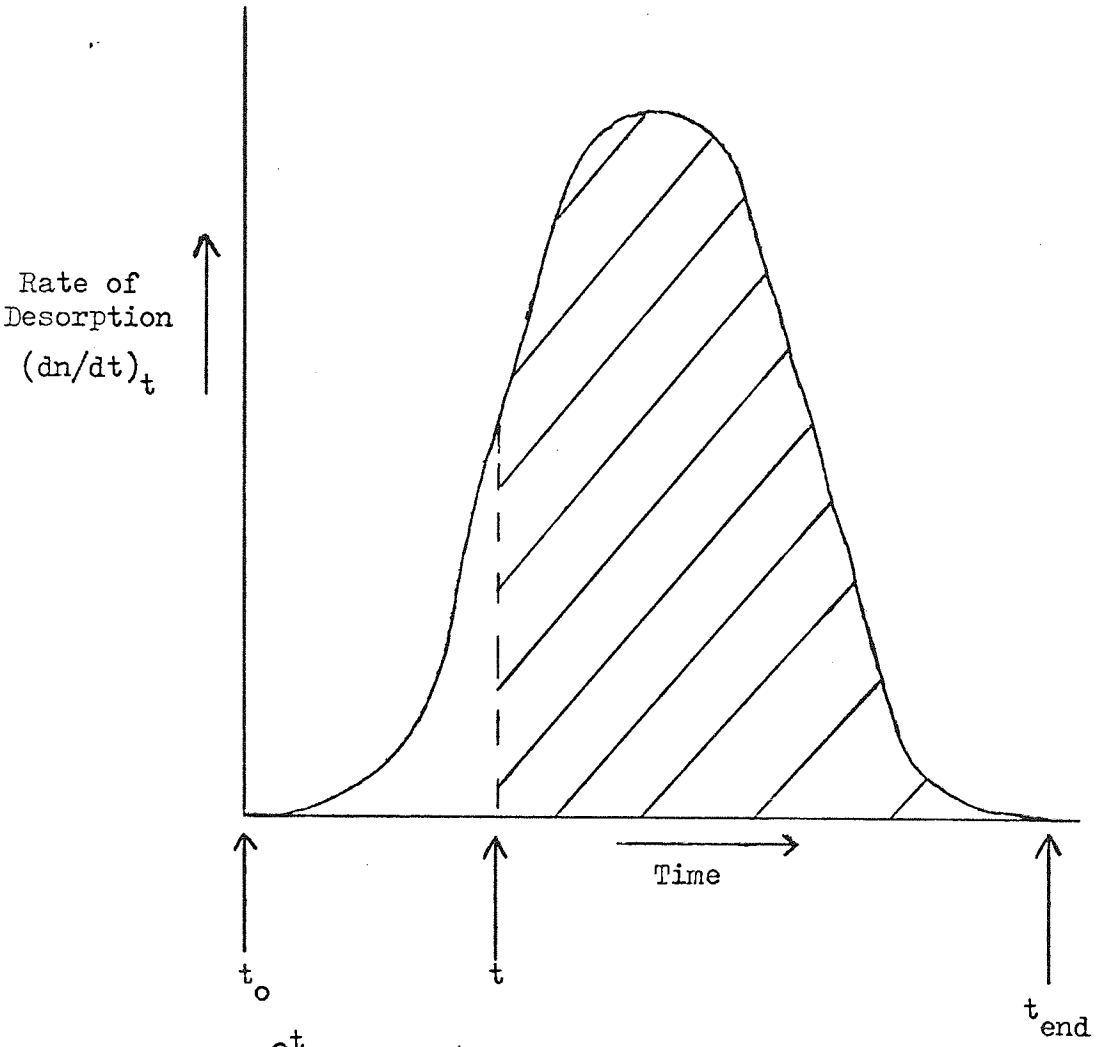

$$\sigma_o = \int_{t_o}^{t_{end}} \left(\frac{dn}{dt} \right) dt$$

$$\sigma_t = (\sigma_o - \theta_t) = \int_{t_o}^{t_{end}} \left(\frac{dn}{dt} \right) dt - \int_{t_o}^{t} \left(\frac{dn}{dt} \right) dt = \text{shaded area}$$

σ_o = total surface coverage

σ_t = surface coverage after time t (shaded area under curve)

θ_t = number of molecules desorbed.

E_{exp} is the experimental energy of activation of the reaction. The equation shows that in our case the rate constant is not a constant but varies with temperature.

Taking logs of (4-35)

$$\ln k_d = \ln A - \frac{E_{exp}}{RT} \qquad \ldots\ (4\text{-}36)$$

differentiating equation (4-36) with respect to temperature

$$\frac{d(\ln k_d)}{dT} = \frac{E_{exp}}{RT^2} \qquad \ldots\ (4\text{-}37)$$

Laidler (83) takes equation (4-37) as his definition of the experimental energy of activation.

The relationship between the rate of reaction and the concentration on the surface, the surface coverage, is given in equation (4-38)

$$\text{rate of reaction} = \frac{dn}{dt} = k_d [\sigma_t]^x \qquad \ldots\ (4\text{-}38)$$

and here x is the order of the reaction, k_d is the rate constant which varies with temperature. $[\sigma_t]$ is the concentration of the reactants and for our purposes this will be the number of molecules adsorbed on the surface, the surface coverage. The rate is the rate of the rate determining step in the desorption process. Combining (4-35) and (4-38)

$$\frac{dn}{dt} = r_d = A [\sigma_t]^x \; e^{-E_{exp}/RT} \qquad \ldots\ (4\text{-}39)$$

The concentration on the surface σ_t has already been calculated and is $[\sigma_o - \theta_t]$.

$$[\sigma_t] = [\sigma_o - \theta_t]$$

$$\frac{dn}{dt} = A [\sigma_o - \theta_t]^x \; e^{-E_{exp}/RT} \qquad \ldots\ (4\text{-}40)$$

taking logs

$$\ln\left(\frac{dn}{dt}\right) = \ln A + x \ln\left[\sigma_o - \theta_t\right] - \frac{E_{exp}}{RT} \quad \ldots\ldots (4\text{-}41)$$

rearranging,

$$\frac{E_{exp}}{RT} = \ln A + \ln\left[\frac{(\sigma_o - \theta_t)^x}{(dn/dt)}\right] \quad \ldots\ldots (4\text{-}42)$$

differentiating with respect to 1/T

$$\frac{E_{exp}}{R} = \frac{d \ln\left[\frac{(\sigma_o - \theta_t)^x}{dn/dt}\right]}{d(1/T)} \quad \ldots\ldots (4\text{-}43)$$

Now using equation (4-43) both the order of reaction and the experimental energy of activation can be found. A graph of $\ln\left[\frac{(\sigma_o - \theta_t)^x}{dn/dt}\right]$ against 1/T for various values of the order of reaction **x** gives the order of reaction. The value of **x** which gives the best straight line is the order of reaction. Using this value of the order of reaction the same graph will give the activation energy. The gradient of the line obtained is $\Delta E_{exp}/R$ and from this the experimental energy of activation can be calculated.

The value of the order of reaction obtained may be checked by a second method using the variation of the surface coverage with time (32). The results from several experiments are used with a variation of the initial surface coverages over them of a FACTOR OF 10-100 molecules per cm^2. Graphs of $(\sigma_o - \theta_t)/\sigma_o$ against t are drawn for each of the experiments. These graphs are shown in Fig. 50 for the first and second order reactions. By comparing the graphs obtained whether the order is first or second can be estimated.

FIG. 50 Graphs Showing Variation of n/n_o Against Time for a First and Second Order Reaction.

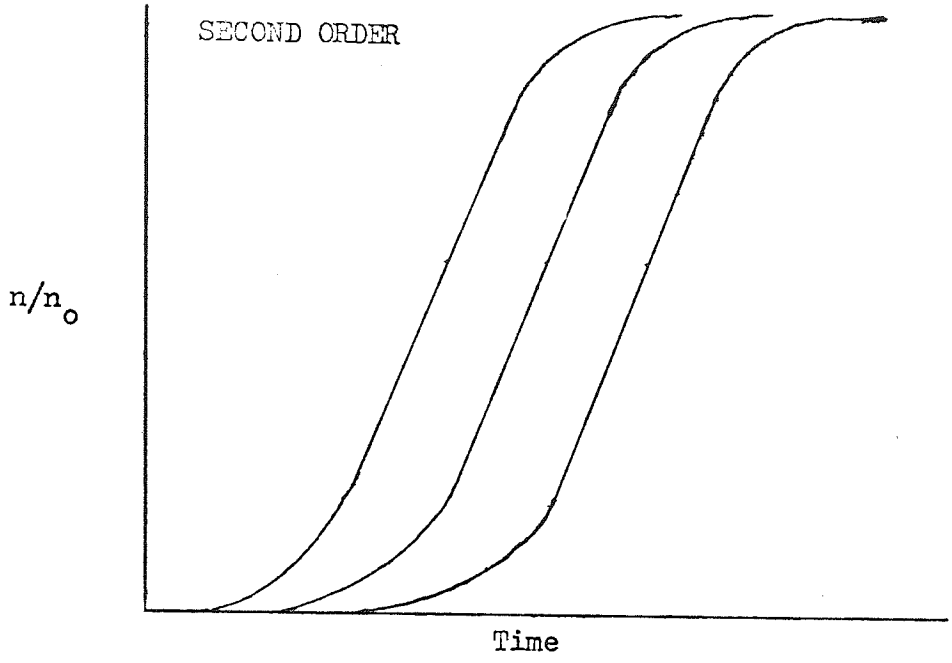

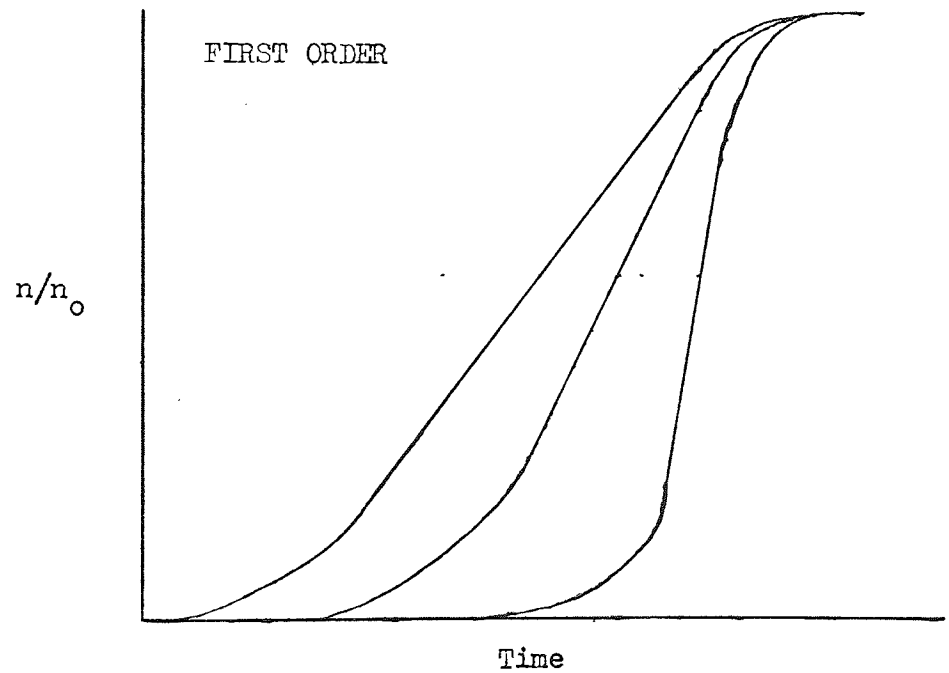

The general trends of the graphs give the information required. The desorption reaction is assumed to be first or second order. The second order graphs have a more pronounced S shape than the first order graphs. The first order curves are independent of the initial surface coverage whereas the second order curves move slightly to higher temperatures with an increase in the surface coverage. The shape of the second order curves is independent of the surface coverage. The use of this alternative approach should confirm the value already obtained for the order of the reaction. However neither method is very accurate and both methods may be needed to estimate the right order.

From equation (4-43) it can be seen that all the quantities have been previously calculated. The temperature has been calculated and the reciprocal is easily found. The surface coverage has also been calculated from the knowledge of the rate of the reaction and so the surface coverage divided by the rate at any time t may be calculated. This term is equal to the reciprocal of rate constant at a particular time and hence temperature, since $dT = dt$. Rearranging equation (4-38),

$$k_d = \frac{dn/dt}{\left[\sigma_o - \theta_t\right]^x} \qquad \ldots\ (4\text{-}44)$$

Calculation of the rate constant allows us to trace its change with temperature. The pre-exponential term A can also be calculated once the rate constant is known.

By this method of analysis, the temperature, the rate of the reaction, the surface coverage, the rate constant, the order of the reaction and the experimental energy of activation have all been calculated. The order of the reaction and the experimental energy

of activation should correspond for all the different experiments for each of the peaks. This information can now be used to evaluate a mechanism for desorption.

4.3 RELATION TO THE SURFACE REACTION

4.3.1 Use of the Absolute Reaction Rate Theory

Consider the reaction

$$A + B \longrightarrow C + D \qquad \ldots\ldots (4\text{-}45)$$

It is postulated that A + B initially combine together to form an intermediate X which then forms the two products. This intermediate is known as the transition state or activated complex.

$$A + B \longrightarrow X \longrightarrow C + D \qquad \ldots\ldots (4\text{-}46)$$

In many cases for the reaction to take place an amount of energy will have to be supplied. This means that the activated complex will be higher in energy than the reactants. The activated complex will then decompose to the products and so the products will be less in energy than the activated complex. The activated complex was first proposed by Eyring (84) in 1935.

For the absolute reaction rate theory to be applied to this system two postulates have to be made. These have been shown to be valid by Petermann (42).

The first states that the reactants must come together to form an activated complex if the reaction needs activation energy to start it. If the rate is dependant on a factor of $e^{-\alpha/t}$ an activated state is formed and this is regarded as being at the top of an energy barrier as shown in Fig. 51. The rate of the reaction will be the frequency at which the activated complexes pass over

FIG. 51 Potential Energy Curve for A Reaction Showing An Imaginary Potential Box Containing The Activated State.

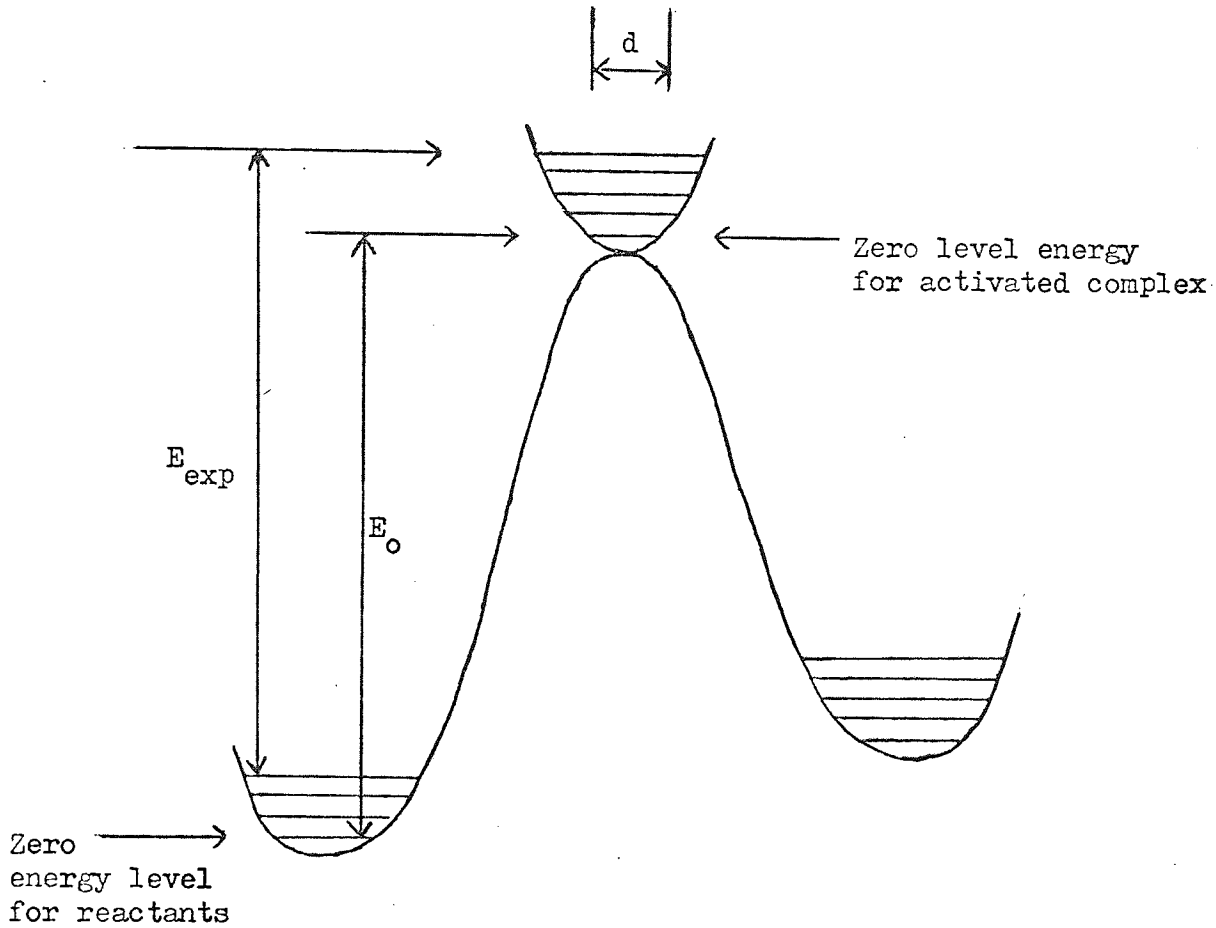

Initial State ⟶ Final State

A + B + C ... X + Y + Z ...

this barrier. The top of the barrier is usually regarded as being flat over a length d so that when the activated complex is in this area it is said to exist.

The difference between an activated complex and an ordinary molecule is that in one of the directions of vibration it falls apart. To put this in another way the normal vibrational frequency in the co-ordinate of decomposition has an imaginary value.

The second postulate states that the activated complex and the reactants are always in equilibrium and that the activated complex always decomposes at a definite rate. For reaction in equation (4-46)

$$A + B \underset{k_2}{\overset{k_1}{\rightleftharpoons}} X \text{ (activated complex)} \qquad \ldots. (4\text{-}47)$$

$$X \xrightarrow[k_3]{} C + D \qquad \ldots. (4\text{-}48)$$

where A and B are in equilibrium with X and then X breaks down at a constant rate k_3 to form the products.

The general equation of the transition state theory is

$$k_d = \frac{k\,T}{h} \quad \frac{F'}{F_A F_B \ldots} \quad e^{-E_o/RT} \qquad \ldots. (4\text{-}49)$$

the derivation of which can be found in most text books on the subject (85). This is assuming the transmission coefficient as shown in Fig. 52 is equal to 1. Here the equation is similar to (4-35). F' is the partition function of the activated complex and F_A and F_B are the partition functions of the reactants A and B (86). E_o is defined as the difference between the zero level energy per mole of activated complex and that of the reactants as shown in Fig. 52. E_o is the activation energy required at 0 K, the amount

FIG. 52 Basic Equation of the Absolute Reaction Rate Theory.

For Reaction

$$A + B \longrightarrow X$$

$$k_f = \frac{kT}{h} \; \bar{r} \; \frac{F^1}{F_A F_B} \; e^{-E_o/RT}$$

$\frac{F^1}{F_A F_B}$ ↓ partition function ratio

$\bar{r}$ ↓ transmission coefficient $\simeq 1$

$\frac{kT}{h}$ ↓ harmonic oscillator

$k = R/N_o$

$h = 6.62 \times 10^{-27}$ erg sec

$R = 8.314$ joules deg^{-1}

$N_o = 6.02 \times 10^{23}$ $mole^{-1}$

1 joule $= 10^7$ ergs

of energy required so that the reactants, A, B, C ... can form an activated complex. Using equation (4-44) with (4-49) we get

$$k_d = \frac{dn/dt}{[\sigma_t - \theta_t]^x} = \frac{kT}{h} \quad \frac{F'}{F_A F_B \cdots} \quad e^{-E_o/RT} \qquad \ldots. (4\text{-}50)$$

It can also be shown that

$$k_d = \frac{dn/dt}{[\sigma_t - \theta_t]^x} = \frac{kT}{h} \; e^{-\Delta H^\circ/RT} \; e^{\Delta S^\circ/R} \qquad \ldots. (4\text{-}51)$$

since

$$\Delta G^\circ = - RT \ln K_c \qquad \ldots. (4\text{-}52)$$

and

$$k_d = \frac{kT}{h} \; K_c \qquad \ldots. (4\text{-}53)$$

Comparing (4-50) and (4-51) it can be seen that

$$\frac{F'}{F_A^n} \equiv e^{\Delta S^\circ/R} \qquad \ldots. (4\text{-}54)$$

where ΔS° is the entropy of activation. This is assuming that the partition function is independent of temperature and

$$e^{-\Delta H^\circ/RT} \equiv e^{-E_o/RT} \qquad \ldots. (4\text{-}55)$$

where $-\Delta H^\circ$ is the standard enthalpy of the reaction. The comparison of the equations cannot be made unless the temperature independence of the partition functions is made. In this case

$$\Delta H_o \equiv E_o \qquad \ldots. (4\text{-}56)$$

and

$$\Delta S^\circ = R \ln \frac{F'}{F_A^n} \qquad \ldots. (4\text{-}57)$$

(4-57) is known as the Sackur-Tetrode equation.

Now taking logs and RE-ARRANGING (4-50)

$$+\frac{E_o}{RT} = +\ln\frac{F'}{F_A^n}\frac{k}{h} + \ln T - \ln\frac{dn/dt}{[\sigma_o - \theta_t]^x} \quad \ldots\ldots (4\text{-}58)$$

differentiating with respect to 1/T and rearranging

$$+\frac{E_o}{R} = \frac{\Delta H_o}{R} = \frac{d \ln\left[\frac{[\sigma_o - \theta_t]^x \; T}{dn/dt}\right]}{d\left[1/T\right]} \quad \ldots\ldots (4\text{-}59)$$

Using equation (4-52)(4-53) and $\Delta G^\circ = \Delta H^\circ - T\Delta S$

$$\Delta S = R\left[\ln\frac{dn/dt}{[\sigma_o - \theta_t]^x} - \ln\left(\frac{kT}{h}\right) + \frac{\Delta H^\circ}{RT}\right] \quad \ldots\ldots (4\text{-}60)$$

Using the absolute rate theory approach further parameters relating to the surface can be calculated such as the standard enthalpy of the reaction, the entropy and the ratio of the partition functions. However thermodynamic data needs to be calculated at a particular temperature. We take this temperature to be the temperature of the maximum in the rate of desorption against time curve. This is the temperature of the maximum rate of reaction and can be regarded as the temperature at which the reaction takes place. Once this temperature has been defined the values can be substituted into equation (4-61)

$$E_{exp} = RT + \Delta H^\circ \quad \ldots\ldots (4\text{-}64).$$

The value of the standard enthalpy of reaction is then substituted in equation (4-60) to find the value of the entropy. The

value of the entropy can then be used to find the ratio of the partition function in equation (4-57).

The value of the entropy and the ratio of the partition functions is used to try and give an estimation of the mobility of the adsorbed species and the transition complex.

4.3.2 Mass Spectrometry

The information obtained so far is not capable of giving a complete picture of what is happening on the surface. When a gas is adsorbed on the surface it may be adsorbed as the gas is in the gas state, it may be adsorbed with dissociation or it might form complexes with the metal. Similarly when the gas is desorbed many mechanisms are possible.

The desorbed species need to be identified so that a complete picture of the mechanism of desorption is found. In some cases more than one peak is desorbed and both the desorbed species in this case need to be identified.

The species are identified with a mass spectrometer attached to the apparatus near to the filament. The mass spectrometer has a range of 1-200 atomic mass units and so any desorbed species in this range could be identified. The full spectrum can be spanned over a short time or one particular peak (mass number) can be followed through the flash. This is very useful since the pressure measured by the gauge is the total pressure and not the partial pressure. The mass spectrometer means that the effect of the desorption process on one particular peak can be followed.

Unfortunately the mass spectrometer can not distinguish between two atoms which gives rise to the same mass peak. For instance peak 28 which can be nitrogen or carbon monoxide. To

be able to try and work out the percentage of this peak due to each one of the masses the past history of the system must be known.

The mass spectrometer needs to be used in a closed system if the whole range of the spectrum is to be scanned since the scan takes a period of time and some of the peak may be preferentially pumped. Also some of the peaks will be opened to the pumps for a longer time than some of the lower mass units and this might effect the relative height of the peaks.

Once the desorbed species have been identified it will greatly help us to try and form a mechanism for the desorption and adsorption of the gas from the metal surface.

With the information obtained from the mass spectrometer added to the information obtained from the numerical analysis we should be able to postulate a reasonably accurate mechanism for adsorption and desorption.

4.3.3 Interpretation of the Experimental Parameters

Once the experimental results have been obtained they must be related to the reaction at the gas-metal surface and be able to be explained by the reaction mechanism. The reaction mechanism put forward must be able to explain all the experimentally obtained parameters. One of the main assumptions is that the desorption process is the opposite of the adsorption process. We will assume this assumption to be true and take the desorption process to be the reverse of the adsorption process, so that if a molecule is desorbed with dissociation we assume it dissociates as it is adsorbed.

The experimental energy of activation gives a measure of the energy needed to break the bonds attaching the molecule to the

surface. If this is of the order of a few kilojoules it indicates the bond is of the weak Van der Waals type, while if the activation energy is greater than this it indicates that the bonds are stronger and that chemical bonds with electron interactions are formed.

The order of reaction gives an indication of the number of molecules involved in the rate determining step of the reaction. This is usually assumed to be either one or two and that either one or two bonds are broken in the rate determining step. It is this that would give an indication as to the nature of the transition state.

The temperature T_o is taken to be the temperature at which the reaction takes place. The reaction takes place over a small range of temperatures and so the temperature T_o is taken to be the temperature at the maximum rate of desorption and can be obtained from the dn/dt against t graph. It is found as expected that T_o occurs just before the maximum in the pressure against time graph. This temperature is then used for calculating thermodynamic relationships where the temperature must be defined. The value of the term RT_o even for high temperatures is only of the order of a few kilojoules and this term would be comparable to the errors expected in the experiment.

The entropy can be used as an indication of the mobility of the molecules on the surface. The value can show whether a molecule is mobile and moves across the surface or whether it is immobile. The value of the Gibbs free energy of activation gives an indication of the reactivity of the reaction. The more negative the Gibbs free energy the more likely the reaction would be to proceed.

The surface coverage shows how the molecules are adsorbed on the surface. The change in the surface coverage with time can show how one state is preferentially adsorbed and whether or not one state is being changed into a second adsorbed state. A molecule may be physically adsorbed and then move around on the surface until it finds a state where it can become chemically adsorbed.

By using this approach parameters relating to adsorption and desorption can be calculated and the desorbed species can be identified. An accurate picture of the reaction on the surface can be suggested with the large amount of information obtained.

4.4 THEORETICAL AND EXPERIMENTAL ERRORS

4.4.1 Accuracy of Results

In order to determine the uncertainty of the results it is necessary to calculate the errors due to the theoretical treatment and the errors due to the experimental measurements. The maximum possible error gives an indication of how good an experiment is and gives a comparison between two experiments which give the same experimental results. A knowledge of where the errors occur and where the largest errors appear means that care can be taken at these points in order to reduce them and possibly improve the technique.

4.4.2 Errors in Calculating the Temperature

The temperature is calculated from the measurements taken off the oscilloscope. The values of the voltage and current are found from the oscilloscope trace. To measure the voltage and current we measure the difference between two lines on the oscilloscope front. The accuracy with which this can be done depends on several factors, the width of the line, the response of the instrument and of the accuracy of the measuring device. For the voltage the distance the trace rises varies along the time base in one flash and also varies when comparing two flashes. We can only take an approximate average value of the trace increase but on a suitable volts/cm setting it usually rose about 5 cms. This could be measured using a rule to an accuracy of $\pm$ 0.1 cms, giving an error of 2%. The error in the volts/cm setting was checked using a measured voltage input and found to be very accurate on all settings and so the error due to this both for the current and voltage, were negligible. The enlargement factor due to the use of the enlarger could also be measured to an accuracy of 1 mm in 150 mm, an error of less than 1%. The enlargement factor was 2.5, a one centimeter square was enlarged to a 2.5 cm square. The total error involved in measuring the voltage was 2$\frac{1}{2}$%. For a typical voltage of 5 V the error was $\pm$ 0.125 volts.

The error in measuring the current was greater because the increase in the trace used to measure the current was smaller.

The change in voltage measured to give the current was very small. A typical voltage change across the shunt would give a change of 2 cms giving an error of 5%. The resistance of the shunt was given by the makers as 0.0075 $\pm$ 0.00001 ohms, an uncertainty of less than 1%. The other errors are similar to that of the voltage trace and so the total error in the measurement of the current is 6%. A typical current of 5 amps would give an error of $\pm$ 0.3 amps. For the filament the resistance at room temperature was measured as 0.4131 ohms. Using our estimations of measuring the resistance, the resistance of the filament was 0.4131 $\pm$ 0.04 ohms. The resistance could be measured to an accuracy of 10%.

To find the resistivity we also need to know the cross sectional area and the length of the filament. The length of the filament was measured with a travelling microscope giving an error of 0.002 cm in 6 cms a very small error indeed. The width was also measured with a travelling microscope and the thickness was given by the makers with an error of $\pm$ 5%. The change in these parameters during the flash can not be estimated and the values used all refer to room temperature.

The total error in the resistivity will be 15%. For a resistivity of 40×10^{-6} ohms cm^{-1} the error would be $\pm 6 \times 10^{-6}$ ohms cm^{-1}. In order to find the temperature we have to look up these values on a graph.

A resistivity of 40×10^{-6} ohms cm^{-1} would give a temperature of 1000 K. The error in the resistivity would give possible temperatures of minimum 850 K and maximum 1160 K giving a total error in the temperature of still 15%. However we only need to know that

FIG. 53 Graph Showing the Temperature Variation Along the Filament.

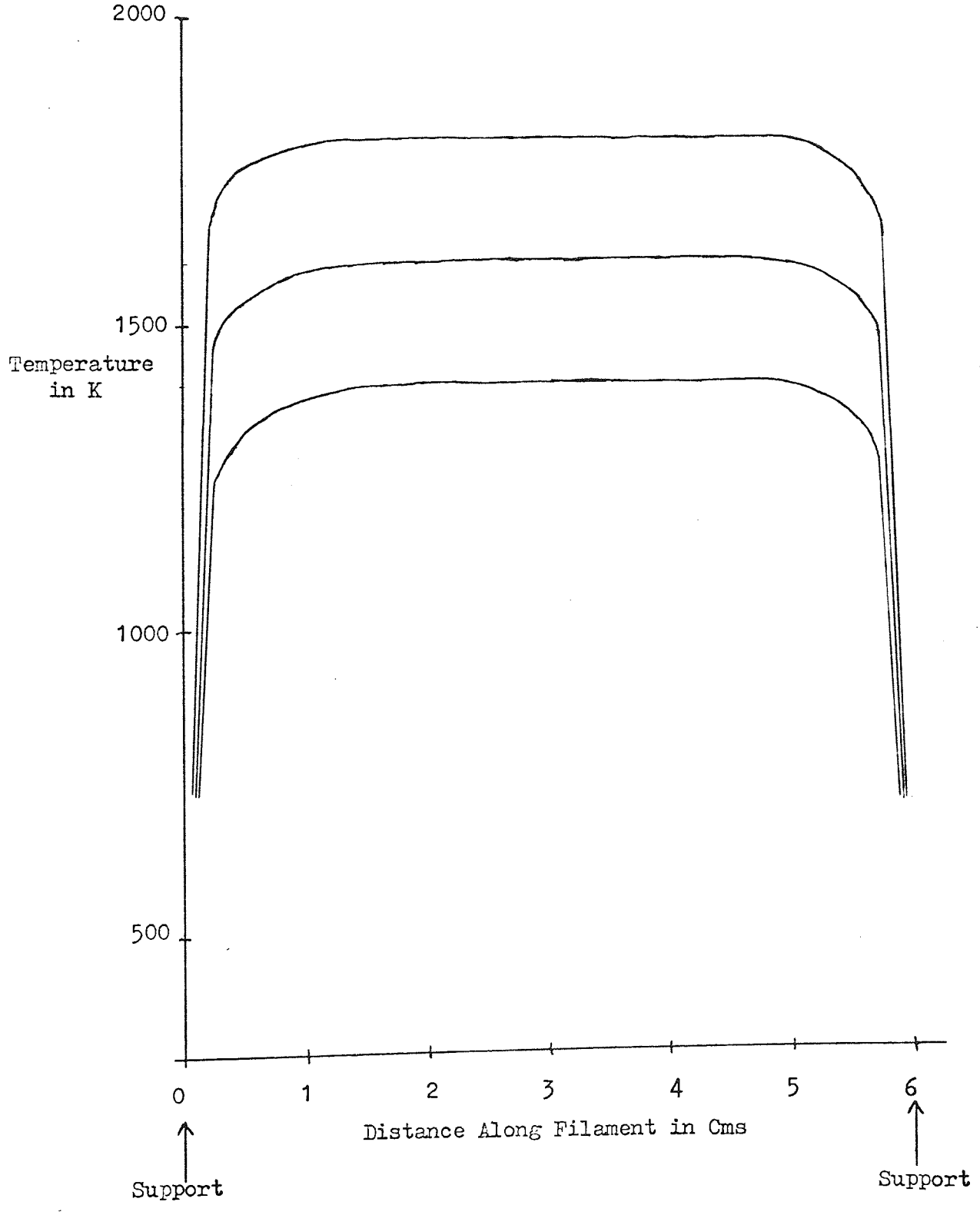

the change in temperature with time is a straight line and this method enables us to show that. Since the method also enables us to measure the temperature directly rather than making assumptions about the temperature relationship between two similar flashes it is a better method.

The temperature is also measured with an optical pyrometer but not during the flash. The optical pyrometer shows the temperature always reached a similar temperature maximum within $\pm$ 50 K for a given current. The maximum temperature for a range of currents were measured and the maximum temperature expected during the flash could be calculated. This was compared to the temperature calculated from the oscilloscope trace and in all cases they compared favourably, they were always within 100 Å of each other.

By measuring the temperature and checking the maximum temperature the value of the temperature obtained is very reliable.

4.4.3 Errors in Measuring the Pressure

The pressure measurement in the system during the flash is probably the most important part of the experiment. The factors effecting the accuracy of this fall into two categories. The actual measurement of the pressure and secondly the external effects which alter the pressure due to the desorption from the filament. The design of the apparatus and experimental precautions try to eliminate the latter. Assuming that the pressure rise is just due to the gas desorbing we wish to estimate how accurately it can be measured.

The pressure increase is very rapid and the oscilloscope must have a fast response time so it is capable of measuring such a quick increase. Rough experiments indicate that the measuring device

copes very accurately with fast pressure increases. So we can assume the error in the response of the gauge is very small and the pressure read off the oscilloscope corresponds to the time and therefore temperature indicated.

The pressure trace suffers from mains interference which appeared to come from the ion gauge control unit. This increased the width of the trace slightly and effected the accuracy of the results slightly. The pressure trace was transferred onto log graph paper using the enlarger so that the pressure could be directly read off the log graph paper. Limitations imposed by the enlarger used meant that 10 cycle log graph had to be used and since each cycle on the graph paper was not very large it meant the accuracy in reading off the pressure suffered especially at the upper end of the cycle.

In any one order of magnitude the pressure can be read off to an accuracy of 1% in the lower range but in the higher region an accuracy of 10% was the best that could be obtained. An average value of the uncertainty of the pressure throughout any one range would be $\pm$ 5%. A pressure of 1×10^{-8} torr would have an error of $\pm 0.1 \times 10^{-8}$ torr.

4.4.4 Error in Measuring the Rate of Desorption

The terms involved in measuring the rate of desorption are a constant, the pumping speed, the pressure, the rate of change of pressure with time and the volume. The error in the pressure is 5% and the error in measuring the volume is very large since only an approximate method is used. The volume of the system was calculated

FIG. 54 Graph Used to Calculate dp/dt.

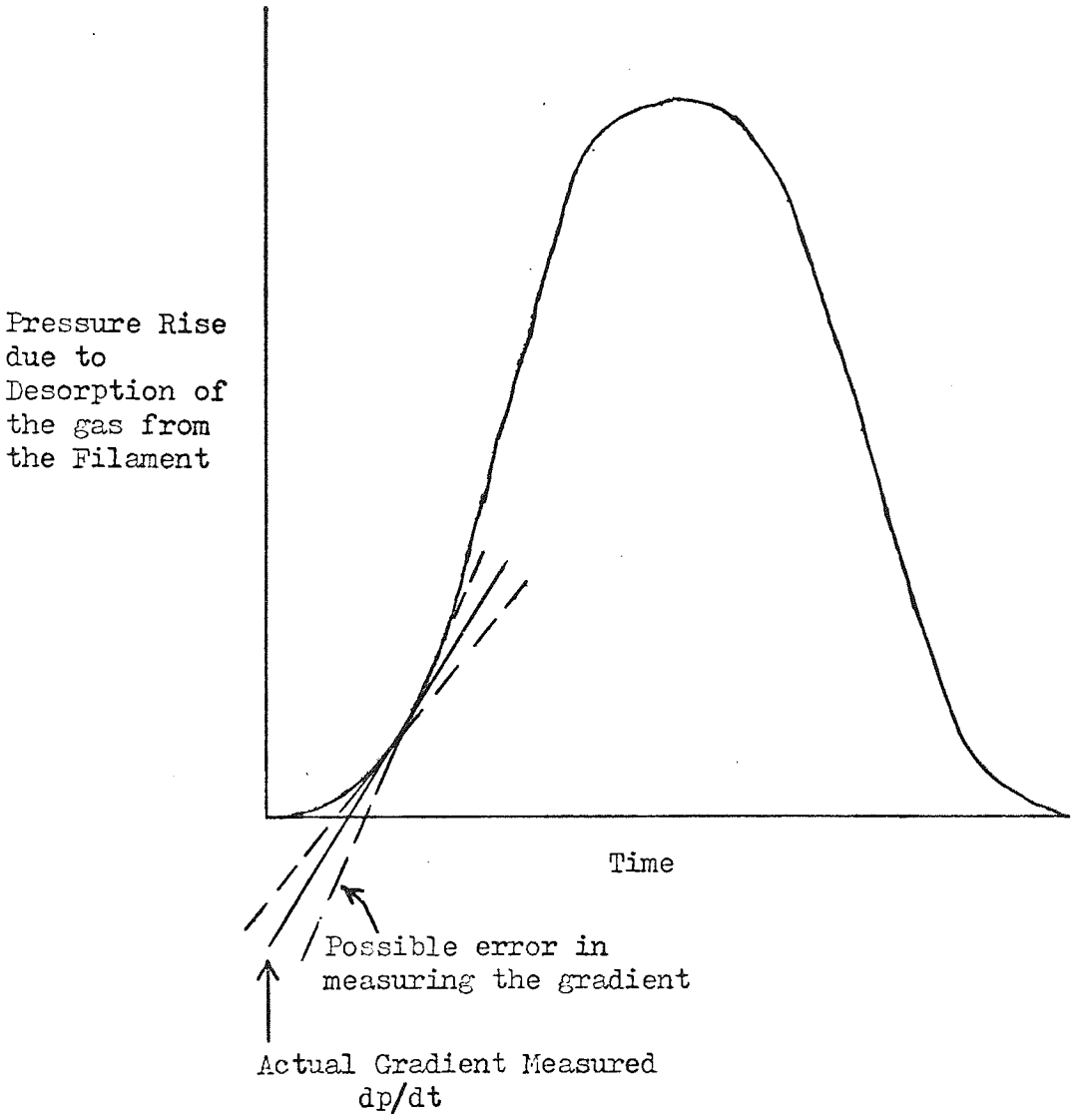

to be 3.5 litres. A reasonable error in this would be 10%. The measurements for the system were obtained either by direct measurements or from the vacuum generators catalogue.

There is also a large error involved in the estimation of the pumping speed. The pumping speed calculation involves using the pressure, volume and the time. The error in the pressure measurement and the volume together would come to 20%. The time can be measured accurately to 0.004 seconds. Over a one second period of time the error is less than 0.1%. Total error involved in measuring the pumping speed is 20% which seems a very conservative estimate.

The error in measuring dp/dt will also be large because gradients are being measured. Fig. 54 shows the graphs and the tangents to the graph. A small change in the gradient gives a very large change in the value of dp/dt. The difficulties in drawing gradients was the main problem although with great care reasonable attempts were made. An accuracy of 10% is the best that could be expected.

The total error in measuring the rate of desorption will be 50%. This may seem very large but when we consider that we are trying to count the number of molecules leaving a surface in a certain time we would expect a very large error. It is more valuable as an order of magnitude calculation and looked upon in this light the error value is reasonable.

For a value of the rate of desorption of 3.38×10^{15} molecules per sec per cm^2, the error value would be very small when we consider the importance of the parameter we have just measured.

4.4.5 Error in Calculating the Surface Coverage

The rate of desorption is used to calculate the surface coverage. A graph is drawn of the rate of desorption against time. However the values of the rate of desorption can vary by ± 50% and this has an effect of increasing and decreasing the area underneath the curve as shown in Fig. 55 .

The area under the graph is either increased or decreased by 50% and so the total surface coverage is either increased or decreased by 50%. A typical value of the surface coverage 8.28×10^{14} molecules per cm^2 would have an error factor of $\pm 4 \times 10^{14}$ molecules per cm^2. So in this case the total surface coverage could vary from 0.4 monolayers to 1.2 monolayers with the most likely value being 0.8 monolayers.

This shows the value of the technique that it can detect very low surface coverages with not too great an error involved.

4.4.6 The Order of Reaction

The order of reaction itself is taken to be either one or two and because of this one cannot consider it an error. We can consider how the errors in the other parameters effect the decision as to whether it is a first or second order reaction.

When plotting the graphs one should, instead of placing a dot where the point is, place a line which covers all possible values due to the errors involved in all the other parameters as shown in Fig. 56 . In some cases this might make it easier to judge whether the reaction is first or second order.

FIG. 55 Graph Showing the Effect of an Error of 50% in the Rate of Desorption on the Surface Coverage.

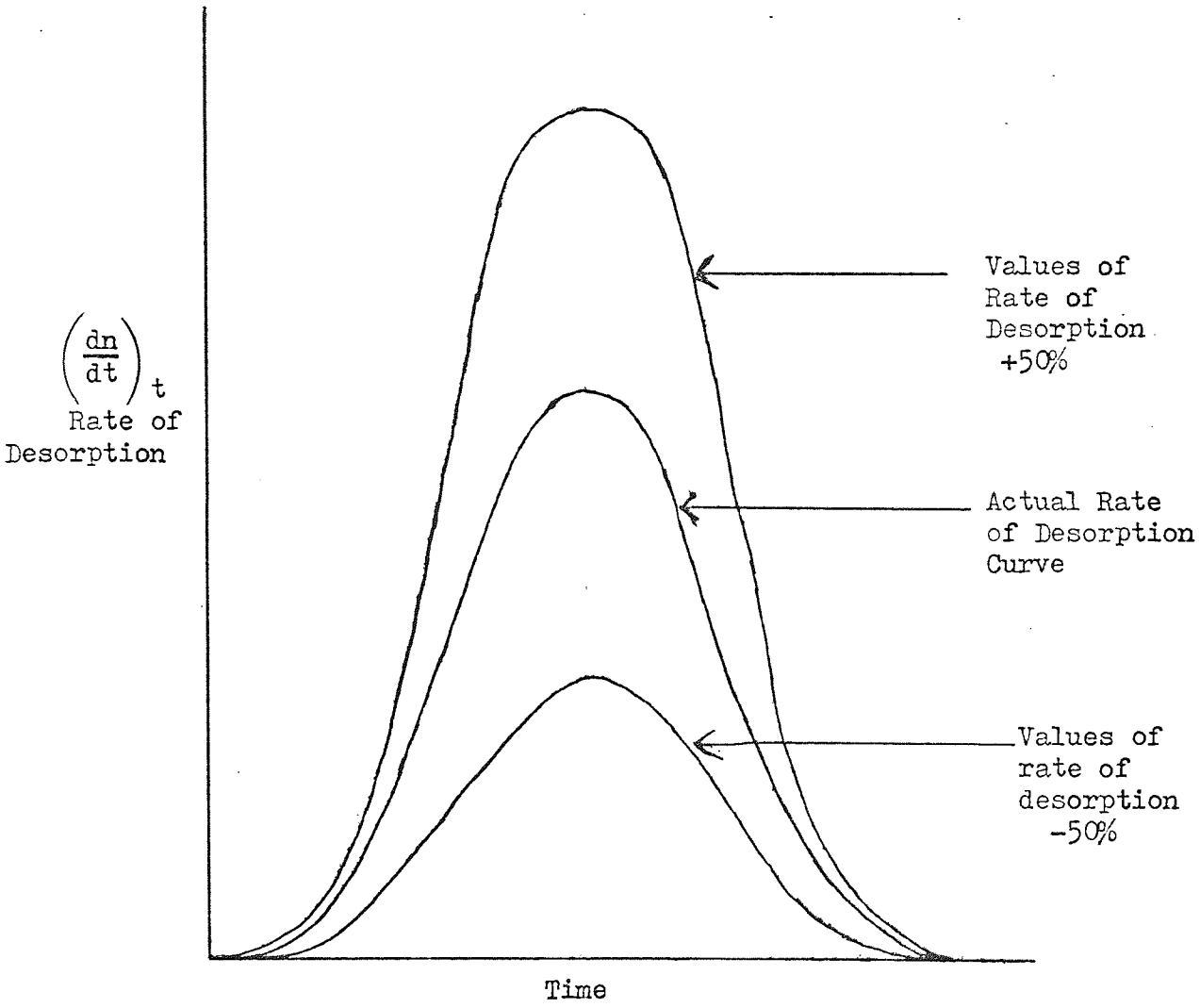

FIG. 56 Graphs Used to Determine the Order of Reaction.

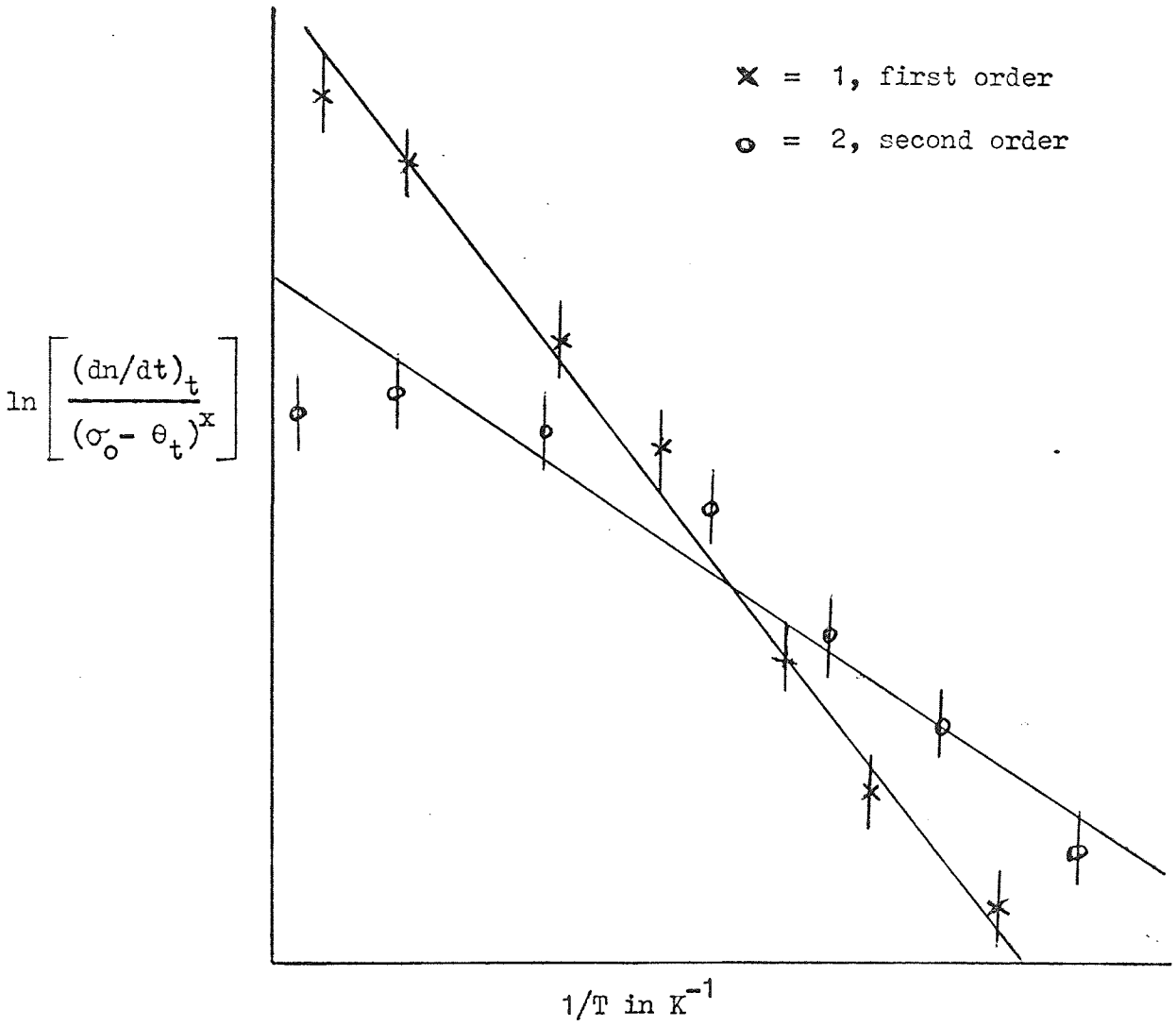

4.4.7 The Experimental Energy of Activation

This is calculated from the gradient of the graph of the change in the rate constant against the reciprocal of the temperature. Once again the errors in the points need to be taken into account, both the error in the rate constant and in the temperature.

The error can be estimated from the graph. The best straight line through the points was drawn to give the correct value of the activation energy. Two other lines parallel to this are drawn through the two extreme points above and below the first line. The diagonals of the rectangle are now drawn in and the gradient of each of the diagonals calculated. This gives a maximum and minimum value for the activation energy for the points drawn on the graph. This is shown in Fig. 57 . The error in calculating the activation energy can be found by comparing the maximum and minimum values with the mean value. If this procedure is repeated for many sets of values an average error for the whole experiment can be found.

The error in calculating the activation energy was found to be $\pm$ 50% over the series of experiments.

FIG. 57 Graph Used to Measure the Error in the Activation Energy.

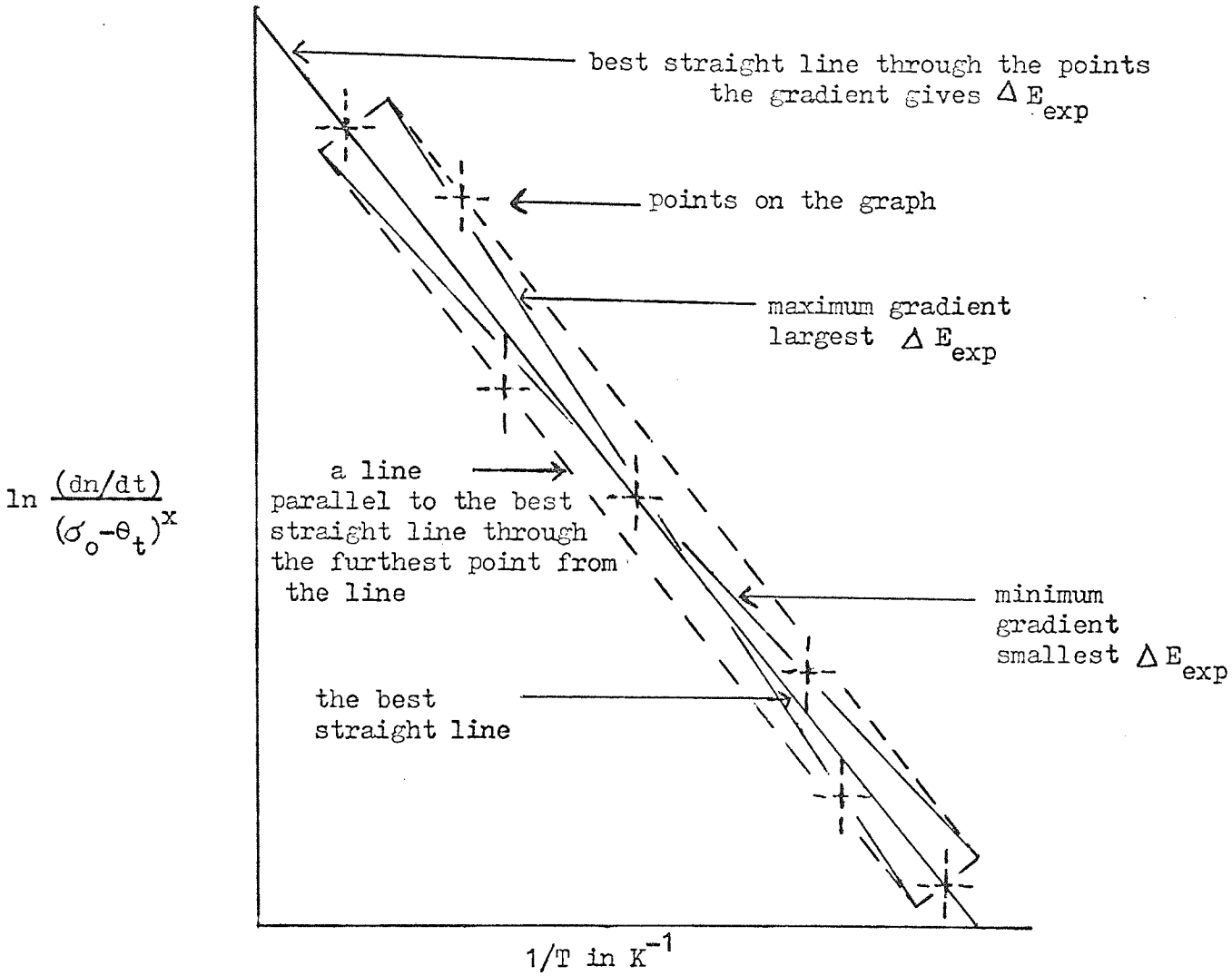

5 CARBON MONOXIDE RESULTS

5.1 PUMPING SPEED

5.1.1 Theory

The pumping speed S in litres per sec is defined by

$$dP/dt = -S\ P_o/V \qquad \ldots\ (5\text{-}1)$$

where V is the volume of the system and P_o is the pressure. Where

$$P_o = P - P_{equ} \qquad \ldots\ (5\text{-}2)$$

and P_{equ} is the equilibrium pressure. At equilibrium P_o is zero and so the change in pressure with time is also zero. The leak rate is never zero because of degassing and although the leaks can be minimised it is very hard to eliminate them completely. At the equilibrium pressure some pumping is occurring and it is only the calculated pumping speed which is zero. By integrating (5-1) assuming the pumping speed is constant, setting $P = P_1$ at $t = t_1$ and $P = P_2$ at $t = t_2$ then

$$\ln \frac{(P_2 - P_{equ})}{(P_1 - P_{equ})} = \frac{S}{V}\ (t_1 - t_2) \qquad \ldots\ (5\text{-}3)$$

If the equilibrium pressure is negligible compared to P_2 and P_1 the equation simplifies to

$$\ln \frac{P_2}{P_1} = \frac{S}{V}\ (t_1 - t_2) \qquad \ldots\ (5\text{-}4)$$

however this is not always valid.

A graph of the left hand side of equation (5-3) against t_1 should give a straight line of gradient 2.303 S/V from which the value of S can be found. By substituting the values into equation (5-3) the value of S may also be found.

The pumping speed calculated is the total pumping speed due to all processes which reduce the number of molecules in the system. This includes the pumps, the pumping of the pressure gauge, adsorption onto the walls of the system and any other pumping mechanism.

The pumping speed needs to be calculated so that the number of molecules lost by pumping can be calculated and this is used to compensate for the molecules lost, in the calculation.

5.1.2 Calculated Pumping Speed

The pumping speed is calculated from the drop in the pressure at the end of the flash. This is shown in Fig. 58 for a carbon monoxide experiment. By substituting the values obtained into the equation the pumping speed is calculated. Fig. 59 shows the pumping speed falls as the equilibrium pressure is approached. This graph of the change in pumping speed against pressure shows the pumping speed falls off rapidly.

The pressure at the end of the flash varies over two or three orders of magnitude and so it is possible to get a graph of pressure against pumping speed using a series of desorption experiments. This graph for a set of experiments is shown in Fig. 60 .

The pumping speed is not constant over the whole pressure range and this should be taken into account when calculating the rate of desorption. Fig. 61 shows, over an order of magnitude above the equilibrium pressure, the pumping speed varies rapidly and linearly over a short pressure region. Fig. 60 shows the pressure against pumping speed graph and that the pumping speed does not change greatly at higher pressures.

FIG. 58 Graph Showing Oscilloscope Trace at the End of the Flash for a Carbon Monoxide Experiment.

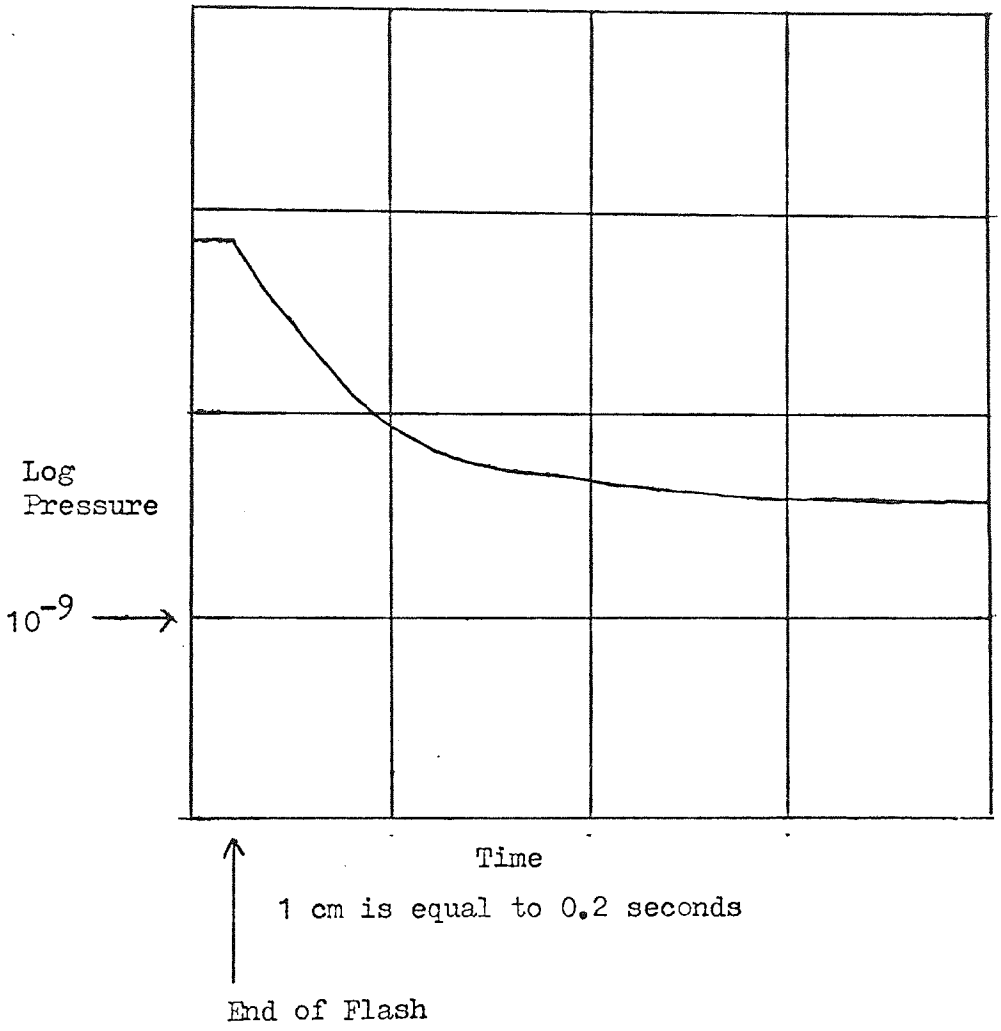

FIG. 59 Graph Showing Change of the Calculated Pumping Speed with Pressure.

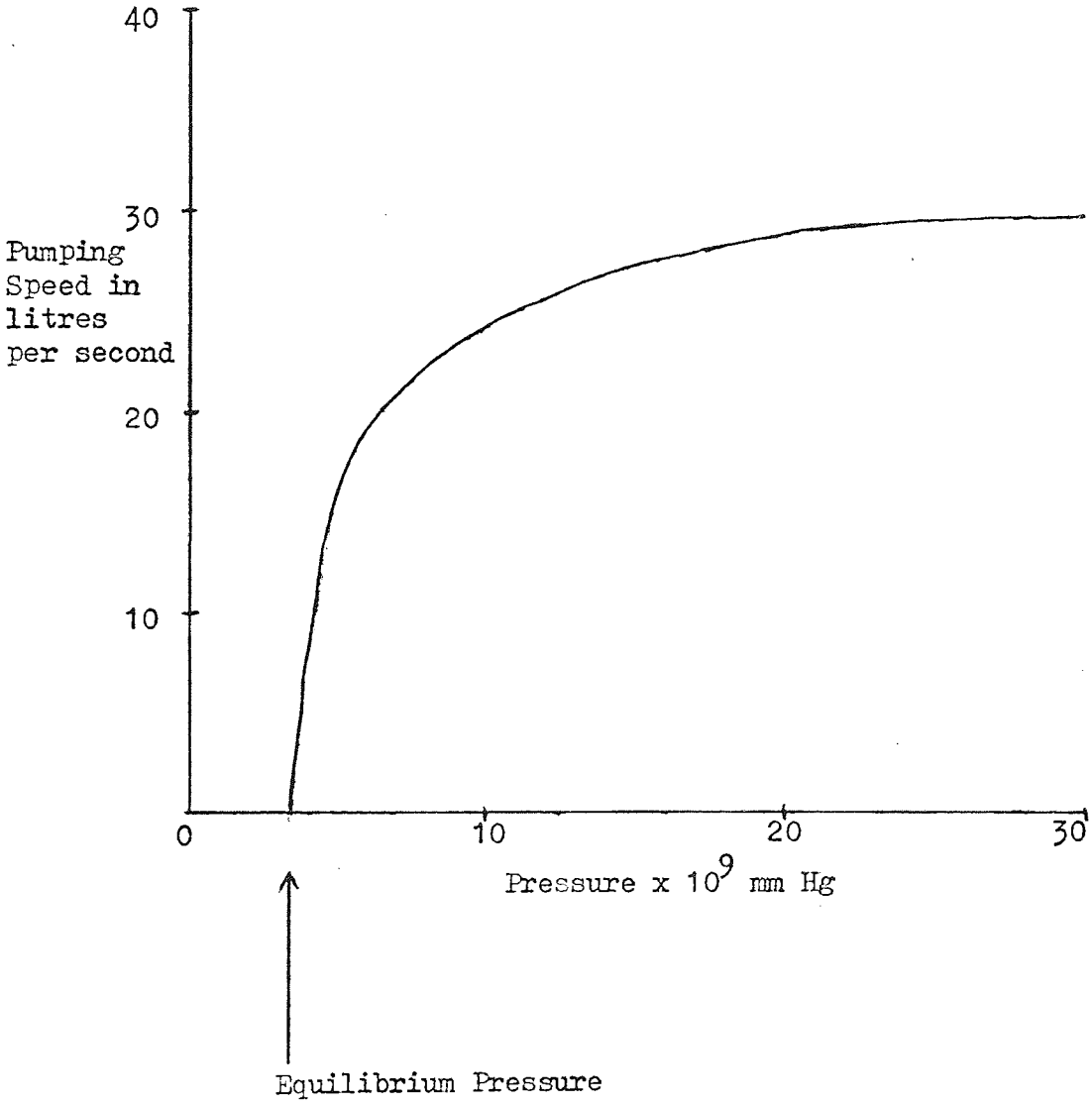

FIG. 60 Graph Showing Measured Pumping Speed Against Pressure for a Series of Carbon Monoxide Experiments.

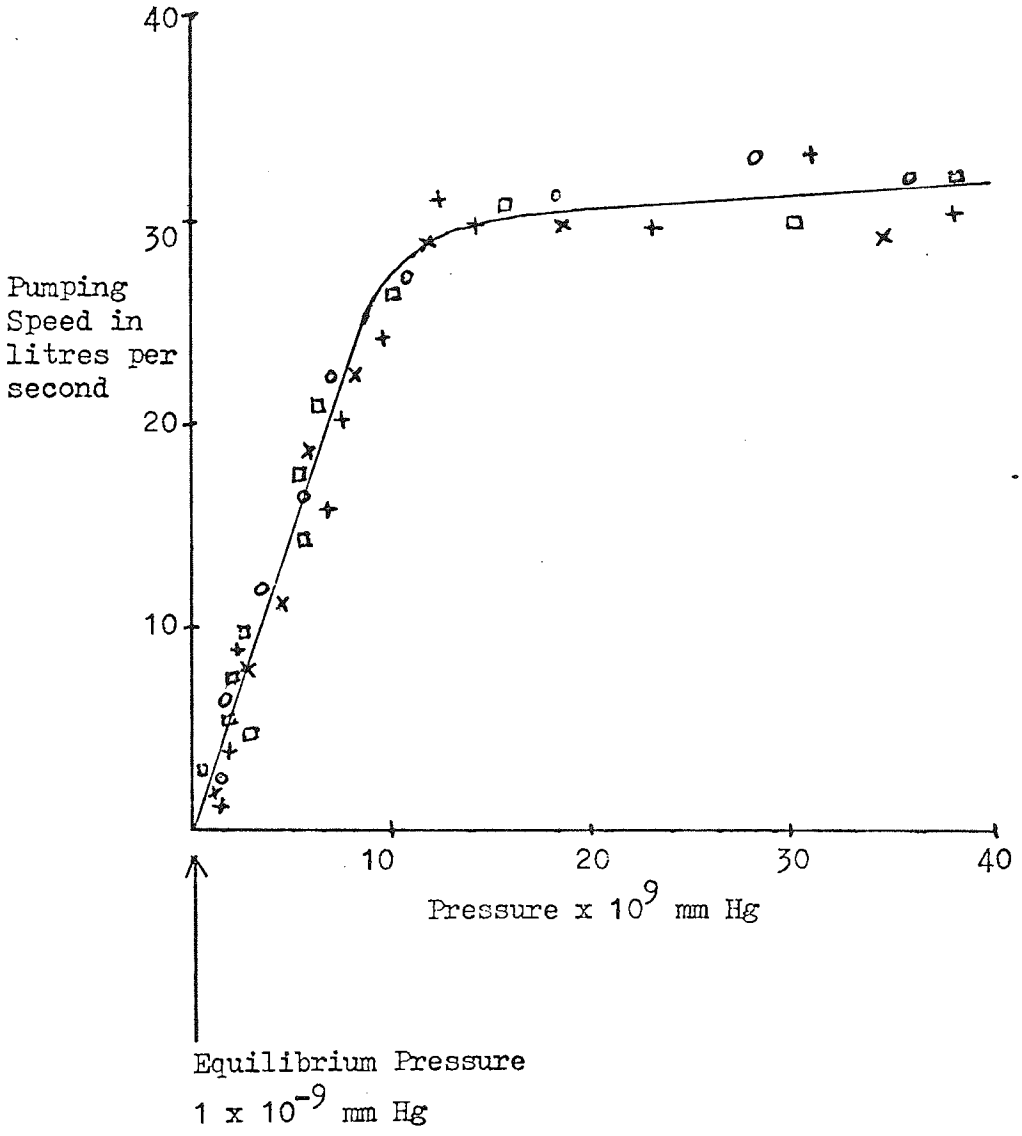

FIG. 61 Graph Showing Change of Pumping Speed with Pressure Over an Order of Magnitude Above the Equilibrium Pressure.

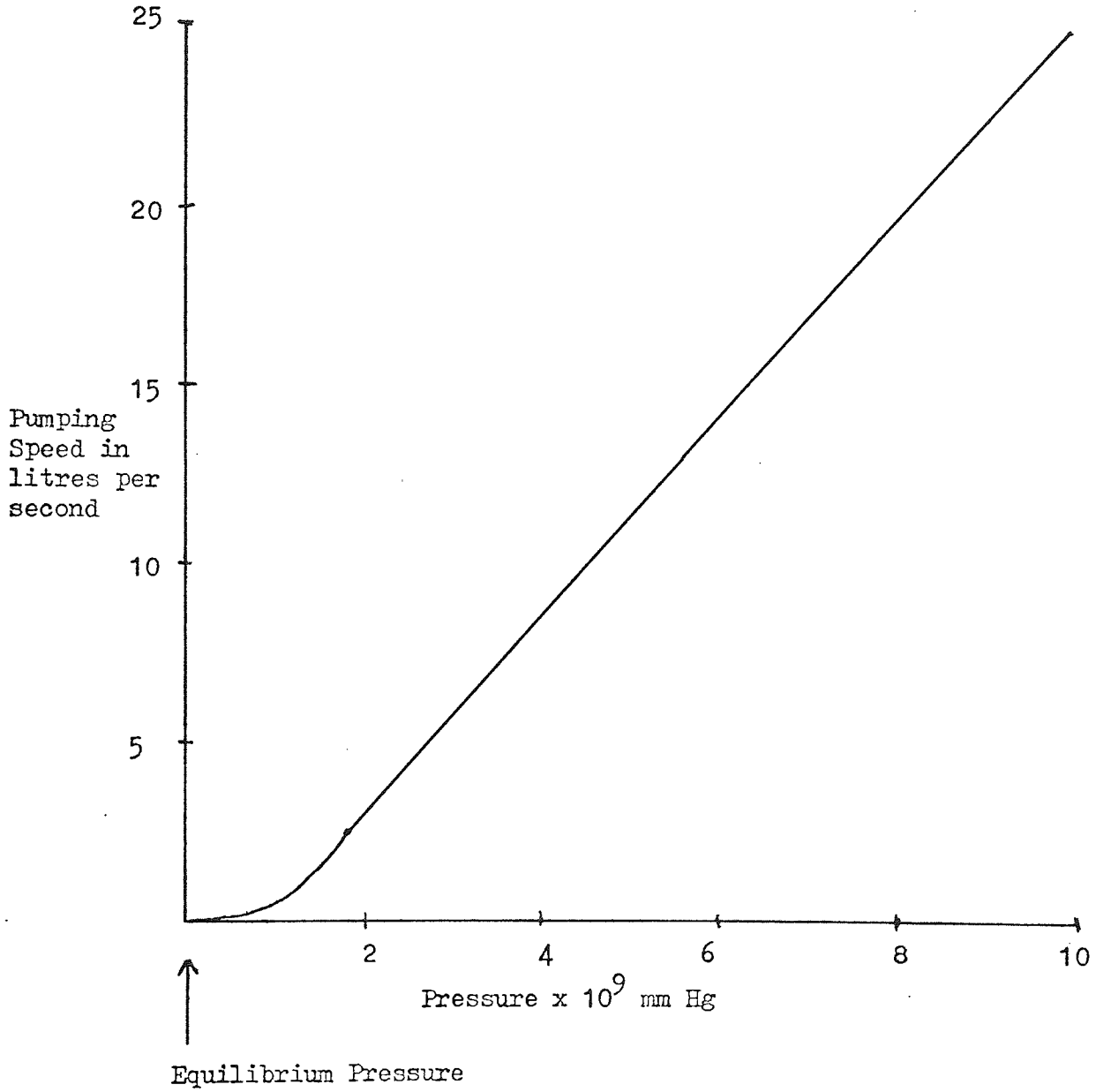

By plotting a graph of the variation of pumping speed with pressure the value of the pumping speed at any pressure can be calculated and substituted into the equation. A constant value for the pumping speed is obtained at pressures two or three orders of magnitude above the equilibrium pressure.

5.2 EXPERIMENTAL PROCEDURE

5.2.1 Carbon Monoxide

In initial U.H.V. studies carbon monoxide serves as a valuable molecule for a variety of reasons. Carbon monoxide does not contaminate the vacuum system unlike some other gases; can be easily pumped by most vacuum pumps and gives realistic readings on the vacuum gauges used. Carbon monoxide is a relatively simple molecule so that interpretation of the results is relatively straightforward. For these reasons, many parameters relating to carbon monoxide have already been determined from U.H.V. studies.

5.2.2 Pump Down Parameters

After the system had been purged out and baked the pressure in the vacuum system was reduced to 5×10^{-11} mm Hg. Experiments were now performed to investigate the maximum temperature obtained when a particular current, read off an ammeter, was used. The filament was flashed and by observing it through an optical pyrometer the maximum temperature obtained during the flash could be measured. This was repeated for a range of current values. It was found for a particular current that the maximum temperature obtained was nearly always the same within $\pm$ 50 K. The readings on the ammeter could now be used as a guide in estimating the maximum temperature during the experiment.

The background photographs that were obtained prior to the CO adsorption are shown in Fig. 62 . The essential features are that there is only one clear background peak seen which is a very sharp peak on the high temperature flash photograph and at lower temperatures this peak spreads out but is not resolved into more than one peak. The background is also seen to be relatively small at temperatures up to 2000 K. A very large rise in background pressure occurs at temperatures greater than 2000 K to a steady pressure of $> 10^{-7}$ mm Hg.

The peak seen in the background is probably due to one of the background gases but when the size of this is compared to the peak obtained from carbon monoxide the ratio is found to be only about 1:100.

The large high temperature background peak could be responsible for masking any high temperature peak from CO. In the case of carbon monoxide no high temperature ($>$ 2000) peaks were found.

Adsorption of the background gases was allowed to take place over a range of adsorption times similar to those to be used in the experiment itself. This meant for any particular adsorption time, the background spectrum was known and could be allowed for in the calculation.

5.3 CALCULATED PARAMETERS FROM THE OSCILLOSCOPE TRACE

5.3.1 Preliminary Investigation of the Peaks

The gas to be investigated was allowed into the system and a series of experiments were performed. The adsorption time was varied and photographs of the oscilloscope trace taken during

FIG. 62 Background Spectra.

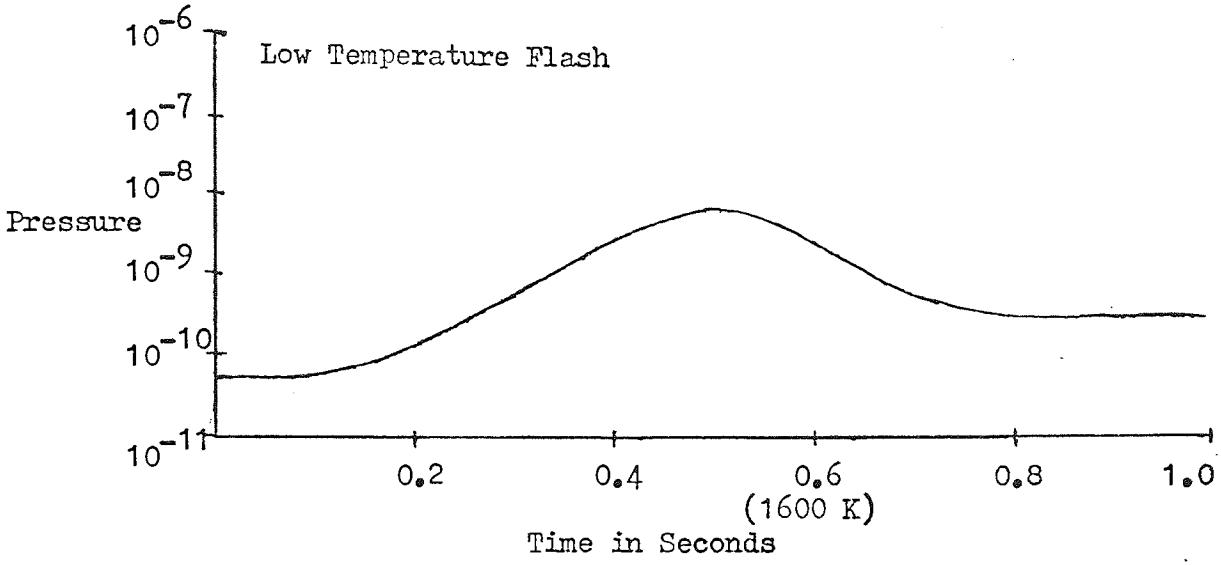

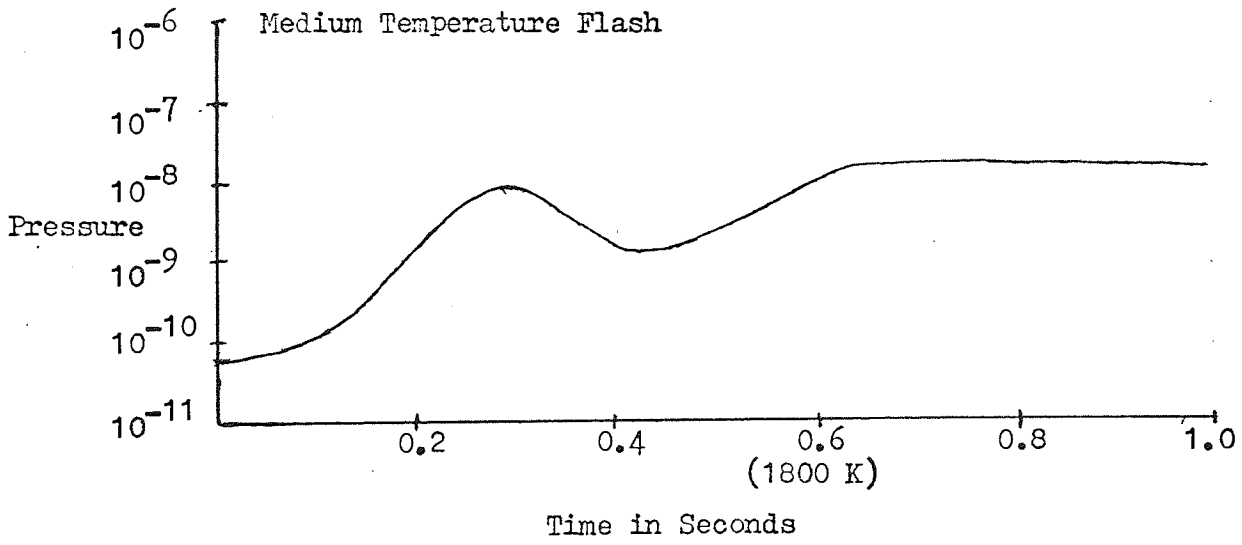

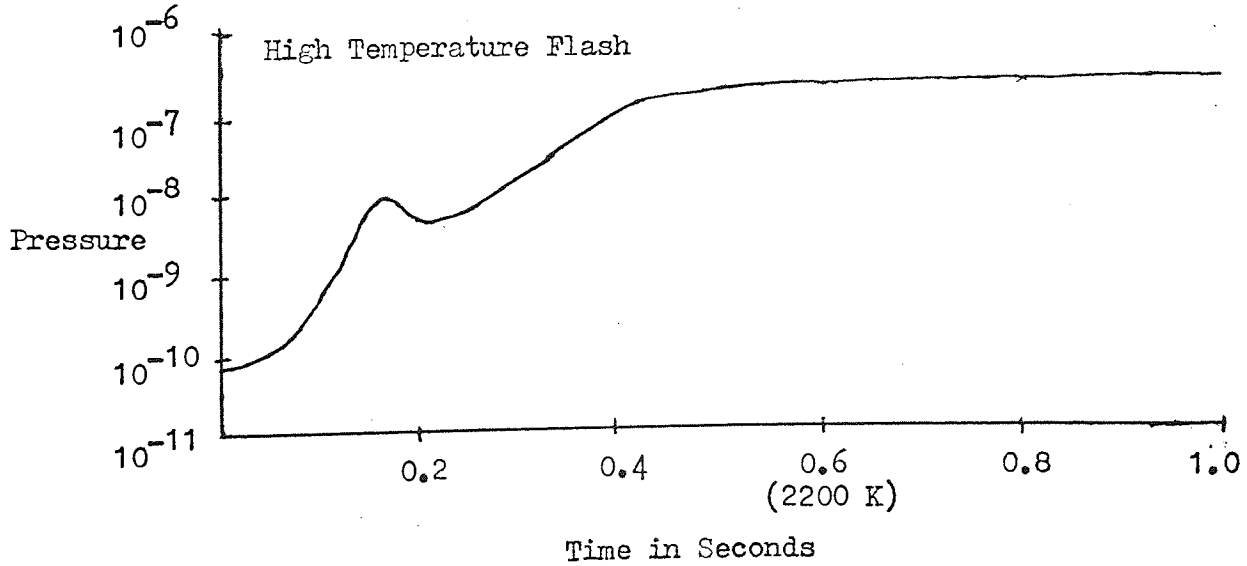

a flash. The current and hence the rate of temperature rise and maximum temperature was altered and a further series of experiments was performed. This latter experiment allowed us to obtain the best possible resolution of the peak.

A high temperature flash ($>$ 2000 K) was observed and two peaks were seen. Each of these occurred at a temperature much less than the maximum obtained on the high temperature flash which was 2200 K. No peaks were observed at very high temperatures but it is possible any small peak could have been masked by the background. A very low temperature flash showed there were no peaks at very low temperatures even at very long adsorption times. A trial and error method revealed the flash current and temperature at which best resolution of the peaks occurred. This was found to be at a maximum temperature at the end of the flash of 1700 K.

Table 9 gives the data for a typical series of experiments at various adsorption times. The table shows the temperature maximum at the end of flash is approximately constant, varying over only 60 K which is within the error calculated for measuring the maximum temperature. The carbon monoxide was leaked into the system whilst the system was being pumped and this is why the adsorption pressure varies even though attempts were made to keep it at 1×10^{-7} mm Hg. Attention to other details and adjustment of the apparatus meant control of the adsorption pressure was significantly easier at the larger adsorption times.

5.3.2 The Temperature Rise

A typical graph of the rise in temperature with time is

Table 9. Typical Data for a Series of Carbon Monoxide Experiments.

Adsorption Time In Minutes	Estimated Final Temperature K	Initial Pressure x 10^{9} mm Hg	Adsorption Pressure x 10^{8} mm Hg	Reading ∝ Current
1	1920	22	15	16
2	1960	20	7.6	16.5
3	1920	20	18	16
5	1920	10	4.4	16
10	1960	2	15	16.5
15	1920	5	13	16
30	1900	3	10	15.5
60	1920	2	10	16
120	1920	2	15	16

shown in Fig. 63 . The graph is linear over the first 0.6 secs and flattens out at the maximum temperature. Graphs similar to this were obtained for all flashes. All reach the maximum temperature after about 0.6 secs and so the shape is similar, the only change is the maximum temperature obtained and the gradient of the graph during the initial 0.6 secs.

The temperature rise over the linear region i.e., the first 0.6 secs is of the form

$$T = T_o + bt \qquad \ldots\ (5\text{-}5)$$

where T_o = 300 K and b varies with the particular temperature maximum but when the maximum temperature is 2100 K, b is equal to 3000 K sec^{-1}.

For a temperature rise to a particular temperature maximum in each case the graphs were found to be identical within the limits of experimental error. Table 10 and 11 show a typical set of values obtained when the temperature is calculated from the oscilloscope trace. The voltage and current are worked out from the values obtained directly from the oscilloscope trace and the temperature is found after calculation of the resistance and resistivity.

5.3.3 The Pressure Rise

The pressure scale on the oscilloscope was logarithmic. The output of the gauge was 0.2 volts per decade. By setting the oscilloscope trace to 0.2 volts per cm, each cm on the grid corresponds to an order of magnitude rise in pressure. To improve the accuracy in the reading off of the results the negative was enlarged onto semi-log graph paper so that each centimetre on the oscilloscope grid covered one order of magnitude

FIG. 63 Graph Showing the Temperature Increase Against Time.

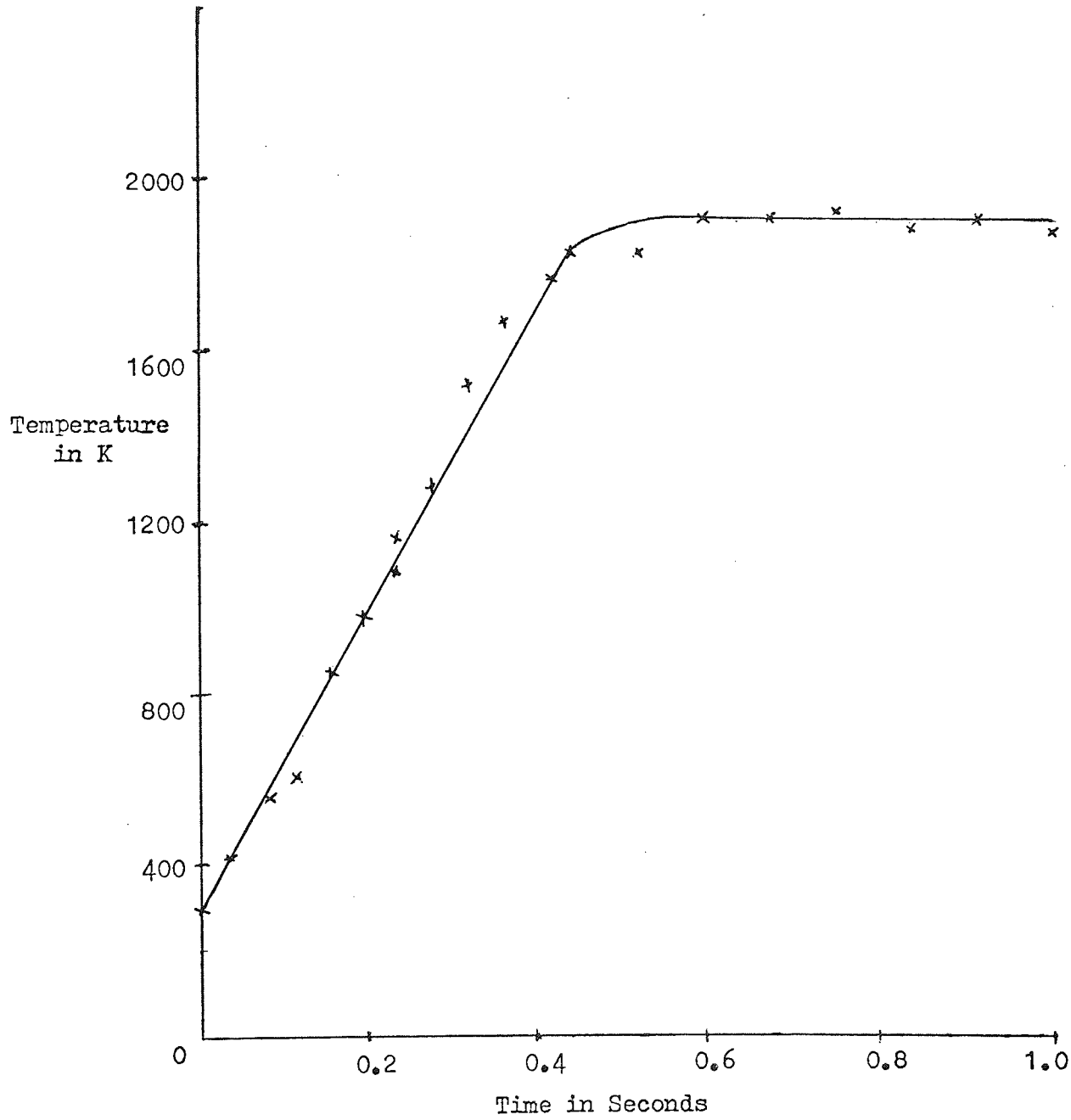

Table 10. Data Used to Calculate the Temperature Rise I.

Time in secs	Voltage in volts	Current in amps	Resistance in ohms	Resistivity x 10^6 ohm cm^{-1}	Temperature in K
0	1.44	4.90	0.2938	13	290
0.04	1.48	4.88	0.3032	18	410
0.08	1.52	4.86	0.3127	23	510
0.12	1.54	4.84	0.3181	26	590
0.16	1.58	4.80	0.3291	35	840
0.20	1.62	4.78	0.3389	40	970
0.24	1.64	4.76	0.3445	43	1060
0.28	1.66	4.74	0.3502	46	1140
0.32	1.70	4.72	0.3601	51	1280
0.36	1.72	4.70	0.3659	59	1510
0.40	1.76	4.65	0.3783	64	1660
0.44	1.76	4.58	0.3845	70	1840
0.48	1.76	4.58	0.3845	70	1840
0.52	1.76	4.58	0.3845	70	1840
0.56	1.76	4.58	0.3845	70	1840
0.60	1.80	4.58	0.3959	73	1920

Table 11. Data Used to Calculate the Temperature Rise II.

Time in Secs	Voltage in volts	Current in amps	Resistance	Resistivity x 10^6 ohm m^{-1}	Temperature in K
0	1.32	2.97	0.4444	13	290
0.04	1.34	2.96	0.4511	17	390
0.08	1.36	2.95	0.4610	23	510
0.12	1.37	2.95	0.4644	26	590
0.16	1.39	2.94	0.4711	30	700
0.20	1.4	2.93	0.4778	34	800
0.24	1.42	2.93	0.4846	38	930
0.28	1.44	2.92	0.4914	43	1060
0.32	1.46	2.91	0.5017	49	1230
0.36	1.47	2.90	0.5051	52	1300
0.40	1.48	2.89	0.5138	57	1450
0.44	1.49	2.88	0.5173	59	1510
0.48	1.50	2.88	0.5208	61	1560
0.52	1.50	2.88	0.5225	63	1640
0.56	1.51	2.88	0.5243	64	1660
0.60	1.51	2.88	0.5243	64	1660
0.64	1.51	2.88	0.5243	64	1660
0.68	1.51	2.88	0.5243	64	1660
0.72	1.51	2.88	0.5243	64	1660
0.76	1.51	2.88	0.5243	64	1660
0.80	1.51	2.88	0.5243	64	1660

on the logarithmic scale. The oscilloscope scale had previously been checked to ensure it was accurate.

A diagram of the photograph of the oscilloscope display and an actual photograph obtained for a flash are shown in Fig. 64 . The total pressure is corrected for the background pressure rise throughout the flash so the pressure increase obtained is due to the desorption of the sample gas only.

The variation of pressure with time is shown in Fig. 65 together with the background pressure and also the actual pressure rise due to CO only.

Table 13 shows the variation of the pressure rise due only to the CO with adsorption time. The higher temperature peak is present throughout the range whilst the lower temperature peak appears after five minutes adsorption time. The lower temperature peak will be referred to as the α peak because it is desorbed at temperatures less than 1000 K and the higher temperature peak, the β peak. The surface coverage of both peaks increases with adsorption time. With an adsorption time of 120 minutes the pressure increase for the β peak is of the order of three orders of magnitude and the α peak over two orders of magnitude.

Graphs of the actual pressure rise due to desorption of CO against temperature for both the α and β peaks are shown in Fig. 67 .

The α peak does not appear until after five minutes adsorption time which means the β peak can be analysed for short adsorption times and the experimental parameters thus found for the β peak

Table 12. This Table Shows the Measured Pressure, the Pressure Rise Minus the Equilibrium Pressure and the Actual Pressure Rise Due to the Desorption of Carbon Monoxide For a β Peak.

Time in secs	Temperature in K	Measured Pressure x 10^9 mm Hg	Pressure Rise x 10^9 mm Hg	Actual Pressure Rise Due to Desorption of Carbon Monoxide $\times 10^9$	
0	290	2	0	0	
0.04	390	2	0	0	
0.08	440	2	0	0	
0.12	510	2	0	0	
0.16	660	2.2	0.2	0	No α Peak
0.20	740	2.4	0.4	0	
0.24	970	2.4	0.4	0	
0.28	1040	2.4	0.4	0	
0.32	1140	2.4	0.4	0	
0.36	1200	2.7	0.7	0.3	
0.40	1340	4.0	2.0	1.0	
0.44	1450	7.5	5.5	3.0	
0.48	1550	12	10	7.5	
0.52	1600	18	16	12	
0.56	1660	20	18	14.5	
0.60	1660	18	16	13	
0.64	1660	15	13	10.5	β Peak
0.68	1660	10	8	5.7	
0.72	1660	6.5	4.5	2.5	
0.76	1660	5.2	3.2	1.2	
0.80	1660	4.7	2.7	0.7	
0.84	1660	3.7	1.7	0.2	
0.88	1660	3.5	1.5	0.1	
0.92	1660	3.5	1.5	0	
0.96	1660	3.5	1.5	0	
1.00	1660	3.5	1.5	0	

FIG. 64. Oscilloscope Trace Obtained for a Typical Carbon Monoxide Experiment.

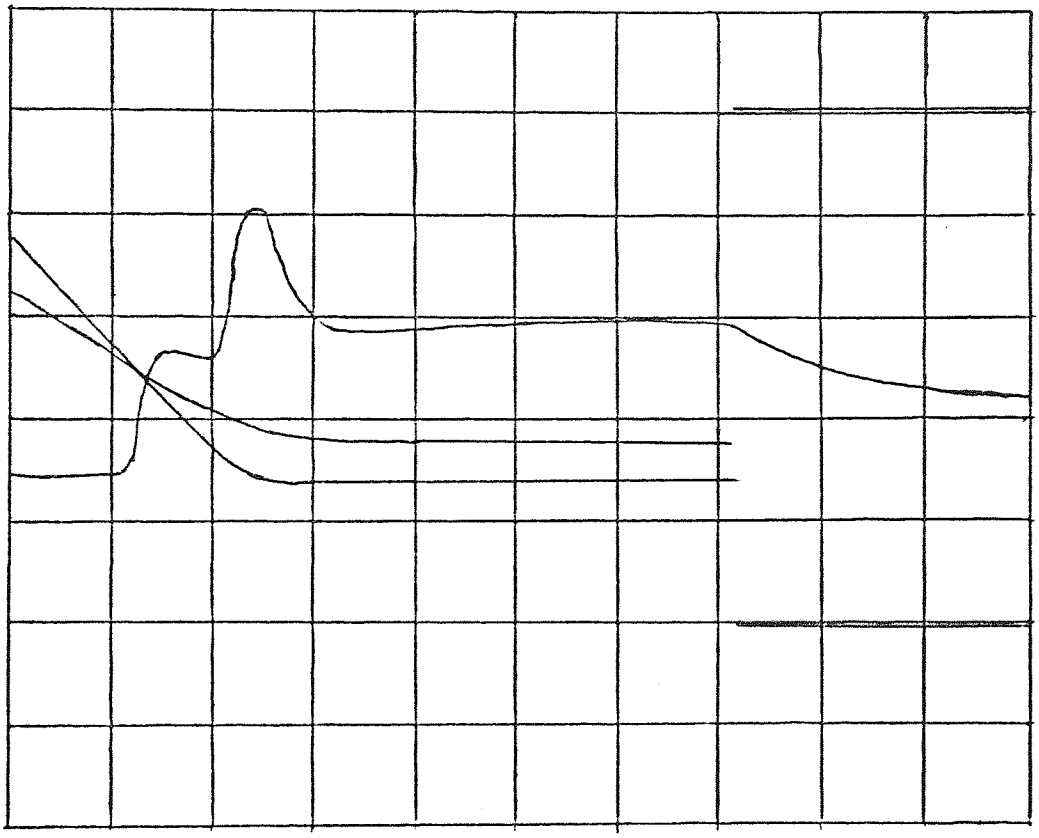

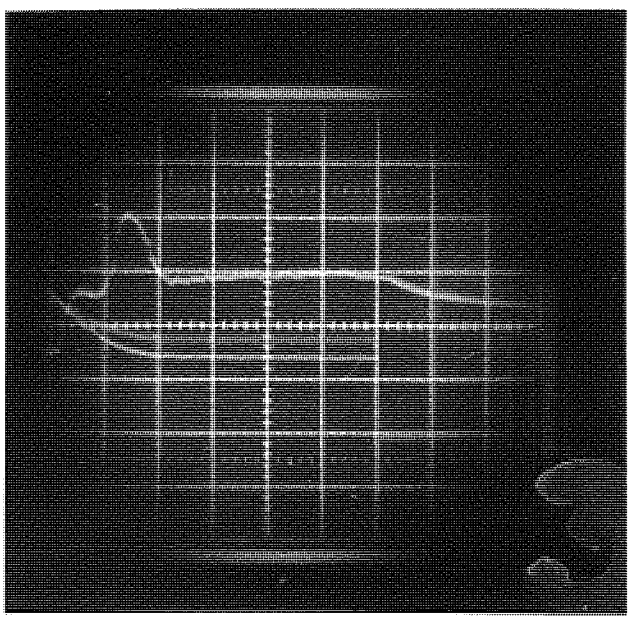

FIG. 65 Graph of Pressure Against Time, Showing the Background and the Actual Rise in Pressure Due to Carbon Monoxide Desorption.

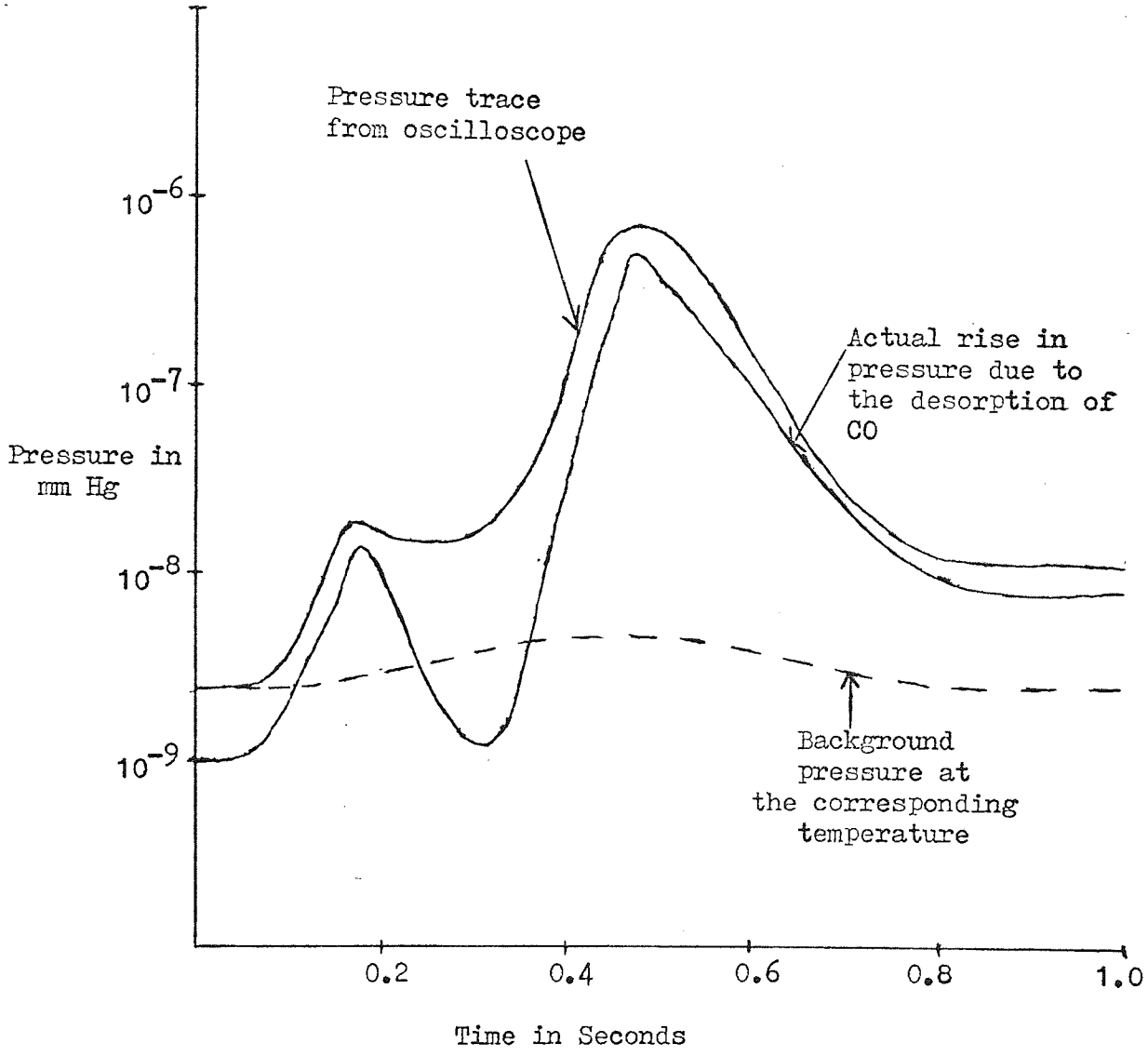

Table 13. The Increase in the Peak Height Due to the Desorption of Carbon Monoxide with Adsorption Time.

Adsorption Time in mins	Actual Pressure Rise due to CO	
	α peak max pressure x 10^9	β peak max pressure x 10^8
1		1.3
2		1.45
5	1.44	6.3
10	5.8	11.3
15	12.2	59.0
30	20.4	74.0
60	46	104.0
120	343	175.0

are used to extrapolate the β peak into the area when the α and β peaks overlap.

A schematic diagram of the increase of the overlap between the α and β peaks is shown in Fig. 66 . In the region where the two peaks overlap the contribution of each peak to the pressure rise needs to be assessed so this could be used in the analysis of the results.

5.4 THE CALCULATED PARAMETERS

5.4.1 The Rate of Desorption

Fig. 68 shows a graph of the pressure rise due to the desorption of CO against time together with a graph of dP/dt and also rate of desorption both plotted against time. The rate of desorption was calculated by substituting in Equation (4-32). This maximum value of the rate of desorption for the β peak was found to be 3×10^{12} molecules cm^{-2} sec^{-1} at one minute adsorption time and 4.2×10^{15} molecules cm^{-2} sec^{-1} at two hours adsorption time.

In the case of the α peak the rate of desorption was found to be lower than for the β peak and the maximum value of the rate of desorption after 2 hours adsorption time was 1×10^{15} molecules cm^{-2} sec^{-1}.

A graph of $(dn/dt)_t$ against t is shown in Fig. 69 . Values are shown in Table 14 for the rate of desorption for a flash which shows both an α and a β peak; both peaks are clearly resolved.

The graph of rate of desorption against time for both peaks is used to calculate the surface coverage.

FIG. 66 Schematic Diagram Showing Rise of α and β peak with Adsorption Time.

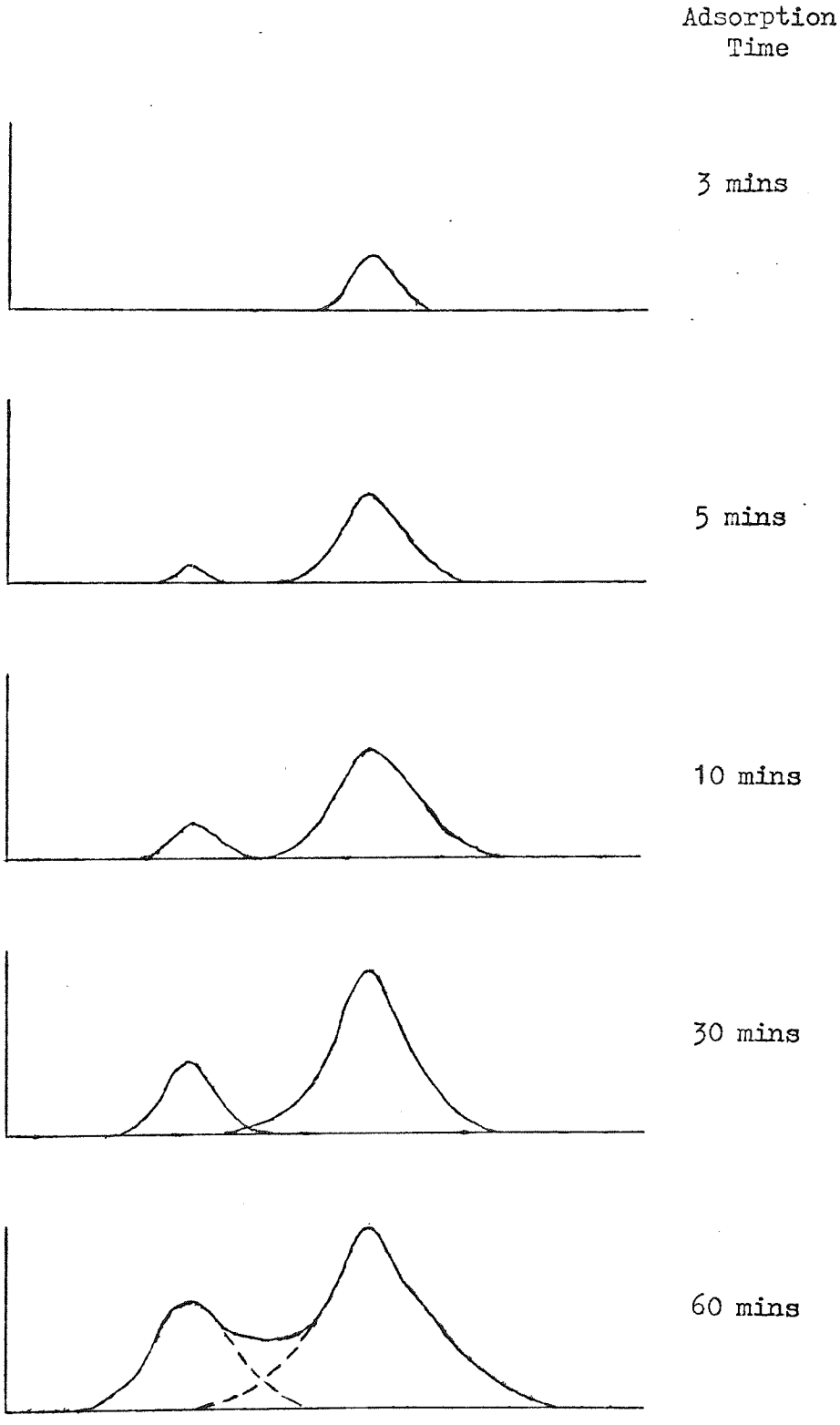

FIG. 67 Graph of Pressure Rise Against Temperature for an ∝ and β Peak.

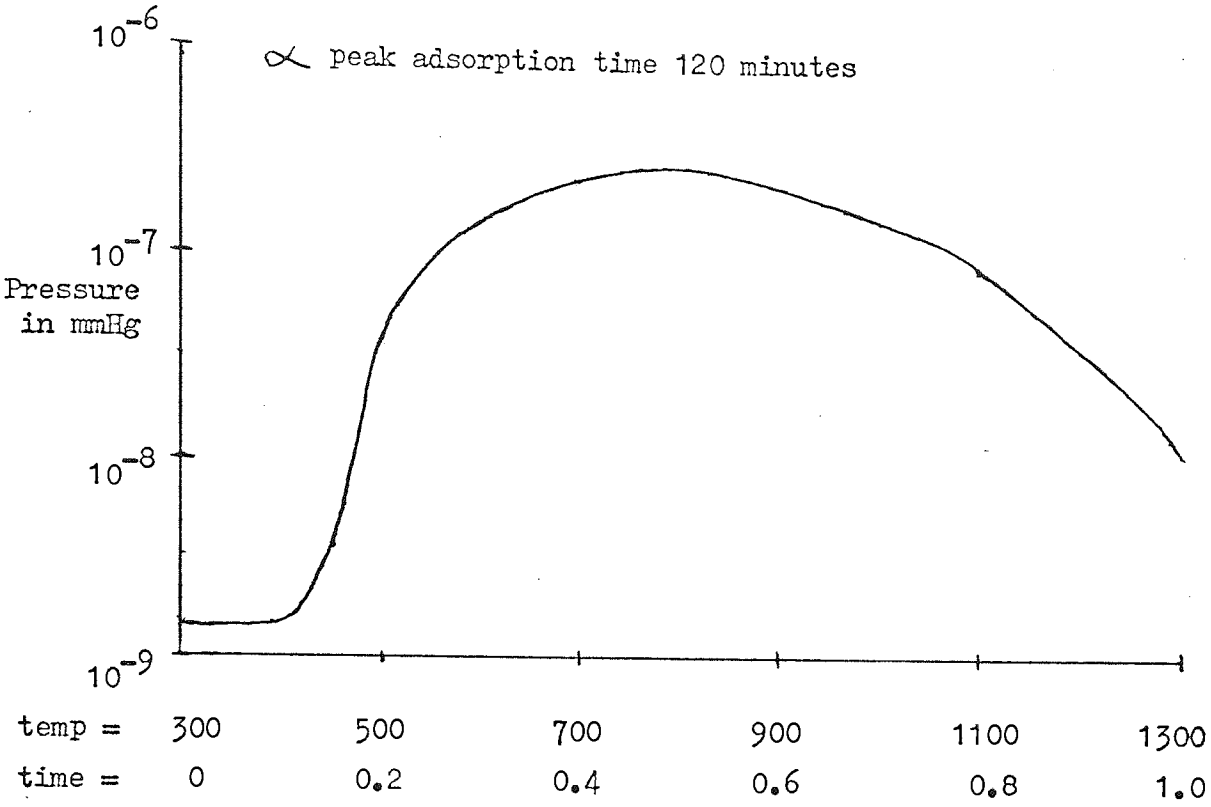

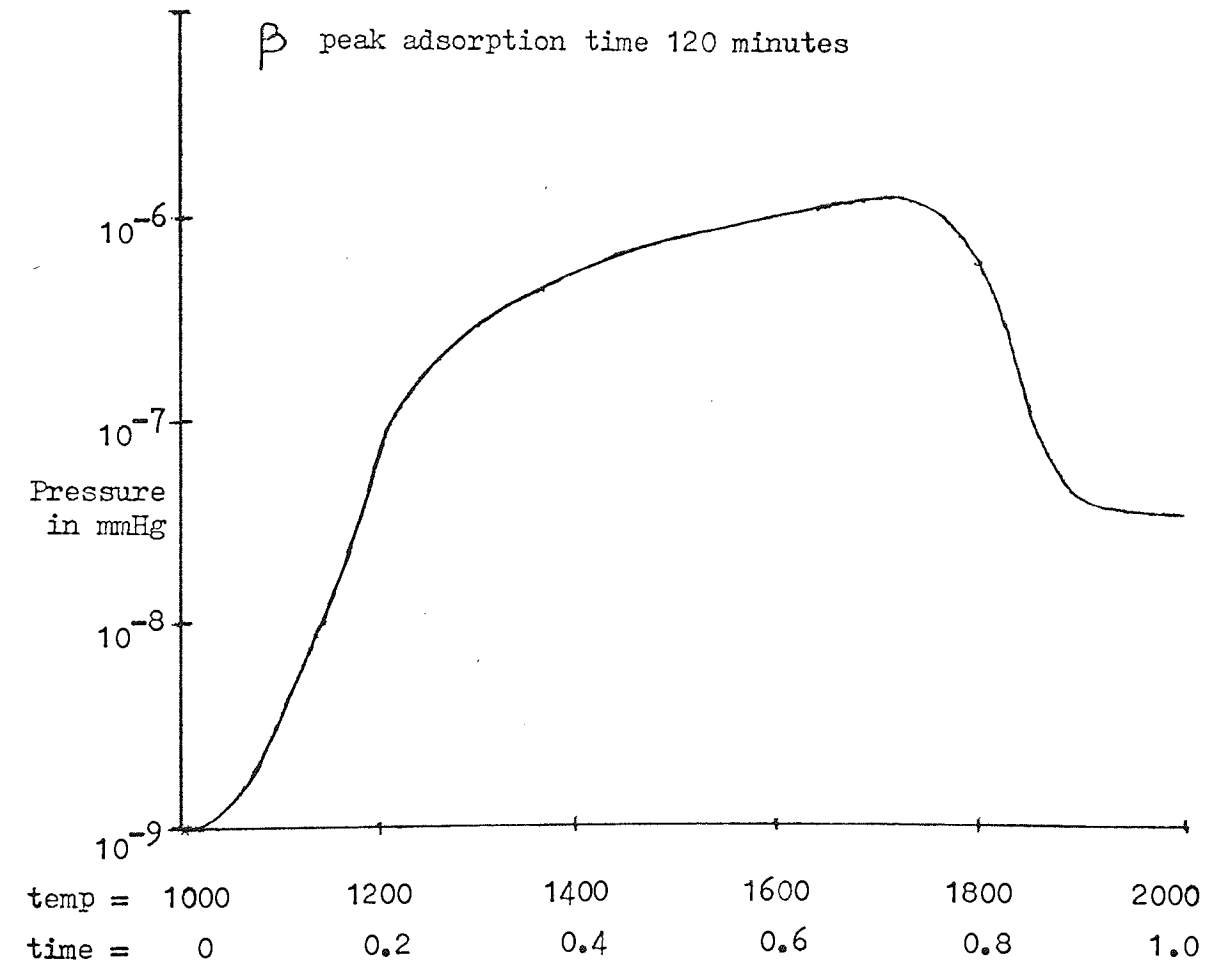

FIG. 68 Graph Showing 1) P against t, 2) dP/dt against t, 3) dn/dt against t.

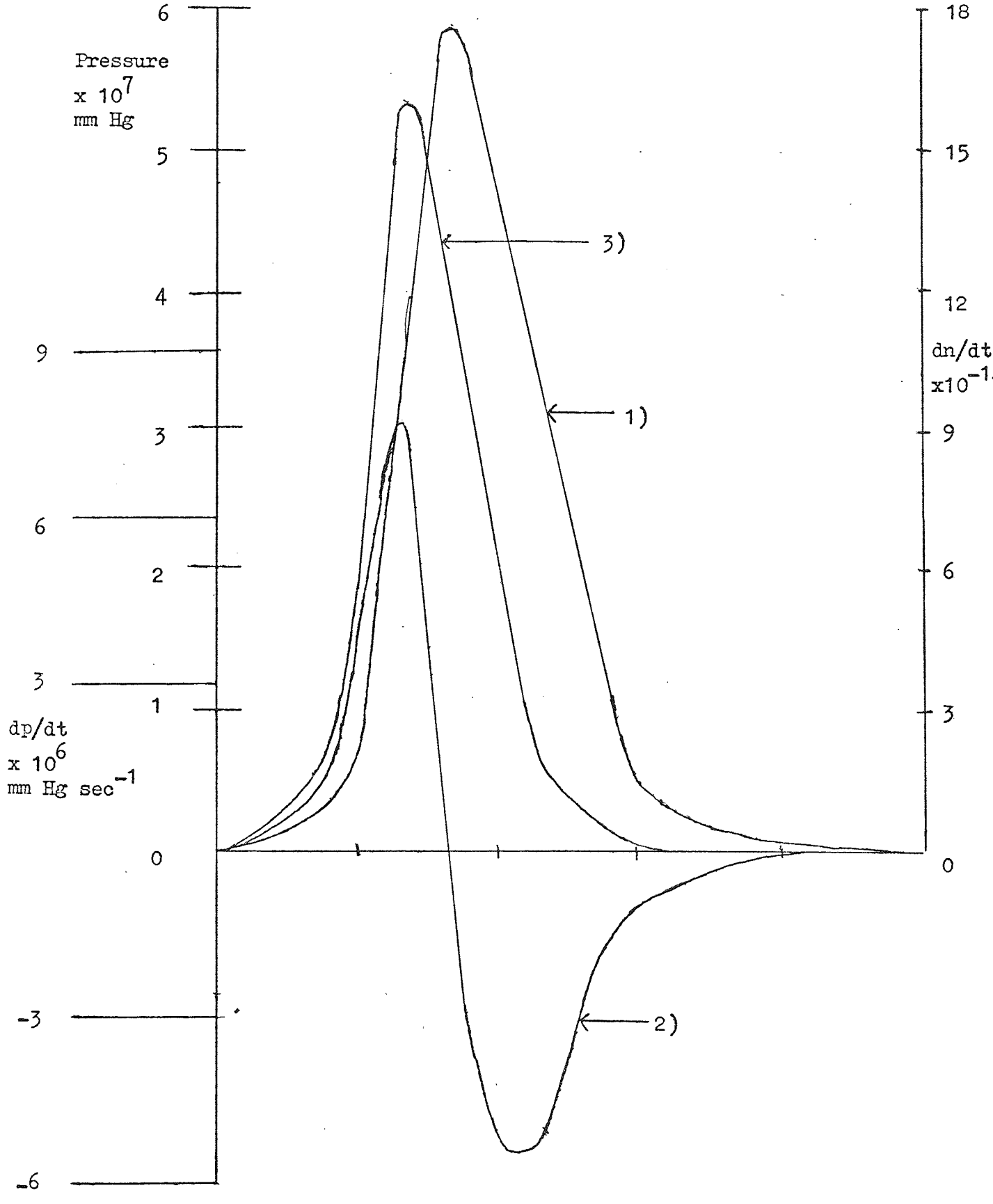

FIG. 69 Graph Showing the Rate of Desorption Against Time for a β Peak for Adsorption Time of 5 Minutes.

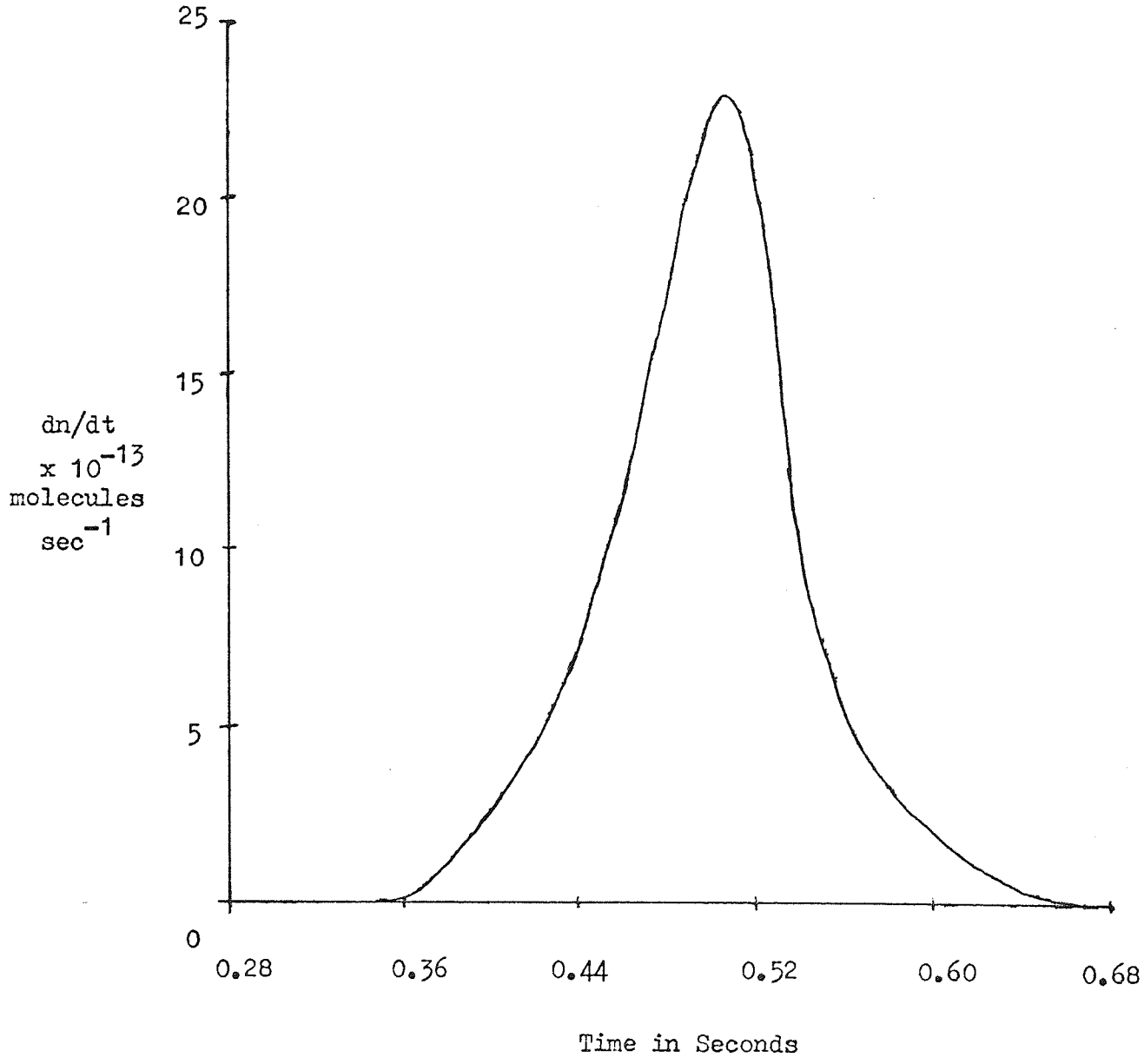

Table 14. Rate of Desorption Data for the α and β Peak.

Time in secs	dn/dt α peak x 10^{-12} molecules sec^{-1}	dn/dt β peak x 10^{-14} molecules sec^{-1}	Temp in K
0	0		300
0.04	0.28		400
0.08	3.3		440
0.12	33.0		520
0.16	53.1		670
0.2	10.4		740
0.24	4.3		960
0.28	0	0	1030
0.32		0.04	1140
0.36		0.08	1200
0.4		1.1	1350
0.44		10.2	1460
0.48		24.1	1590
0.52		84.8	1600
0.56		0.11	1630
0.6		0	1650

5.4.2 The Surface Coverage

The surface coverage is calculated by counting all the molecules which have been desorbed from the surface during the flash. This is done by integrating numerically dn/dt, i.e. by calculating the total area under the curve. The number of molecules remaining on the surface at a particular time t is calculated by subtracting from σ_o which is the total surface coverage, the number of molecules which have been desorbed at time θ, this gives σ_t, the number of molecules left on the surface at time t. θ is given by the area under the curve from t = 0 to t = t. The graph of rate of desorption against time is shown in Fig. 69 .

Values are shown in Table 15 of the variation of surface coverage with time and the ratio of the surface coverage to the total surface coverage σ_o. The ratio of σ_t/σ_o can be used to estimate the order of reaction.

Table 16 shows the variation of the total surface coverage with adsorption time for both the α and β peak. The surface coverage of the β peak varies from 3/100th of a monolayer at one minute adsorption time to 1/6th of a monolayer at two hours adsorption time. The α peaks surface coverage changes from 1/10000th of a monolayer after five minutes adsorption time to 1/10th of a monolayer after two hours adsorption time. A graph of total surface coverage, the sum of both the α and β peaks, against time is drawn in Fig. 70 .

Table 15. Surface Coverage Data.

Time in secs	Surface Coverage of the α peak x 10^{-12} molecules	Surface Coverage of the β peak x 10^{-14} molecules	$\frac{\sigma t}{\sigma_0}$	
0	3.07		1	α peak
0.04	3.02		0.983	
0.08	2.68		0.873	
0.12	1.38		0.449	
0.16	0.18		0.059	
0.20	0.002		0.0006	
0.24	0	0	0	
0.28		1.56	1	β peak
0.32		1.55	0.998	
0.36		1.54	0.989	
0.40		1.44	0.925	
0.44		1.01	0.649	
0.48		0.54	0.348	
0.52		0.04	0.027	
0.56		0.01	0.008	
0.60		0	0	

Table 16. Increase of Surface Coverage with Adsorption Time for the α and β Peaks.

Adsorption Time	Surface Coverage α Peak Monolayers	Surface Coverage β Peak Monolayers
1		0.0037
2		0.0048
5	0.0001	0.017
10	0.0008	0.031
15	0.003	0.15
30	0.008	0.17
60	0.011	0.29
120	0.15	0.61

FIG. 70 Variation of Surface Coverage with Adsorption Time.

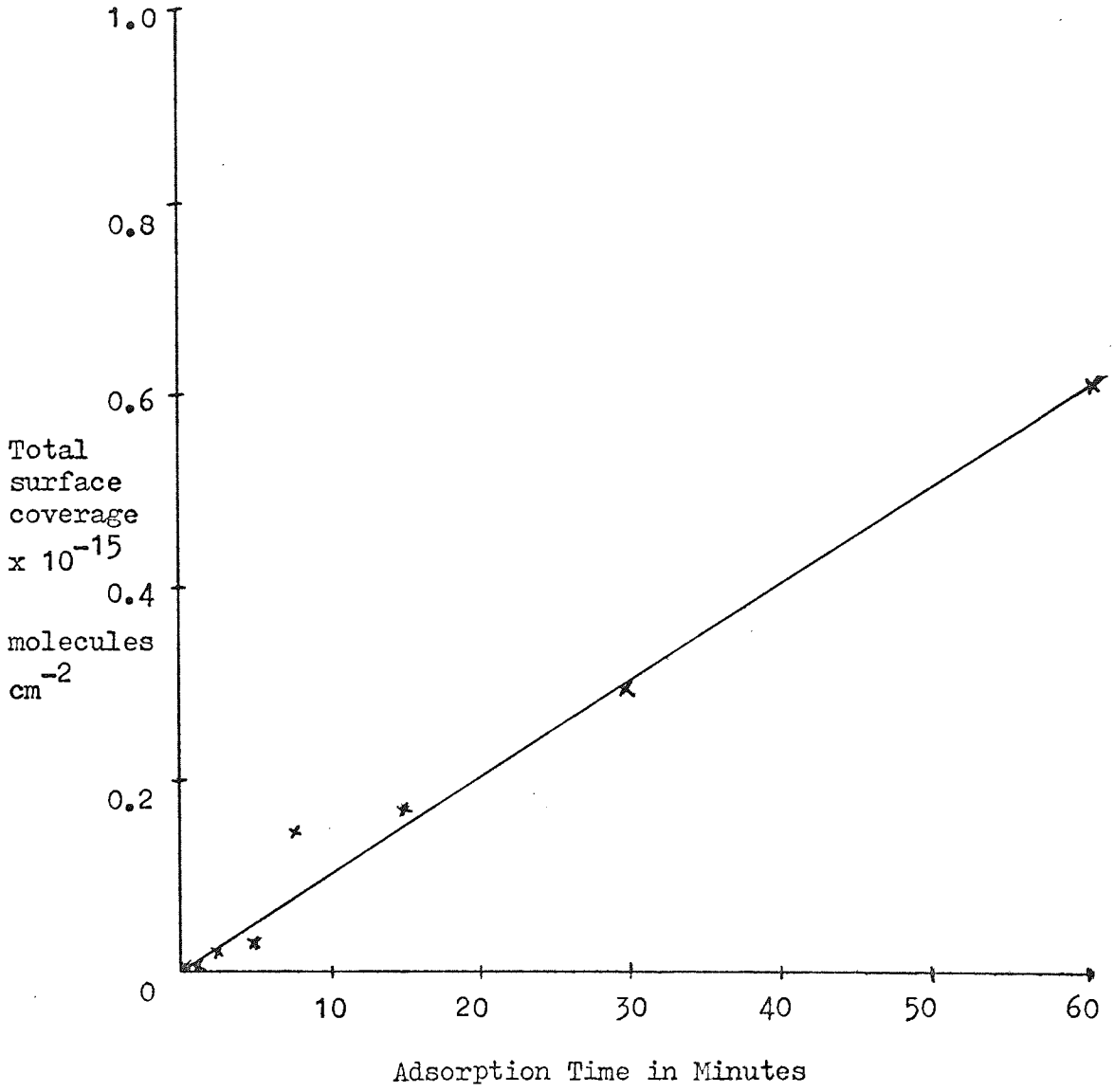

5.4.3 Desorption Kinetics

The kinetics are defined by the equation

$$(dn/dt)_t = k\left[\sigma_o - \theta\right]^x \quad \ldots\ (5\text{-}6)$$

k at a given temperature is the rate constant of the reaction.

$$k = (dn/dt)_t/\left[\sigma_o - \theta\right]^x = A_e^{-E/RT} \quad \ldots\ (5\text{-}7)$$

$$\ln(dn/dt)_t/\left[\sigma_o - \theta\right]^x = \ln A - \frac{E}{RT} \quad \ldots\ (5\text{-}8)$$

A graph of the left hand side against 1/T should be a straight line for the correct value of x, the order of reaction. The correct value of x, which will be either 1 or 2 can be found.

The slope of the line is E/R and so E can be found and finally using equation (5-8) A can be calculated. The rate constant can also be found and the change of this with temperature is shown in Table 17 and Fig. 71 .

The order of reaction was found by a second method of plotting a series of graphs of σ_t/σ_o against t for various values of σ_o. The shape and general trend of these graphs suggested the order of reaction was first order for both desorption peaks which supported the value of the order of reaction obtained by the other method. The graphs of $\ln(dn/dt)_t/\left[\sigma_o - \theta\right]^x$ against 1/T are shown for the α and β peak in Figs. 72 and 73 respectively. The graphs of σ/σ_o against t are shown in Fig. 74 .

The possibility of mixed order kinetics was also investigated.

Table 17. Rate Constant as a Function of Temperature.

Temperature K	1/T K $\times 10^{-4}$	Rate Constant
740	1.35	-
970	1.03	0.747
1040	0.96	2.255
1140	0.87	5.485
1200	0.83	20.76
1340	0.74	76.66
1450	0.68	216.28
1600	0.62	241.09
1660	0.60	241.93

FIG. 71 Variation of Rate Constant with Temperature for the ∝ Peak after Adsorption Time of 120 Minutes.

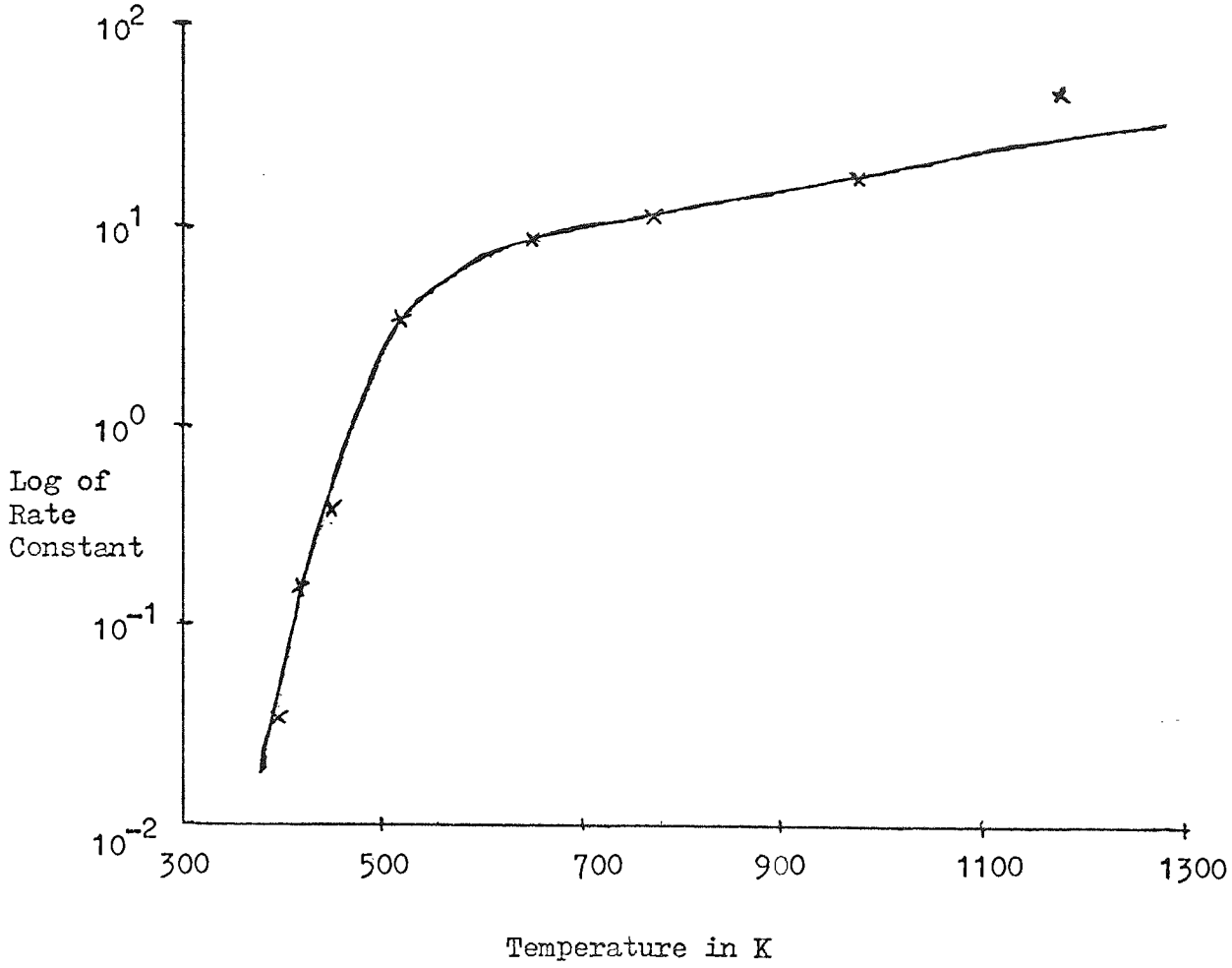

FIG. 72 Calculation of the Order of Reaction of the α Peak.

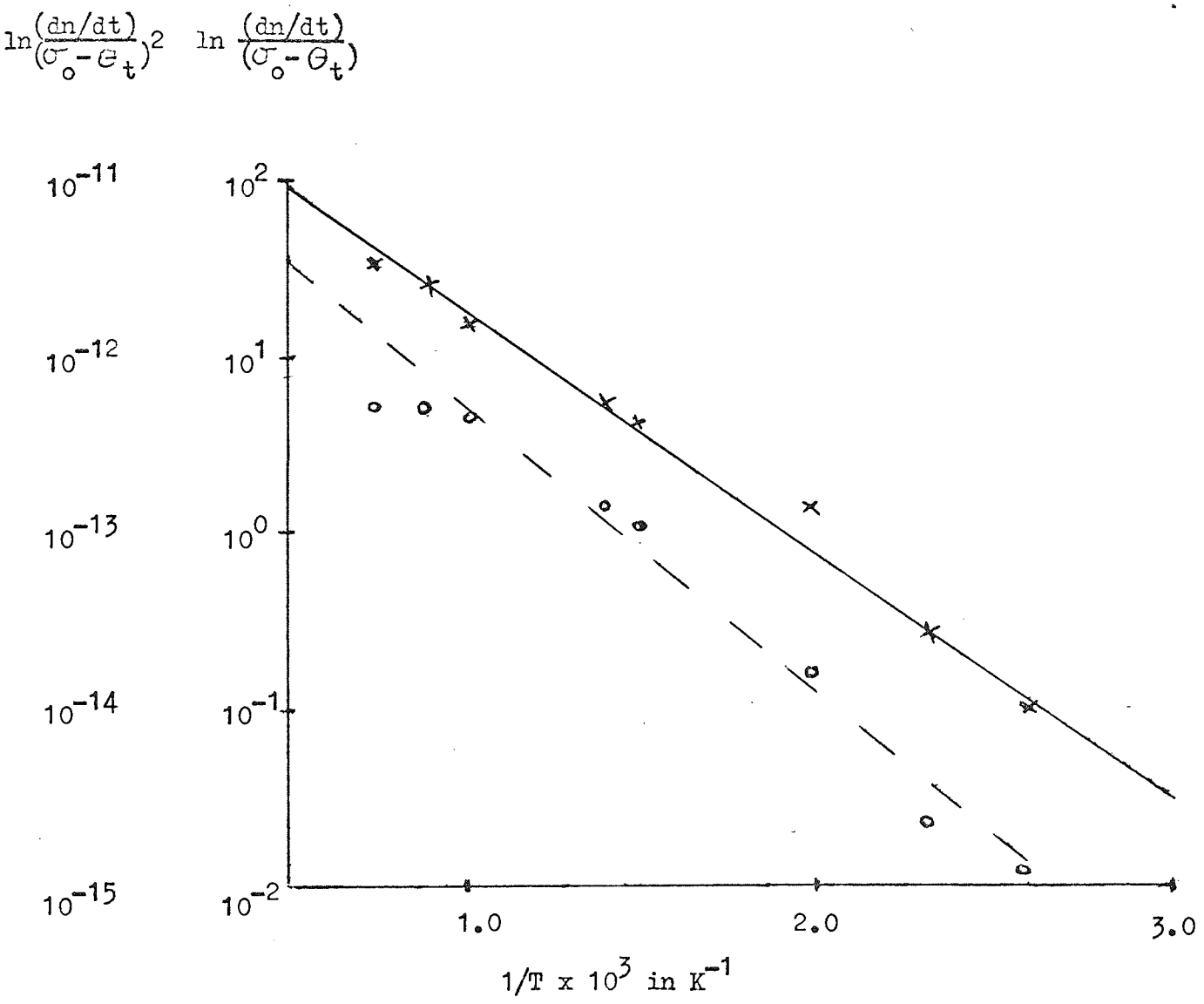

× = First Order

o = Second Order

FIG. 73 Calculation of the Order of Reaction of the β Peak.

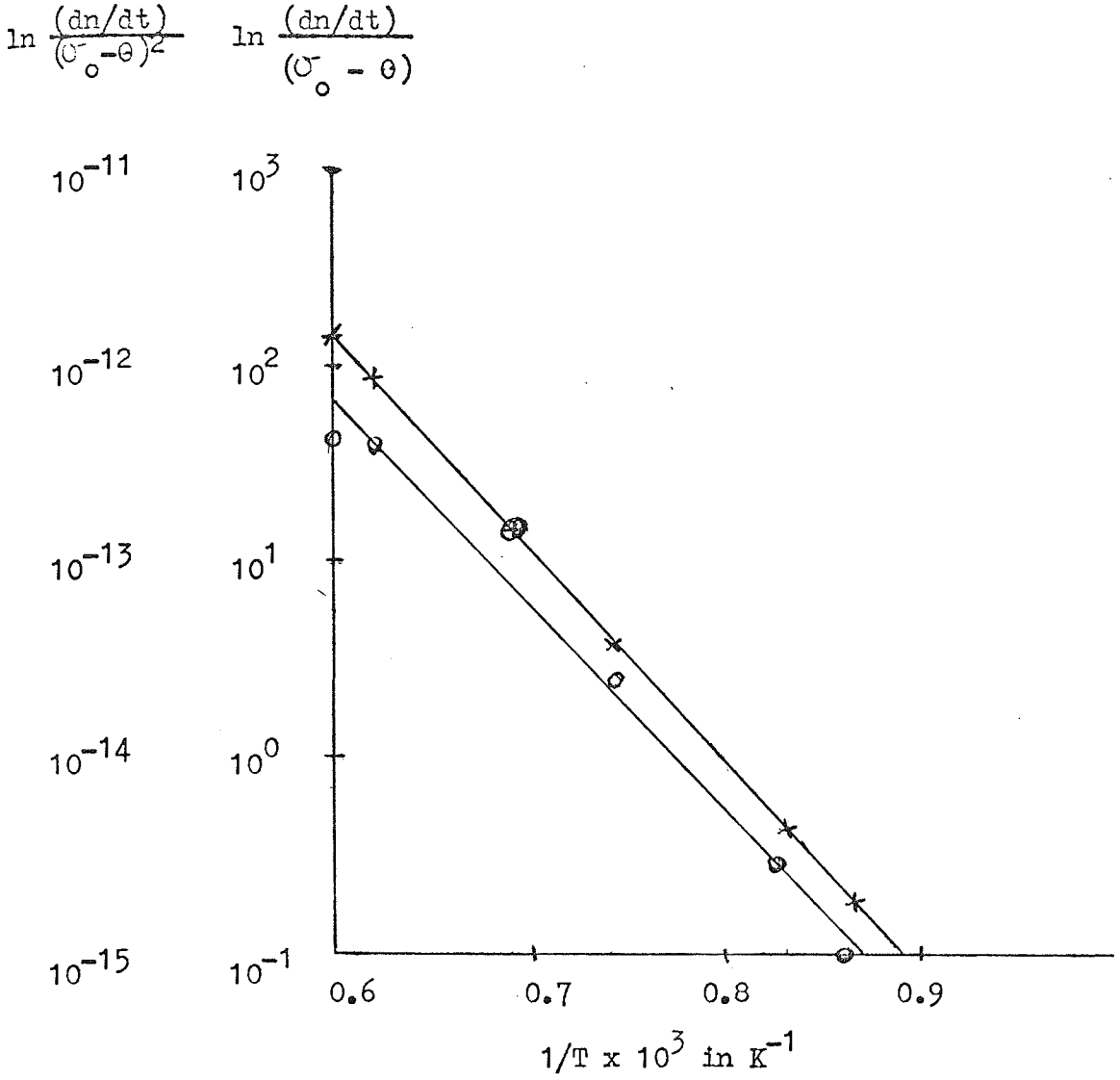

X = First Order

O = Second Order

FIG. 74 Graph of σ_t/σ_o against Time for the α and β Peaks.

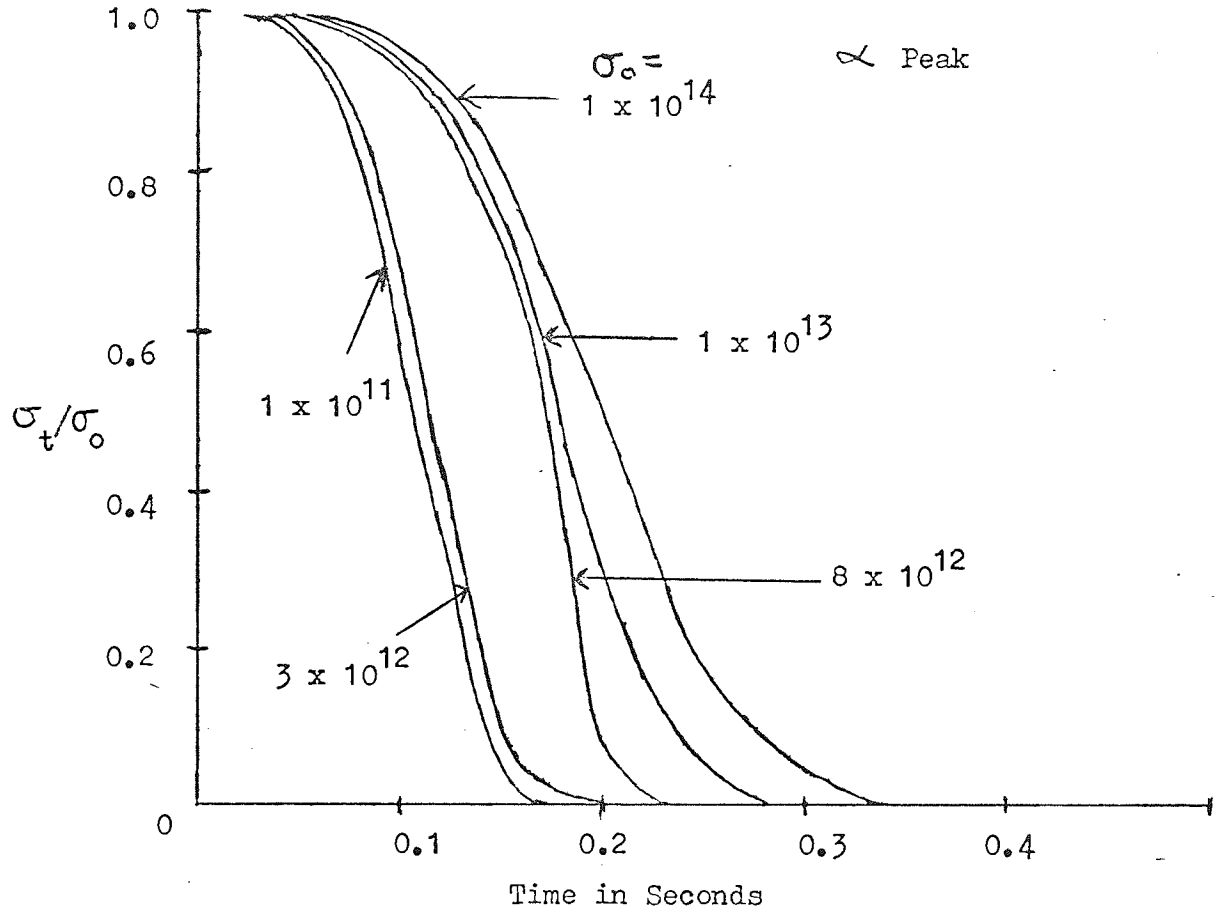

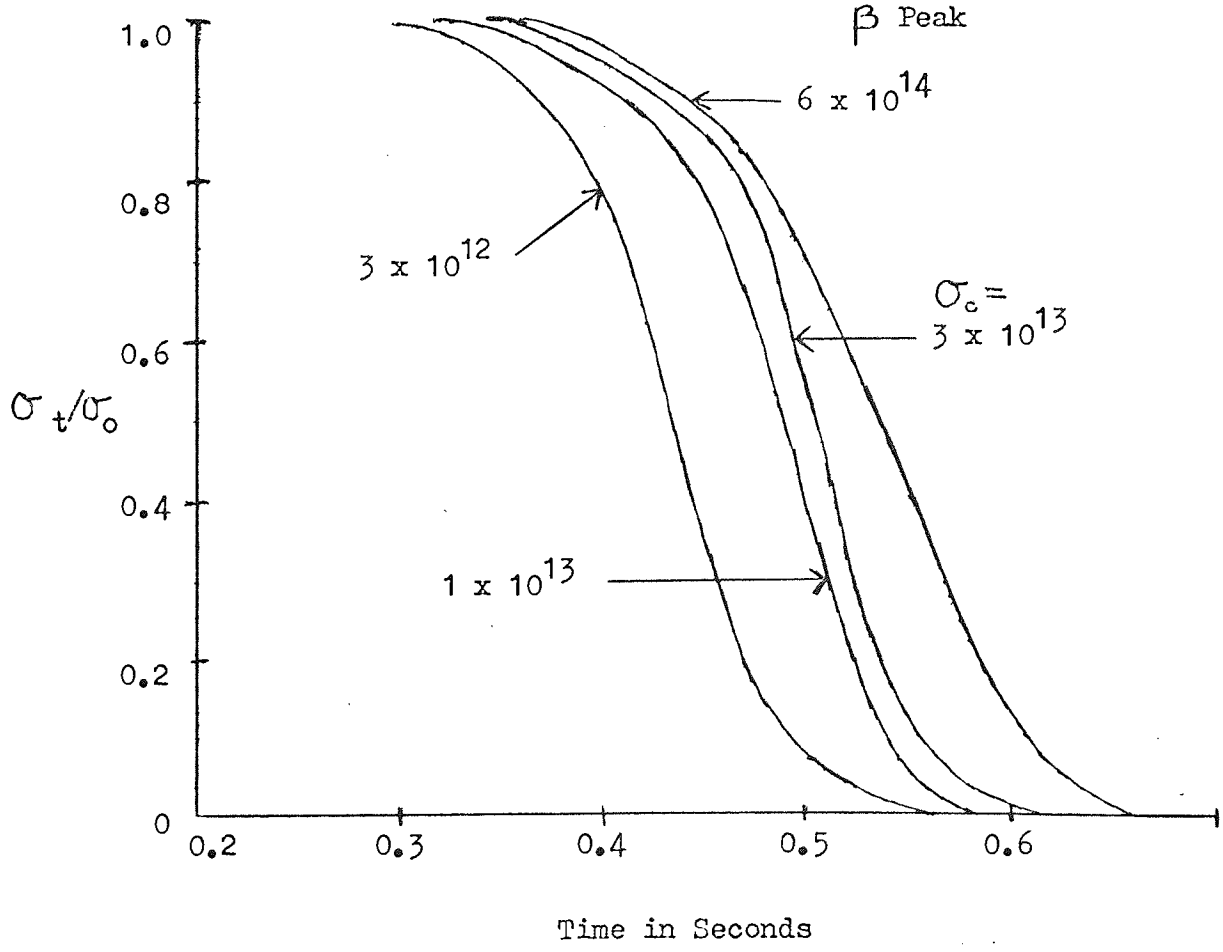

The equation for mixed first and second order kinetics is

$$(dn/dt)_t = k_1 \sigma_t + k_2 \sigma_t^2 \quad \ldots\ldots (5\text{-}9)$$

where k_1 is the rate constant for the first order desorption and k_2 is the rate constant for the second order desorption,

$$(dn/dt)_t / \sigma_t = k_1 + k_2 \sigma_t \quad \ldots\ldots (5\text{-}10)$$

A graph of the left hand side against σ_t for a series of values of σ_t all at the same temperature in each of the runs should give a straight line if mixed order kinetics are responsible for any spread in the value of the order of reaction. This graph showed a spread in the points with no clear straight line through the points and this suggested any discrepancy in the order of reaction calculated was due to errors in the number obtained.

5.4.4 The Sticking Probability

The sticking probability was calculated from the ratio of the number of collisions made by the molecules in the adsorption time to the number of molecules on the surface. The number of molecules on the surface was given by the surface coverage and the number of collisions was calculated from the kinetic theory. By substituting the values in the equation, the sticking probability was found to be 0.2, i.e. approximately one in every five collisions lead to a bound molecule.

When calculating the surface coverage the total number of molecules on the surface was used, that is the sum of both the α and β peaks.

5.4.5 Activation Energy

The experimental energy of activation was found by measuring the gradient of the graph of $\ln\left[(dn/dt)_t/(\sigma_o-\theta_t)^x\right]$ against 1/T. The gradient is equal to $\Delta E_{exp}/2.303R$. This is done for the correct value of the order of reaction. The graphs when x = 1 for the α and β peaks are shown in Figs. 75 and 76 respectively. The values obtained for the activation energy are shown in Table 18.

The values obtained for the α peak for 5 and 10 minutes adsorption time are subject to a large error because of the small number of points on the graph. It was thought the values obtained are from the extremes of the graph and not very accurate but it is possible they could be due to a change of activation energy with surface coverage. The average values for the activation energy were 34.7 k joules $mole^{-1}$ for the α peak and 183.9 k joules $mole^{-1}$ for the β peak. The values obtained would suggest both peaks are due to chemisorbed species but the α peak may indicate physisorbed material with an unusually high adsorption energy.

By substituting into the Arrhenius equation the pre-exponential function can be calculated. The pre-exponential functions were found to be 10^{14} s^{-1} and 10^{7} s^{-1} for the β and α peaks respectively.

5.5 THE THERMODYNAMIC PARAMETERS

5.5.1 The Temperature and the Enthalpy of Activation, $\Delta H^{\ddagger}$

We take the temperature of the reaction to be the temperature

FIG. 75 Graph Used to Calculate the Experimental Energy of Activation for the α Peak.

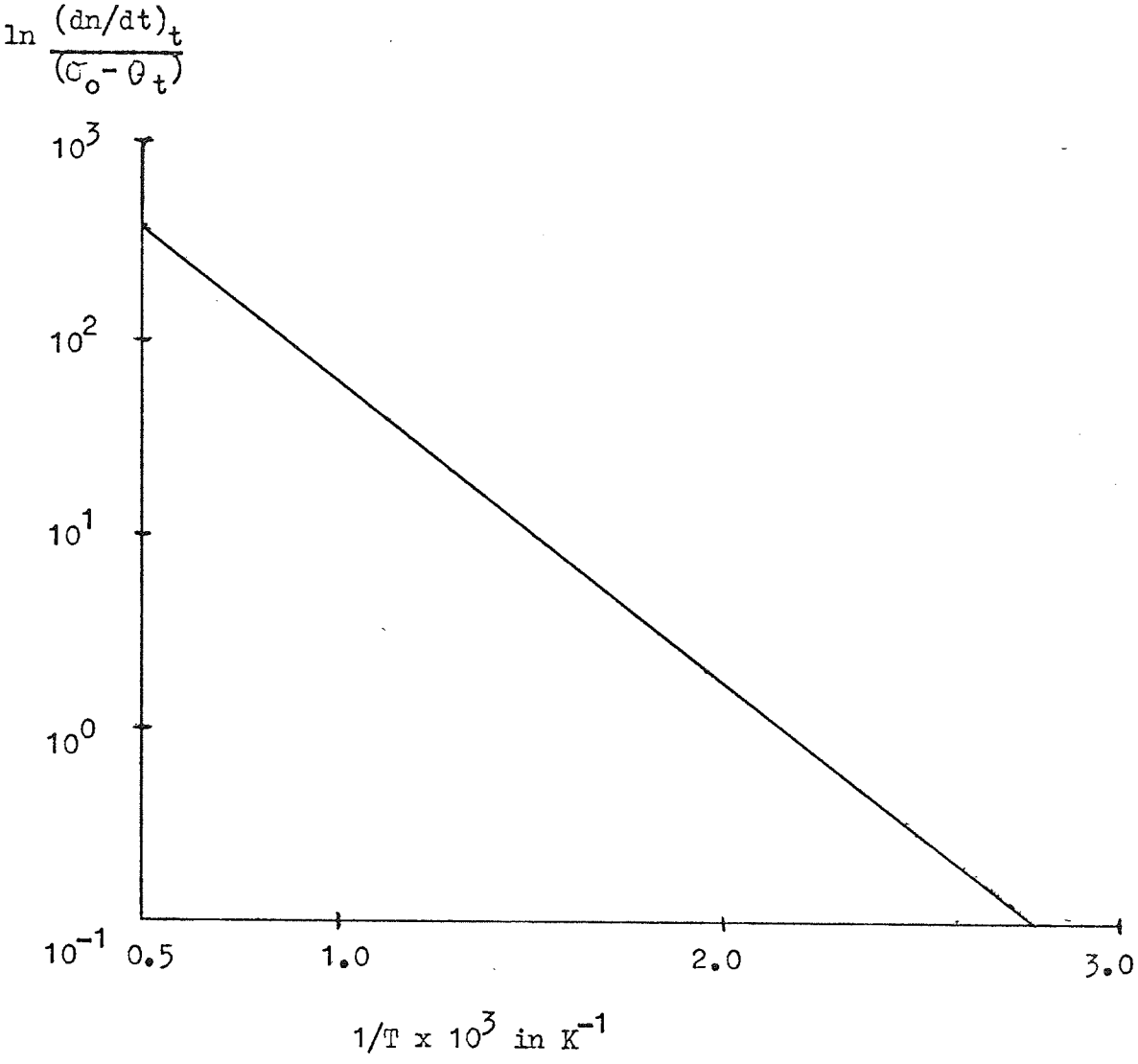

FIG. 76 Graph Used to Calculate the Experimental Energy of Activation for the β Peak.

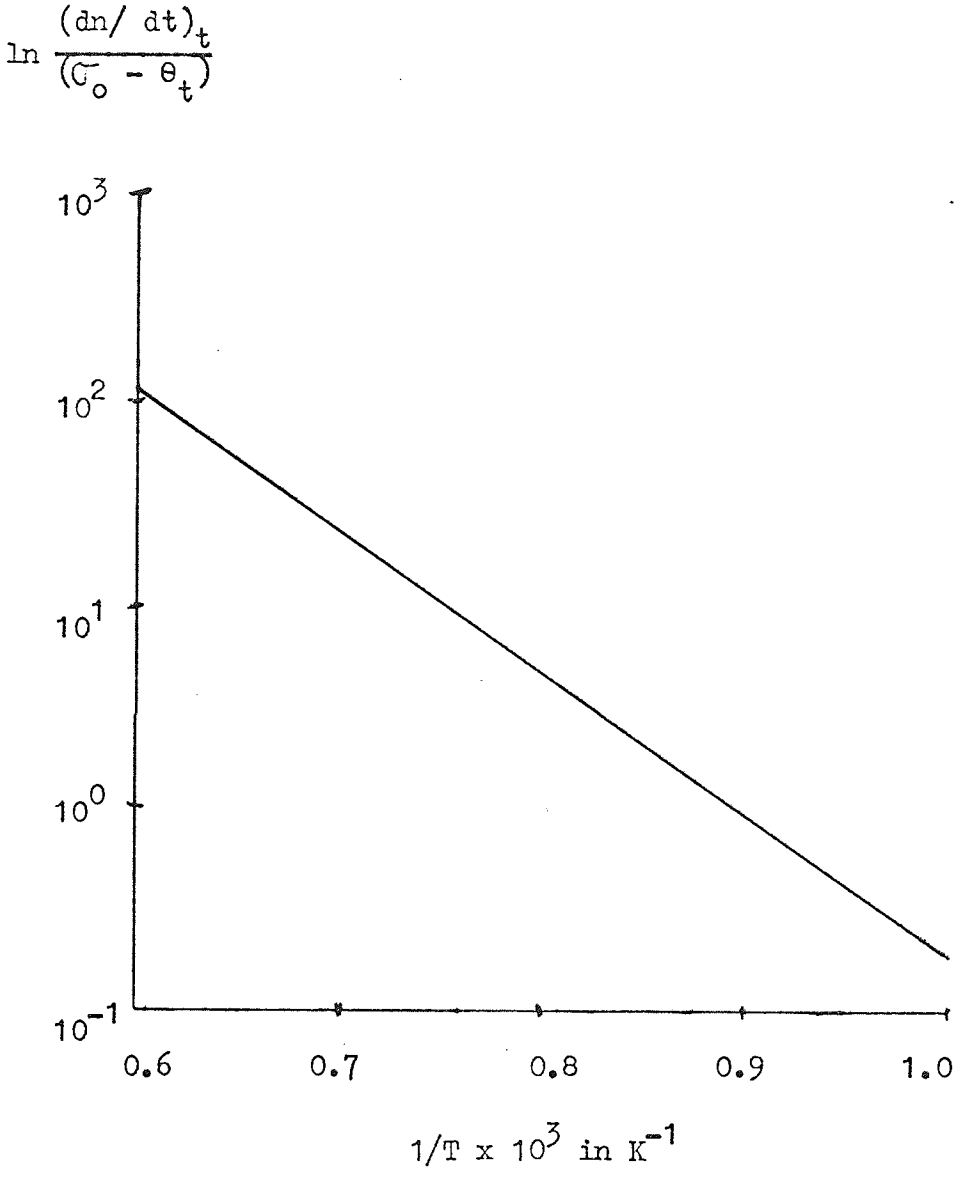

Table 18. The Spread of Activation Energies.

Adsorption time in minutes	ΔE_{exp} α peak in k joules mole^{-1}	ΔE_{exp} β peak in k joules mole^{-1}
1		185
2		155
5	(60)	168
10	(48)	193
15	33	193
30	33	231
60	28	185
120	28	147
Average	32.7	184
Error	$\pm$ 5	$\pm$ 30
Standard Deviation	$\pm$ 3	$\pm$ 24.5

of the maxima in the rate of desorption against time graph. For the α peak this temperature is found to be 700 K and for the β peak 1600 K.

The enthalpy differs from the experimental energy of activation by a term RT. $\Delta H_{\alpha}^{\neq}$ was found to be 20.4 k joules $mole^{-1}$ and $\Delta H_{\beta}^{\neq}$ = 170.5 k joules $mole^{-1}$.

5.5.2 The Entropy

The entropy of activation gives information about the state of order or disorder which exists on the surface i.e. whether the molecules are mobile or stationary.

The entropy is found by substituting the values in equation (4-60). The entropy of activation of the β peak at 1600 K was found to be 5. Joules K^{-1} mol^{-1} and for the α peak at 700 K -160 Joules K^{-1} mol^{-1}.

Using the Sackur Tetrode equation which is equation (4- 57) the ratio of the partition functions can be found. For the α peak

$$(F/F_A)_{\alpha} = 10^{-7} \quad \ldots. (5\text{-}11)$$

and for the β peak

$$(F/F_A)_{\beta} = 10^{0.6} \simeq 1 \quad \ldots. (5\text{-}12)$$

A summary of the experimental results is given in Table 19.

5.5.3 Mass Spectrometer Results

The results obtained for the desorption of carbon monoxide from tantalum are shown. Standard gases were used to establish the linearity of the mass scale, with slight discrepancies of m/e > 100 (error not more than $\pm$ 2 mass units).

Table 19. Summary of Data Obtained.

Parameter	α peak	β peak
Temperature of Maximum desorption rate, T_o	700 K	1600 K
Order of reaction	First	First
Rate constant at T_o	30 sec^{-1}	23 sec^{-1}
Experimental energy of activation	32.7 k joules $mole^{-1}$	184 k joules $mole^{-1}$
A factor	10^7 sec^{-1}	10^{14} sec^{-1}
F/F_A	10^{-7}	1
Entropy	-60 joules K^{-1} $mole^{-1}$	5. Joules K^{-1} $mole^{-1}$
Enthalpy	20.4 k joules $mole^{-1}$	170.5 k joules $mole^{-1}$

The background spectrum obtained from the system before the carbon monoxide experiments is shown in Fig. 77 . The mass 28 peak is the largest from the "boiled off" nitrogen. Other relatively small peaks are seen at mass 2, 14, 16, 17, 18 arising from traces of hydrogen and water.

The spectrum of Fig. 77 was obtained whilst carbon monoxide was being adsorbed. The size of the mass 14 peak due to atomic nitrogen can also be used as an indication of the amount of molecular nitrogen contributing to the mass 28 peak. From this it was estimated 90% of the mass 28 peak was due to the carbon monoxide.

A spectrum after the flash is shown in Fig. 77 where any increase in any of the peaks is due to any desorption from the filament. The only peak which increased was the mass 28 peak and all other peaks remain the same within the limits of the recording apparatus. The effect of the system on the desorption mass spectrum must be carefully considered. The mass spectrum takes several minutes to run and if the pumps are still open to the system one desorbed species could be preferentially pumped and reactions with the wall of the cell could effect the desorbed species. Also the lifetime of some of the desorbed species must be taken into account. From the evidence of the mass spectrum the only peak to increase was the mass 28 peak due to the desorption of carbon monoxide. The mass 12 and 16 peaks appear to increase very slightly but this may be due to variation in pressure and response of the recording device. The other peaks except for a slight trace of nitrogen were not detectable. There was no peak at the upper end of the spectrum indicating that no tantalum

FIG. 77 Mass Spectra of the Desorption of Carbon Monoxide.

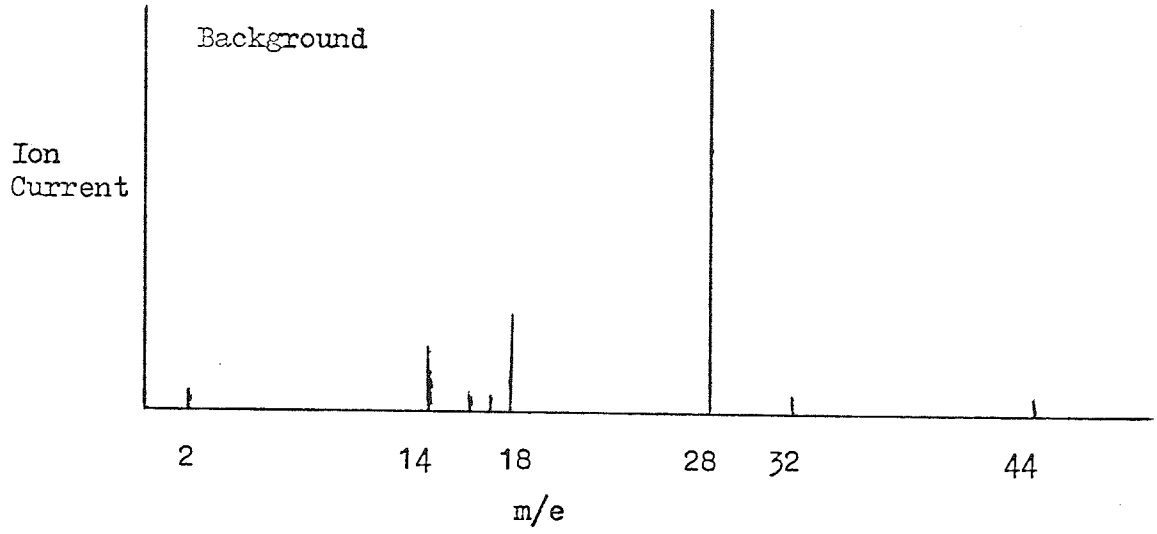

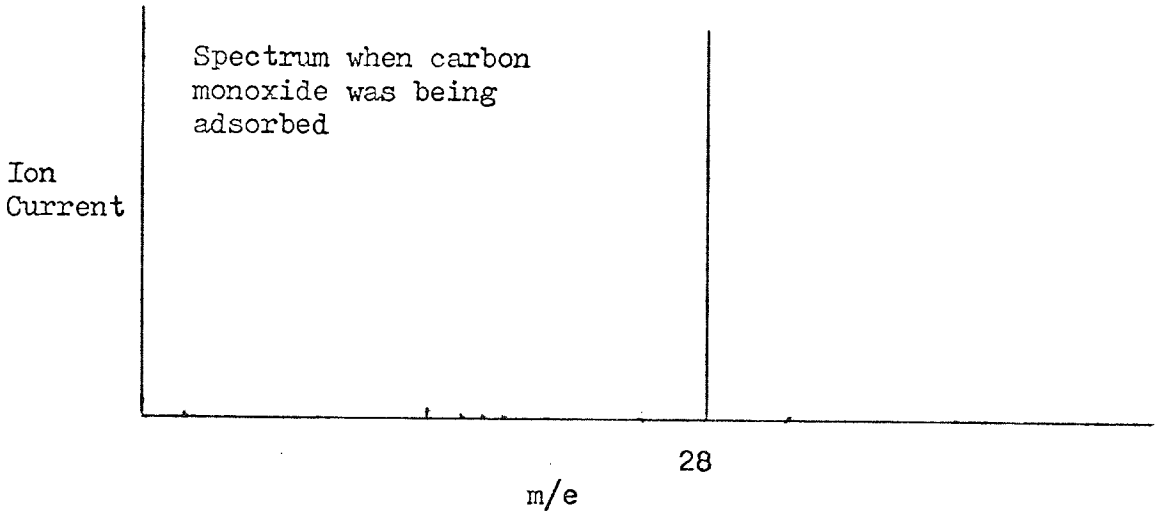

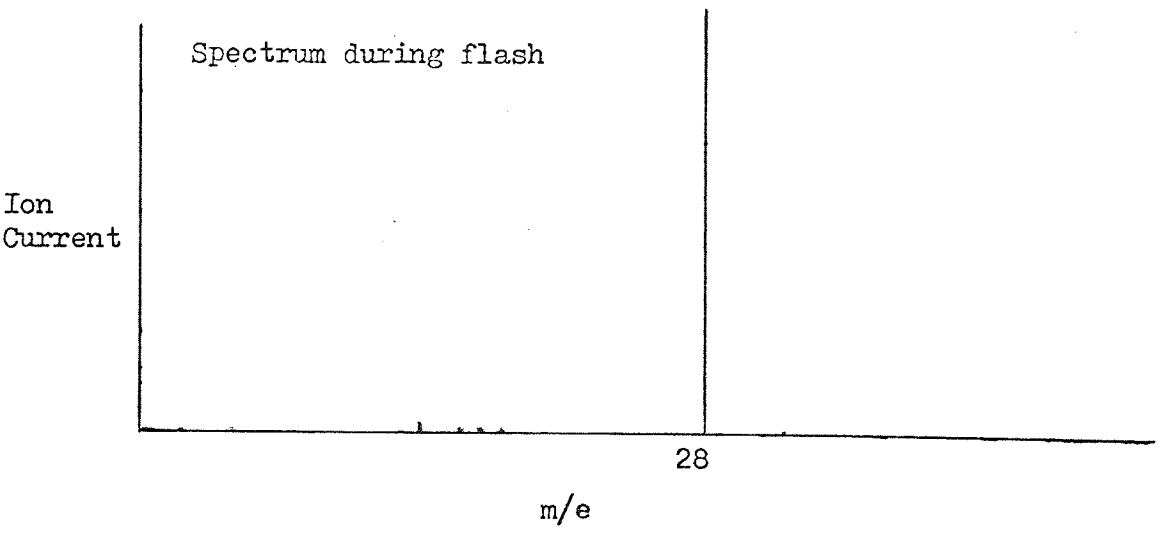

was being desorbed in species such as TaCO, TaC or TaO. No dissociation was seen to occur and no complex radical formation with the tantalum. The only desorbed species found was the carbon monoxide molecule.

Two pressure peaks were seen in the flash desorption of CO from tantalum. Mass spectrometric scans during the flash showed that desorption of carbon monoxide molecules only was occurring throughout each desorption peak. Only the peak at m/e = 28 showed measurable changes throughout the flash.

All the peaks seen on the mass spectrum were followed through the flash. The only peak which increased appreciably when the filament was flashed was the mass 28 peak. A very slight increase was seen in the 12 and 16 peaks but even on a low sensitivity the increase was only very small and little information could be gained from this.

The mass spectrometer could be used as a partial pressure measuring device. Experiments prior to the flash had shown that the ion current when the mass spectrometer was set on the mass 28 peak was proportional to the pressure. A straight line was obtained when a graph of the ion current was plotted against pressure. The mass spectrometer could be used in place of the trigger gauge and the same method of analysing the results should give the experimental parameters. The trigger gauge is still preferable to the mass spectrometer as a pressure measuring device because it is capable of accurately detecting much lower pressures and the response time is much quicker.

The only peak seen to increase appreciably during the flash was the mass 28 peak and the peaks 12 and 16 increased only slightly. The other peaks followed 2, 14, 27, 29 and 44 showed no increase at all.

5.6 ANALYSIS OF THE RESULTS

5.6.1 Introduction

The information obtained needs to be combined so that we can make feasible deductions about the reactions taking place on the surface. A detailed discussion is given in later sections but the main conclusions can be summarised as follows. The presence of two peaks in the desorption spectra show there are at least two desorbed states. The mass spectrometric results show only one species, mass 28, is desorbed during both pressure peaks; i.e. carbon monoxide in the molecular form is being desorbed from two differently bonded states on the surface. The direct surface studies indicate the surface is tantalum only, both before and after the reaction.

5.6.2 Observed Changes in the Filament

Direct observations of the filament were made by electron microscopy and X-ray diffraction. These both indicated that no compounds of tantalum had been formed on the surface. The electron microscope showed only changes in crystal structure and etching due to the heat treatment as expected. The X-ray diffraction pattern was identical to that of the unused filament with the exception that the lines were somewhat blurred because of the crystals formed on heating.

Previous evidence from a field emission microscope suggests that dissociation occurs when carbon monoxide is adsorbed. The carbon monoxide pattern was found to be converted to an oxygen pattern after a few seconds at 1550 K (94).

No high mass peaks up to m/e = 200 were found when the mass spectrum was analysed and this shows no tantalum compounds were

desorbed during the flash. Results for the desorption of carbon monoxide from other transition metals have shown no dissociation occurs on the surface (96).

5.6.3 Kinetics of Desorption

In these experiments the sticking probability for carbon monoxide on tantalum was found to be 0.2. This compares favourably with the value of 0.14 obtained by Gasser (97) for the adsorption of carbon monoxide on tantalum. Similarly the sticking probability was also found to be independent of temperature.

Gasser found the maximum surface coverage was 3.3×10^{14} molecules cm^{-2} compared with 7×10^{14} from the present study. With a surface roughness factor of unity Gasser's value corresponds to a carbon monoxide/surface tantalum atom ratio of 1:4.

The order of reaction was found to be first order for both the α and β peak. Gasser found the order of reaction for his desorption curves also to be first order over a much reduced temperature range. Similar behaviour has also been observed for the carbon monoxide-tungsten system(96).

The experimental energy of activation was found to be 33 k joules $mole^{-1}$ for the α peak and 185 k joules $mole^{-1}$ for the β peak. The high value of the activation energy for the β peak suggests it is chemisorbed with some form of chemical bond holding the molecule to the surface. The α peak may also be chemisorbed but the low value of the activation energy could allow the possibility of it being physisorbed. These are similar orders of magnitude to the adsorption energies for the α and β peak on other transition metals (96). King (23) found activation energies for carbon monoxide on tungsten of 220 k joules $mole^{-1}$ for the β peak and 100 k joules $mole^{-1}$ for the α peak.

The pre-exponential function was found to be 10^{14} sec^{-1} for the β peak and 10^{7} sec^{-1} for the α peak. A value of 10^{13} sec^{-1} for the pre-exponential factor has frequently been assumed in evaluating Arrhenius activation energies in similar studies (92).

5.6.4 Nature of the Adsorbed Species

The desorption spectra indicate that there are at least two desorbed species, the α and β states. Similar states are found for the desorption of carbon monoxide from tungsten (23). The β peak for tungsten is split into several peaks but this is probably due to adsorption on different crystal faces.

The α state for tantalum does not appear until the β state is firmly established on the surface. This is similar to the results obtained for the behaviour of carbon monoxide on tungsten by Redhead (92). Conversion from the α state into the β state is a possibility after adsorption. The carbon monoxide molecules which are adsorbed in the α state move around the surface until an unoccupied β state is found. At low adsorption time most of the molecules would be desorbed from β states. The α sites do not fill up appreciably until most of the β sites are filled. It was assumed that there are 10^{15} sites per cm^{2} but this is only a very approximate value and the precise number of β sites on the surface is unknown. The possibility of conversion from the α state to the β state for the adsorption of carbon monoxide on tungsten has been considered by King (23).

Field emission studies have been performed by Klein and Leder (94) for the system carbon monoxide on tantalum. They found three states which were desorbed at temperatures of 125 K, 650 K and one at greater than 900 K. Our investigations started at temperatures

above 125 K but two peaks were found, one which occurred with a maximum rate of desorption at 700 K, and one with desorption maximum at 1600 K. Klein found that at higher temperatures the tantalum oxide field emission pattern was obtained and at 2000 K a clean field emission pattern was obtained.

When a tantalum filament is heated above 2400 K in an atmosphere of carbon monoxide then an irreversible adsorption of carbon monoxide takes place. This was explained by Scheer and Fine (99) in terms of the equation,

$$Ta + CO \longrightarrow TaO + C$$

and both these and Klein (94) have found that no carbon is thermally desorbed during the experiments.

Using an omegatron mass spectrometer Madey (100) has investigated the possibilities of isotopic mixing when $^{12}C^{18}O$ and $^{13}C^{16}O$ are adsorbed on tungsten. No evidence of isotopic mixing was found but King (23), using a more sensitive instrument, found an extremely small amount of CO_2 when carbon monoxide was desorbed from a tungsten surface.

The mass spectrometric evidence suggests the desorbed species from both the α and β peaks is carbon monoxide. No evidence for the desorption of a tantalum oxide or carbide was found. This is similar to the results obtained for the desorption of carbon monoxide from tungsten and this system is regarded as the ideal system which represents the complete non-dissociative chemisorption of a diatomic molecule on the surface. However King (23) has questioned this and has presented results which are consistent with the dissociative adsorption of the β peak. The results from the present study are that the desorbed species is molecular carbon

monoxide and no dissociation occurs on the surface.

5.6.5 Possible Adsorbed Structures

The β peak was found both with low and high surface coverages but the α peak was only found at relatively high surface coverages. The α peak was found to be weakly bonded to the surface, but the β peak was tightly held. A normal pre-exponential factor was found for the β peak but a low value of 10^7 sec^{-1} was found for the α peak. Little change in the entropy was found for the β state but the α state produced a large negative change in the entropy. For both peaks the only desorption product was molecular carbon monoxide. The conclusions made from these observations are below.

The β peak is adsorbed without dissociation and tightly held to the surface and this is shown by the high value of the activation energy. The carbon monoxide is initially bonded to the β sites and will be immobile. The small entropy and normal pre-exponential function suggests that the β site will be immobile.

The α peak is only weakly bound to the surface, this is shown by the lower value of the activation energy. The carbon monoxide is adsorbed and desorbed without dissociation. The low pre-exponential function and large negative value of the entropy suggests that the α state is relatively free and mobile on the surface. The late appearance of the α peak at relatively high adsorption times could be attributed to the mobile α adsorbed carbon monoxide at low surface coverages moving around the surface until it finds and becomes attached to a more firmly bound β site. As the β sites are filled more and more α adatoms are unable to find a β site on which to adsorb and are desorbed as α-CO.

An analogy can be made between the bonding on the surface and metal carbonyls. In metal carbonyls the carbon monoxide molecule has three different structural functions (102). The structures are

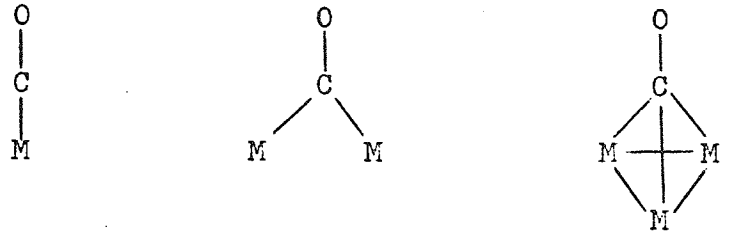

(a) (b) (c)

Tungsten has a metal carbonyl with the formula $W(CO)_6$ where the six CO are placed octahedrally around the tungsten with a W-C bond length of 2.06 A. Tantalum forms a carbonylate ion with the structure $[Ta(CO)_6]^-$.

Lanyon and Trapnell (101) have suggested the following structures for the β peak when carbon monoxide is adsorbed on tungsten

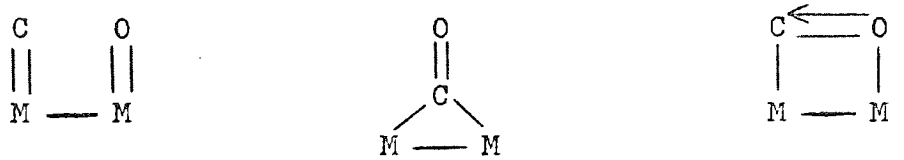

(a) (b) (c)

The generally accepted structure for the β site adsorption is (b). Our results cannot support any structure but since the carbon monoxide is found to be undissociated, model (a) seems unlikely. The α peak is regarded as a single site adsorption.

Further information is needed before a model of the adsorbed carbon monoxide on the surface can be made. For carbon monoxide

infra-red spectroscopy could give this information.

A review of the information pertaining to the infra-red studies of carbon monoxide adsorbed on metal surfaces has been made by Eischens and Pliskin (104). It is suggested that infra-red bands above 2000 cm^{-1} represent a linear M-C-O structure and bands below 2000 cm^{-1} were due to a bridging carbon monoxide group.

Blyholder (103) has investigated the adsorption of carbon monoxide on various transition metals. The main bands found are for

V	1940 cm^{-1}	1890 cm^{-1}
Cr	1940 cm^{-1}	1880 cm^{-1}
Co	2000 cm^{-1}	1880 cm^{-1}.

The bands below 2000 cm^{-1} could be due to a linear structure adsorbed in special sites such as corners and edges.

For most transition metals a broad band was found in the region 2100 cm^{-1} to 1700 cm^{-1} which is similar to the results obtained for the infra-red spectra of metal carbonyls.

6 DESORPTION OF HYDROGEN FROM TANTALUM

6.1 EXPERIMENTAL PROCEDURE

6.1.1 The Hydrogen Sample

The preparation of the hydrogen sample has been previously described. The sample in the bulb was 99.8% pure which was an increase of over 5% on the cylinder hydrogen sample. The sample was sealed in the bulb at a pressure of 30 mm Hg and the bulb was joined to the vacuum line by the glassblower Mr Herricks.

Hansen (38) has found when hydrocarbons are adsorbed on an iridium surface and flash desorbed, hydrogen is the main product observed. Knowledge of the behaviour of hydrogen in vacuum systems will be helpful if we are to use hydrocarbons in the system and obtain hydrogen as one of the decomposition products.

Hydrogen is found in the vacuum system as one of the background gases. When the titanium sublimation pump filaments are degassed, the gas desorbed is found to be mainly hydrogen. Hydrogen is known to be pumped and held by hot metal filaments and these concentrate the hydrogen and prevent it from being removed from the system.

Besides these reasons hydrogen is a very reactive and useful gas and knowledge of its behaviour will help in catalysis and other gas metal systems.

6.1.2 The Pump Down for Hydrogen

The apparatus was checked to make sure it was leak free and purged out with "boiled off" nitrogen several times to ensure the gas in the vacuum system was nitrogen. The sorption pumps were used to pump the system down to a pressure at which the ion pump and sublimation pump could be started. The pressure was reduced

using these pumps to 8×10^{-8} mm Hg.

The apparatus was baked at 500 K for 72 hours so desorbed gas could be removed from the sides of the system and from the filament and leads. The pressure rose very quickly when the heating began and care had to be taken to make sure the automatic cut out did not switch off the pump.

When the temperature, after the bake out, was reduced to room temperature the pressure in the system was 5×10^{-11} mm Hg which was measured on the trigger gauge.

6.1.3 The Background

For various maximum temperatures at the end of the flash the background spectra are shown in Fig. 78 . One or possibly two poorly resolved peaks are seen at very low temperatures. The background peak is relatively large at very short adsorption times and strongly resembles the shape of the hydrogen peak obtained in the experiment. It is quite possible the background gas could consist of a lot of hydrogen because a very large hydrogen peak, much greater than the mass 28 peak, was observed on the mass spectrometer when the filament was flashed. The size of the background peak was about 10% of the peak obtained during the experiments. The resolution of the desorption spectrum could not be improved because the minimum maximum temperature was being used at the time.

6.2 PARAMETERS CALCULATED FROM THE OSCILLOSCOPE TRACE

6.2.1 Preliminary Investigation of the Peaks

Experiments were performed and the results analysed so that the best resolution and peak heights could be obtained. Flashes

FIG. 78 Background Spectra Obtained for Hydrogen

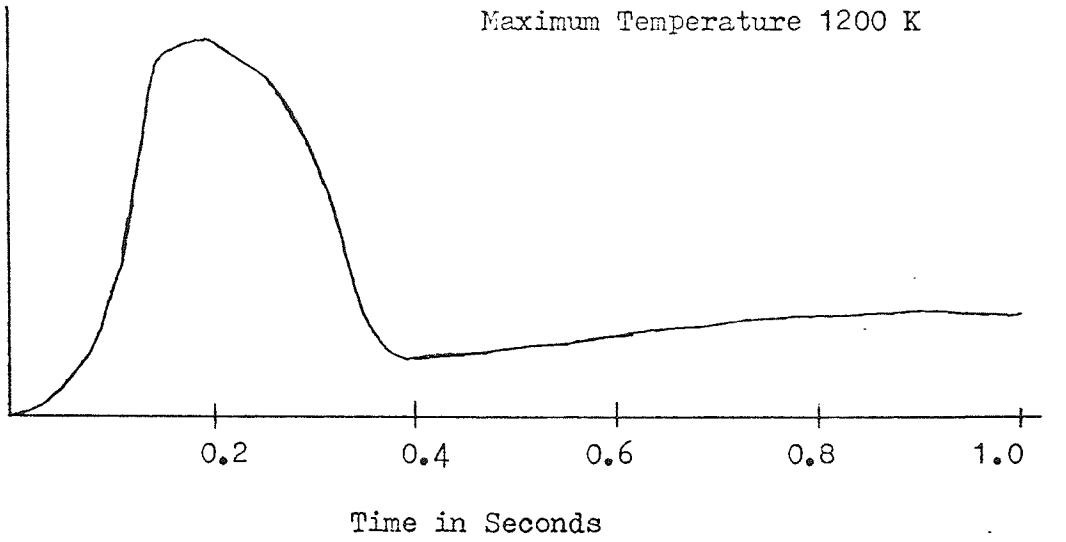

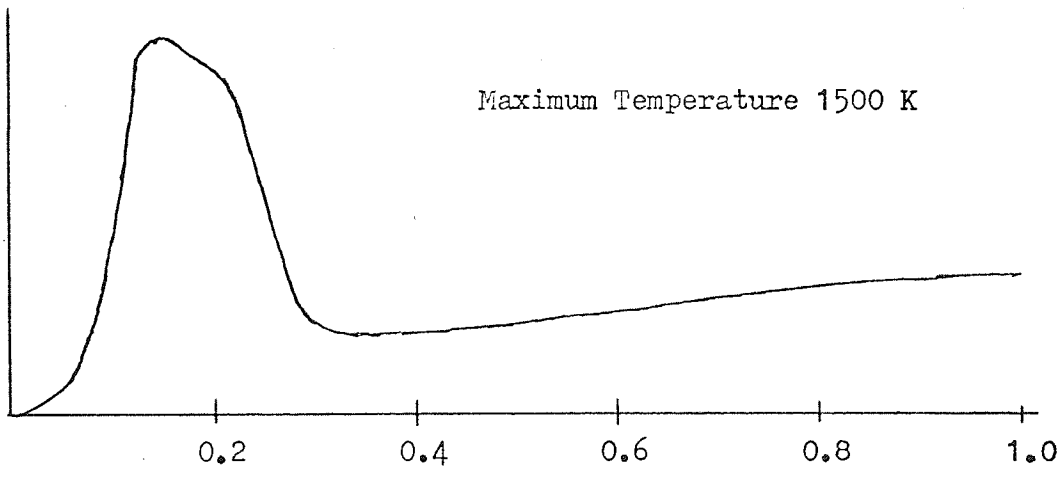

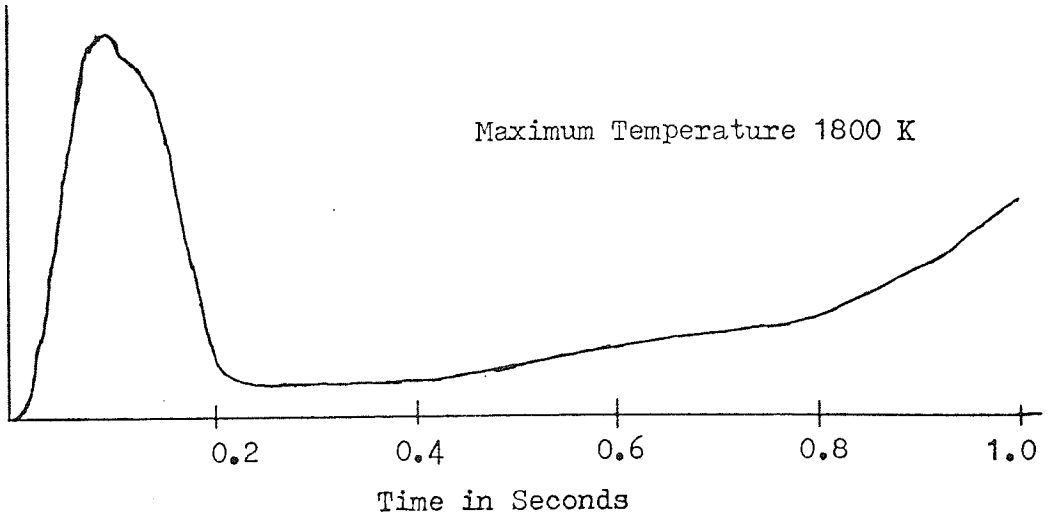

to various maximum temperatures revealed the only peaks seen were low temperature peaks. The peaks were at a temperature maximum so that the lowest maximum temperature obtainable was used.

The hydrogen was adsorbed very rapidly and too high an adsorption time at high pressures would result in a pressure rise during the flash which was too high for the trigger gauge and the gauge would cut out. By trial and error methods the adsorption times and pressures were found at which the gauge did not "cut out".

A typical desorption trace for hydrogen is shown in Fig. 79. The main feature of this is only one desorption peak is seen at very low temperatures. The pressure rises and falls very rapidly from 10^{-9} mm Hg to 10^{-5} mm Hg in 0.08 seconds and this occurs after a very short adsorption time of 1 minute at a pressure of 5×10^{-8} mm Hg.

Table 20 shows the data from a typical set of adsorption experiments.

6.2.2 Temperature Rise

No peaks were found at very high temperatures. The temperature rise was only a low temperature flash up to a maximum temperature of just over 1000 K. Fig. 80 shows the rise of temperature with time.

Table 21 shows the figures used in calculating the temperature rise for a flash. The temperature was calculated as in previous chapters.

The change in voltage across the known resistance was only very small and the lowest sensitivity on the oscilloscope had to

FIG. 79 Oscilloscope Trace Obtained for a Typical Hydrogen Experiment.

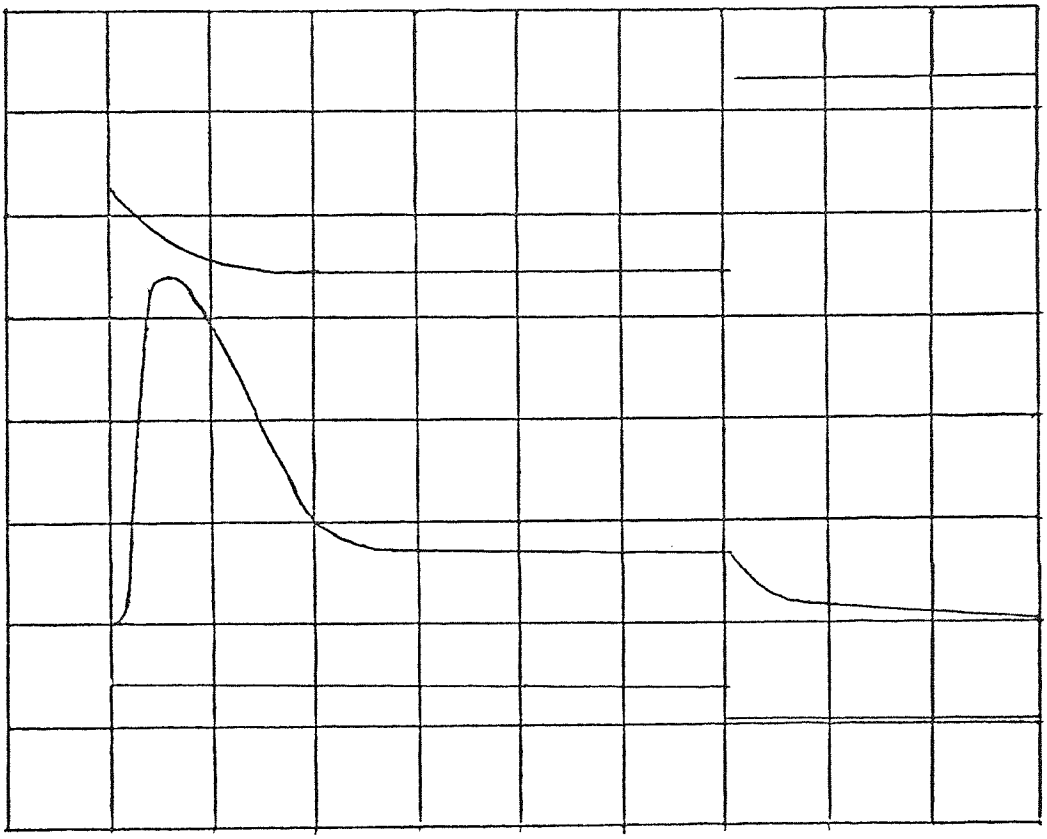

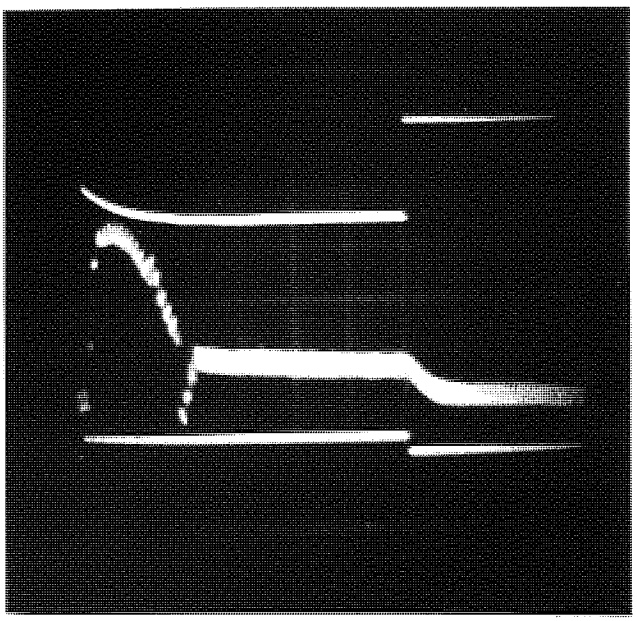

Table 20. A Typical Series of Adsorption Experiments

Adsorption Time In Minutes	Maximum Temperature K	Equilibrium Pressure in mm Hg	Maximum Pressure During Flash in mm Hg	Number ∝ Current
1	1380	3×10^{-9}	7×10^{-6}	4
2	1390	3×10^{-9}	1.25×10^{-5}	4
3	1380	3×10^{-9}	1.13×10^{-5}	4
5	1360	4×10^{-9}	1.23×10^{-5}	4
10	1390	2×10^{-9}	1.5×10^{-5}	5
15	1370	3×10^{-9}	3×10^{-5}	4
30	1380	3×10^{-9}	4.2×10^{-5}	4.5
60	1380	2×10^{-9}	4.7×10^{-5}	4

FIG. 80 A Typical Temperature Against Time Curve Obtained in the Hydrogen Experiments.

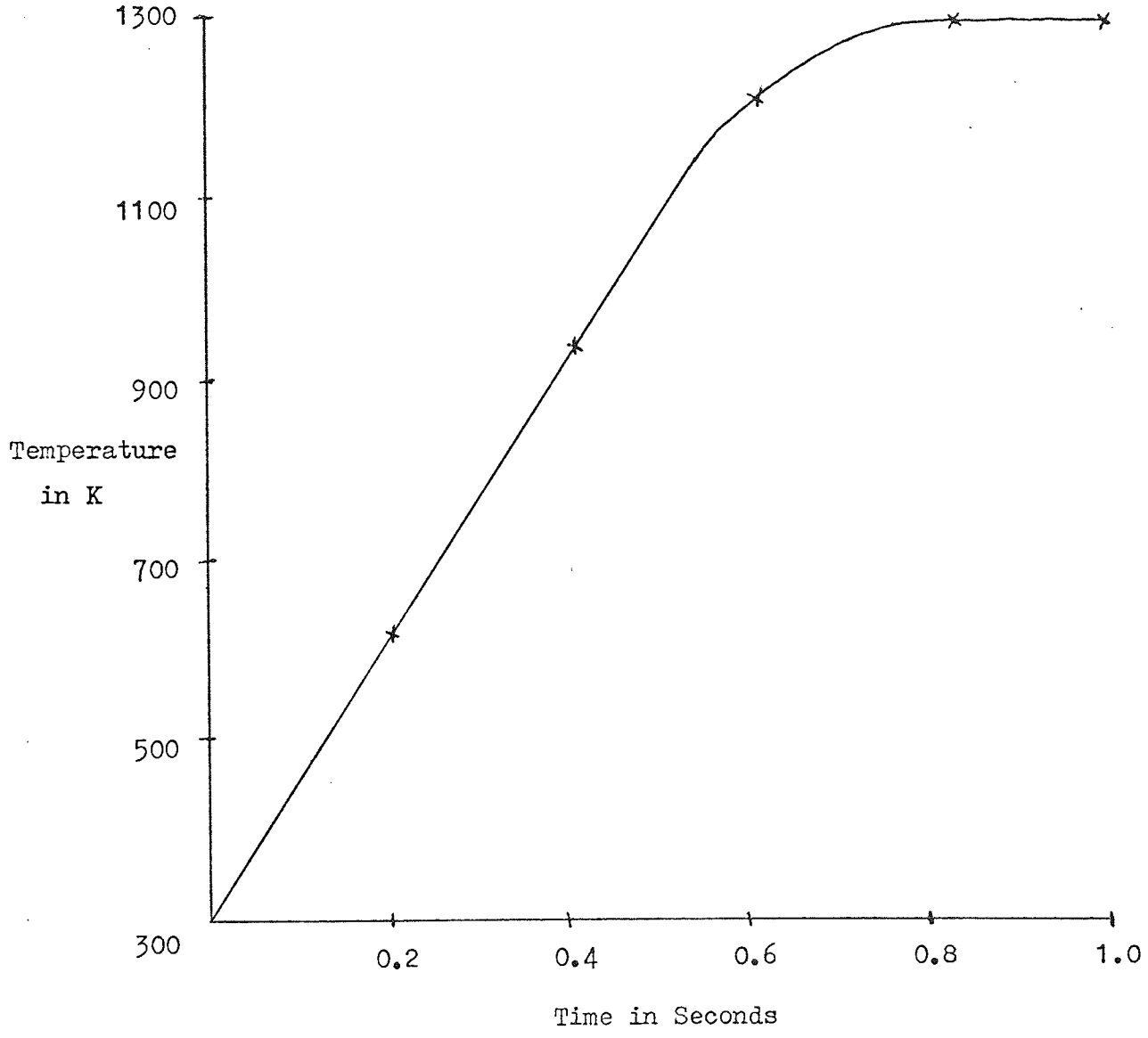

Table 21. Data Showing Relationship Between Temperature and Time

Time in secs	Current in Amps	Voltage in Volts	Resistivity $\times 10^{-6}$ ohm m^{-1}	Temperature in K
0	1.86	1.0	13	290
0.04	1.84	1.05	16	350
0.08	1.82	1.08	18	410
0.12	1.79	1.13	20	450
0.16	1.76	1.17	23	510
0.2	1.73	1.22	30	700
0.24	1.70	1.26	33	760
0.28	1.65	1.3	36	860
0.32	1.60	1.33	44	1080
0.36	1.60	1.36	46	1140
0.4	1.60	1.38	48	1200
0.44	1.60	1.4	49	1230
0.48	1.60	1.41	50	1250
0.52	1.60	1.43	51	1280
0.56	1.60	1.44	52	1300
0.6	1.60	1.44	52	1300
0.64	1.60	1.45	52	1300
0.68	1.60	1.45	52	1300
0.72	1.60	1.46	53	1340
0.76	1.60	1.46	53	1340
0.8	1.60	1.47	53	1340

be used. Even so, the change in the trace was very small and this was a source of error in measuring the temperature.

The temperature rises linearly 900 K in 0.4 secs, this gives an equation describing the rise

$$T = 298 + 2250\,t \qquad \ldots. (6\text{-}1)$$

where $\beta = 2250\ K\ sec^{-1}$.

6.2.3 The Pressure

The pressure rise is very rapid in this experiment, some 4 to 5 orders of magnitude in 0.08 seconds. Tables 22 and 23 show an increase in pressure for the flash together with the time, pressure minus the background pressure and the actual pressure rise due to the desorption of hydrogen. Figs. 81 and 82 show typical hydrogen desorption spectra for different adsorption times.

Only one desorption peak can be clearly seen but this could be a combination of poorly resolved peaks. The peak occurs very soon after the start of the flash and is desorbed by the time the temperature has reached 700 K. No peaks were detected at between room temperature and where the peak occurred and no peaks were observed at higher temperatures.

6.3 CALCULATED PARAMETERS FOR HYDROGEN

6.3.1 The Rate of Desorption

The graph of actual increase in pressure due to hydrogen desorption against time is shown in Fig. 83 . The gradient of the graph was calculated and a table of the values used to calculate the rate of desorption is shown in Table 24 . The hydrogen desorption experiments present a problem with working

Table 22. Data Used to Calculate the Actual Pressure Rise Due to Hydrogen I

Time in secs	Pressure $\times 10^9$ mm Hg	Pressure minus the equilibrium $P_o \times 10^9$ mm Hg	Pressure - P_o - Background $\times 10^9$ mm Hg
0	3	0	0
0.04	10	7	7
0.08	2300	2297	2292
0.12	8500	8497	8477
0.16	12000	11997	11957
0.2	13000	12997	11397
0.24	9500	9497	8497
0.28	7500	7497	6797
0.32	5500	5497	5550
0.36	3900	3897	3867
0.4	2700	2697	2685
0.44	1900	1897	1897
0.48	1100	1097	1097
0.52	650	647	647
0.56	250	247	247
0.6	120	117	117
0.64	60	57	57
0.68	45	42	42
0.72	30	27	27
0.76	21	18	18
0.8	17	14	14
0.84	12	9	9
0.88	11	8	8
0.92	10	7	7
0.96	9	6	6
1.00	8.5	5.5	5.5

Table 23. Data Used to Calculate the Actual Pressure Rise Due to Hydrogen II

Time in secs	Pressure $\times 10^9$ mm Hg	Pressure minus the equilibrium $P_o \times 10^9$ mm Hg	Pressure - P_o - Background $\times 10^9$ mm Hg
0	3	0	0
0.04	5	2	1
0.08	3000	2997	1797
0.12	20000	19997	15499
0.16	47000	46997	42997
0.2	40000	39997	39697
0.24	28000	27997	27932
0.28	21000	20997	20967
0.32	15000	14997	14997
0.36	11000	10997	10997
0.4	8000	7997	7997
0.44	5800	5797	5797
0.48	4000	3997	3997
0.52	3000	2997	2997
0.56	2000	1997	1997
0.6	1200	1197	1197
0.64	600	597	597
0.68	300	297	297
0.72	200	197	197
0.76	130	127	127
0.8	80	77	77
0.84	50	47	47
0.88	40	37	37
0.92	32	29	29
0.96	27	24	24
1.00	23	20	20

FIG. 81 A Typical Hydrogen Desorption Spectra. I

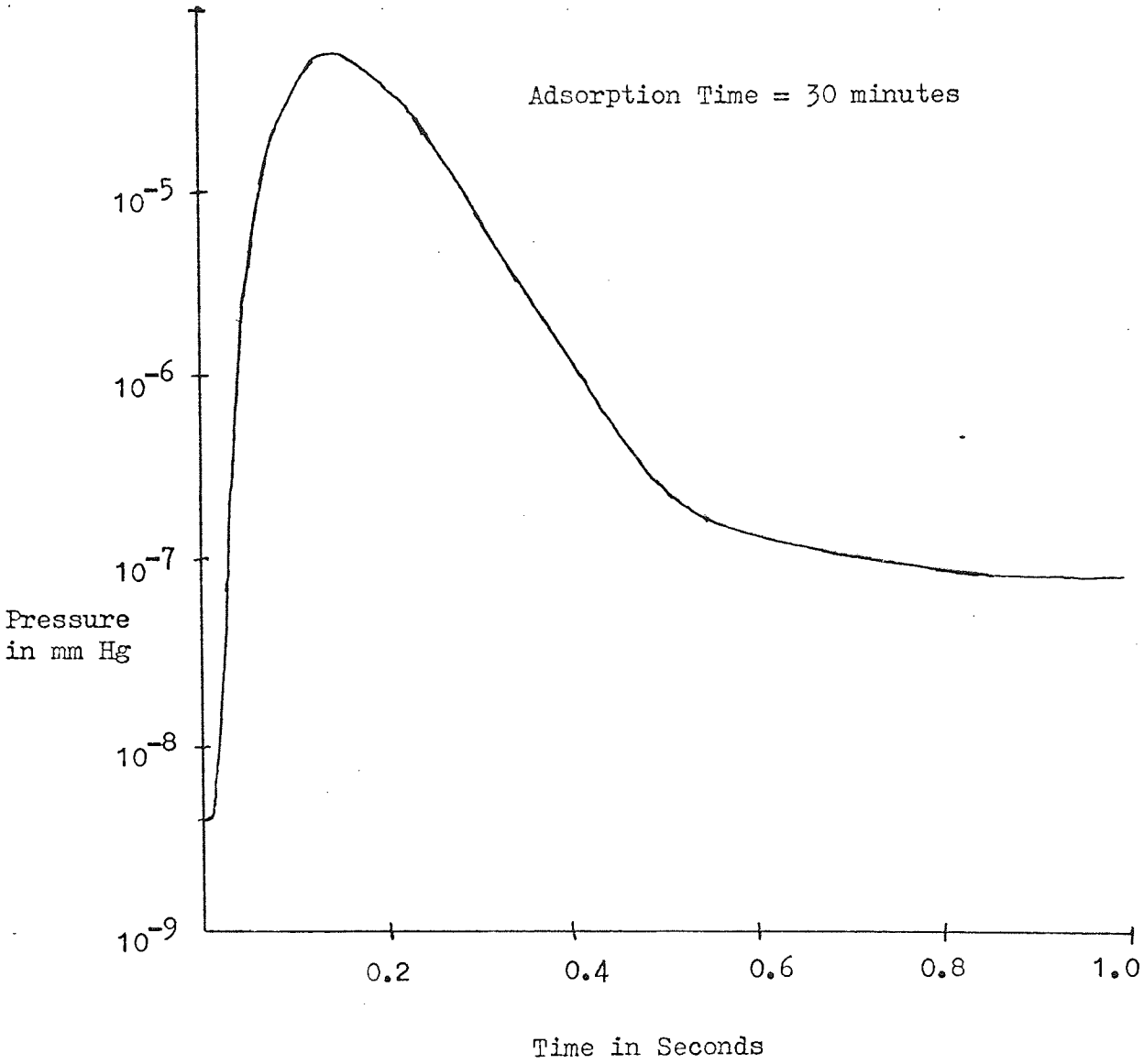

FIG. 82 A Typical Hydrogen Desorption Spectra II.

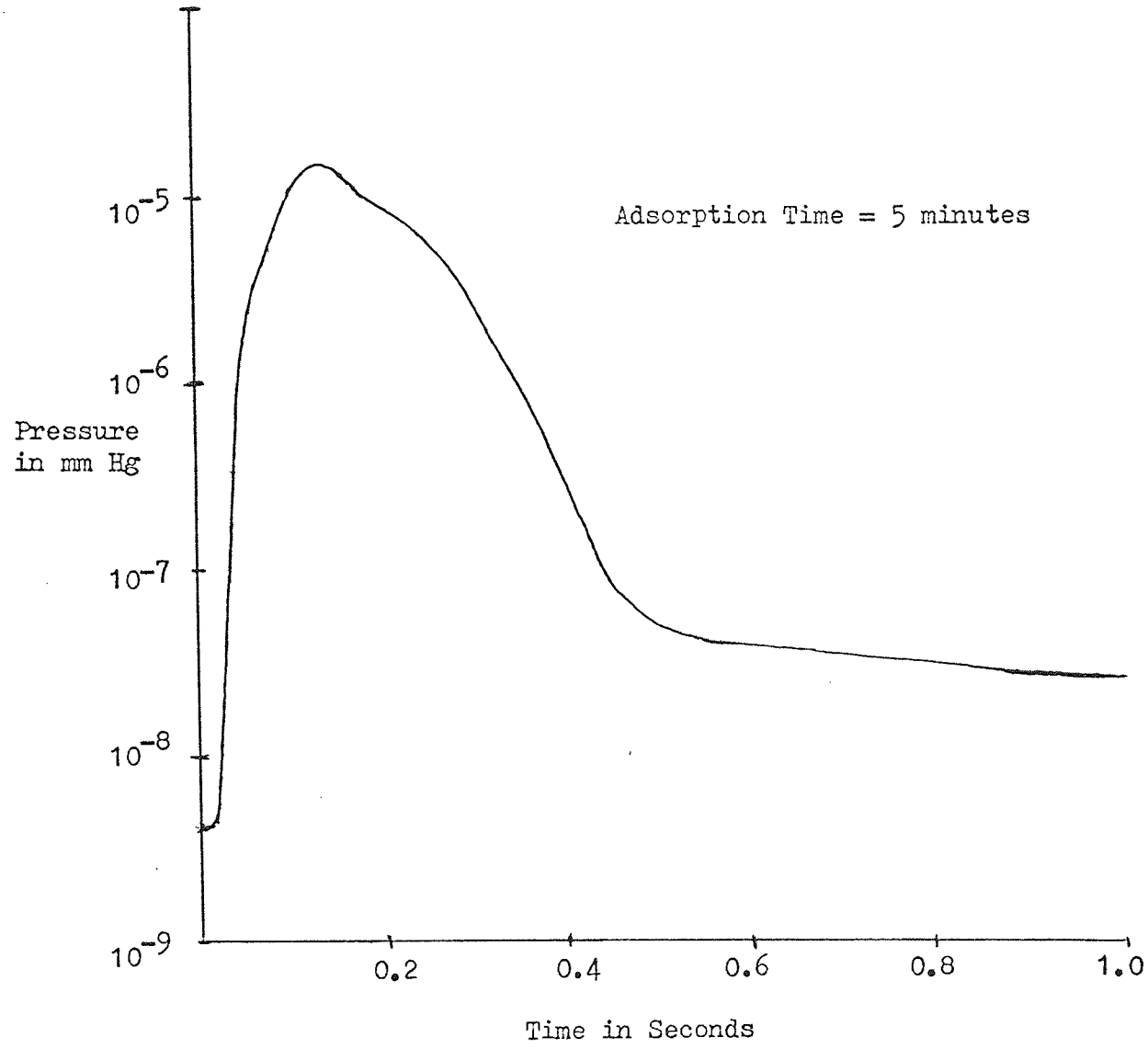

FIG. 83 A Graph of the Pressure Increase Due to the Desorption of Hydrogen Against Time.

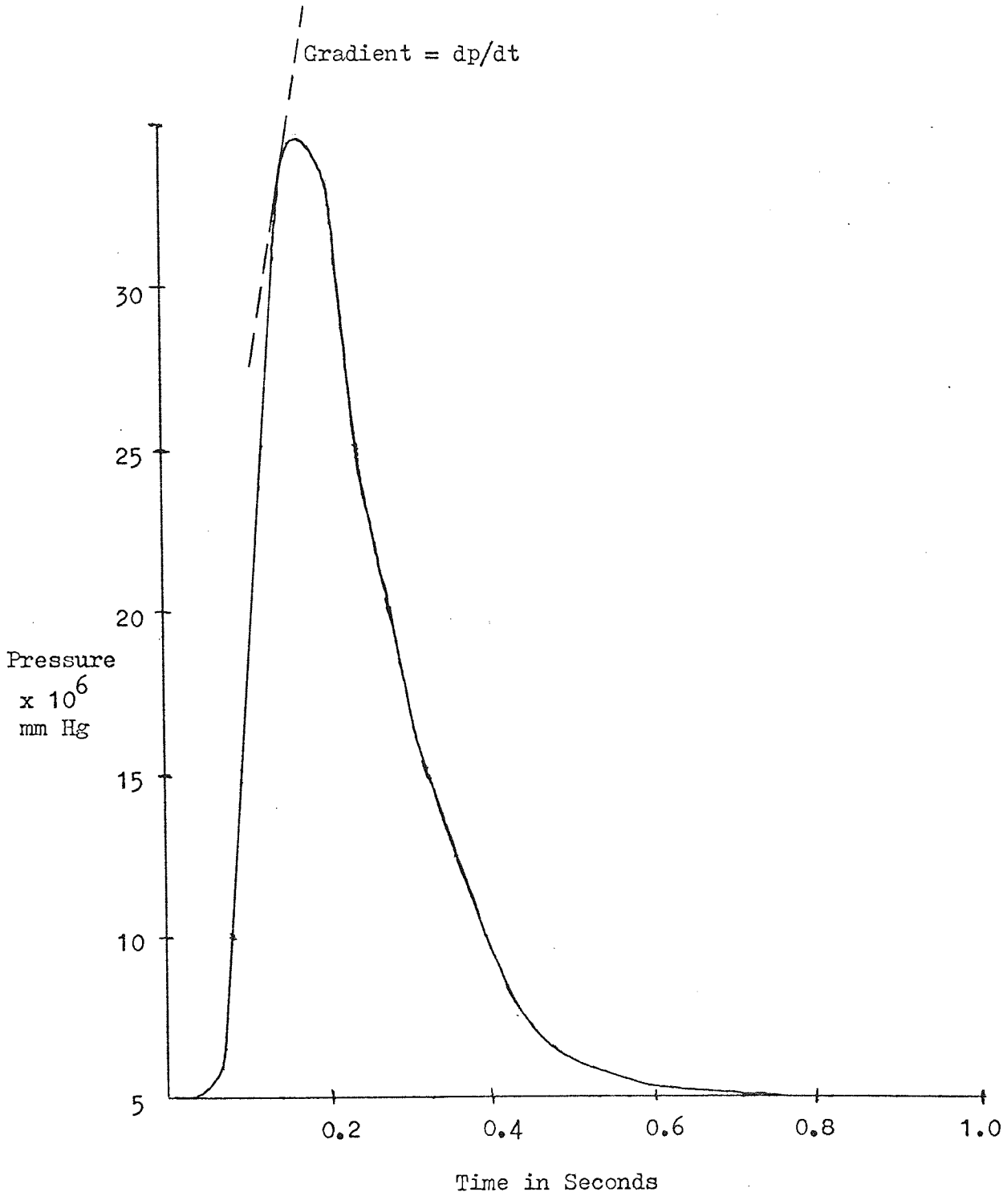

Table 24. Data Used to Calculate the Rate of Desorption

Time in secs	Pressure $\times 10^{9}$ mm Hg	dP/dt $\times 10^{7}$ mm Hg sec^{-1}	dn/dt $\times 10^{-14}$ molecules sec^{-1}
0	0	0	0
0.04	1	125	4.69
0.08	1797	850	31.92
0.12	15497	6850	305.47
0.16	42997	6850	395.65
0.17	45000	0	
0.2	39697	-3500	38.95
0.24	27932	-2500	19
0.28	20967	-2000	10
0.32	14997	-1250	5
0.36	10997	- 750	2
0.4	7997	- 600	0

out the pumping speed. Many pumps behave differently to hydrogen than most other gases. A further complication is the hot filament which is also acting as a pump to the hydrogen. The pumping speed was calculated from the decrease of pressure with time at the end of the flash and the value obtained used to estimate the correction for the number of molecules lost by pumping. However, how reliable this method is when calculating the pumping speed for hydrogen is questionable. The decrease in the pressure after the initial rise indicates the pumping speed should be large and this is in agreement with the value calculated.

Fig. 84 shows a graph of dp/dt against time and Fig. 85 shows the rate of desorption against time graphs for a number of adsorption times.

For an adsorption time of one minute the maximum rate of desorption was 6.6×10^{15} molecules cm^{-2} sec^{-1} and this increased to 4×10^{16} molecules cm^{-2} sec^{-1} at an adsorption time of one hour.

6.3.2 The Surface Coverage

The area under the rate of desorption against time curve, Fig. 85 was calculated and the results tabulated in Table 25 . The hydrogen is rapidly adsorbed and soon forms a monolayer coverage.

Table 26 shows the decrease in surface coverage with temperature and it can be seen that most of the hydrogen is desorbed by the time a temperature of 700 K is reached. A graph of the change in surface coverage with time is shown in Fig. 86.

FIG. 84 Graph of dp/dt Against Time.

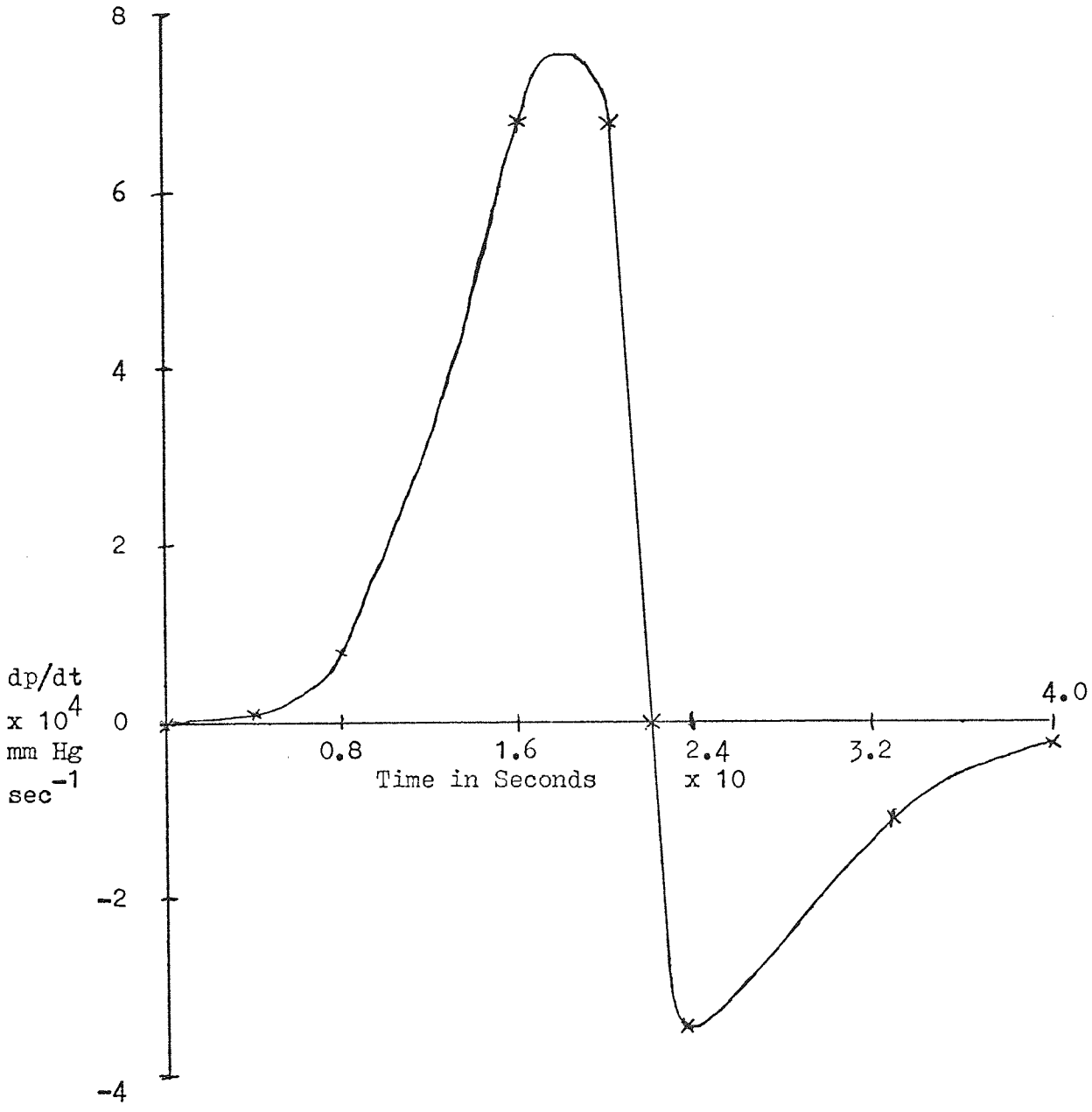

FIG. 85 Variation of the Rate of Desorption.

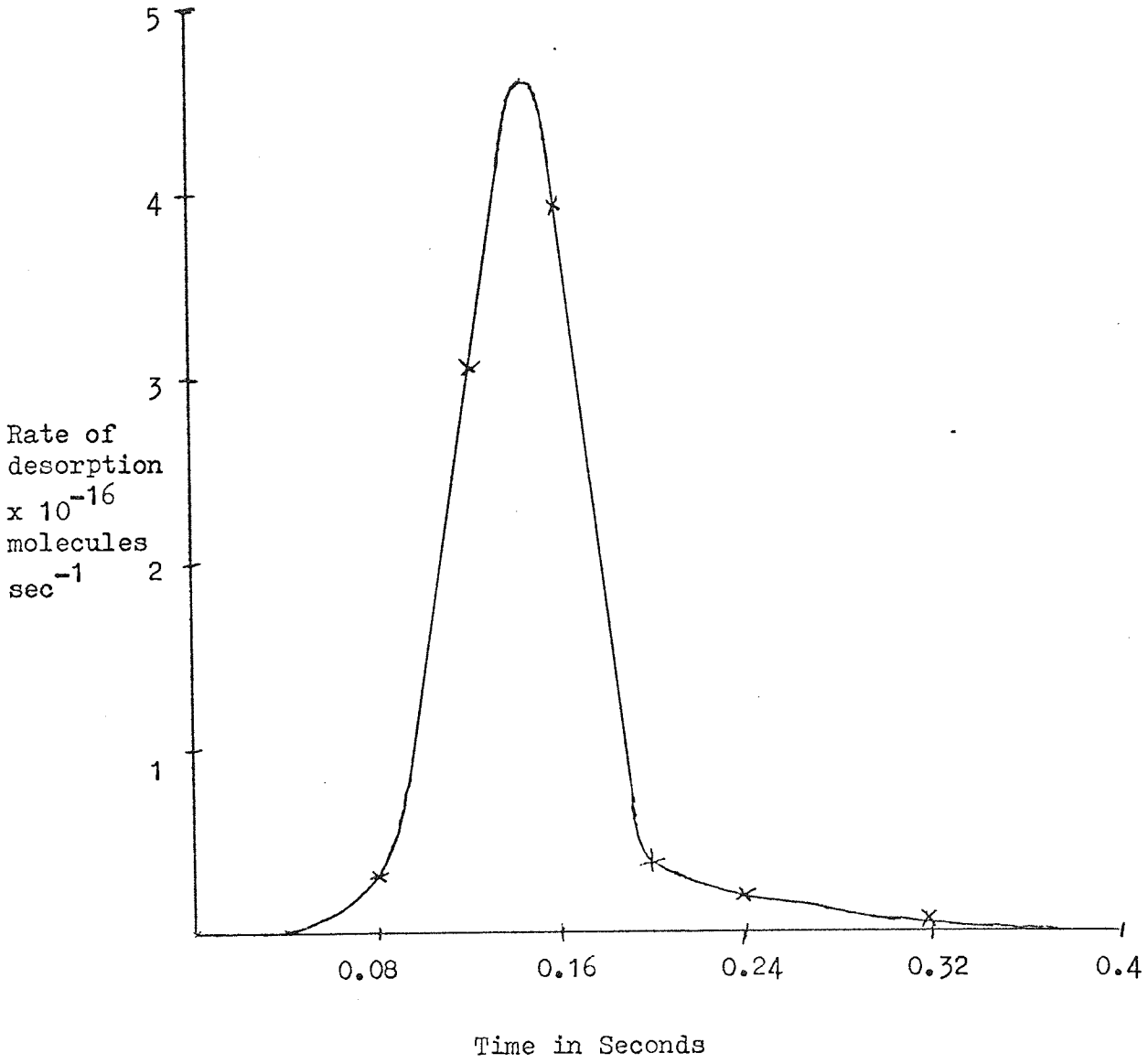

Table 25. Variation of Surface Coverage With Adsorption Time

Adsorption Time in Minutes	Maximum Surface Coverage $\times 10^{-15}$ molecules cm^{-2}
1	0.48
2	0.82
3	0.88
5	0.943
10	0.957
15	1.11
30	1.33
60	1.7

Table 26. Variation of Surface Coverage During the Flash

Time in secs	$\sigma \times 10^{-14}$ Molecules cm^{-2}	$\sigma_o - \theta_t \times 10^{-14}$ Molecules cm^{-2}	$\sigma_o - \theta_t$ Monolayers	Temperature in K
0	0.00	9.57	0.95	290
0.04	0.12	9.45	0.94	350
0.08	1.81	7.76	0.77	410
0.12	6.49	3.08	0.30	450
0.16	8.83	0.74	0.07	510
0.2	9.31	0.26	0.02	700
0.24	9.49	0.08	0.008	760
0.28	9.55	0.02	0.002	860
0.32	9.57	0	0	1080

FIG. 86 Change of Surface Coverage with Adsorption Time.

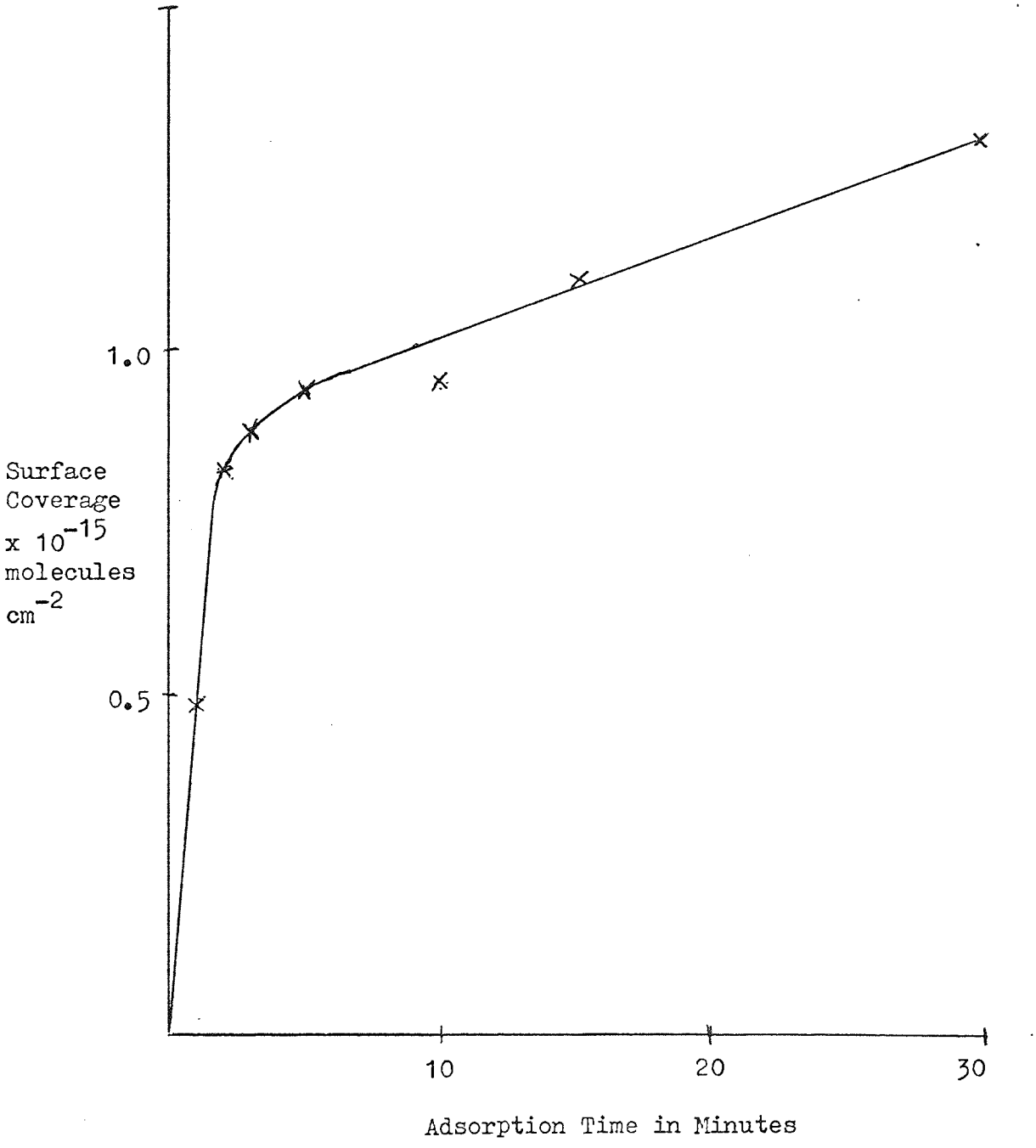

6.3.3 The Sticking Probability

The results obtained for the sticking probability are shown in Table 27. On a clean surface the sticking probability is found to be 0.57 but is probably even higher than this. This is the average value of the sticking probability over the first minute and also the error involved in estimating the surface coverage is larger at short adsorption times and therefore initially the sticking probability could be much larger. The sticking probability falls with adsorption time and a graph showing this is Fig. 87.

6.3.4 The Order of Reaction

Graphs of $\ln\left[(dn/dt)_t/(\sigma_o - \theta)^x\right]$ against $1/T$ for $x = 1$ or 2 were drawn and these are both shown in Fig. 88. The second order graph gave the best straight line in each case and order of reaction was concluded to be second order. This was confirmed by using graphs of $\sigma_o - \theta_t/\sigma_o$ against t which are shown in Fig. 89. The rate constant for the desorption reaction at a particular temperature is equal to $(dn/dt)_t/(\sigma_o - \theta)^2$ and at 490 K was found to be 11×10^{-14} molecule^{-1} cm^2 sec^{-1}. The values of the rate constant at various temperatures calculated for different experiments are shown in Table 28. The differences in the values could be due to the inaccuracy in measuring the temperature.

6.3.5 The Experimental Energy of Activation

A graph of ln k against $1/T$ is shown in Fig. 90 and the slope of this gives the value of ΔE. Over a series of experiments the value of ΔE calculated lay between 46 k joules mole^{-1} to 84 k joules mole^{-1} and this is shown in Table 29. The average value for the experimental energy of activation was found

Table 27. Sticking Probability Results

Time for Adsorption In Minutes	Calculated number of Collisions $\times 10^{-14}$ molecules cm^{-2}	Surface Coverage $\times 10^{-14}$ molecules cm^{-2}	Sticking Probability
1	8.4	4.8	0.57
2	16.8	8.2	0.49
3	25.2	8.8	0.35
5	42	9.4	0.22
10	84	9.5	0.11
15	126	11.1	0.088
30	252	13.3	0.052
60	504	17.0	0.033

FIG. 87 A Graph Showing the Change in the Sticking Probability.

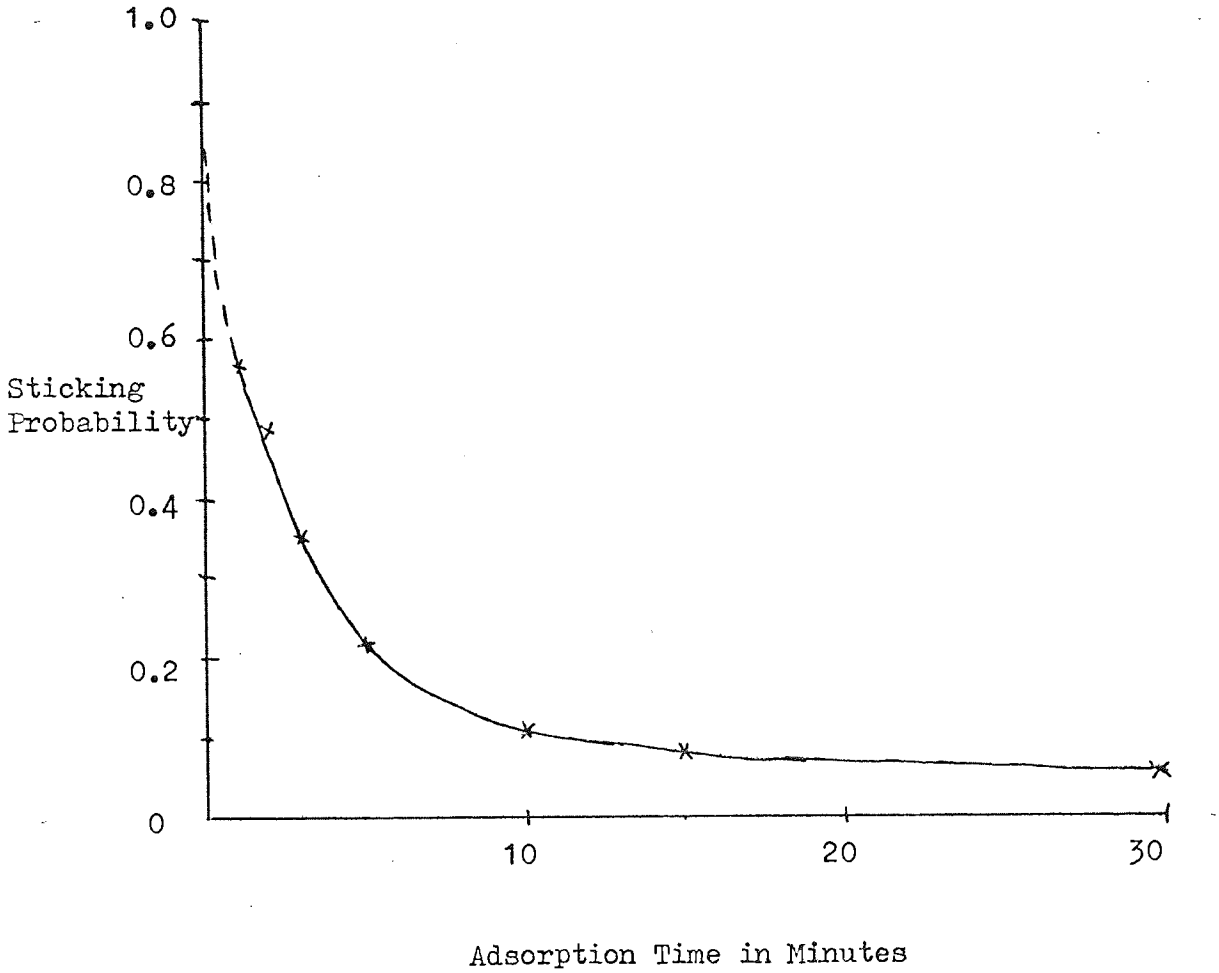

FIG. 88 Graph of Log Rate Constant Against the Reciprocal of the Temperature.

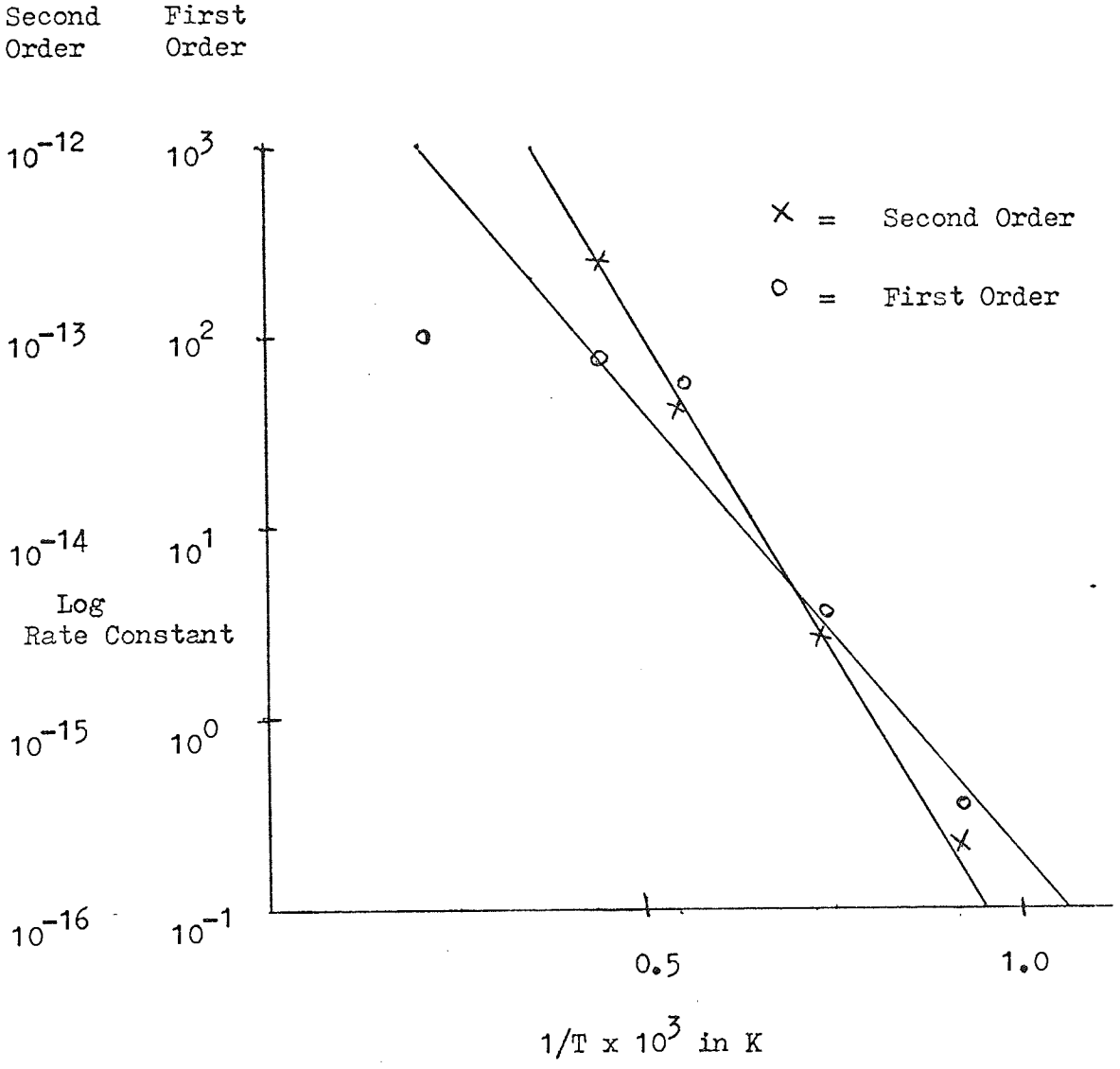

FIG. 89 Graph of $\sigma_o - \theta/\sigma_o$ Against Time for Various Adsorption Times.

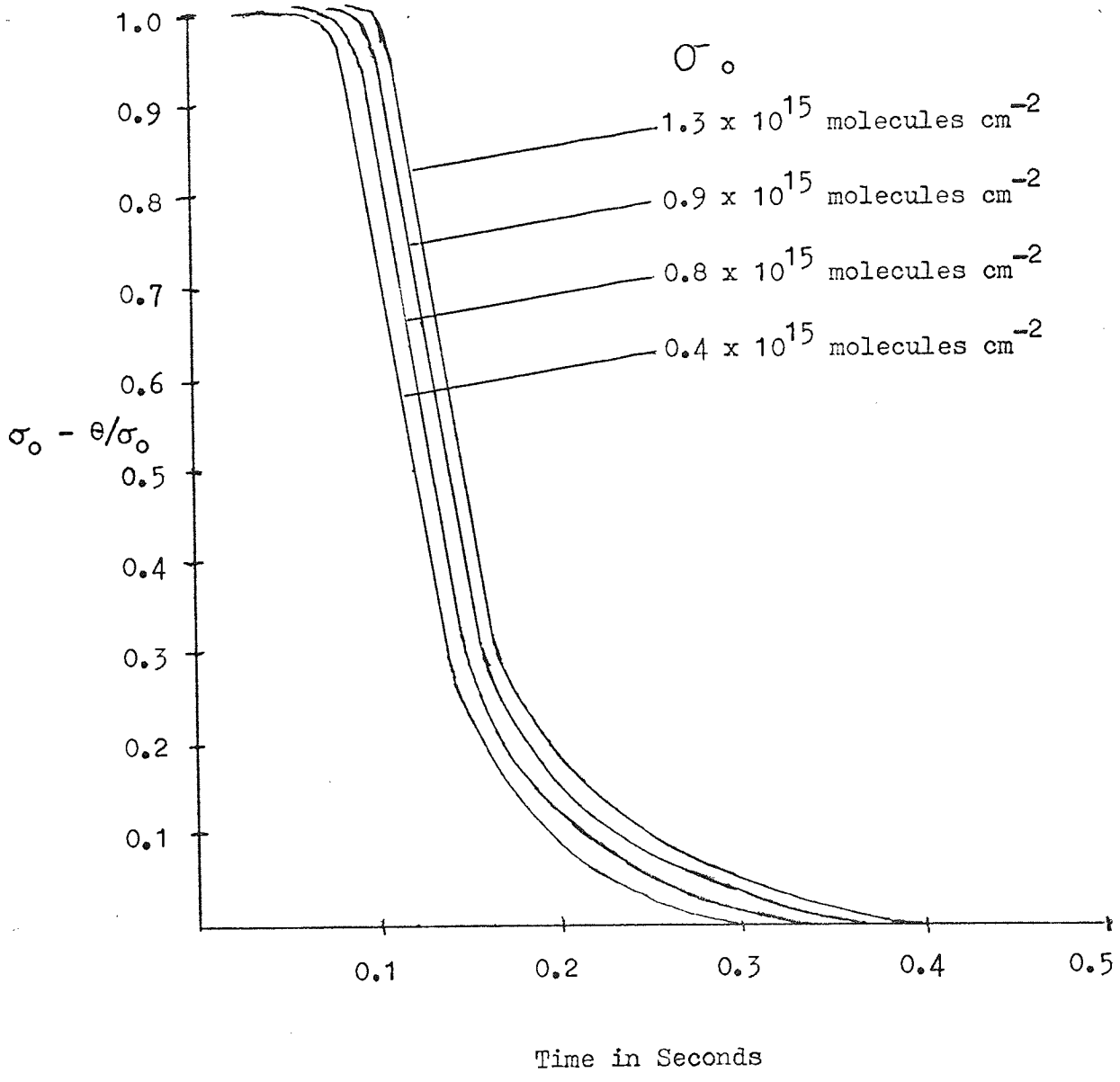

Table 28. Rate Constant at Various Constant Temperatures

Adsorption Time In Minutes	Rate Constant in cm^2 $mole^{-1}$ sec^{-1}		
	at 350 K $\times 10^{12}$	at 490 K $\times 10^{14}$	at 700 K $\times 10^{14}$
1	1.21	8.36	24.29
2	0.035	13.56	301
3	3.11	12.44	48.29
5	4.08	7.05	42.40
10	2.51	11.87	111.0
15	0.02	15.3	278
30	0.02	12.24	148
60	0.012	11.01	380

FIG. 90 Graph Used to Calculate the Activation Energy of the Reaction.

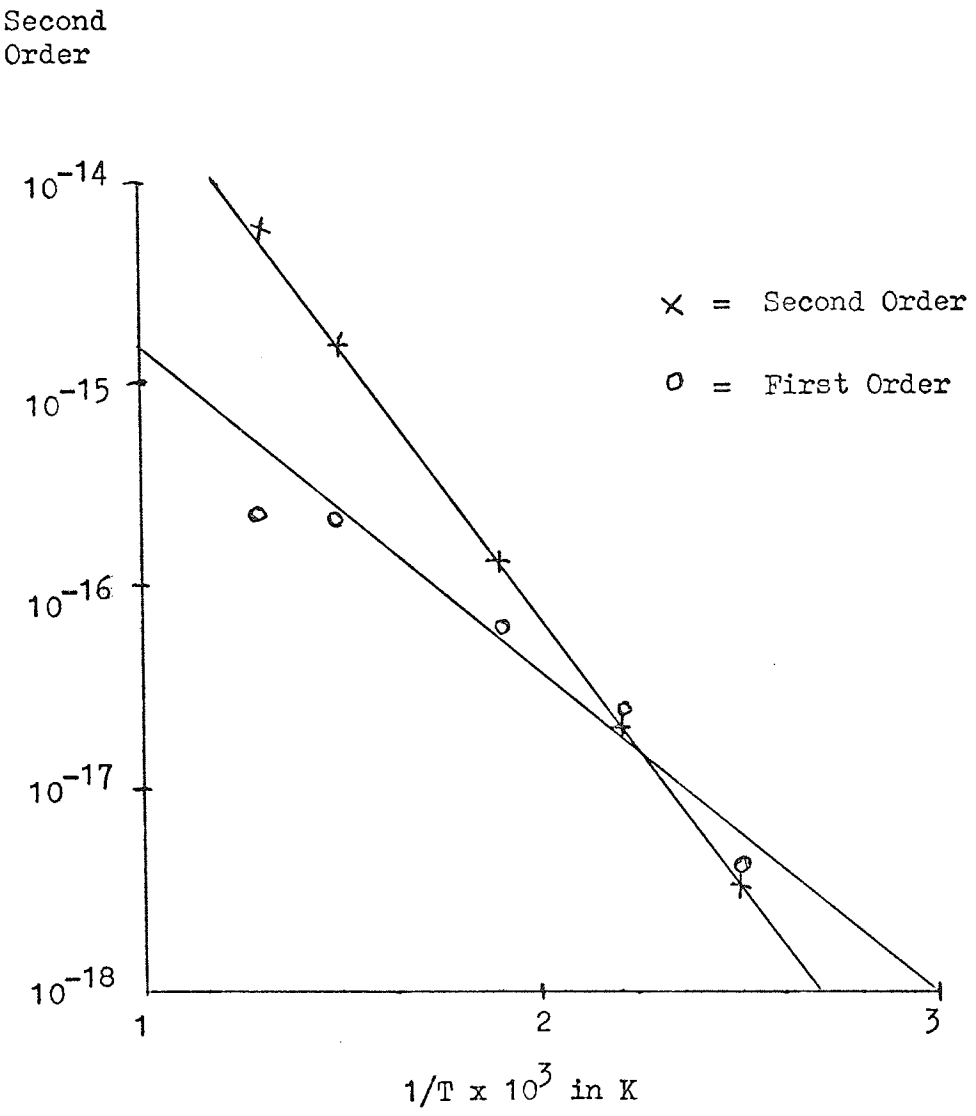

Table 29. Activation Energy Data for Hydrogen

Adsorption Time in mins	Activation Energy in k J $mole^{-1}$	maximum surface coverage in molecules cm^{-2} x 10^{-15}
1	53	0.48
2	84	0.82
3	72	0.88
5	78	0.943
10	66	0.957
15	63	1.11
30	46	1.33
60	57	1.7

to be 65 k joules $mole^{-1}$. All lay within a range of $\pm$ 20 k joules $mole^{-1}$.

The hydrogen is adsorbed rapidly and one would expect a low value of the activation energy.

By substituting the known values into the Arrhenius equation the pre-exponential function was found to be $\bar{1}0^{6}$ $molecule^{-1}$ cm^{2} sec^{-1}, a low value of the pre-exponential function. The Arrhenius equation for the reaction could be written

$$k = \bar{1}0^{6} \quad e^{-65000/RT} \qquad \ldots\ (6\text{-}2)$$

6.3.6 The Thermodynamic Parameters

The maximum of the rate of desorption curve occurred at a temperature between 450 K and 510 K. The average value was 490 K and the thermodynamic parameters are calculated at this temperature. The enthalpy was found to be 62.2 k joules $mole^{-1}$ at 490 K.

The entropy was found to be-383 joules deg^{-1} $mole^{-1}$. The ratio of the partition functions was found, using equation (4-57), to be $\bar{1}0^{20}$.

Table 30 gives a summary of the calculated parameters.

6.3.7 Mass Spectrometer Results

The products of the desorption were analysed using the quadrupole mass spectrometer. The background spectrum prior to allowing hydrogen into the system is shown in Fig. 91. The major peak is the nitrogen 28 peak. There is a small 44 peak and a series of very small peaks 12, 14, 16, 17, 18. This spectrum was taken at a pressure of 1×10^{-8} torr, the lowest which could be obtained with the mass spectrometer on the system and the attenuation on the controls was set as low as possible.

Table 30. Kinetic and Thermodynamic Parameters

ΔE_{exp}	65 k joules $mole^{-1}$
Order of Reaction	2nd
ΔH^{o}	60 k joules $mole^{-1}$
$T^{o}K$	490 K
ΔS^{o}	-383 joules deg^{-1} $mole^{-1}$
A	10^{6} $mole^{-1}$ cm^{2} sec^{-1}
k at 490	11.14 x 10^{-14} cm^{2} $mole^{-1}$ sec^{-1}
F/F^{n}_{A}	10^{20}

FIG. 91 Mass Spectra Obtained for Hydrogen I.

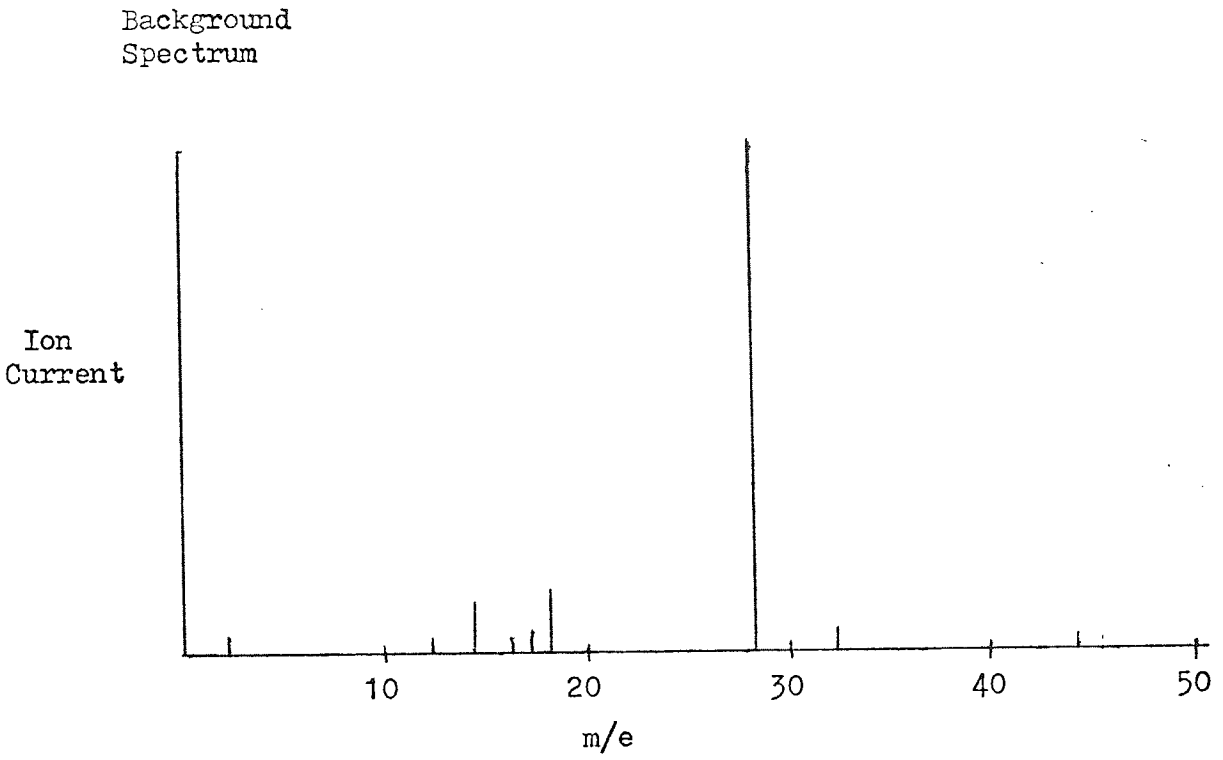

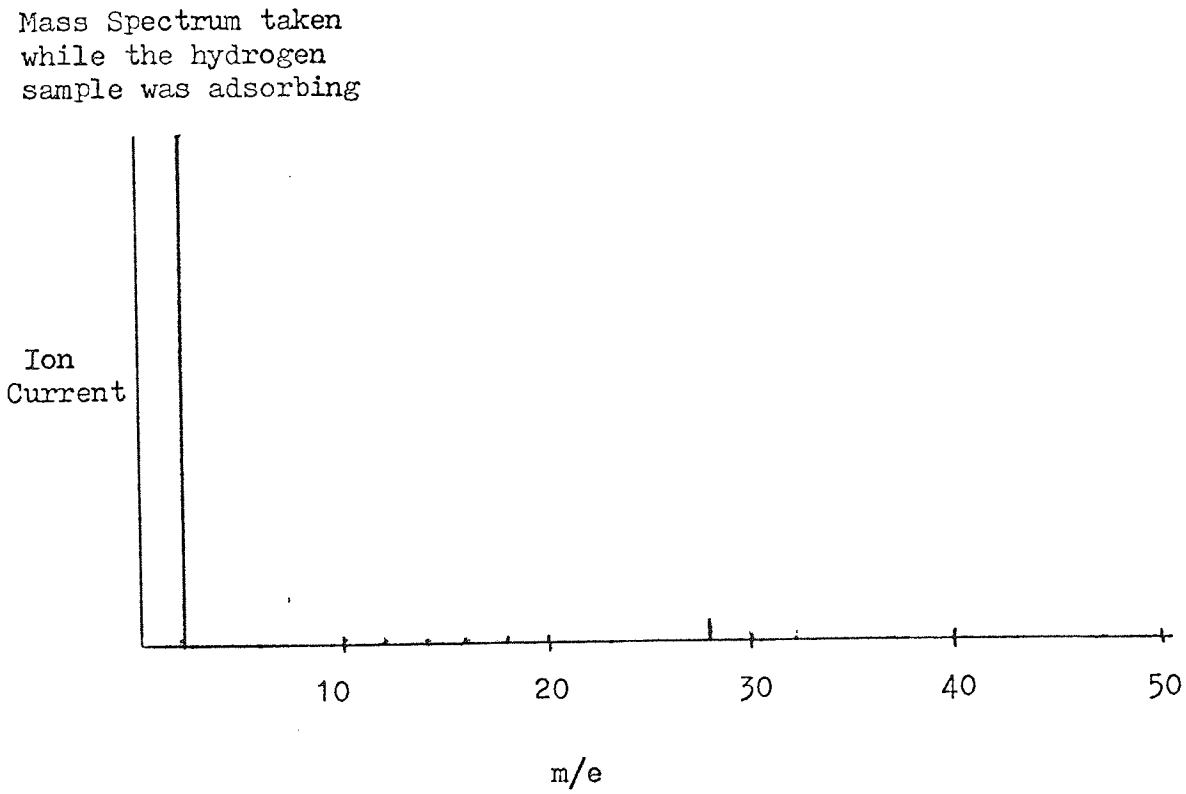

When hydrogen was allowed into the system a very large mass 2 peak was obtained and the remainder of the peaks with the exception of mass 28 were negligible. The nitrogen 28 peak could be detected but was very small. This spectrum is shown in Fig. 91 . The ratio of the two peaks was, hydrogen 70 to nitrogen 1. This gave an indication of the purity of the hydrogen being adsorbed on the surface. The percentage of impurity gases in the system was less than 2%. A spectrum was taken while the hydrogen was adsorbing and found to be identical to the spectrum in Fig. 91 .

The hydrogen gas was allowed to adsorb and the gas was allowed to pump away and another background spectrum taken. The background spectrum before the flash is shown in Fig. 92 . The hydrogen peak is greatly reduced and the background gases remain in approximately the same proportions they were in before the hydrogen was allowed into the system. No new peaks were seen and no great difference in any of the other peaks except the hydrogen mass 2.

The filament was flashed and the spectrum taken. The scan of the mass spectrometer takes a lot longer than the flash if we are to get it to record on the recorder. The leak valve between the pumps and the reaction vessel is closed and the filament is flashed. The spectrum of the hydrogen desorption is shown in Fig. 92 . The only peak which increases greatly is the hydrogen 2 peak. The height of some of the other peaks vary but not by a great amount and this may be due to the recording system. Over

FIG. 92 Mass Spectrum Obtained for Hydrogen II.

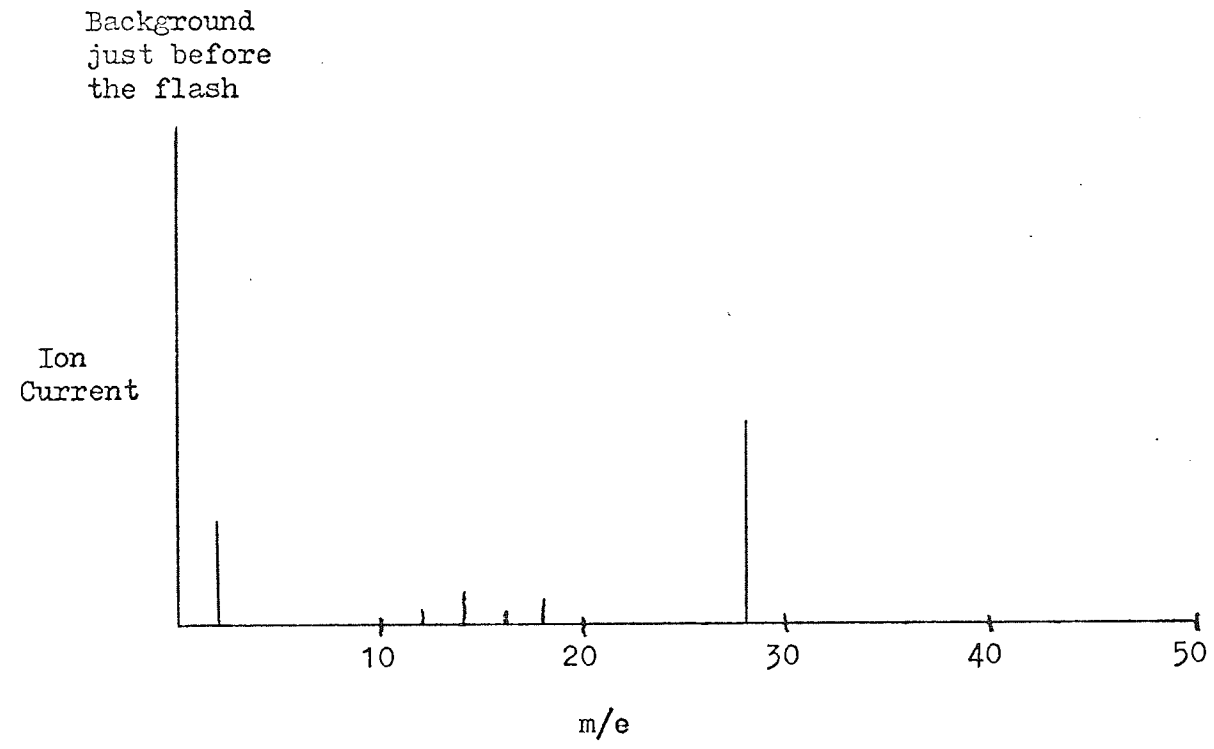

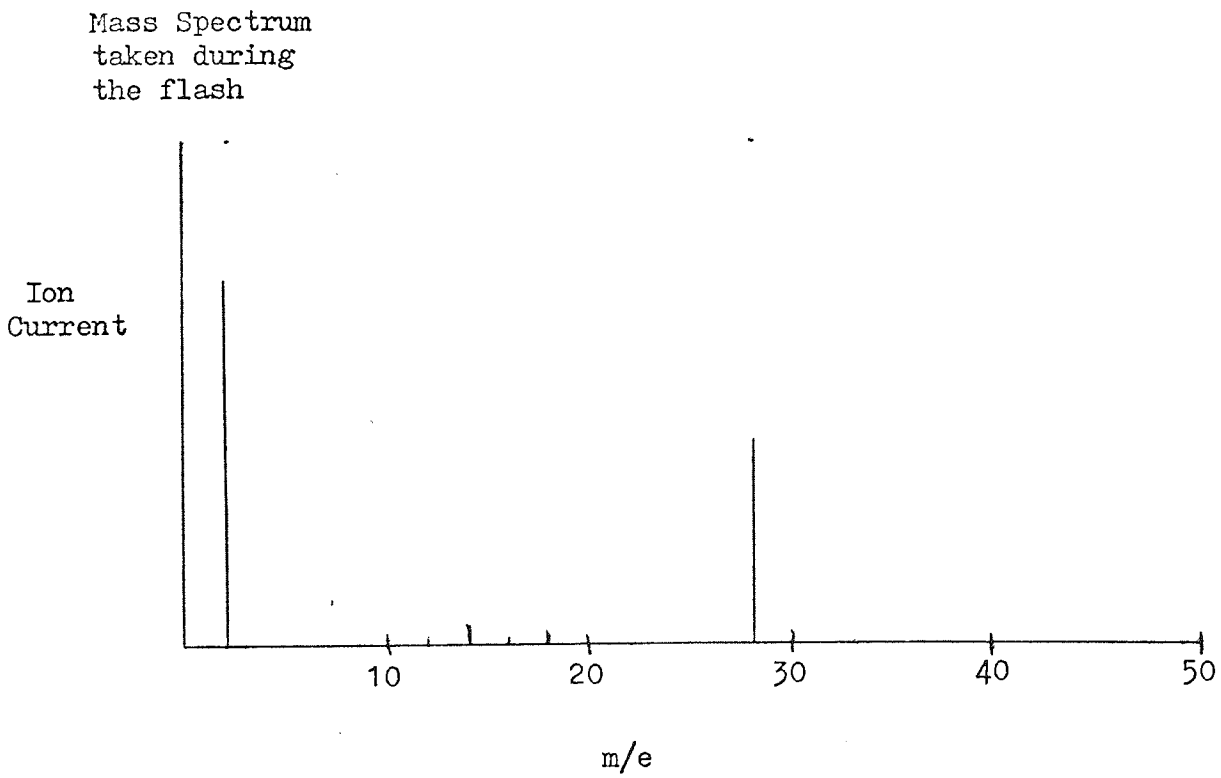

a series of scans for the same peak and pressure there was a slight variation in the heights of the peaks. Table 31 gives a list of the peaks and increase in the various peaks due to the desorption of the hydrogen. This table gives the average over a series of experiments at varying adsorption times.

Attempts were made to investigate any change in the mass 1 peak. However the mass 1 peak could not be detected and whether or not there was any change in this it is difficult to tell.

In order to obtain further information the mass spectrometer was set on a particular peak and this peak was followed through the flash. This was a very good technique since it allowed observation of the change in the peak when the temperature was raised. The mass 2 peak was followed through a flash and the result of this is shown in Fig. 93. This peak increases rapidly when the temperature of the filament is increased. Due to limitations on the minimum current obtainable extremely low temperatures below 700 K were not obtained. Other peaks were followed through the flash. The mass 28 peak being the second major peak on the desorption spectrum was followed and no change in this was seen, this is shown in Fig. 93. The change in the mass 12, 14, 16, 17 and 18 peaks were also observed but no changes could be noticed in the size of these peaks due to the flash.

Throughout the experiments only the hydrogen mass 2 peak was seen to increase. None of the other peaks increased and no very high mass peak, indicating desorption of a tantalum hydride, was seen. The mass 1 peak would have given us a lot of information about the desorbed species but the mass 1 peak could not be detected.

Table 31. Analysis of Mass Spectra for Hydrogen

Peak	Background Peak Height	Peak Height During Flash	Increase in Peak	Percentage Increase
2	5	16	11	100
14	1	1	-	
15	0.5	0.5	-	
16	0.5	0.5	-	
18	0.5	0.5	-	
28	23	22.5	-	

FIG. 93 Change of the m/e = 2 peak and m/e = 28 peak During a Flash.

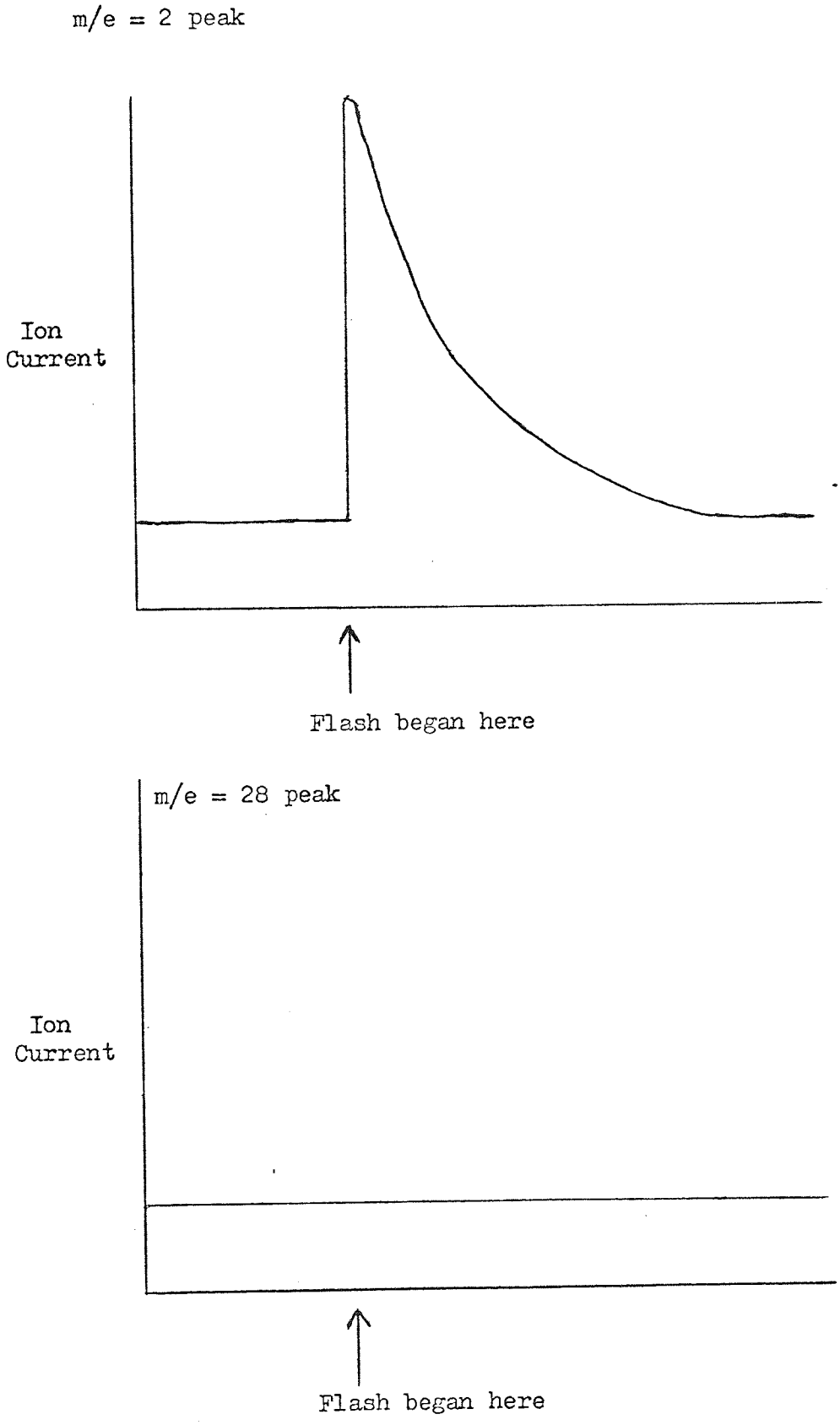

6.4 INTERPRETATION OF THE RESULTS

6.4.1 The Adsorption of Hydrogen

The hydrogen was rapidly adsorbed on the tantalum surface. This was shown by the high value of the surface coverage at low adsorption times. The value of the sticking probability was initially found to be 0.57. As the surface coverage increases this value drops rapidly as the hydrogen is quickly adsorbed and after two hours adsorption time the sticking probability is measured at 0.033. Values of the sticking probability cited by other workers are lower than the 0.57 found in the present study. Eley (105) found the sticking probability on a clean surface to be 0.17 and Eisinger 0.2 (106).

The low value of the activation energy of desorption found is a combination of the binding energy of the hydrogen and the activation energy for adsorption. The rapid adsorption of hydrogen suggests that the activation energy for adsorption is very small and in this case the binding energy is nearly equal to the activation energy for desorption.

6.4.2 Direct Observation of the Filament

The filament was analysed after the experiments using X-ray diffraction and electron microscopy. Apart from the expected changes in crystal structure on the surface the results showed the filament was tantalum. The results of direct observation of the filament for hydrogen were identical to those obtained when the filament used for the carbon monoxide experiment was analysed. The crystal structure obtained was similar to that of Lapujoulade (41) who used a nickel filament.

6.4.3 Information from the Desorption Spectrum

Only one desorption peak could be clearly seen although previous workers have found more than one peak for hydrogen desorption on other metals (107) (108). As Fig. (80) indicates the observed peak shape suggests that more than one peak was present but not resolved.

The peak was desorbed in the temperature range 300-1000 K and the rate of desorption maxima occurred at 490 K. The desorption of hydrogen from many other transition metals has been investigated. Generally more than one desorption peak was found but all the peaks were desorbed below 1000 K. Rigby (109) observed three peaks when hydrogen was desorbed from tungsten which he designated the α, β_1 and β_2. All of these peaks were desorbed between 300 and 900 K. Ageev (107) after a long adsorption time observed two poorly resolved peaks for the desorption of hydrogen from tungsten. At low adsorption times of less than three hours he observed only one peak. Yates and Madey (108) observed several weakly bound states of hydrogen on (100) tungsten but in the flash desorption spectra they could see only two major peaks.

6.4.4 Kinetics of Desorption for Hydrogen

The reaction was found to be second order. This was also found by Ageev (107), Hickmott (48) and Hansen (38) for tungsten and Lapujoulade (41) for nickel. Lapujoulade and Hansen assume that the second order kinetics mean that the hydrogen exists as atoms on the surface.

The activation energy for the desorption reaction was found

to be 64 k joules $mole^{-1}$ at the high surface coverages used. Hansen (38), Lapujoulade (41), Hickmott and Eley (105) have all found that the activation energy varies with surface coverage. The activation energy for hydrogen on nickel was found by Lapujoulade to vary linearly with surface coverage from a value of $\Delta E \simeq$ 120 k joules $mole^{-1}$ at a coverage of 10^{12} atoms cm^{-2} to a $\Delta E \simeq$ 20 k joules $mole^{-1}$ at 10^{15} atoms. A value of the surface coverage used in the present study gave $\Delta E \simeq$ 52 k joules $mole^{-1}$ from Lapujoulade's graph which is close to the 64 k joules $mole^{-1}$ measured. On a tungsten surface Eley found on a clean surface the activation energy was 263 k joules $mole^{-1}$, but this fell rapidly to a value of 92 k joules $mole^{-1}$ at a surface coverage of 0.52 monolayers.

Hansen investigated the behaviour of hydrogen on tungsten, iridium and rhodium. He assumed a linear variation of the activation energy obeying an equation

$$\Delta E = \Delta E_o - \alpha n \qquad \ldots\ (6\text{-}3)$$

where α is a constant, n the surface coverage and ΔE_o the activation energy at zero surface coverage. Hansen found for tungsten ΔE_o = 35 kcals $mole^{-1}$ and $\alpha = 28 \times 10^{-2}$ cal/mole/molecule/cm^2, for indium ΔE_o = 24, α = 14 and for rhodium ΔE_o = 18 and α = 24.

Hansen for hydrogen desorbed from tungsten found a value for the pre-exponential function of 2×10^{-3} cm^2 $molecule^{-1}$ sec^{-1}. This was in close agreement with the value of the frequency factor calculated from the two dimensional hard sphere collision theory of 3.6×10^{-3} cm^2 $molecule^{-1}$ sec^{-1}. This is also close to the value

of the pre-exponential function calculated for the desorption of hydrogen from tantalum in the present study of 10^{-4} cm^2 $molecule^{-1}$ sec^{-1}.

Lapujoulade found that the pre-exponential factor varied with the activation energy of desorption.

Using $\Delta E = 64$ k joules $mole^{-1}$ for tungsten he obtained a value $\log A \simeq -5$.

6.4.5 Nature of the Desorbed Species

The species desorbed during the flash were analysed using the mass spectrometer. The only peak in the mass spectrum which increased in height when the filament was flashed was at m/e = 2. Various peaks were tuned in and observed during the flash and efforts were made unsuccessfully to tune into the m/e = 1 peak. No high mass peaks m/e $\simeq$ 200 were found indicating that no tantalum hydrides were desorbed.

The only species detected due to desorption from the filament during the flash was molecular hydrogen. Although attempts were made no atomic hydrogen was traced.

6.4.6 Synthesis of the Results

The value of the activation energy for desorption indicates that the hydrogen is weakly chemisorbed on the surface. The hydrogen is rapidly adsorbed on the surface suggesting that it has a very small activation energy of adsorption. If this is so the activation energy for desorption will be nearly equal to the binding energy holding the hydrogen on the surface and most of the energy supplied for desorption will be used in breaking the bonds of the hydrogen with the surface.

Ageev, who used a time of flight mass spectrometer for his

work on hydrogen, has stated that it should be possible to neglect desorption of hydrogen atoms the fraction of which was less than 1%.

The mass spectrometer evidence in the present study indicates that the hydrogen is desorbed as hydrogen molecules and we have found the reaction to be second order.

Lapujoulade has shown that the entropy of activation decrease with increasing surface coverage. Considering the translational degrees of freedom on the surface he concludes that his values show that at low surface coverages both the activated complex and adatoms are immobile but as the coverage increases the adatoms become increasingly more mobile. This variation of mobility supports earlier ideas of Sweett and Rideal (110).

In the present study comparatively high values of the surface coverage were used. Lapujoulade's coverages varied over four orders of magnitude but in the present study they varied over only one order of magnitude close to a monolayer coverage. A great change in the activation energy was not observed although a small gradual trend could be seen, the value of the activation energy decreasing towards high surface coverages. To affect the value of the entropy the activation energy must change by more than a few kilojoules and so no change in entropy was found. Further work needs to be performed at lower surface coverages if the entropy change and hence change of mobility of the adatoms is to be investigated.

7 DESORPTION OF ETHYLENE FROM TANTALUM

7.1 INTRODUCTION

7.1.1 The Ethylene Sample

The experiments with carbon monoxide have given an indication of the value of the experiments and the technique. They have shown the accuracy of the experiments and given an indication of the problems expected both in using the apparatus and in analysing the results.

Ethylene was the first of the hydrocarbons to be studied. Ethylene is a simple but very reactive hydrocarbon taking part in addition and substitution reactions with other compounds. The ethylene has two carbon atoms and four hydrogen atoms and this means if it were to decompose, it could do so by several routes each one leading to different products. There is also the possibility of other reactions involving addition to the unsaturated double bond and only an investigation of the system and analysis of the products will tell by which pathway the reaction took place.

The ethylene sample was prepared by purifying cylinder ethylene. The cylinder ethylene contained impurities which were the products of the ethylene decomposing mainly along with small amounts of the other background gases. After purification it was found that the mass 28 peak was relatively much larger but also were the radicals with a mass very close to ethylene's, i.e. mass 26, 27, 29 and 30.

The ethylene sample in the bulb was at a pressure of 30 mm Hg. This ensured there was enough ethylene for several runs at various adsorption pressures.

7.1.2 The Pump Down for Ethylene

The ethylene bulb was attached to the apparatus and the apparatus purged out with nitrogen. The apparatus was checked to make sure there were no leaks and pumped down with the sorption pumps to a pressure below 10^{-4} mm Hg when the ion pump was started. The ion pump reduced the pressure into the 10^{-8} mm Hg range overnight and the apparatus was baked-out for seventy-two hours over the weekend at a temperature of 510 K. The degassing of the various parts of the apparatus made the pressure rise sharply and care had to be taken so the ion pump did not "cut out". The filament and titanium sublimation pump filaments were flashed during the bake-out.

When the heaters were turned off and the temperature returned to room temperature the pressure was in the 10^{-11} mm Hg range and a minimum pressure in the 10^{-12} mm Hg range was reached before the experiments were begun.

7.1.3 The Background Spectrum

The background spectra were taken so that the increase in pressure due to the background gases during the flash could be observed. The background spectra obtained at various maximum temperatures of the flash are shown in Fig. 94 . The background pressure begins to rise at a temperature of about 1500 K, below this there is no noticeable increase in pressure. A very low temperature flash below a maximum flash temperature of 1500 K revealed no increase in the background pressure at any adsorption time.

FIG. 94 The Background Spectra Obtained for the Ethylene Experiments.

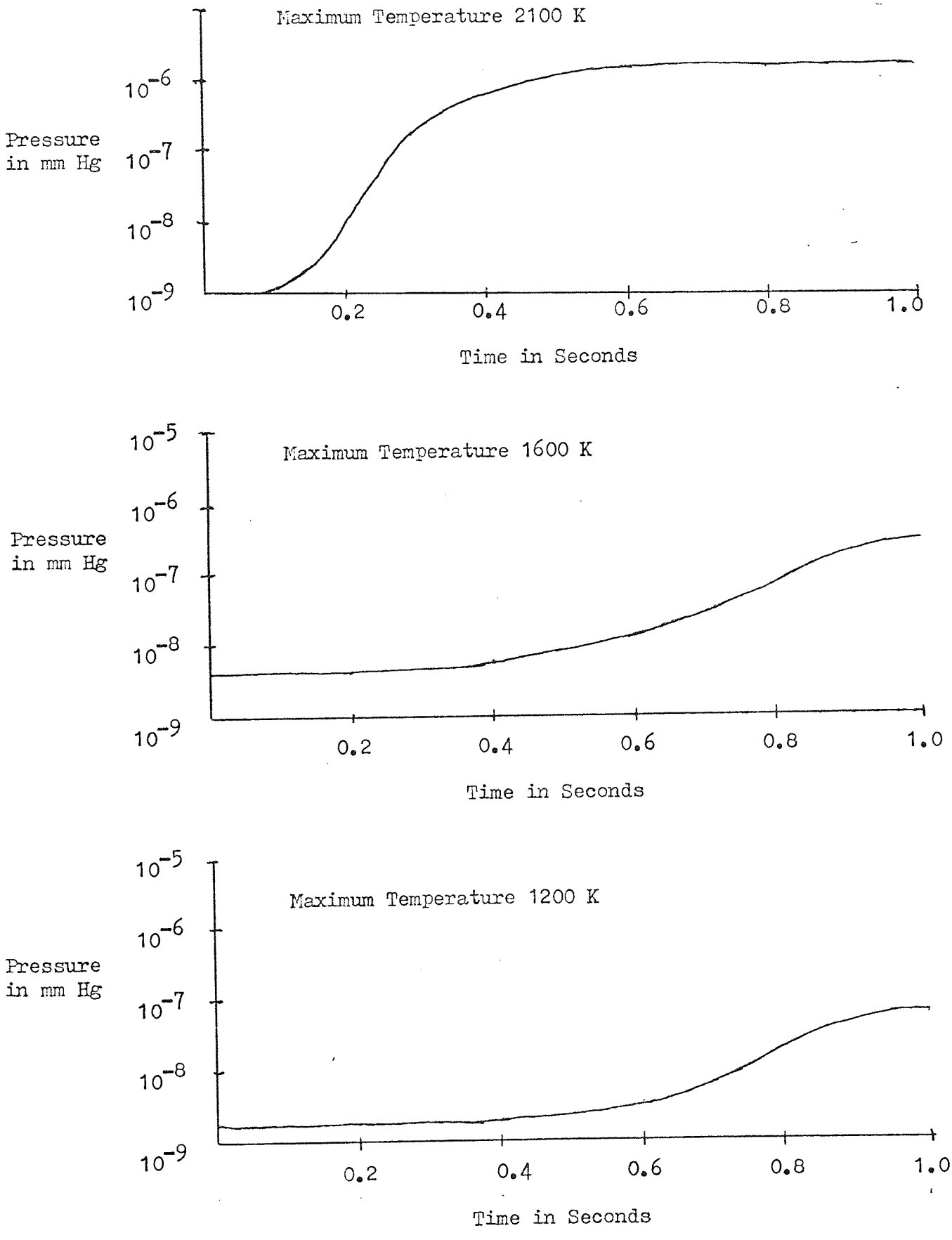

7.2 CALCULATED PARAMETERS FROM THE OSCILLOSCOPE TRACE

7.2.1 Preliminary Investigation of the Peaks

Observation of the flashes show that there is at least one peak in the desorption spectrum. This peak occurs at about 1300 K but the maximum varies slightly. The desorption traces obtained are shown in Fig. 95 . Only one broad peak is clearly seen.

7.2.2 The Temperature Rise

The preliminary photographs of the ethylene flashes show that all the desorption due to the adsorption of the ethylene gas is over when the temperature reaches 1800 K. A graph of the rise of temperature with time is shown in Fig. 96 .

A graph of temperature against pressure is shown in Fig. 97 . Since the temperature is linear with time for a large portion of the graph the pressure against temperature graph is the same shape until the maximum temperature is reached.

A table showing a typical temperature rise with time is shown in Table 32 . The temperature rises from room temperature to 1840 K in 0.6 seconds.

Flashes were performed using a maximum temperature at the end of the flash of 2200 K down to 1300 K and it was found that the best results for ethylene desorption occurred when using a maximum temperature of 1800 K.

7.2.3 The Pressure Rise

The pressure rise in this experiment is over three orders of magnitude at large surface coverages but only one order of magnitude at low surface coverages. This pressure rise gives at least one major peak and takes 0.4 seconds. A typical oscilloscope

FIG. 95 Desorption Spectra Obtained for Ethylene.

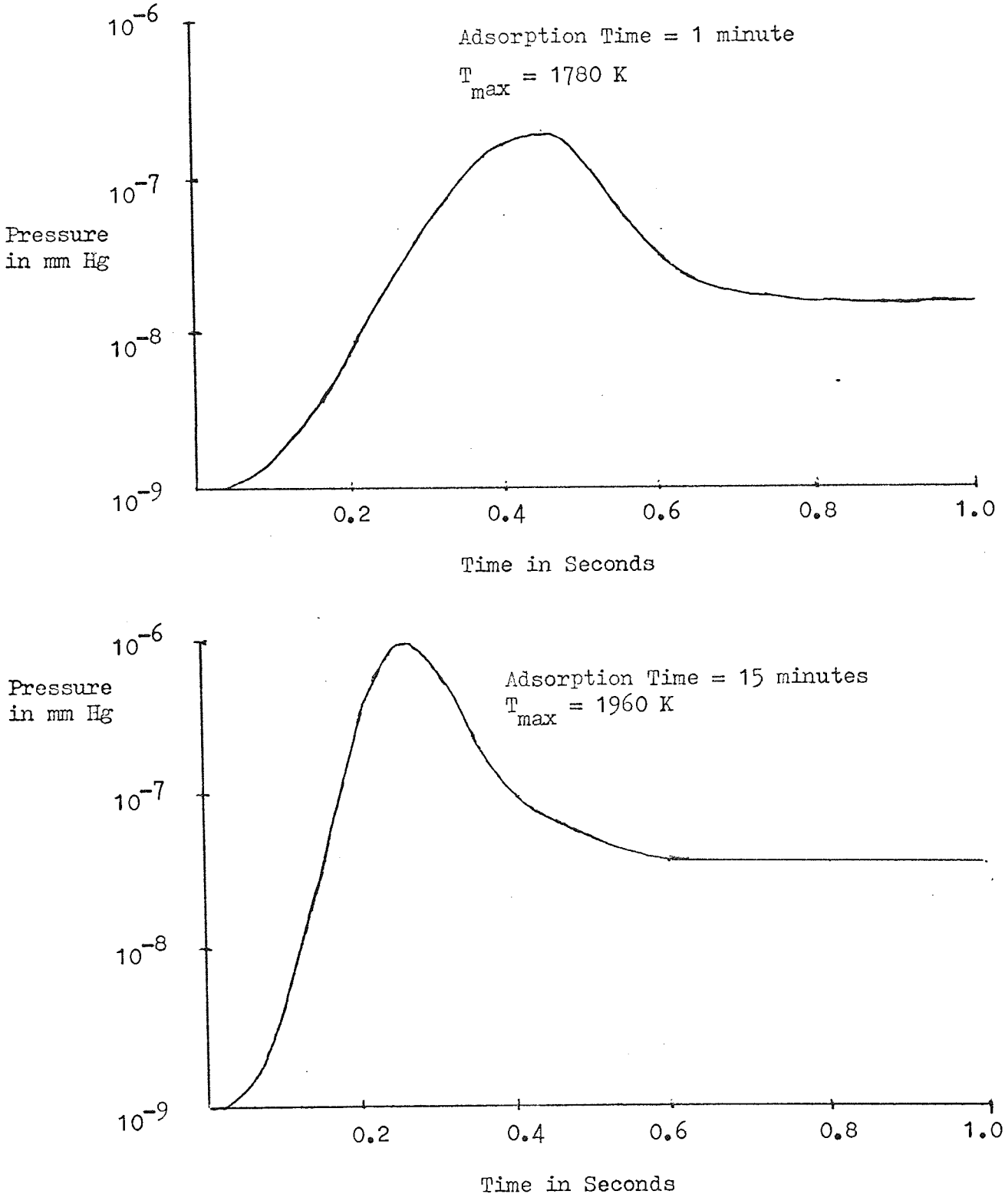

FIG. 96 A Typical Temperature Against Time Graph Obtained During the Ethylene Experiments.

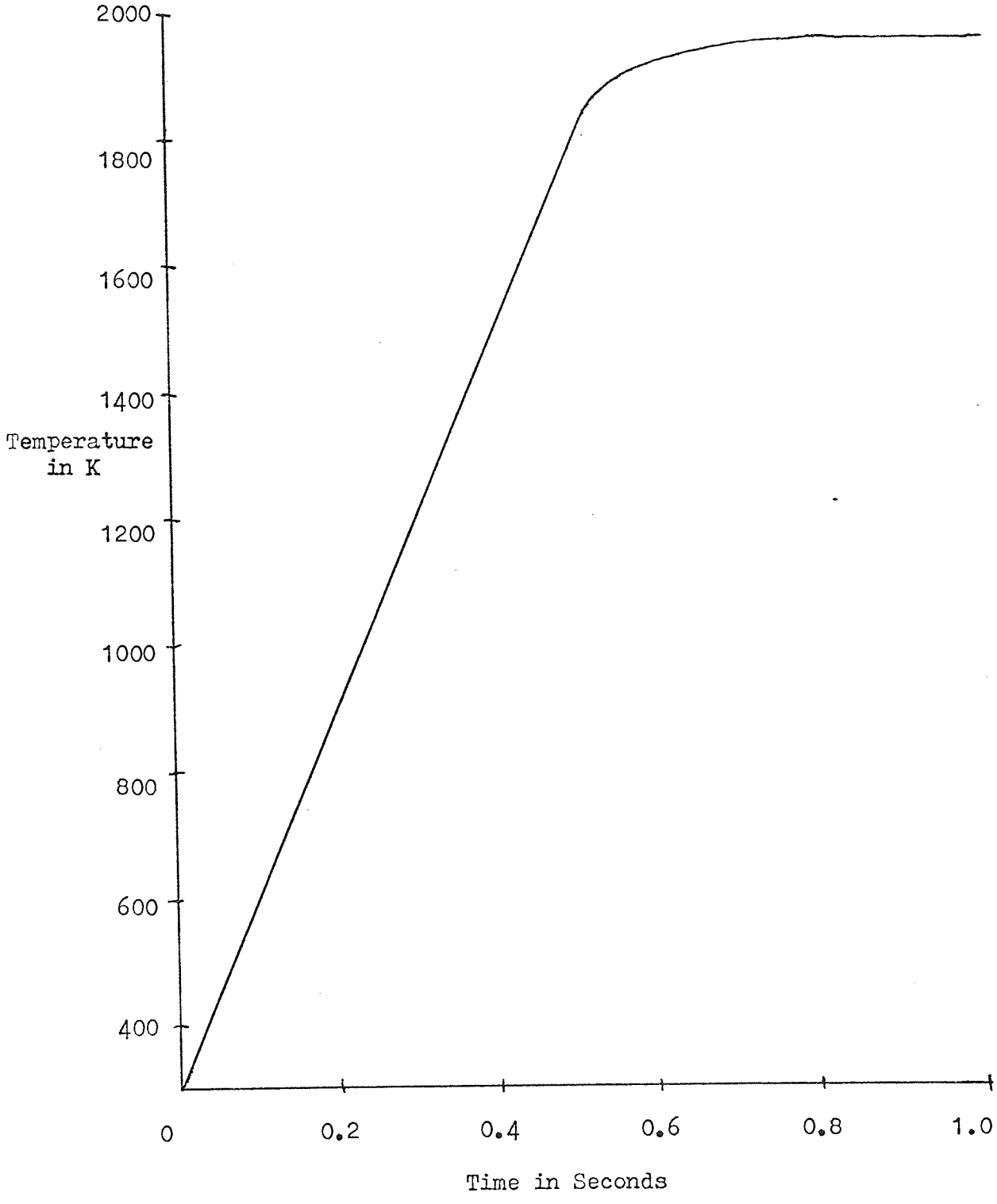

FIG. 97 A Pressure Against Temperature Curve Obtained for an Ethylene Desorption Experiment.

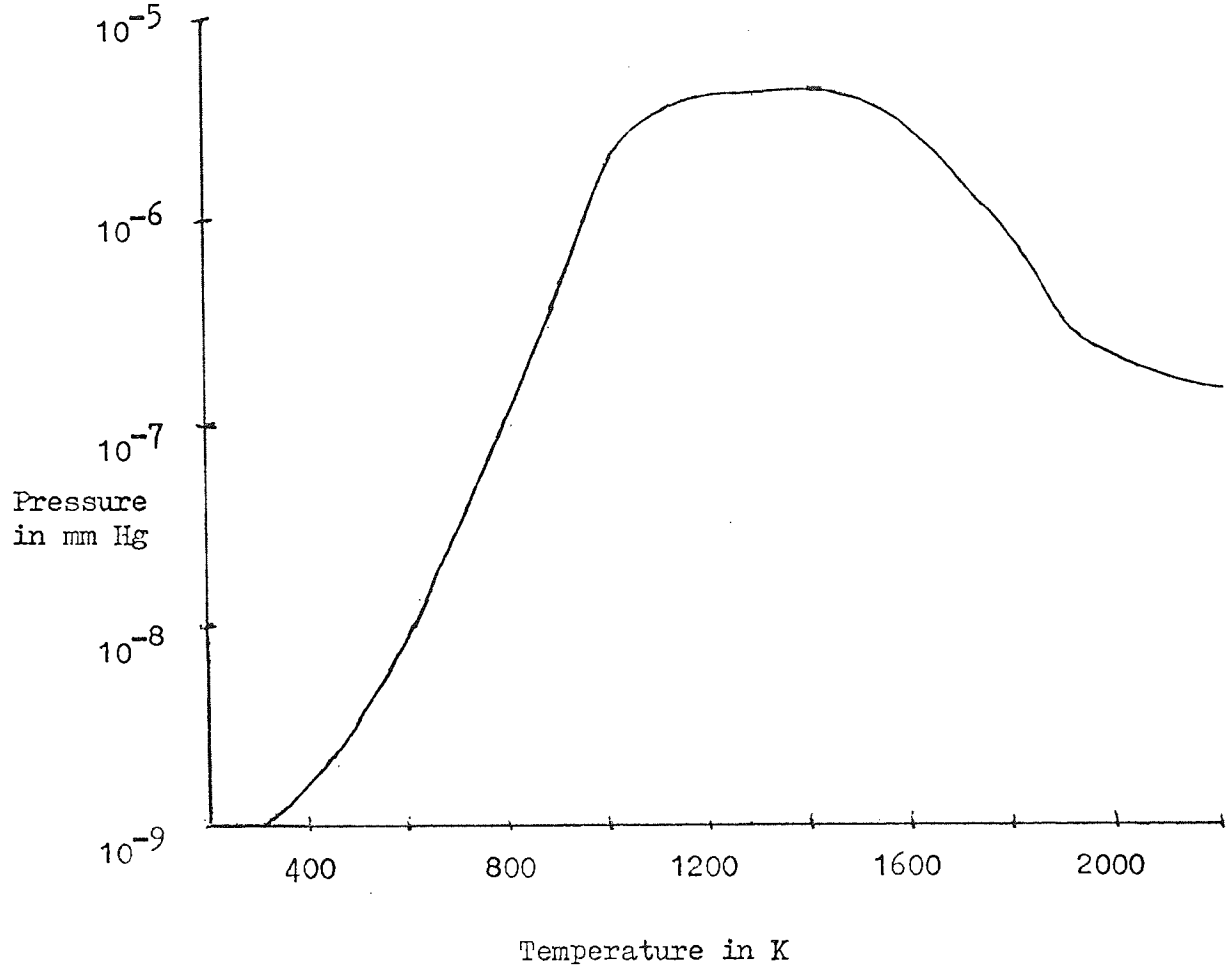

Table 32. A Typical Temperature Rise Against Time Used for Ethylene

Time in secs	Resistivity in ohm m^{-1} x 10^6	Temperature in K
0	13	290
0.04	15	330
0.08	18	430
0.12	22	490
0.16	27	610
0.20	31	725
0.24	36	870
0.28	40	990
0.32	45	1130
0.36	51	1280
0.40	56	1410
0.44	61	1530
0.48	64	1660
0.52	67	1740
0.56	68	1760
0.60	69	1830
0.64	70	1840
0.68	70	1840
0.72	70	1840
0.76	70	1840
0.8	70	1840

trace showing the increase of pressure with time is shown in Fig. 98 . Table 33 shows the increase of pressure against time together with the background pressure. The last column gives the total pressure rise due to the desorption of the ethylene only. Table 34 gives a summary of the data over a series of runs for ethylene desorption. The maximum temperature at the end of the flash varies slightly between the runs but the maximum temperature is always about 1800 K.

Throughout all the flashes only one desorption peak is seen which is desorbed over a temperature range 900 K to 1700 K. The peak of the curve occurs usually mid-way between these two temperatures.

When the temperature was reduced in order to obtain a better resolution of the peak it was found that there was still only one peak seen and if this one peak was a combination of two peaks they were so close together they could not be clearly resolved by this method.

Fig. 99 shows a graph of the total pressure rise due to the desorption of the ethylene against time. The background pressure as a percentage of the total pressure varies but at higher pressures the background correction is only roughly 1% of the total pressure.

7.3 THE CALCULATED PARAMETERS FOR ETHYLENE

7.3.1 The Rate of Desorption

Table 35 shows the values used to calculate the rate of desorption for a typical flash.

The maximum rate of desorption in this case is 3.2×10^{15} molecules sec^{-1} cm^{-2}.

FIG. 98 Oscilloscope Trace Obtained for a Typical Ethylene Desorption Experiment.

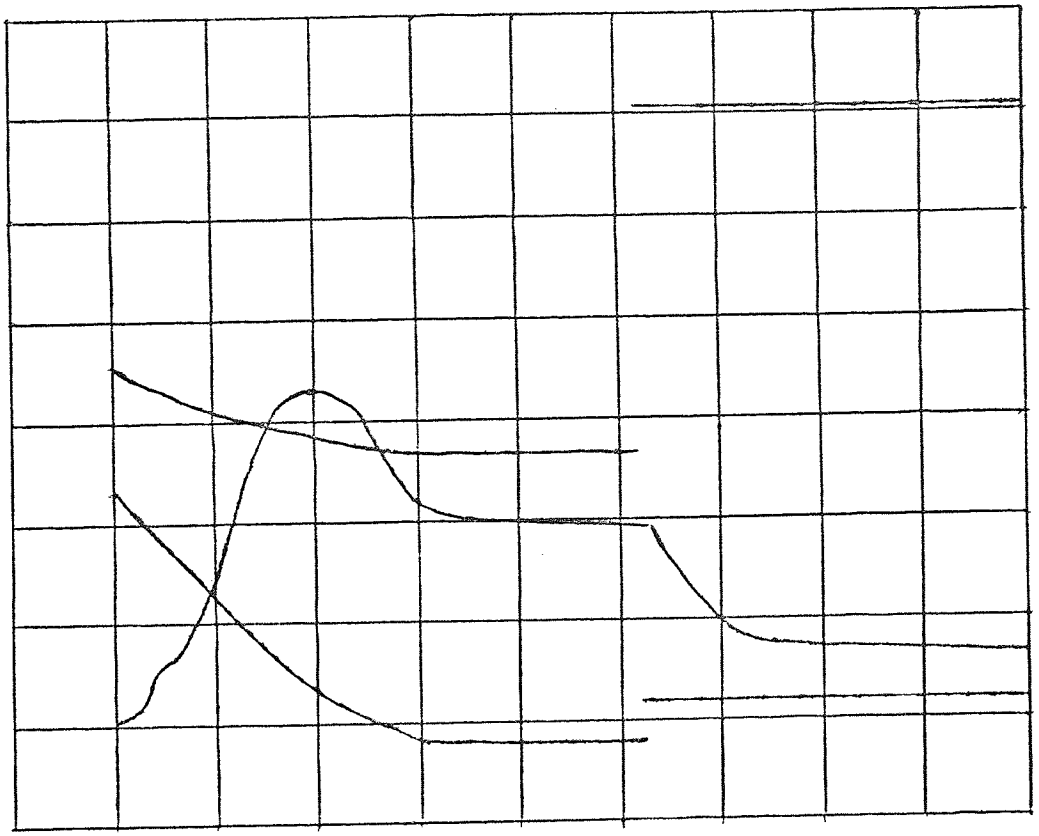

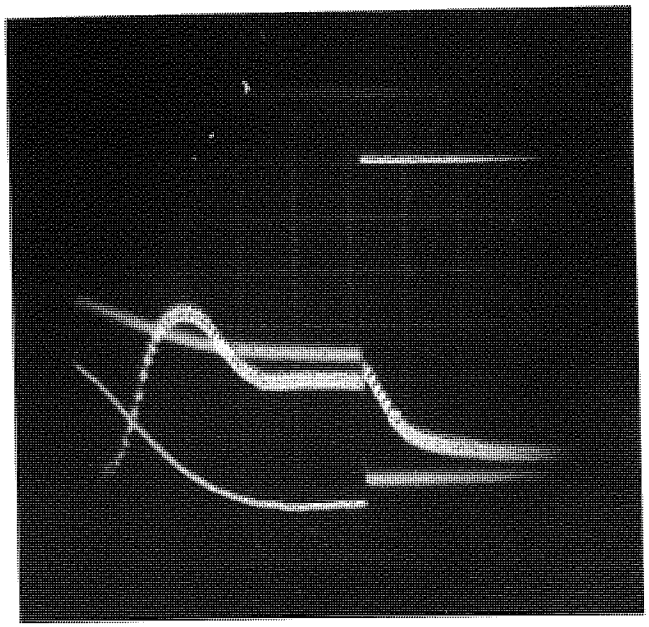

Table 33. Data for the Calculation of Pressure Rise Due to Ethylene Desorption Only

Time	Pressure $\times 10^9$ mm Hg	Background Pressure $\times 10^9$ mm Hg	Pressure Rise Due to Ethylene Desorption $\times 10^9$ mm Hg
0	1	0	0
0.04	1.2	0.2	0.2
0.08	2.2	1.2	1.2
0.12	5.6	4.6	4.6
0.16	11	10	10
0.2	57	56	56
0.24	300	299	299
0.28	1100	1099	1099
0.32	2400	2399	2399
0.36	3700	3699	3699
0.4	4000	3999	3997
0.44	3500	3499	3494
0.48	2400	2399	2383
0.52	1200	1199	1160
0.56	680	579	520
0.6	400	399	330
0.64	260	259	180
0.68	220	219	120
0.72	210	209	50
0.76	205	204	35
0.8	200	199	20

Table 34. Data for a Series of Ethylene Desorption Flashes

Adsorption Time in Minutes	Pressure max. x 10^9 mm Hg	Temperature of peak max. K	Time of peak max. in secs	Temperature max. K
1	199	1215	0.4	1780
2	270	1570	0.4	1960
3	330	1410	0.4	1840
5	580	1410	0.4	1840
10	750	1215	0.4	1780
15	999	1230	0.28	1960
30	1300	1570	0.4	1960
60	2000	1380	0.4	1840
120	2998	1380	0.48	1780
150	3999	1410	0.4	1840

FIG. 99 Graph of the Pressure Rise Due to the Desorption of Ethylene Against Time.

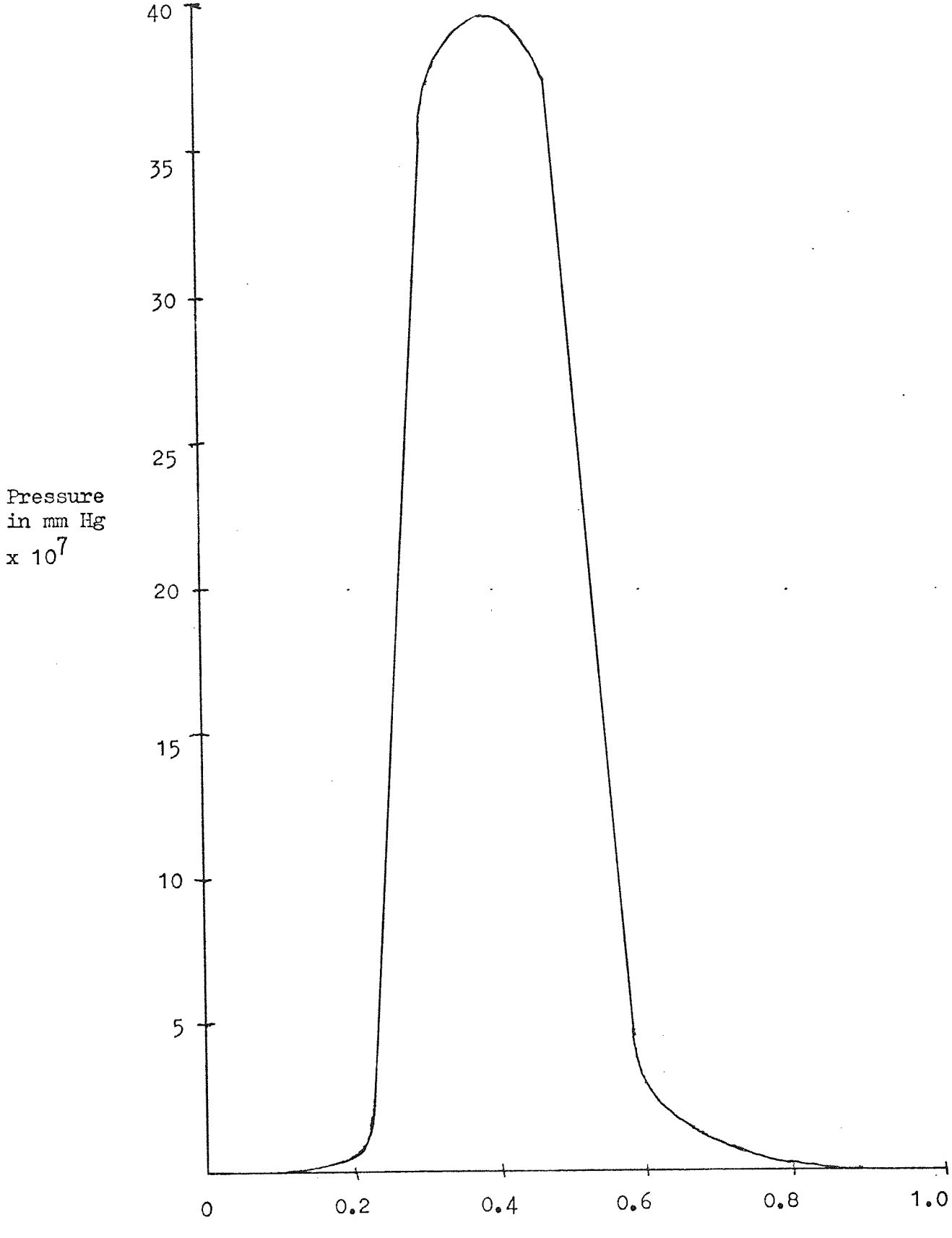

Table 35. Data for the Rate of Desorption Calculation

Time in secs	Pressure $\times 10^{8}$ mm Hg	dP/dt $\times 10^{7}$ mm Hg sec^{-1}	dn/dt $\times 10^{-8}$ molecules sec^{-1}
0	0	0	0
0.04	0.07	0.17	0.006
0.08	0.35	0.7	0.029
0.12	1.4	2.6	0.15
0.16	1.6	2.6	0.20
0.20	2.0	2.6	0.30
0.24	3.3	10	0.51
0.28	10.9	32.5	1.80
0.32	39.9	100	5.89
0.36	109.9	197	13.31
0.40	199.9	197	18.14
0.44	259.9	197	21.36
0.48	299.8	0	16.08
0.52	249.7	-250	4.00
0.56	149.6	-250	2.5
0.60	94.5	- 95	1.5
0.64	54.0	- 87.5	0.5
0.68	28.8	- 45	-
0.72	15.0	- 25	-
0.76	9.0	- 10	-
0.80	6.5	- 7.5	-

A graph of dp/dt against t is drawn in Fig. 100 . A graph of the rate of desorption against time is shown in Fig. 101 .

7.3.2 The Surface Coverage

Fig. 101 shows a graph of the rate of desorption against time which was used to calculate the surface coverage. The area under the curve was calculated and this gave the surface coverage in molecules per cm^2.

A typical set of results is shown in Table 36 . A graph of surface coverage against time is shown in Fig. 102 .

The variation of surface coverage with various adsorption time is shown in Table 37 . This shows how the surface coverage rises from 2.2×10^{13} molecules per cm^2 at one minute adsorption time up to 4.3×10^{14} molecules per cm^2 at $2\frac{1}{2}$ hours adsorption time. A graph of this variation is shown in Fig. 102 showing the increase in surface coverage against adsorption time for ethylene.

7.3.3 The Sticking Probability

The total number of collisions can be worked out theoretically and this is compared to the number of molecules on the surface and the sticking probability calculated. Table 38 shows a typical set of values.

With a clean filament there is a very high sticking probability of 0.91. This drops steadily as the adsorption time increases to 0.12.

FIG. 100 Graph of dp/dt Against Time for Ethylene.

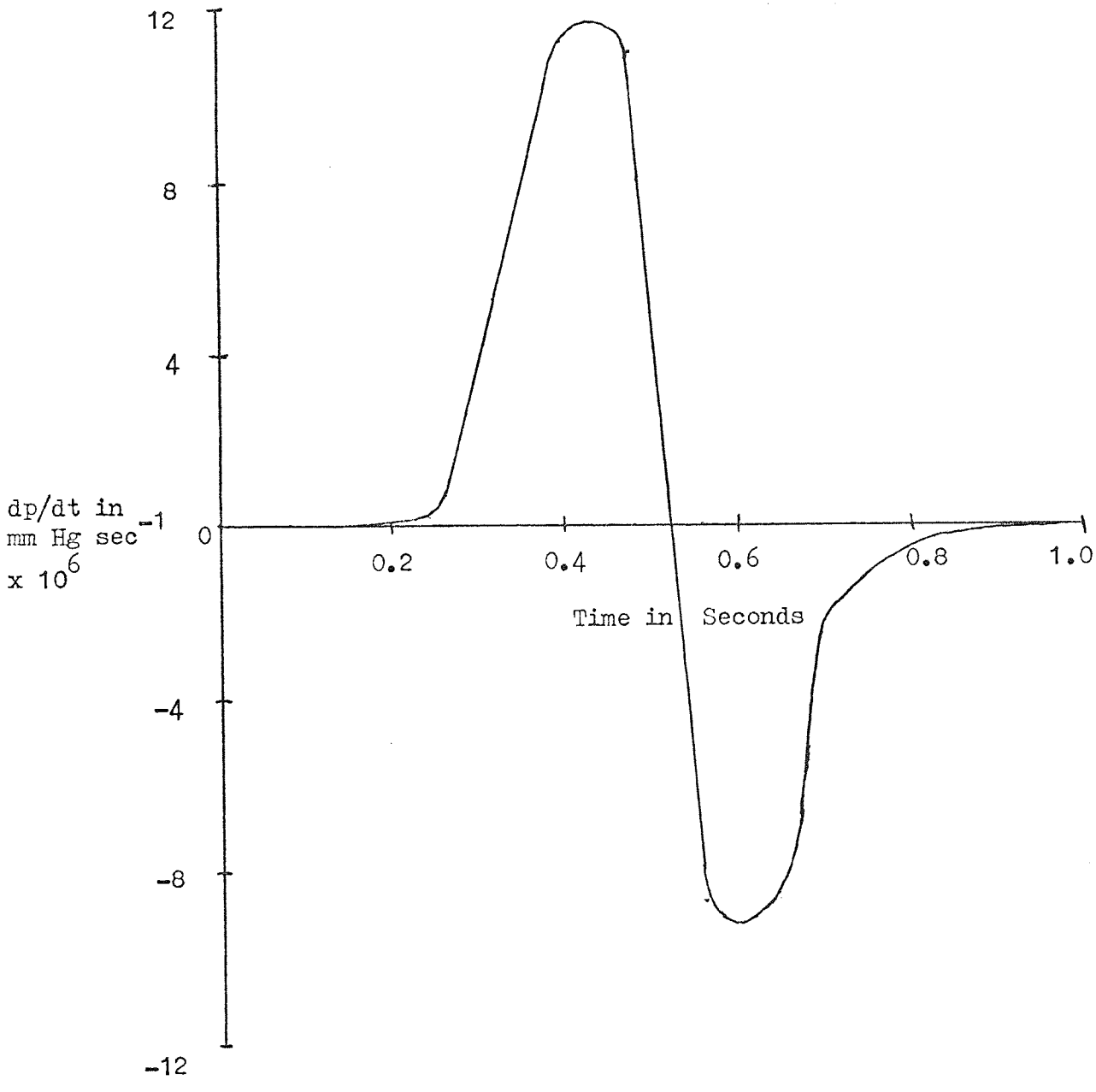

FIG. 101 Rate of Desorption Graph Used to Calculate the Surface Coverage for Ethylene.

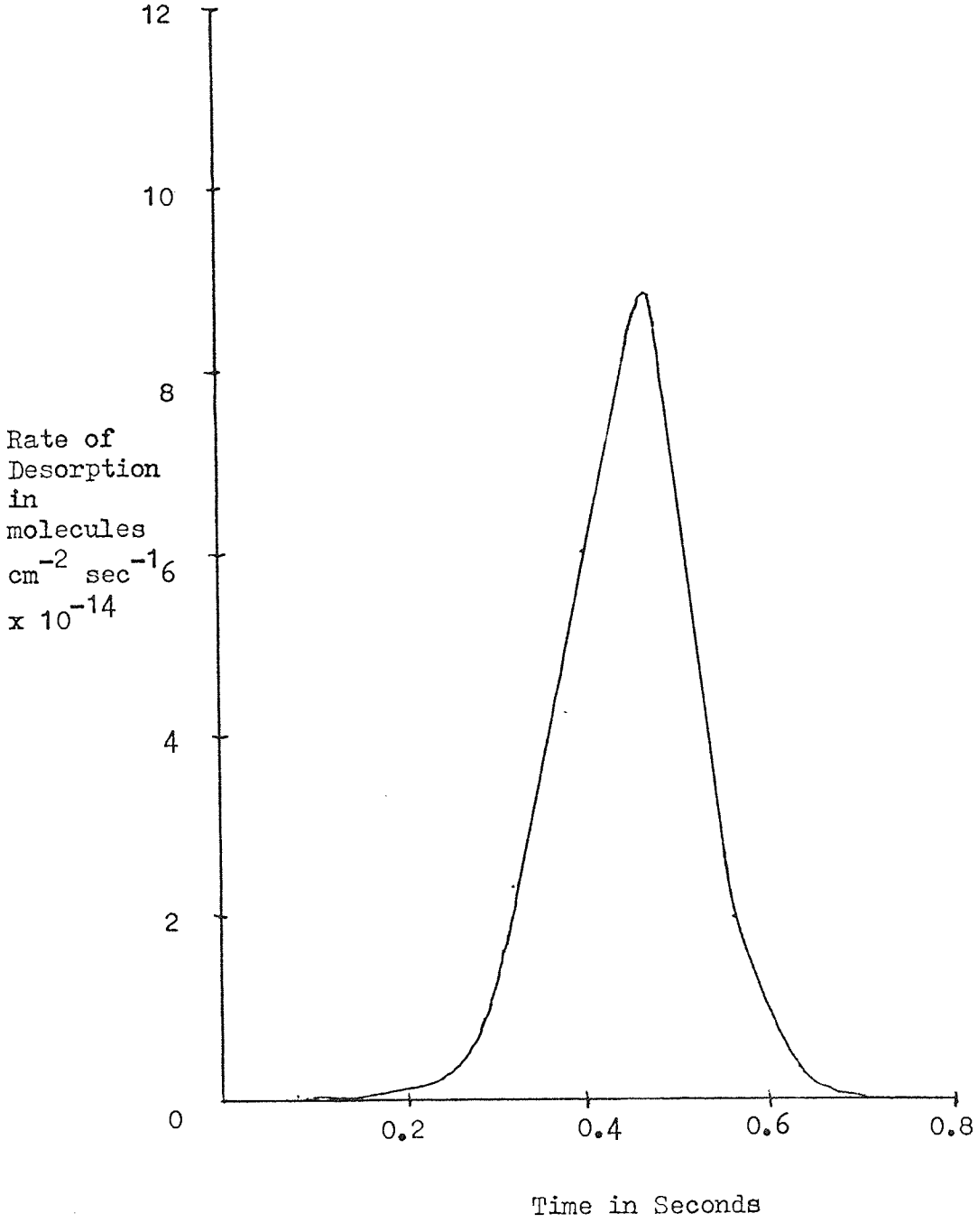

Table 36. Surface Coverage Data

Time in secs	Rate of Desorption molecules sec^{-1} $\times 10^{-13}$	Surface Coverage in molecules cm^{-2} $\times 10^{-13}$	$\frac{\sigma_t}{\sigma_o}$	Temperature in K
0.12	0.056	9.29	1	520
0.16	0.42	9.28	0.998	620
0.20	6.36	9.18	0.988	720
0.24	32.5	8.43	0.907	810
0.28	45.9	6.78	0.729	930
0.32	58.2	4.53	0.487	1030
0.36	44.8	2.28	0.245	1110
0.40	35.4	0.63	0.067	1215
0.44	1.93	0.03	0.003	1280
0.48	0.0	0.00	0	1340

FIG. 102 The Variation of Surface Coverage with Adsorption Time.

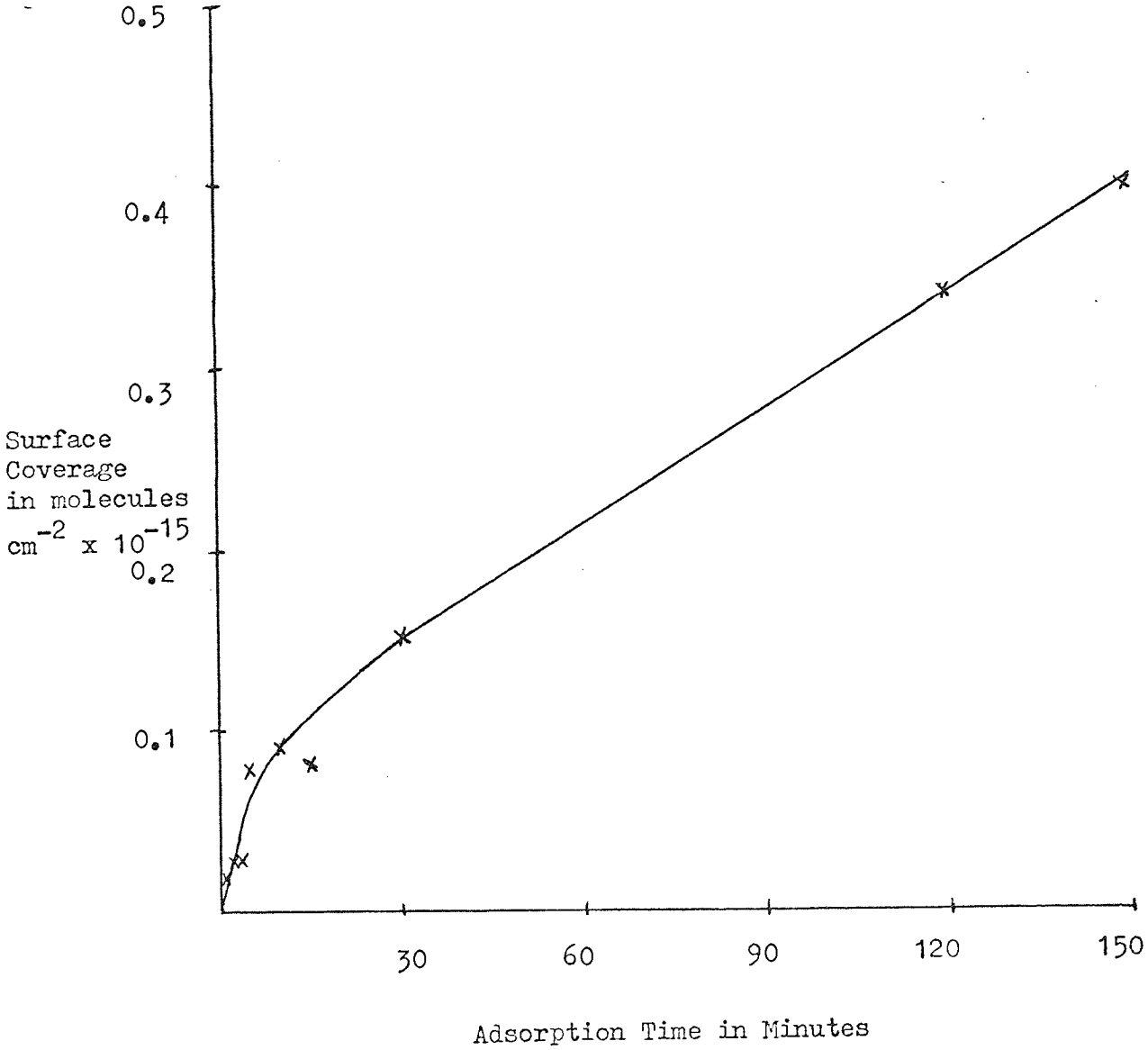

Table 37. Change of Surface Coverage with Adsorption Time

Adsorption Time in Minutes	Surface Coverage in molecules cm^{-2} x 10^{-14}
1	0.22
2	0.30
3	0.35
5	0.75
10	0.9
15	0.8
30	1.5
60	2.5
120	3.4
150	4.3

Table 38. Sticking Probability Data

Time for Adsorption In Minutes	Calculated number of Collisions $\times 10^{-14}$ molecules sec^{-1}	Surface Coverage $\times 10^{-14}$ molecules cm^{-2}	Sticking Probability
1	0.24	0.22	0.91
2	0.48	0.30	0.62
3	0.72	0.35	0.48
5	1.20	0.75	0.625
10	2.40	0.92	0.38
15	3.60	0.83	0.23
30	7.20	1.5	0.20
60	16.0	2.5	0.15
120	28.80	3.4	0.12
150	36.00	4.3	0.12

So on a clean filament the ethylene is readily adsorbed and nine out of ten collisions lead to adsorption. As the surface coverage increases and more and more sites become occupied the sticking probability drops and after two hours only one in ten collisions lead to adsorption.

A graph of sticking probability against adsorption time is drawn in Fig. 103.

7.3.4 The Order of Reaction

It would seem an easy choice to pick between first and second order reactions. However, for ethylene, graphs of log rate constant against the reciprocal of the temperature give approximate straight lines for both first and second order reactions. It is very difficult to choose using this method only. These graphs are shown in Fig. 104.

The second method to work out the order of reaction, plotting graphs of $\sigma_o - \theta_t/\sigma_o$ against time, where σ is the surface coverage, suggest the order of reaction is second order but this is not conclusive. These graphs seem to have more second order characteristics than first order. The series of graphs for ethylene are shown in Fig. 105.

From this it was concluded that the order of reaction was second order. However the proof is not conclusive so we must bear in mind that there is a chance the reaction could be first order. The experimental energy of activation was calculated using the order of reaction being second order.

Values of $(dn/dt)_t$ and σ_t were calculated at a constant temperature for a series of experiments. A graph of $(dn/dt)_t/\sigma_t$

FIG. 103 Variation of Sticking Probability with Adsorption Time.

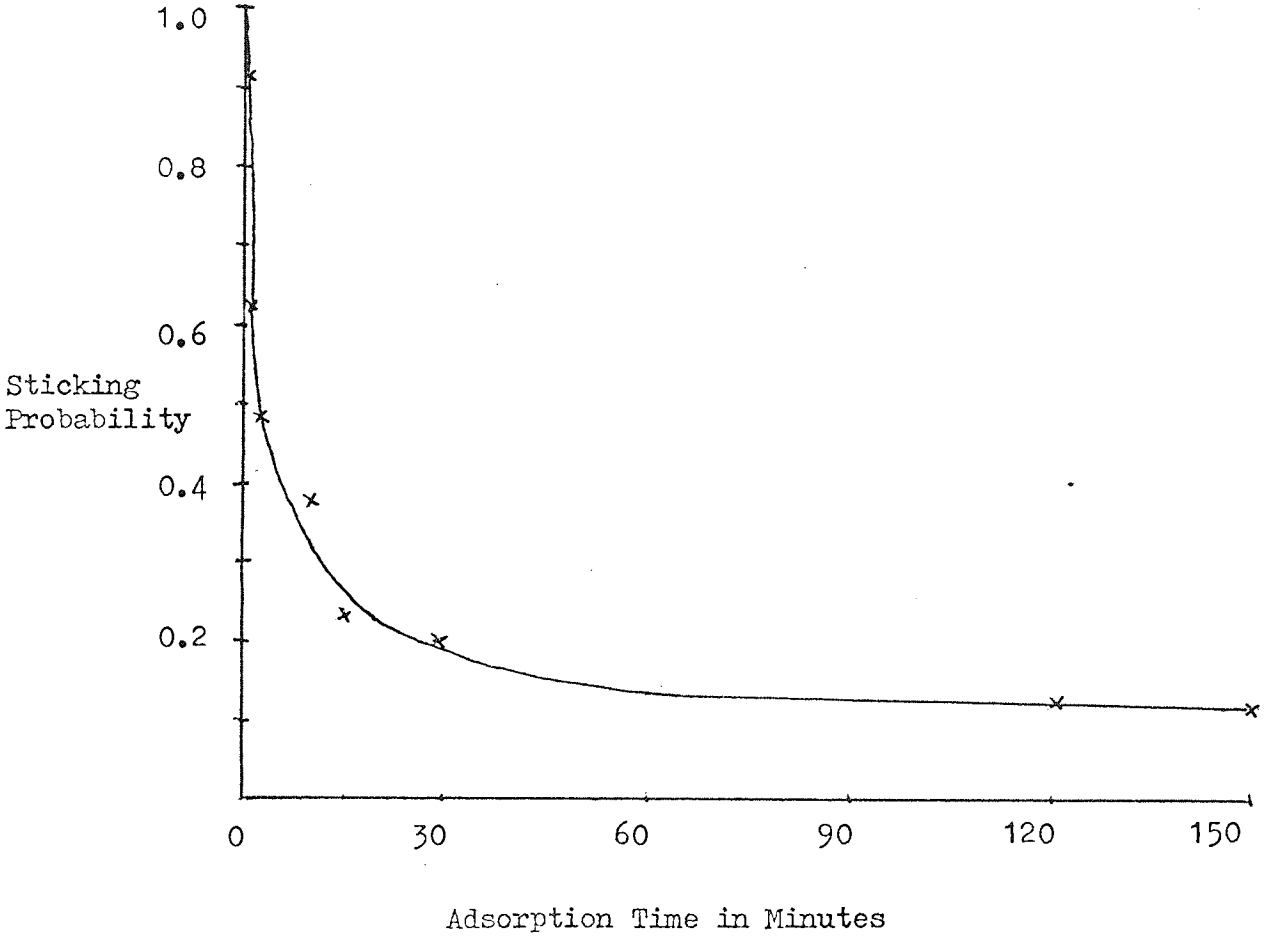

FIG. 104 Graph of Log Rate Constant Against the Reciprocal of Temperature Used to Find the Order of Reaction.

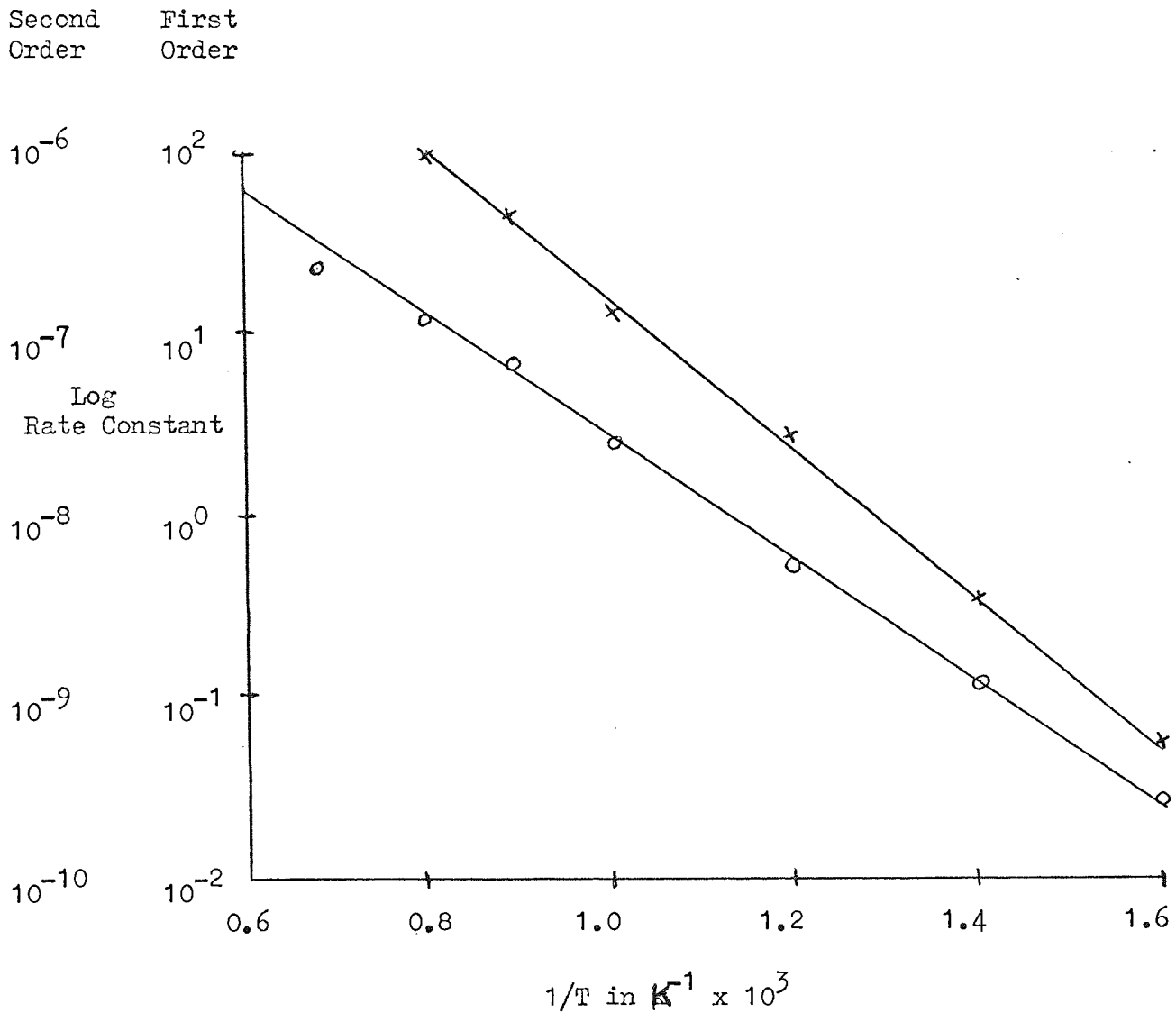

X = Second Order

O = First Order

FIG. 105 Graphs of $\sigma_o - \theta/\sigma_o$ Against Time.

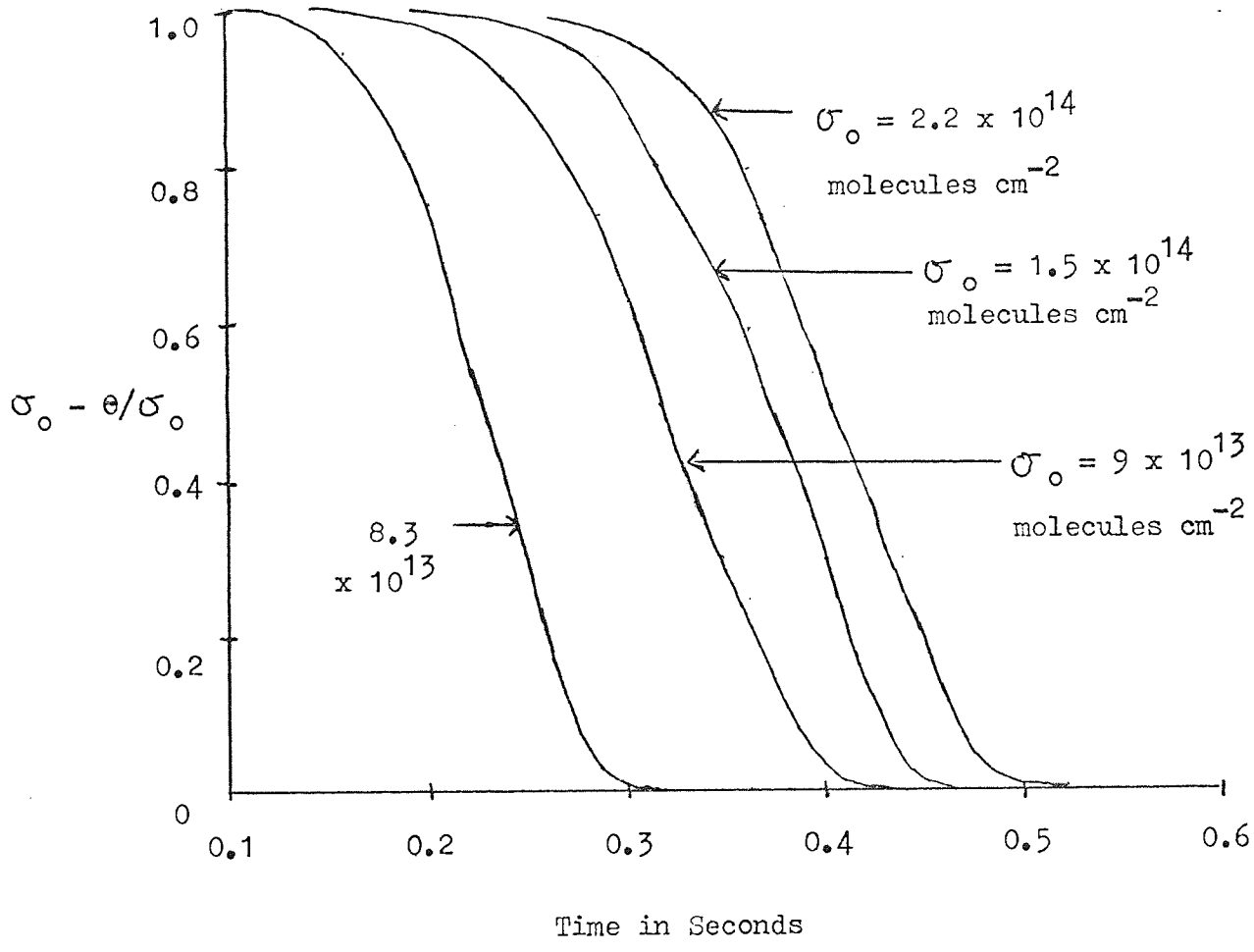

against σ_t was plotted to test for mixed order kinetics. There was some spread in the results but the graph passed through the origin suggesting that the reaction is definitely not first order. The gradient of the graph would give the rate constant for the second order reaction. This graph is shown in Fig. 106 .

A graph of the rate constant against the reciprocal of the temperature should give a straight line if the experimental energy of activation is constant and does not vary with surface coverage. A graph of the rate constant against temperature is drawn to observe the effect of temperature on the rate constant. This is shown in Fig. 107 .

For the series of experiments the rate constant should be a constant at a particular temperature and Table 39 gives a series of values of the rate constant at a constant temperature. The rate constant does vary but is constant within a reasonable experimental error.

7.3.5 The Experimental Energy of Activation

Fig. 108 shows the graph of the $\ln[(dn/dt)_t/(\sigma_o - \theta)^2]$ against the reciprocal of the temperature. The gradient of this graph is equal to the experimental energy of activation divided by R. There is a spread of experimental energies of activation over a range from 42 k joules $mole^{-1}$ to 126 k joules $mole^{-1}$ with many of the values being close to 84 k joules $mole^{-1}$. The average value is found to be 79.5 k joules $mole^{-1}$ and all the values lie inside a range expected from the error calculations.

Table 40 gives the range of experimental energies of activation together with the adsorption time at which they were

FIG. 106 Graph Used to Test for Mixed Order Kinetics.

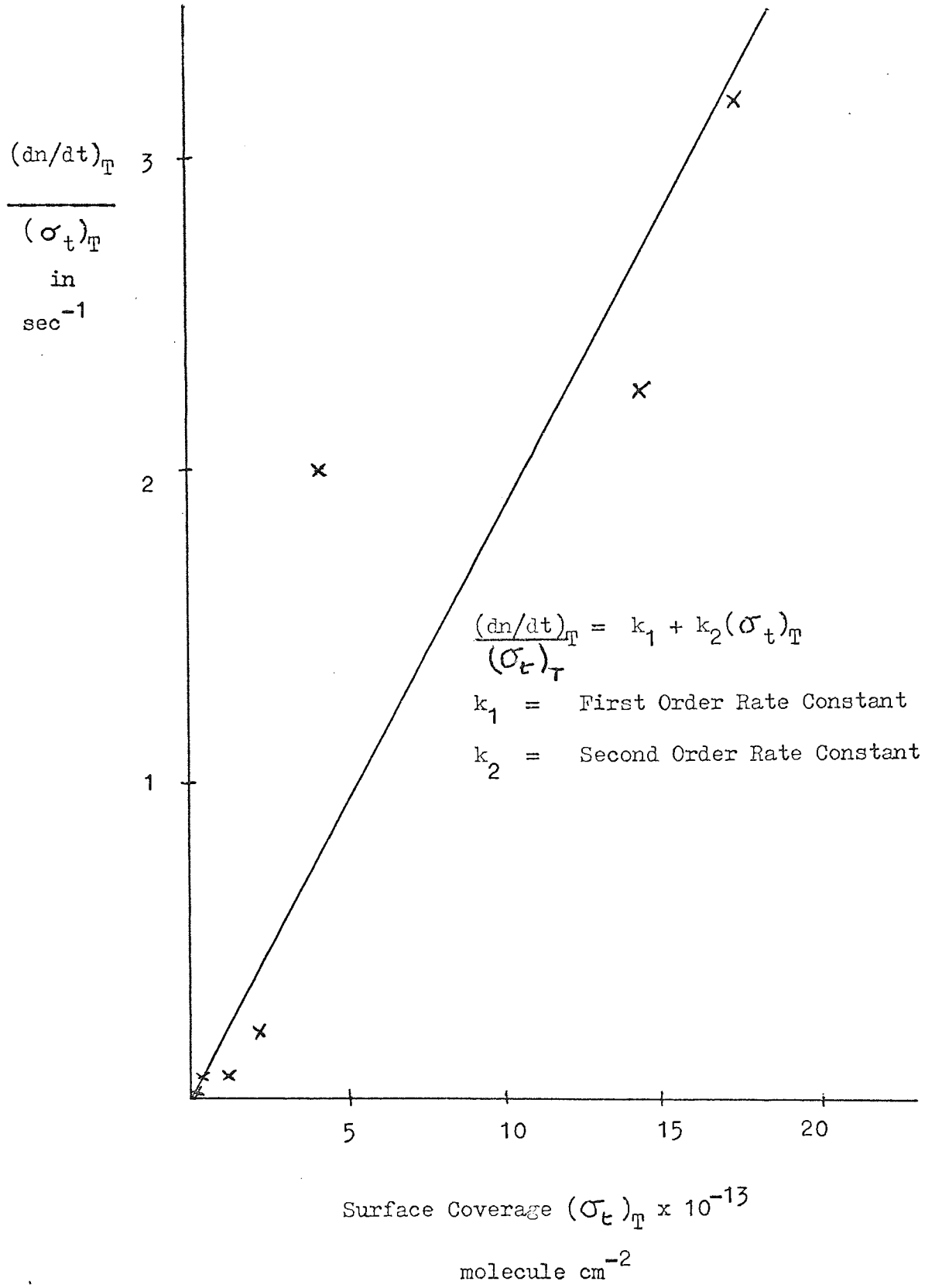

FIG. 107 Variation of Rate Constant with Temperature.

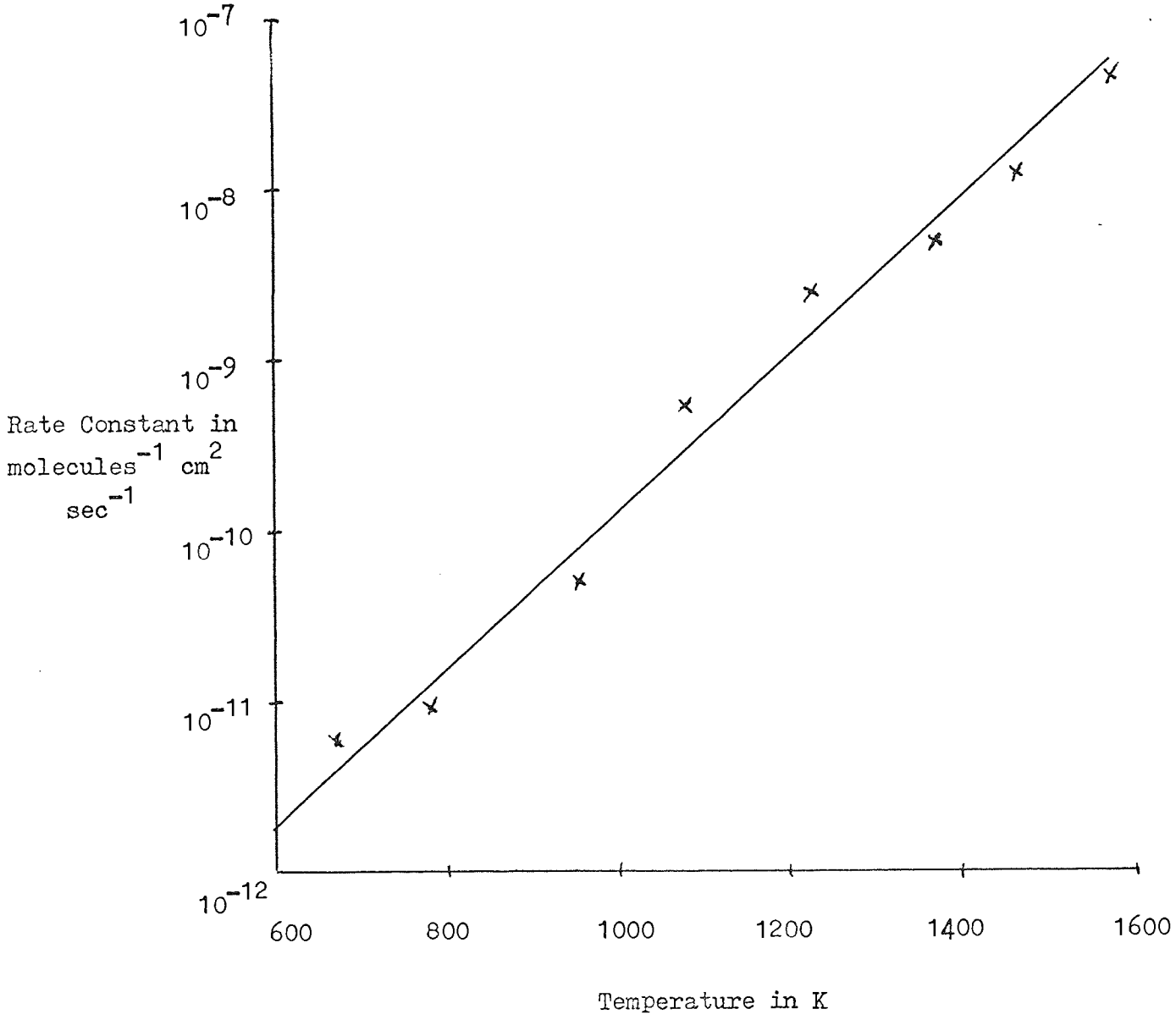

Table 39. Rate Constant at Constant Temperature for a Series of Ethylene Desorption Experiments

Rate Constant x 10^{15} in molecule^{-1} cm^{2} sec^{-1}			
600 K	1000 K	1280 K	1500 K
0.0012	0.073	5.53	142
0.0024	0.016	1.80	147
0.007	0.023	21.44	609
0.0027	0.059	0.264	1.16
0.0078	0.062	5.004	115

FIG. 108 Graph Used to Calculate the Activation Energy.

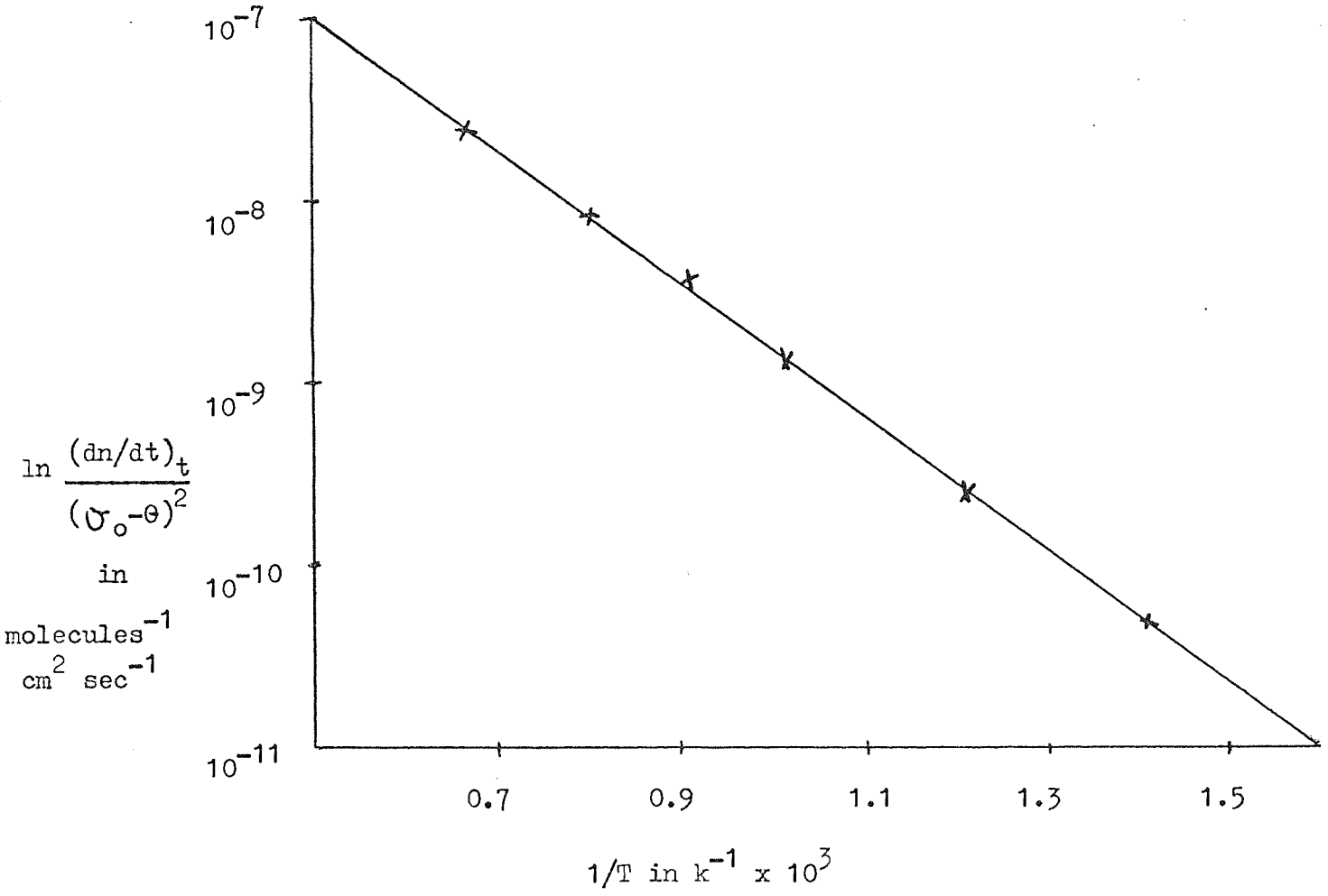

Table 40. Spread of Activation Energies

Adsorption Time in Minutes	Activation Energy in k joules $mole^{-1}$
1	85
2	79
3	88
5	55
10	96
15	78
30	82
60	80
120	92
150	54
Average = 79 k joules $mole^{-1}$ $\pm$ 13.4 k joules $mole^{-1}$	
Standard Deviation = 13.4	

obtained.

A histogram to show the spread of activation energies is shown in Fig. 109 .

The value of the experimental energy of activation is a high value for a physisorbed peak and rather low for a chemisorbed peak, however it is known some chemisorbed species have very low experimental energies of activation.

The value of the pre-exponential function in the Arrhenius equation is found by substituting in the values of the known functions. The value of the pre-exponential function was found to be 10^{10} cm^2 $molecule^{-1}$ sec^{-1}.

The generally accepted value of the pre-exponential function for the Arrhenius equation is 10^{13}. This is close to the value obtained. The Arrhenius equation for this reaction at a temperature of 1280 K is

$$k = 10^{10} \quad e^{-79500/RT} \qquad \ldots\ (7\text{-}1)$$

7.3.6 Thermodynamic Parameters

The temperature at which we consider the reaction to take place is the temperature where the rate of desorption is maximum. A survey of the experiments show that there is a spread of temperatures between the experiments but most give a temperature close to 1300 K and the average value of all the values is 1280 K. This is the temperature at which we will consider the reaction to take place.

The enthalpy is calculated by substituting the known values into the standard thermodynamic equation. This gives

$$78540 = \Delta H^{\circ} + 9840 \qquad \ldots\ (7\text{-}2)$$

A value of the enthalpy of 67859 joules $mole^{-1}$.

FIG. 109 Histogram Showing the Spread of Activation Energies.

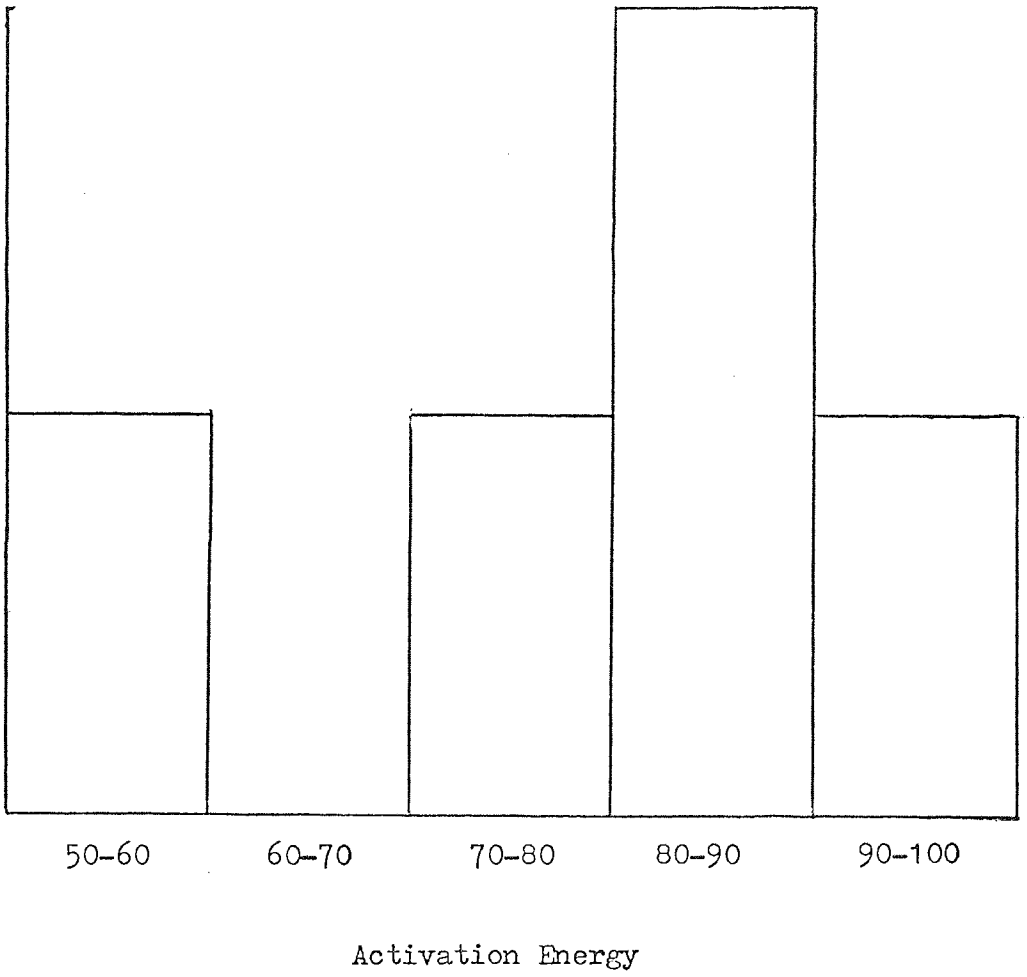

By substituting the known values into the equation the entropy of the reaction can be calculated. This gives a value for the entropy of -475 J deg^{-1} $mole^{-1}$. This value can now be used in equation (4-57) and the ratio of the partition functions found.

$$\frac{F'}{F_A^n} = e^{-475/8\cdot3\cdot2\cdot3} \quad \ldots\ldots (7\text{-}3)$$

the ratio of the partition function is

$$\frac{F'}{F_A F_B} = 10^{-25} \quad \ldots\ldots (7\text{-}4)$$

~~This suggests that the mobility of the activated complex is very similar to the mobility of adsorbed species on the surface.~~

The free energy of ACTIVATION was found to be 50 k joules $mole^{-1}$.

Table 41 gives a summary of the calculated parameters for the ethylene experiments.

7.3.7 Mass Spectrometer Results

The vacuum system was purged and pumped down and a background spectrum obtained. This is shown in Fig. 110. There is a large background peak at 28 which is due to the "boiled off" nitrogen with which the system was purged. Other peaks were seen at 12, 14, 15, 16, 18, 20 and 44. The largest of these smaller peaks prior to allowing the ethylene into the system was the 18 peak but this was only a quarter the size of the nitrogen 28 peak.

Table 41. Summary of Calculated Parameters

T_o	1280 K
Order of Reaction	2nd
Enthalpy	67.8 k joules $mole^{-1}$
Activation Energy	79 k joules $mole^{-1}$
A Factor	10^{-12} cm^2 $mole^{-1}$ sec^{-1}

FIG. 110 Mass Spectra for Ethylene I.

Background Spectra of the Clean System

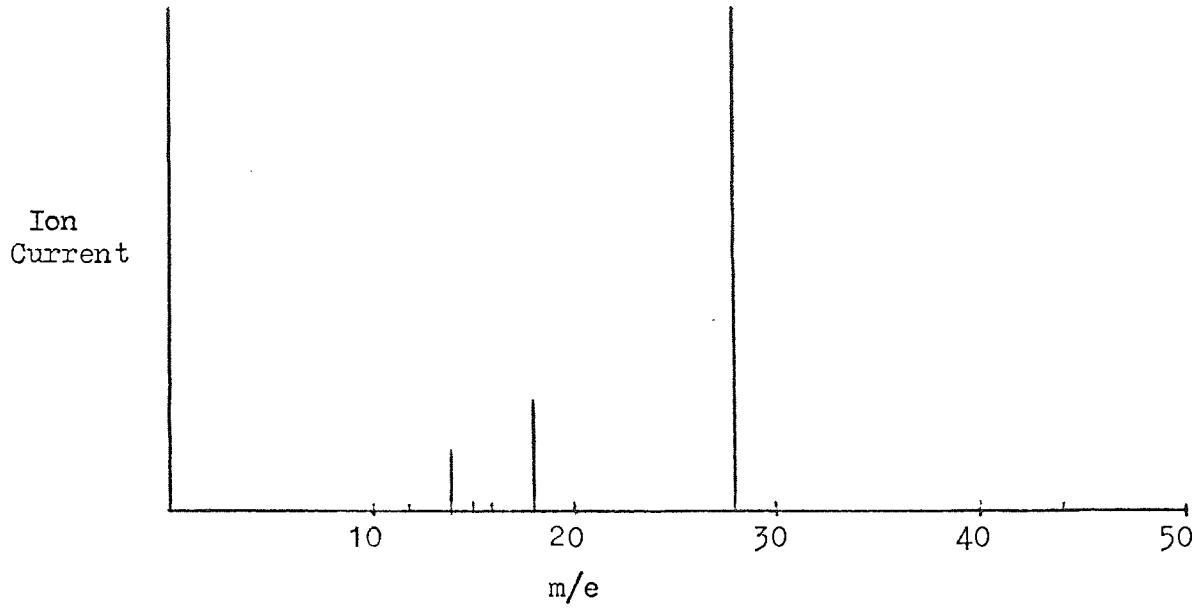

Mass Spectrum While the Ethylene was Adsorbing

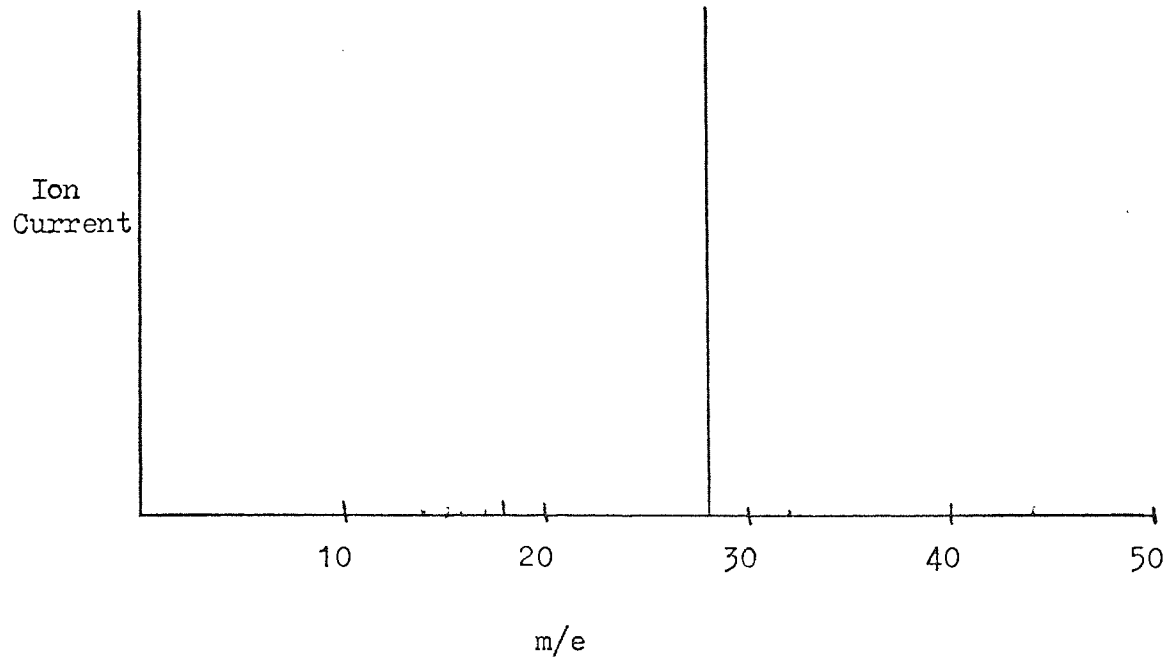

The spectrum when the ethylene sample was allowed into the system is shown in Fig. 110. Table 42 gives a summary of the increase in each of the peaks. The peaks which increased are the 2, 12, 14, 15, 16 and 28. These peaks are from ethylene and the fragmentation of the ethylene into C, CH_2, CH_3 and CH_4. The 28 peak was due to the ethylene C_2H_4 but part of it would be due to the nitrogen in the background and possibly some carbon monoxide. The mass spectrometer was not sensitive enough to resolve these three compounds, all of which have an atomic mass of 28. The very large MS9 mass spectrometer which was used to analyse the sample after purification was able to distinguish between these three peaks.

Prior to the flash the gas is pumped out of the system and a background spectrum obtained. This is shown in Fig. 111.

When the system is flashed there is an increase in the mass 2,14, and 16 peaks. This is shown in Fig. 111 and a summary of the increases is shown in Table 43. Also the data from a second run is shown in Table 43. The major increases are in the mass 14 and 15 peaks. The mass 28 peak also increases but the mass 28 peak was initially large and the percentage increase in the peak is only 3 units in 30 units, a relatively small rise compared to the 14 and 15 peaks. The hydrogen mass 2 peak increases by a small amount.

No peaks at 26, 27 and 29 were detected in the mass spectrum even though when the ethylene was analysed on a more sensitive mass spectrometer these peaks were found. The peaks which were observed to increase were the 14 and 15 peak. The 14 peak was probably due to dissociation of ethylene into two CH_2^+ radicals.

Table 42. Mass Spectrometer Data Taken While Ethylene Sample is Adsorbing

Peak	Background Peak Height	Peak Height During Flash	Increase in Peak	Percentage Increase
2	4	5	1	0.1
12	1	5	4	0.5
14	4	90	86	14.2
15	1	5	4	0.5
16	5	10	5	0.6
17	10	10	-	-
18	20	15	-	-
20	1	5	4	0.5
28	33	680	647	84.1
32	1	5	4	0.5
44	2	10	8	1.0

FIG. 111 Mass Spectrum for Ethylene II.

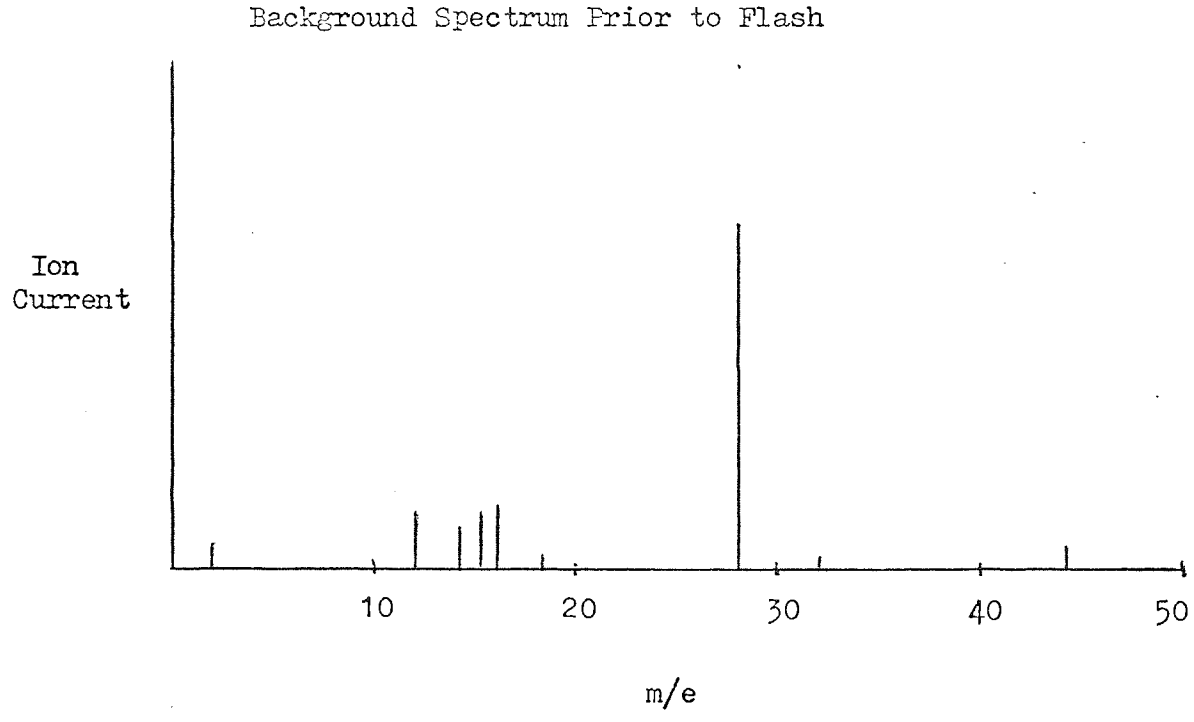

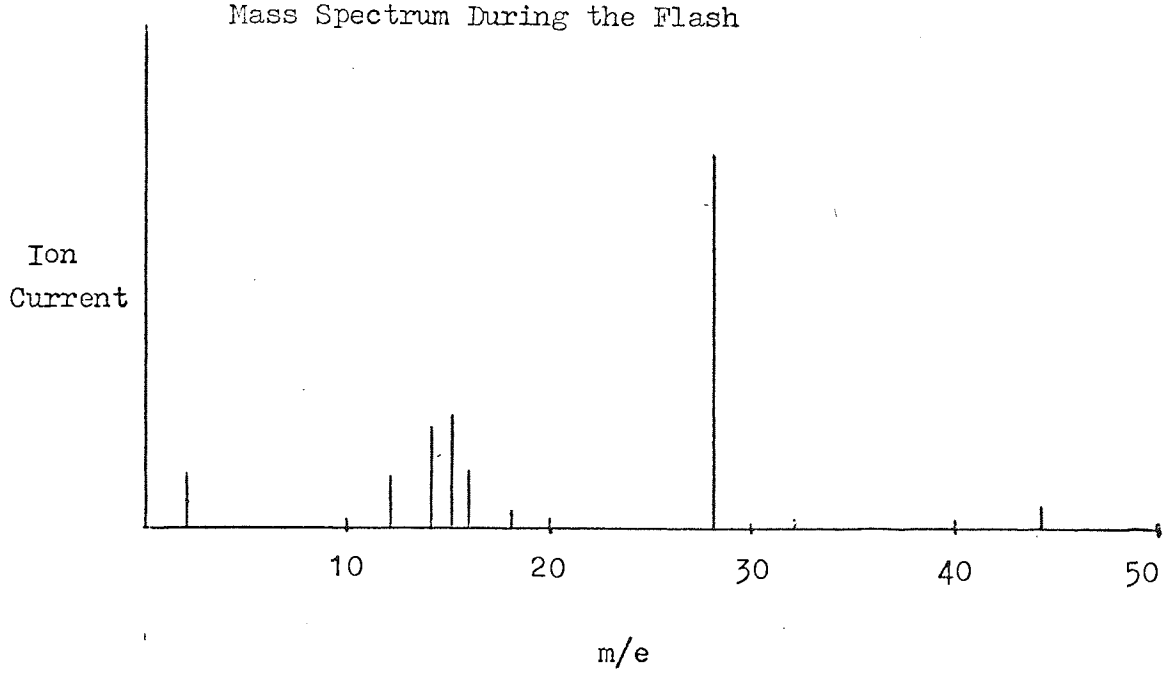

Table 43. Mass Spectrometer Data for an Ethylene Flash Desorption Experiment

	Peak	Background Peak Height	Peak Height During Flash	Increase In Peak	Percentage Increase
a	2	2	5	3	17
	12	5	5	-	
	14	4	10	6	33
	15	5	11	6	33
	16	6	6	-	
	18	1	1	-	
	28	34	37	3	17
	32	1	1	-	
	44	2	2	-	
b	2	4	7	3	21
	12	5	5	-	
	14	3	8	5	33
	15	4	9	5	33
	16	4	4	-	
	18	1	1	-	
	28	41	43	2	13
	32	2	-	-	
	44	1	-	-	

The mass 15 peak is probably due to the existence of a CH_3 radical. The presence of the radicals indicate that some of the ethylene is dissociated on adsorption or decomposed on desorption. The increase in the mass 28 peak is seen in all cases but is proportionally very small when considering the size of the peak. The mass 28 peak rise could be due to desorption of ethylene or the desorption of two CH_2 radicals which combine to form an ethylene molecule. The increase in the mass 2 will be due to desorption of hydrogen which once again suggests some dissociation takes place.

7.4 INTERPRETATION OF RESULTS

7.4.1 The Adsorption of Ethylene

On a clean tantalum surface the sticking probability was 0.91 which is a very high value indicating that most collisions with the surface lead to adsorption. The value of the sticking probability drops steadily to 0.12 at relatively long adsorption times. The initial value of the sticking probability is very high but the fall in sticking probability is what would be expected as the adsorption sites are filled. The number of molecules on the surface after 150 minutes adsorption time is found to be 0.4×10^{14} molecules cm^{-2}. There are approximately 10^{15} adsorption sites on the tantalum surface. The ethylene molecule is a comparatively large molecule and when adsorbed may occupy more than one adsorption site.

7.4.2 Direct Observation of the Filament

X-ray diffraction data indicates that a change in the filament has taken place during the treatment. The X-ray diffraction

pattern is changed and when analysed it was found to be the X-ray diffraction pattern of tantalum carbide. An attempt was made to see if the tantalum carbide was a surface layer or whether the whole filament was tantalum carbide. An attempt was made to "photograph" the filament end with the X-rays but unfortunately the filament was too thin and too fragile to give any results.

The electron microscope pictures of the filament used for the carbon monoxide experiments showed a smooth surface with clear crystal boundaries. The pictures of the filament after treatment with ethylene were quite different. The crystal boundaries caused by the heating could still be seen but at low magnifications the surface did not look smooth but appeared to have many small scratches on it. At much higher magnifications what appeared to be a fibrous coating was seen as shown in Fig. 42. This indicated that the ethylene had reacted with the surface and caused some change. Once again observation of the end of the filament was attempted but again experimental difficulties meant that no information was obtained.

When the filament used for the carbon monoxide experiments was removed from the apparatus it was still a metallic silver colour. The ethylene filament was much darker and so even casual observation of the filament indicated some change.

The electron microscope evidence showed that the ethylene had affected the surface and this was supported by the X-ray diffraction data which showed the surface of the tantalum to be

tantalum carbide. Whether all of the filament had been changed to tantalum carbide or just the surface could not be discovered.

7.4.3 Information From the Desorption Spectrum

Only one clear broad peak is seen in the desorption spectrum. No other clearly resolved peaks could be seen but there was a suggestion of a very small lower temperature peak at high adsorption times. Attempts were made to make the peak larger and better resolved but no peak, which it would be possible to analyse, was obtained. The broad peak is desorbed in the temperature range 300 - 1600 K with the maximum rate of desorption at 1380 K.

Two peaks are seen in the flash desorption spectrum of ethylene adsorbed on iridium at 300 K (38)(58). The peaks are desorbed in the temperature range 400 - 900 K.

7.4.4 Kinetics of Desorption for Ethylene

The reaction was found to be second order and the activation energy for the desorption reaction 80 k joules $mole^{-1}$. The pre-exponential function was found to be 10^{10} cm^2 $molecule^{-1}$ sec^{-1}.

Robertson has investigated the decomposition of ethylene on niobium (26). The reaction was found to be first order at low pressure but to have zero order kinetics at higher pressures. The equation which described the decomposition reaction was

$$P = 10^{2.2} \exp(-57 \text{ k J mol}^{-1}/RT) \qquad \ldots\ (7.1)$$

The parameters are measured when the ethylene is decomposed in the presence of the hot filament and so cannot strictly be compared to the values obtained in this work since the techniques are different.

7.4.5 Nature of the Desorbed Species

The peaks which increased during the flash are the 2, 14, 15 and 28. The major increases are seen in the 14 and 15 peaks which are probably due to desorption of CH_2 and CH_3. The mass 28 peak increases and this could be due to desorption of molecular ethylene or recombination of two CH_2 radicals. The mass 2 peak will be due to molecular hydrogen.

Each of the peaks was followed through the flash and the increase in each could be seen. Other peaks which should be present in the ethylene mass spectrum, but were not detected, were also followed through the flash.

No high mass peaks, m/e $\simeq$ 200, were found which suggests no tantalum hydride or carbide were desorbed. It was stated in the carbon monoxide chapter that no carbon or tantalum carbide had been found to desorb from a carbided surface (94).

For the desorption of ethylene from niobium (58) and iridium (38) the only gaseous product found was hydrogen. Hydrogen was the only product found when acetylene was desorbed from niobium and iridium and butadiene was desorbed from niobium.

7.4.6 Synthesis of the Results

The change in the surface of the filament complicates the reaction. Where do we stop investigating the desorption of ethylene from tantalum and start investigating the desorption of ethylene from tantalum carbide? Robertson has considered a similar problem for the decomposition of ethylene from niobium. He found that Nb_2C filaments gave very similar results to the clean niobium surface but the NbC filaments did not give similar

results. Experiments with a carbon filament had suggested that the deposited carbon would be unlikely to affect the results obtained.

We were unable to say if the carbide was a surface layer or if it had penetrated the bulk of the material. If the whole filament was tantalum carbide then the whole experiment could be effected. The resistivity of tantalum carbide varies greatly from that of tantalum and so the temperature calculation could be seriously effected.

For the carbon monoxide and hydrogen it was assumed that the desorption reaction is the reverse of the adsorption reaction. For ethylene dissociation occurs at high temperatures and so if ethylene is adsorbed it will be dissociated at the temperatures required for a flash desorption reaction. It is the decomposition of hydrocarbons that has been studied and it was found that the only product found was hydrogen (58). Hansen found a small quantity of ethylene desorbed at 100 K (38).

The large quantity of carbide on the surface suggests that our investigations had been concerned with the desorption of ethylene from tantalum carbide. The broad desorption spectrum is probably due to a combination of many peaks with similar reaction kinetics.

BIBLIOGRAPHY

1. GASSER, R.P.H., Chem. Soc., Quart. Rev., 25, 2, 223 (1971).
2. HAYWARD, D.O., TRAPNELL, B.M.W., "Chemisorption" 2nd Ed., (Butterworths, 1964).
3. PAINTER, M.R., Ph.D. Thesis, University of Aston (1973).
4. BAYARD, R.T., ALPERT, D., Rev. Sci. Instrum., 21, 571 (1950).
5. ALEXANDER, C.S., PRITCHARD, J., J. Chem. Soc., Faraday Trans., 68, 202, (1972).
6. BECKER, J.A., Bell System Tech., 30, 907, (1951)
7. GOMER, R., WORTMAN, R., LUNDY, R., J. Chem. Phys., 26, 1147, (1957).
8. MULLER, E.W., Chem. Soc., Quart. Rev., 23, 177, (1969).
9. ANDERSON, J.S., Rec. Austral. Acad. Sci., 1, 109, (1967).
10. DAVIDSSON, C.J., GERMER, L.H., Phys. Rev., 30, 705, (1927).
11. U.H.V. Conference at Warwick, (1974).
12. MORRISON, J., LANDER, J.J., Surf. Sci., 5, 163, (1966).
13. HARRIS, L.A., General Electric Res. Dev. Rep., 67c, 201, (1967).
14. HAAS, T.W., GRANT, J.T., DOOLEY, D.J., "Adsorption-Desorption Phenomena" (Ed J Ricca), Acad. Press, (1972).
15. BORDASS, W.T., LINNETT, J.W., Nature, 222, 660, (1969).
16. AL-JOBOURY, M.I., TURNER, D.W., J. Chem. Phys., 37, 3007, (1962).
17. BRUNDLE, C.R., ROBIN, M.B., KUEBLER, N.A., BASCH, H., J. Amer. Chem. Soc., 94, 1466, (1972).
18. BRUNDLE, C.R., ROBIN, M.B., J. Amer. Chem. Soc., 92, 5550, (1970).
19. REDHEAD, P.A., Canad. J. Phys., 42, 886, (1964).
20. MENZEL, D., GOMER, R., J. Chem. Phys., 41, 3311, (1961).

21. NISHIJIMA, M., PROPST, F.M., J. Vac. Sci. and Tech., 7, 410, (1970).

22. NISHIJIMA, M., PROPST, F.M., J. Vac. Sci. and Tech, 7, 420, (1970).

23. GOYMOUR, C.G., KING, D.A., J. Chem. Soc., Farad. Trans., 4, 736, (1973).

24. KING, D.A., MADEY, T.A., YATES, J.T., J. Chem. Soc., Farad. Trans., 68, 1347, (1972).

25. AGEEV, V.N., IONOV, N.I., USTINOV, Y.K., Sov. Phys-Tech. Phys., 9, 3, 424, (1964).

26. MORGAN, J.A., ROBERTSON, A.J.B., J. Chem. Soc., Farad. Trans., 70, 936,(1974).

27. LANGMUIR, I., TAYLOR, J.B., Phys. Rev., 51, 753, (1937).

28. URBACH, F., Sitzber. Akad. Wiss. Wien, Math-Naturw. Kl. Abt. IIa, 139, 363, (1930).

29. BECKER, J.A., HARTMAN, C.D., M I T. Physical Electronics Conference, (1950).

30. HARTMAN, C.D., MOLNAR, J.P., Amer. Phys. Soc. Meeting, (Schenectady), (1951).

31. BECKER, J.A., HARTMAN, C.D., J. Phys. Chem., 57, 153, (1953).

32. ERHLICH, G., Jour. of App. Phys., 32, 1, 4, (1961).

33. ERHLICH, G., Gen. Elec. Rep. No 63-RL-(3375M), (1963).

34. SMITH, A.W., ARANOFF, S., J. Phys. Chem., 62, 684, (1958).

35. REDHEAD, P.A., Vacuum, 12, 203, (1962).

36. CARTER, G., Vacuum, 12, 245, (1962).

37. AGEEV, V.N., IONOV, N.I., Sov. Phys-Solid State, 13, 11, 2816, (1972).

38. HANSEN, R.S., MIMEAULT, V.J., "Experimental Methods in Catalytic Research", Academic Press, (1968).

39. PETERMANN, L.A., Nuovo Cimento, Suppl., 5, 2, 364, (1967).

40. DEGRAS, D.A., Nuovo Cimento, Suppl., 5, 2, 426, (1967).

41. LAPUJOULADE, Nuovo Cimento, Suppl., 5, 2, 433, (1967).

42. PETERMANN, L.A., "Adsorption-Desorption Phenomena", J. Ricca (ed), (Academic Press 1972).

43. AMENOMIYA, Y., J. of Catalysis, 12, 410, (1968).

44. AMENOMIYA, Y., CVETANOVIC, R.J., Catalysis Rev., 6, 1, 21, (1972).

45. PAGE, F.M., JENNINGS, T.A., Unpublished Work.

46. HICKMOTT, T.W., EHRLICH, G., J. Phys. Chem. Solids, 5, 47, (1958).

47. HICKMOTT, T.W., EHRLICH, G., J. Chem. Phys., 24, 1263, (1956).

48. HICKMOTT, T.W., EHRLICH, G., J. Chem. Phys., 26, 219, (1957).

49. HICKMOTT, T.W., J. Chem. Phys., 32, 3, 810, (1960).

50. RIGBY, L.J., Can. J. Phys., 43, 532, (1965).

51. HANS, H.R., SCHMIDT, L.D., J. Phys. Chem., 75, 2, 227, (1971).

52. EISINGER, J., J. Chem. Phys., 30, 2, 412, (1959).

53. AGEEV, V.N., IONOV, N.I., Sov. Phys-Tech. Phys., 13, 7, 950, (1969).

54. AVEEV, V.N., IONOV, N.I., Sov. Phys-Tech. Phys., 14, 8, 1142, (1970).

55. AGEEV, V.N., IONOV, N.I., Sov. Phys-Solid State, 13, 6, 1305, (1971).

56. GASSER, R.P.H., PATTESON, T.F., Vacuum, 14, 141, (1964).

57. MADEY, T.E., YATES, J.T., J. Vac. Sci. and Tech., 8, 39, (1971).

58. HANSEN, R.S., ARTHUR, J.R., MIMEAULT, V.J., RYE, R.R., J. Phys. Chem., 70, 9, 2787, (1966).

59. DAWSON, P.H., ROBERTSON, A.J.B., T. Farad. Soc., 60, 157, 1122, (1964).

60. PRIVATE COMMUNICATION, U.H.V. Conference, Swansea, (1972).

61. VACUUM GENERATORS CATALOGUE, Vacuum Generators Ltd.

62. GASSER, R.P.H., Private Communication, (1972).

63. JENNINGS, T.A., Ph.D. Thesis, University of Aston, (1971).

64. TURNBULL, A.H., BARTON, R.S., RIVIERE, J.C., "An Introduction to Vacuum Techniques", Newnes, (1962).

65. REDHEAD, P.A., HODSON, J.P., KORNELSEN, E.V., "The Physical Basis of Ultra High Vacuum", Chapman and Hall, (1968).

66. POWER, B.D., "High Vacuum Pumping Equipment", Chapman and Hall, (1966).

67. JNANANANDA, S., "High Vacuum", Van Nostrand, New York, (1947).

68. DEWAR, J., TAIT, P.G., Nature, 12, 217,(1875).

69. BARRER, R.M., Brit. Chem. Engng., 4, 267, (1959).

70. COPE, J.O., Vacuum, 18, 665, (1968).

71. LECK, J.H., "Pressure Measurement in Vacuum Systems", Chapman and Hall, (1957).

72. PIRANI, M., YARWOOD, J., "Principles of Vacuum Engineering", Chapman and Hall, (1961).

73. McLEOD, H., Phil. Mag., 48, 110, (1874).

74. PENNING, F.M., Physica's Grav., 4, 71, (1937), Phillips Tech. Rev., 2, 201, (1937).

75. PENNING, F.M., NIENHUIS, K., Phillips Tech. Rev., 11, 116, (1949).

76. DAWSON, P.H., WHETTON, N.R., Adv. in Electronics and Electron Physics, 27, 59,(1969).

77. PAUL, W., STEINWEDEL, H., Z. Natur., 8a, 448, (1953).

78. PAUL, W., RAETHER, M., Z. Physik, 140, 262, (1955).

79. QUINN, T.F.J., "X-Rays, Electrons and Crystalline Materials", Butterworths, London, (1970).

80. GUINIER, A, "X-Ray Diffraction", (Freeman and Co, San Francisco, 1963).

81. WANG, G.C.Y., LEE, C.Y., "Thermophysical Properties of High Temperature Solid Materials", Toulaukian, Y.S. (Ed), (Macmillian, New York, 1967).

82. ARRHENIUS, S., MEDDA, K., Vetensk. Akad., Nobelinst, 2, 7, 1, (1911).

83. LAIDLER, K.J., "Chemical Kinetics", McGraw-Hill, London, (1965).

84. EYRING, H., J. Chem. Phys., 3, 107, (1935).

85. GLASSTONE, S., LAIDLER, K.J., EYRING, H., "The Theory of Rate Processes", (McGraw-Hill, New York, 1941).

86. FOWLER, R.H., "Statistical Mechanics", (Cambridge Uni. Press, 1966).

87. PORTER, A.S., TOMPKINS, F.C., Proc. Roy. Soc., A217, 529, 544, (1953).

88. GREENHALGH, E., SLACK, N., TRAPNELL, B.M.W., Proc. Roy. Soc., 52, 865, (1956).

89. PASTERNAK, R.A., WIESENDANGER, H.U.D., J. Chem. Phys., 34, 2062, (1961).

90. WHALLEY, L., DAVIS, B.J., MOSS, R.L., T. Farad. Soc., 67, 8, 2445, (1971).

91. TRASATTI, S., J. Chem. Soc., Fara. Trans., 68, 229, (1972).

92. REDHEAD, P.A., T. Farad. Soc., 57, 641, (1961).

93. MORGAN, A.M., KING, D.A., Fara. Soc., 67, 7, 2145, (1971).

94. KLEIN, R., LEDER, L.B., J. Chem. Phys., 38, 1863, (1963).

95. KLEIN, R., LEDER, L.B., J. Chem. Phys., 38, 1866, (1963).

96. FORD, R.R., Adv. Catalysis, 21, 51, (1970).

97. GASSER, R.P.H., THWAITES, R., T Farad. Soc., 61, 2036, (1965).

98. KING, D.A., GOYMOUR, C.G., Fara. Transactions, 4, 749, (1973).

99. SCHEER, M.D., Fine J., Surface Science, 12, 102, (1968).

100. MADEY, T.E., YATES, J.T., STERN, R.C., J. Chem. Phys., 42, 1372, (1965).

101. LANYON, M.A., TRAPNELL, B.M.V., Proc. Roy. Soc. Ser A, 387, 227, (1955).

102. COTTON, F.A., WILKINSON, G., "Advanced Inorganic Chemistry", (Interscience, 1966).

103. BLYHOLDER, G., ALLEN, M.C., J. Amer. Chem. Soc., 91, 3158, (1969).

104. EISCHENS, R.P., FRANCIS, S.A., PLISKIN, W.A., J. Phys. Chem., 60, 194, (1956).

105. ELEY, D.D., NORTON, P.R., Proc. Roy. Soc. Lond., 314, 301, (1970).

106. EISINGER, J., J. Chem. Phys., 32, 3, (1960).

107. AGEEV, V.N., IONOV, N.I., Sov. Phys-Tech Phys., 9, 1581, (1965).

108. YATES, J.T., MADEY, T.E., J. Vac. Sci and Tech., 8, 63, (1971).

109. RIGBY, L.J., Can. J. Phys., 42, 1256, (1964).

110. RIDEAL, E., SWEETT, F., Proc. Roy. Soc., A257, 375, (1957).

111. PAGE, P.J., TRIMM, D.L., WILLIAMS, P.M., Fara. Trans, 70, 1769, (1974).